ANALYSIS OF FLOW SIGNATURES AND CATCHMENT SIMILARITY INDICES FOR CATCHMENT CLASSIFICATION IN YESILIRMAK BASIN

A THESIS SUBMITTED TO
THE GRADUATE SCHOOL OF NATURAL AND APPLIED SCIENCES
OF
MIDDLE EAST TECHNICAL UNIVERSITY

BY

BATUHAN SOYUGÜR

IN PARTIAL FULFILLMENT OF THE REQUIREMENTS
FOR
THE DEGREE OF MASTER OF SCIENCE
IN
GEOLOGICAL ENGINEERING

MAY 2019

Approval of the thesis:

ANALYSIS OF FLOW SIGNATURES AND CATCHMENT SIMILARITY INDICES FOR CATCHMENT CLASSIFICATION IN YESILIRMAK BASIN

submitted by **BATUHAN SOYUGÜR** in partial fulfillment of the requirements for the degree of **Master of Science in Geological Engineering Department, Middle East Technical University** by,

Prof. Dr. Halil Kalıpçılar
Dean, Graduate School of **Natural and Applied Sciences** ________________

Prof. Dr. Erdin Bozkurt
Head of Department, **Geological Engineering** ________________

Assoc. Prof. Dr. Koray K. Yılmaz
Supervisor, **Geological Engineering, METU** ________________

Examining Committee Members:

Prof. Dr. M. Lütfi Süzen
Geological Engineering, METU ________________

Assoc. Prof. Dr. Koray K. Yılmaz
Geological Engineering, METU ________________

Prof. Dr. İsmail Yücel
Civil Engineering, METU ________________

Assoc. Prof. Dr. M. Tuğrul Yılmaz
Civil Engineering, METU ________________

Assoc. Prof. Dr. Harun Aydın
Environmental Engineering, VAN YYÜ ________________

Date: 30.05.2019

I hereby declare that all information in this document has been obtained and presented in accordance with academic rules and ethical conduct. I also declare that, as required by these rules and conduct, I have fully cited and referenced all material and results that are not original to this work.

Name, Surname: Batuhan Soyugür

Signature:

ABSTRACT

ANALYSIS OF FLOW SIGNATURES AND CATCHMENT SIMILARITY INDICES FOR CATCHMENT CLASSIFICATION IN YESILIRMAK BASIN

Soyugür, Batuhan
Master of Science, Geological Engineering
Supervisor: Assoc. Prof. Dr. Koray K. Yılmaz

May 2019, 182 pages

Catchment classification schemes aim to identify groups of hydrologically similar catchments to enable a mapping between catchment physical characteristics and hydro-climatic conditions with the catchment functioning. This mapping, together with the quantified uncertainties, potentially facilitates improved process understanding, transfer of this understanding to ungauged catchments, model parameter regionalization and hence improve operational applications and watershed management. Although many studies focusing on the topic of catchment classification exist in the literature, there is yet no consensus on the number and type of similarity metrics that should be included in such analysis. The aim of this study is to first carefully derive hydrologically relevant similarity metrics from catchment physical (topography, geology, soil, landcover), climatic (precipitation, evapotranspiration, aridity index) and hydrologic response characteristics (flow signatures), provide a basic framework for catchment classification, utilize Affinity Propagation clustering algorithm to determine the optimal number of groupings based on individual as well as a combination of these similarity metrics then compare results with multiple external clustering validation indices (Cramer's V, Adjusted Rand Index etc.). The study area is comprised of 31 sub-catchments (varying between 6.8 km^2 and 10048.8 km^2) located in the Yesilirmak Basin, Turkey, where daily streamflow and monthly meteorological variables are available. The metrics that are based on flow signatures summarize a number of behavioral functions of the catchment system including those derived from flow duration curve (overall water balance, vertical redistribution) as well as temporal redistribution of flow (seasonality etc.). Comparison of the clusters obtained from flow signatures, catchment physical properties and climatic properties indicated that the climate properties are the most important descriptors of the flow signatures in the catchments. Secondarily, the topographic descriptors have the second correspondence with the flow signature clusters. After climate and topographic group of descriptors, land cover, geology and soil have the correspondence with the flow signatures, respectively.

Keywords: Catchment similarity, Flow signatures, Cluster analysis, Affinity propagation algorithm

ÖZ

YEŞİLIRMAK HAVZASI'NDA HAVZA SINIFLAMASI İÇİN AKIM GÖSTERGELERİ VE HAVZA BENZERLİK İNDEKSLERİNİN ANALİZİ

Soyugür, Batuhan
Yüksek Lisans, Jeoloji Mühendisliği
Tez Danışmanı: Doç. Dr. Koray K. Yılmaz

Mayıs 2019, 182 sayfa

Havza sınıflandırma planları, hidrolojik olarak benzer havza gruplarını fiziksel ve hidro-iklimsel olarak haritalayarak, benzer havza gruplarını sınıflandırmayı amaçlamaktadır. Bu çalışmalar, sayısallaştırılmış belirsizliklerle birlikte, süreç anlayışının geliştirilmesini, bu anlayışın ölçülemeyen havzalara aktarılmasını, model parametrelerinin bölgeselleştirilmesini, dolayısıyla operasyonel uygulamaları ve havza yönetimini geliştirmeyi kolaylaştırmaktadır. Havza sınıflandırması konusunda literatürde birçok çalışma mevcut olmakla birlikte, benzerlik ölçütlerinin nasıl sağlanacağı konusunda genel bir görüş birliği bulunmamaktadır. Bu çalışmanın amacı, öncelikle havzanın fiziksel (topografi, jeoloji, toprak, arazi kullanımı), iklimsel (yağış, potansiyel evapotranspirasyon, kuraklık indeksi) ve akış, göstergelerini üretmek, Benzeşme Yayılması algoritmasını kullanarak havzaların benzerliklerini ortaya koymak, ardından yine bu havzaları benzerliklerine göre sınıflamak ve daha sonra sonuçları dış kümeleme karşılaştırma indeksleri (Cramer V Testi, Düzeltilmiş Rand İndeksi vb.) ile karşılaştırmaktır. Çalışma alanı meteorolojik ve akım gözlem istasyonlarındaki verilerin kullanılabilirliğine göre seçilmiş olup, Yeşilırmak Havzası'ndaki 31 alt havzayı (6.8 km^2 ve 10048.8 km^2 arasında değişen) içermektedir. Akımın zamansal dağılımı (mevsimsellik vb.) dahil olmak üzere akım süreklilik eğrisinden elde edilen (toplam su dengesi, düşey akım dağılımı) akım göstergeleri,

havza sisteminin bir dizi hidrolojik işlevini ortaya koymaktadır. Elde edilen kümeleme analizi sonuçlarına göre havzaların akım göstergelerini tanımlamada, iklimsel özelliklerin en belirleyici olduğu görülmüştür. İkincil olarak ise havzaların akım göstergelerinin kümeleri ile topoğrafik özelliklerinin kümelerinin benzerlik gösterdiği sonucuna varılmıştır. İklimsel ve topoğrafik özelliklerin ardından sırasıyla havzaların arazi kullanımı, jeoloji ve toprak özellikleri akım göstergeleri ile benzerlik göstermektedir.

Anahtar Kelimeler: Havza benzerliği, Akım göstergeleri, Kümeleme analizi, Benzeşme yayılması algoritması

To my mom and my sister & memory of my dad…

ACKNOWLEDGEMENTS

Foremost, I would like to express my special thanks to my supervisor Assoc. Dr. Koray K. YILMAZ for his guidance, support, encouragement and patience throughout all phases of this thesis.

In the name of Temelsu International Engineering Services Inc., I would like to express my special thanks to Ayşe SOYDAM BAŞ for sharing her guidance during my thesis study.

I am very grateful to my dear friends Serdar Görkem ATASOY and Timur ERSÖZ for their mental and technical support during my thesis study.

I would like to thank my colleagues Kadir YERTUTANOL, Egemen FIRAT, Orçun YALÇINKAYA, Nurullah SEZEN, Mustafa DİREN, Ecem Cansu ASAN and Evrim SOPACI for their technical support during my thesis.

Finally, I am deeply grateful to my mom and my sister for their endless assistance and support regarding my life.

TABLE OF CONTENTS

LIST OF TABLES

TABLES

LIST OF FIGURES

FIGURES

LIST OF ABBREVIATIONS

ABBREVIATIONS

ALV: Area percentage of alluvium

ARE: Area, (km^2)

ARI: Aridity index

ASP: Mean aspect (°)

BFI: Baseflow index

CAR: Area percentage of carbonate rocks

CLIM: Climatic properties

CLSL: Percentage of clay and silt

CN: Runoff curve number

DHYF: Day of half year flow

DRD: Drainage density (km^{-1})

DSI: General directorate of state hydraulic works

ELV: Mean elevation (m)

FLOW: All flow signatures

GEO: Geological properties

HI: Hypsometry integral

IAL: Permanently irrigated arable land (%)

LCOV: Landcover properties

LFP: Longest flow path (m)

MTA: General directorate of mineral research and exploration

PET: Mean annual potential evapotranspiration (mm)

PPT: Mean annual precipitation (mm)

Q5: 5th percentile exceedance flow

Q50: 50th percentile exceedance flow

Q95: 95th percentile exceedance flow

RQP: Runoff ratio

SFDC: Slope of flow duration curve

SFE: Streamflow elasticity

SLP: Mean slope (°)

SND: Percentage of sand

SOIL: Soil properties

TOPO: Topographic properties

VOR: Area percentage of volcanic rocks

CHAPTER 1

INTRODUCTION

1.1. Background

In all branches of science, it has always been a matter of concern to examine the effects of the factors that form part of the system. As a result of the complex and heterogeneous structure of the Earth, understanding the causes and consequences of the factors affecting this structure, especially in the sciences related to nature, and characterizing and classifying the system as a whole constitute the focal point of the studies in this field. In hydrology, understanding this system is done directly on the catchment scale (Sawicz, 2011). In order to define the hydrological system in a catchment in a meaningful way, the characteristics acting on the flow in the study area should be determined. Although the catchments are defined as a unique and complex organization (Beven, 2000), soil, climate, vegetation and topography can be the result of this complexity (Sivapalan, 2005). Wagener et al. (2004) discusses the fact that a catchment has all the landscape features in the hydrological cycle and the effects of these features on hydrological behavior should be studied at a certain scale. For example, Winter (2001) stated that hydrological responses may be similar when the landscape features are similar as a result of the studies at the catchment scale in Crow Wing River, Minnesota.

In the light of the above-mentioned information, there are many physical and climatic forces that can affect the hydrological behavior in the catchment. If the dominance levels of these forces in catchments are well understood, healthier interpretations of the hydrological responsiveness of those catchments can be made (Sawicz, 2011). Therefore, if we examine the connection of many physical and climatic variables with flows, we can potentially reveal the dominant characteristics in complex catchment structure. To do this, a classification should be made using the physical and climatic variables in the catchments and the results of this classification should be interpreted together with the catchment flow data. According to this classification; a common language can be developed for the studies to be carried out on the watershed scale, the factors related to hydrological cycle can be investigated, a guide can be created to provide a base for models and empirical research, the similarities of catchments on a global scale can contribute to generalization by allowing them to be investigated hydrologically, it can provide ease of information transfer from gauged basins to ungauged catchments and it gives information about the effects of climatic and land cover variations on water resources (Wagener et al., 2007; Sivapalan et al., 2003; Sivakumar et al., 2008, McDonnel and Woods, 2004, Sawicz, 2011).

In these regards, Buttle (2006) discussed the distribution of water in the catchment and landscape features based on typology, topography and topology features. Wagener et al. (2007) also discusses the ways in which water is stored and divided into different flow paths in the catchment, in which time it is stored or released in the catchment, and in which ways the water is separated from the catchment. According to studies on this subject, hydrological responses such as low flows and flow duration curves (Holmes et al., 2002), average of long-term annual flows (Bower et al., 2004), seasonally averaged flows (Laizé and Hannah, 2010), streamflow elasticity, runoff ratio, baseflow index (Sawicz, 2011) is also studied at the catchment scale. Chiverton et al. (2015) studied 116 catchments in UK to investigate those characteristics of daily river flow in the catchment that are affected by the elevation, physiographic characteristics, soil type and geology. He also discussed how such information can be transferred into ungauged catchments by using various statistic methods such as quadratic discriminant analysis, hierarchical clustering based on Ward's minimum variance method etc. Results of the cluster analysis indicated that hydrological response characteristics and precipitation have a strong relationship in the study. Moreover, it is also indicated that surface and groundwater flows are controlled by topography according to results of the study. Ramachandra Roa and Srinivas (2006) have classified and grouped catchments in Indiana according to the physical characteristics (area, channel length, channel slope, etc.) using hierarchical and partitional clustering algorithms. As a result of this study they stated that the flow and physical characteristics of the catchments are more related. In addition, Rice et al. (2015) also find strong relationship between hydroclimatic conditions and topography while examining hydrologic response characteristics in 967 catchments of U.S. Kuentz et al. (2017) study 35215 European catchments using 16 flow signatures and 35 catchment descriptors. This recent study is one of the important publications on this subject on a global scale. In this study, 35215 catchments across Europe clustered according to flow signatures, physiographic properties and combination of two using hierarchical minimum-variance method. The results reveal that flow signatures mainly controlled by climatic characteristics. Then the land cover is the second important characteristics while examining the hydrological response characteristics of the catchments. On the other hand, Merz and Blöschl (2009), Ali et al. (2012) and Ley et al. (2011) found low correlations between flow signatures and physical characteristics of the catchments that they studied.

Although there are many studies on this issue in world, to the best knowledge of the author, this study is the first study in Turkey focusing on catchment classification based on hydrological response and physical characteristics of catchments. Thus, our motivation is to understand which physical and climatic properties controls the hydrological response characteristic of the catchments located in Turkey. This study can help to motivate the further studies in regionalization of flow signatures. Although there are many abovementioned clustering algorithms and statistical methods which was applied in this subject, Affinity Propagation clustering algorithm is used in this study. Affinity Propagation clustering is generally used in mapping of DNA and face recognition in criminal issues to obtain meaningful results (Frey and Dueck, 2007). According to Jing et al. (2010), performance of the hierarchical, k-means and affinity propagation clustering algorithms were tested using large population of image. Result of the study indicates that performance of affinity propagation is better than other clustering algorithms. Furthermore, abovementioned clustering algorithms such as k-means, hierarchical clustering require some subjective choices that define clustering process, but Affinity Propagation doesn't require any initialization before clustering. Thus, Affinity Propagation clustering provide simple solutions in clustering while classifying flow signatures and catchment properties.

In this study, physical, climatic, geological, soil and land cover characteristics and flow signatures of catchments have been characterized. Then, Affinity Propagation Clustering Algorithm was applied to flow signatures and catchment physical and climatic properties to obtain meaningful groups which shows the hydrologic similarity between catchments. After this stage, the results of the affinity propagation by using internal and external cluster indices were compared according to flow signatures and catchment properties.

1.2. Objectives

Catchment classification schemes aim to identify groups of hydrologically similar catchments to enable a mapping between catchment physical characteristics and hydro-climatic conditions with the catchment functioning. This mapping, together with the quantified uncertainties, potentially facilitates improved process understanding, transfer of this understanding to ungauged catchments, model parameter regionalization and hence improve operational applications and watershed management.

The aim of this study is:

- To carefully derive hydrologically relevant similarity metrics from catchment physical (elevation, area, aspect, slope, etc.), geologic, land cover, soil, climatic and hydrologic response characteristics (flow signatures).

- To utilize Affinity Propagation clustering algorithm to determine the optimal number of groupings based on individual as well as a combination of these similarity metrics.
- To compare the results with external and internal cluster validation indices and find relation between catchments properties and flow signatures.

1.3. Study Area

Yeşilırmak Basin is the one of 25-river basin in Turkey and drains its waters into the Black Sea. It is the fifth largest catchment in Turkey (39.628 km^2); the basin covers approximately 5% of the surface area of Turkey. The narrowest part of the basin is in the vicinity of Koyulhisar with a width of 30.5 km. The widest point is in the direction of Ladik – Zile -Akdeğirmen with a width of 170 km. Location map, hillshade model, river network and the main settlements of the study area are given in Figure 1.1.

Figure 1.1. Location Map of Yeşilırmak Basin.

Yeşilırmak, which flows westwards from the Köse Mountains where it was born, drains through the Tokat and Turhal Plains and heads northwards from the Amasya Plain, splitting the Canik Mountains and opening to the Çarşamba Plain among the Topuzlu and Eğrikiraz Mountains. Yeşilırmak, which forms a wide delta through the Çarşamba Plain, is drains to the sea in Çatlı.

Yeşilırmak River forms one of the largest deltas on the Black Sea coast of Turkey. A very large portion of the delta was dried and converted into agricultural land. There are many fertile plains within the boundaries of Yeşilırmak Basin. The most important of these are; Çarşamba, Turhal, Erbaa, Niksar, Artova, Zile, Merzifon, Suluova, Geldingen, Gümüş, Çorum, Mecitözü, Seydim, Suşehri, Kelkit and Şiran. The river reaches Samsun-Çarşamba from here and finally merges with three important branches before it is disembogued into the Black Sea.

All and/or part of Tokat, Samsun, Amasya, Çorum, Sivas, Yozgat, Gümüşhane, Giresun, Erzincan, Ordu and Bayburt provinces are located in Yeşilırmak Basin. The areas of the provinces together with the area distributions within the basin are given in Table 1.1.

Table 1.1 Provinces in Yeşilırmak Basin

Province	**Total Area (km^2)**	**Area in Yesilirmak Basin (km^2)**	**Propotion of the Province Area in Basin (%)**
Tokat	9982	9982	100
Amasya	5701	4885	86
Samsun	9579	4807	50
Yozgat	14123	4238	30
Çorum	12820	4222	33
Sivas	28488	4115	14
Gümüşhane	6585	2828	43
Giresun	6934	2670	39
Erzincan	11903	1110	9
Ordu	6001	614	10
Bayburt	3652	32	1

This study includes 31 sub-catchments with a total area of 6.8 to 10048.8 km^2 in the Yeşilırmak Basin. The catchments are located in the north, west, east and south of Yesilirmak Basin (Figure 1.2). Name of the stream gauges and catchments were selected based on Yeşilırmak Basin Master Plan (Temelsu, 2016). These catchments with different flow, rainfall and physical characteristics represent a heterogeneous structure.

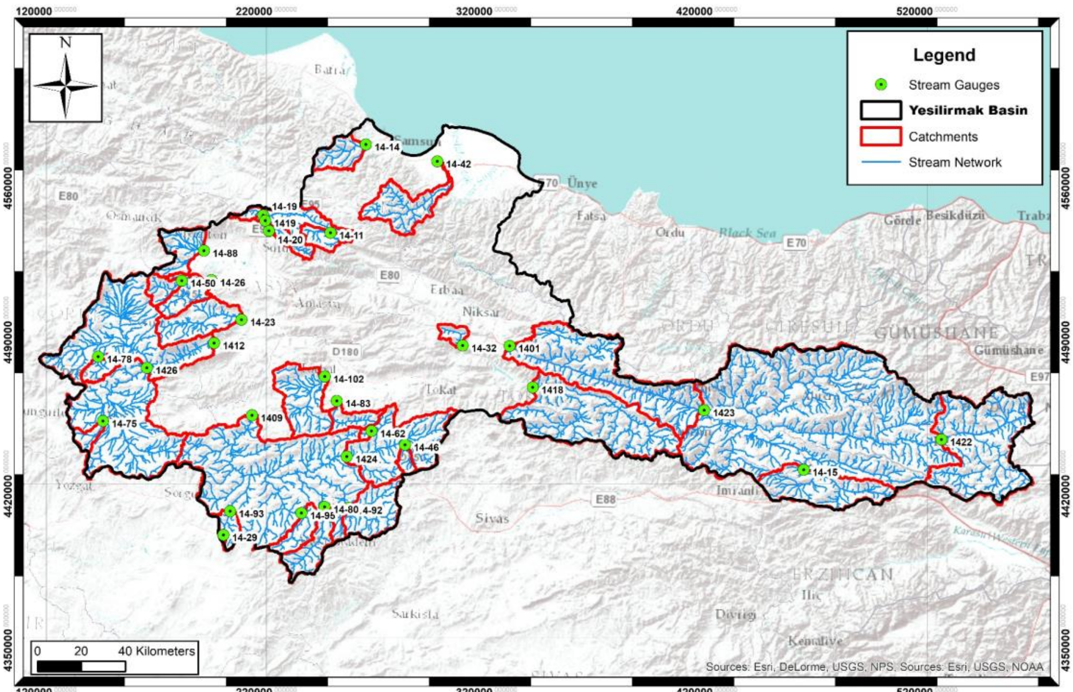

Figure 1.2. Studied Catchments in Yeşilırmak Basin

1.4. Datasets

In this study, completeness of rainfall and flow data was taken into consideration when selecting the study catchments. In addition, human effects to the flow in the study area are minimized. Therefore, attention was paid to avoid dam structures on the main river. In this way, the natural flow response to catchment and climate characteristics was investigated.

The monthly average precipitation and temperature data in the basin were provided by the General Directorate of Meteorology and the flow data were provided by the General Directorate of State Hydraulic Works.

The time period for which the complete data on the main river where the dams are not in operation and for which the daily streamflow, monthly precipitation and temperature values are available without gap, is designated as 1973-1977 period. Therefore, this study covers a period of 5 years in accordance with the available data. The graphs summarizing the availability of the data are given in Figure 1.3 and 1.4. In addition, the general information about important dams and distribution of all dams in Yeşilırmak Basin is given in Table 1.2 and Figure 1.5 respectively. In the figure, the presence of dams in the 31 sub-catchments should not be misleading because the operating years of these dams are after 1977; end of the study period.

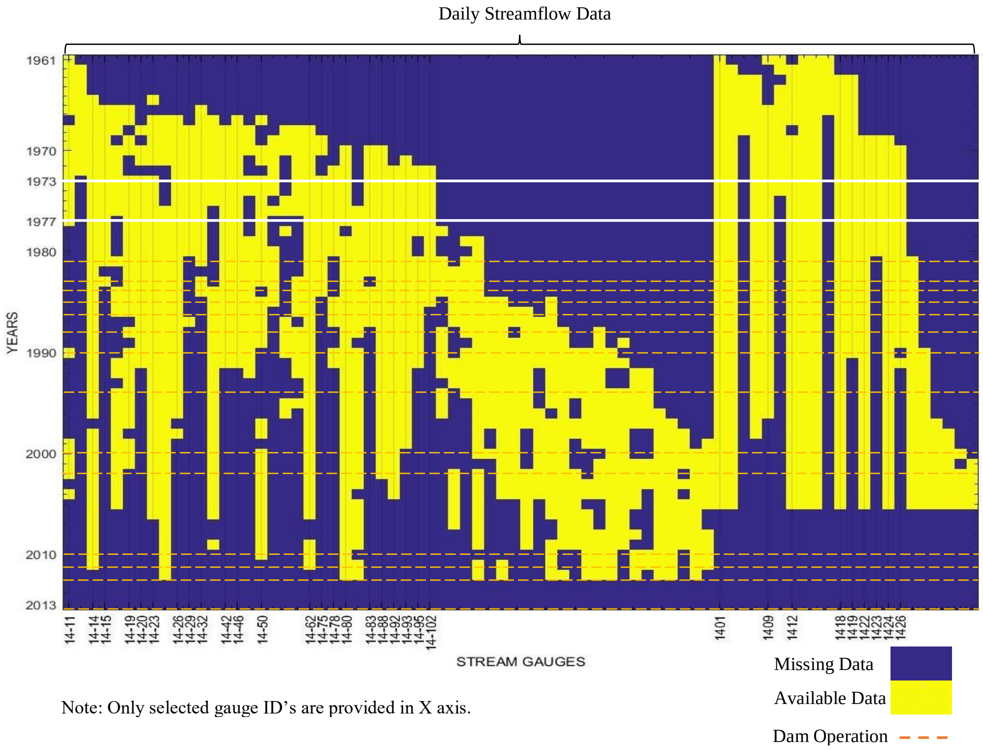

Figure 1.3. Available Streamflow Data

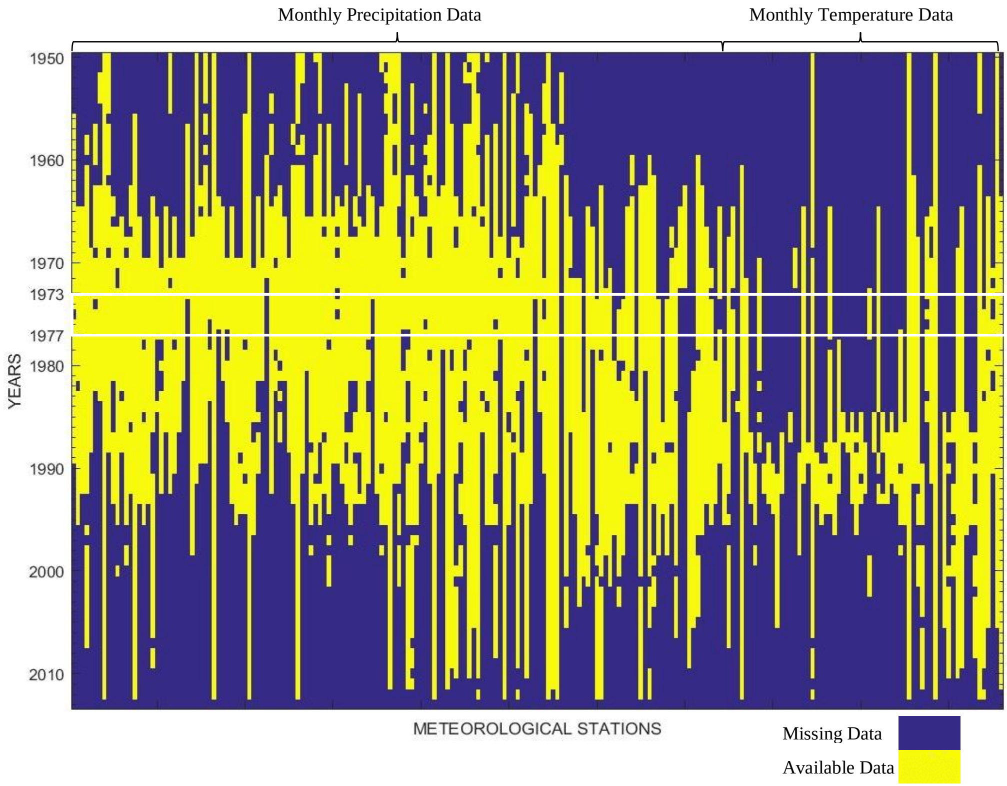

Figure 1.4. Available Meteorological Data

Table 1.2 General Information about Existing Reservoirs in Yeşilırmak Basin

Yesilirmak Basin Existing Reservoirs						
Dam Name	Coordinates		Drainage Area (km^2)	Volume (hm^3)	Purpose	Opening date
	x	y				
Almus*	36.90	40.41	2353.00	855.30	E, I, F	1966
Belpınar	35.95	40.18	258.00	27.30	I	1984
Çakmak	36.63	41.11	477.00	88.90	D	1988
Çamlıgöze	38.08	40.23	8332.00	30.10	E	2000
Derinöz	35.84	40.85	45.00	18.40	I	2002
Gölova	38.62	40.04	748.00	57.40	E,I	1990
H.Uğurlu	36.65	40.94	35900.00	636.10	E	1981
Kılıçkaya	38.19	40.24	8202.00	1033.00	E	1990
S.Ugurlu	36.67	41.07	36100.00	28.10	E	1981
Süreyyabey	35.55	40.04	5123.00	1081.00	E, I, F	2013
Yedikır	35.58	40.79	720.80	57.10	I	1986
Alaca	34.84	40.11	91.00	10.30	I	1985
Boztepe	35.87	40.18	132.00	12.80	I	1983
Çorum	34.99	40.58	51.50	6.10	I,D	1983
Gediksaray	35.66	40.44	98.60	15.80	I	1994
Hatap	34.80	40.37	129.40	11.00	I,D	2010
Uluköy	36.39	40.78	4.20	4.60	I	1984
Yenihayat	34.67	40.39	202.00	29.10	D	2000
Koçhisar	34.94	40.10	721.00	119.00	I	2012
Bedirkale	36.46	40.04	70.00	19.40	I	1983
Koruluk	39.12	40.24	22.00	10.30	I	2004
Köse	39.63	40.24	69.00	14.30	I	2011
I = Irrigation						
F=Flood control						
D=Domastic water supply						
E= Energy						
*Dam is not located on the main river in study catchments.						

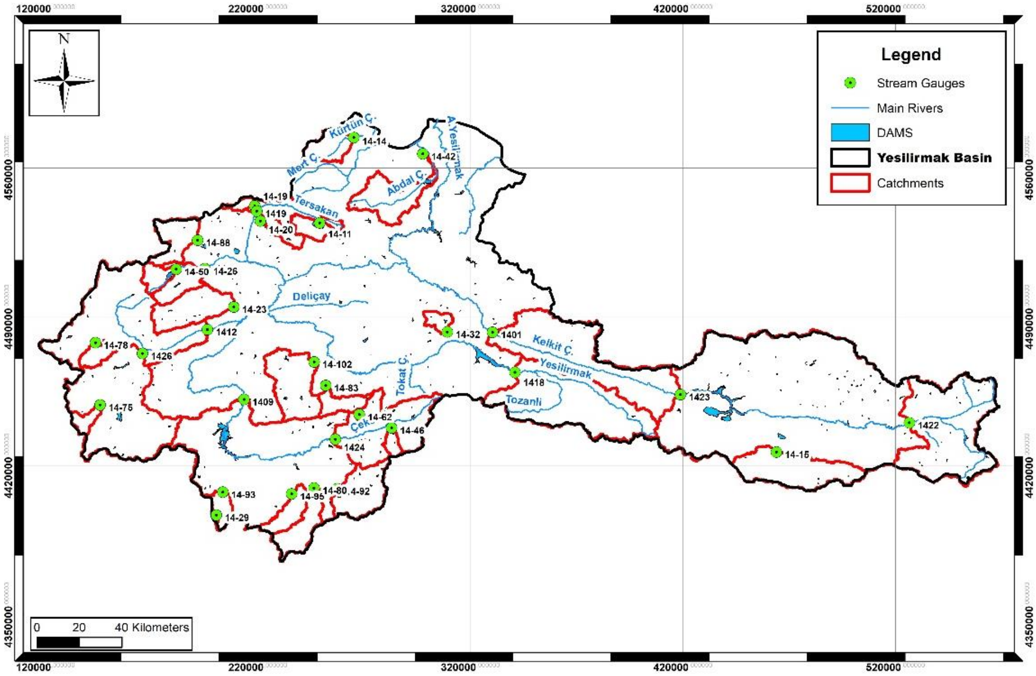

Figure 1.5. Dams in Yeşilırmak Basin

Hydrological data in the basin were analyzed in the ArcGIS® environment. Many hydrological and physical parameters in the catchments were extracted with the help of a Digital Elevation Model (DEM) having a 30mx30m spatial resolution. In the ArcGIS program, sinks in DEM are determined by using sink command. Then with fill command, identified depressions in the sink were filled. Next, with flow direction command, the direction of flow in each cell was found. Then, flow accumulation command is applied to determine the area draining into each cell. The stream definition command by using ArcHydro Toolbox (Strassberg et al., 2011) ensures that the river areas in the basin are at least 2 km^2. Then, the streams have been linked with the stream order. Finally, the stream to feature command created the Streams in the basin (Figure 1.6). The catchment boundaries were created by using the study stream gauges as outlets with the snap pour point command (Parmenter and Melcher, 2012).

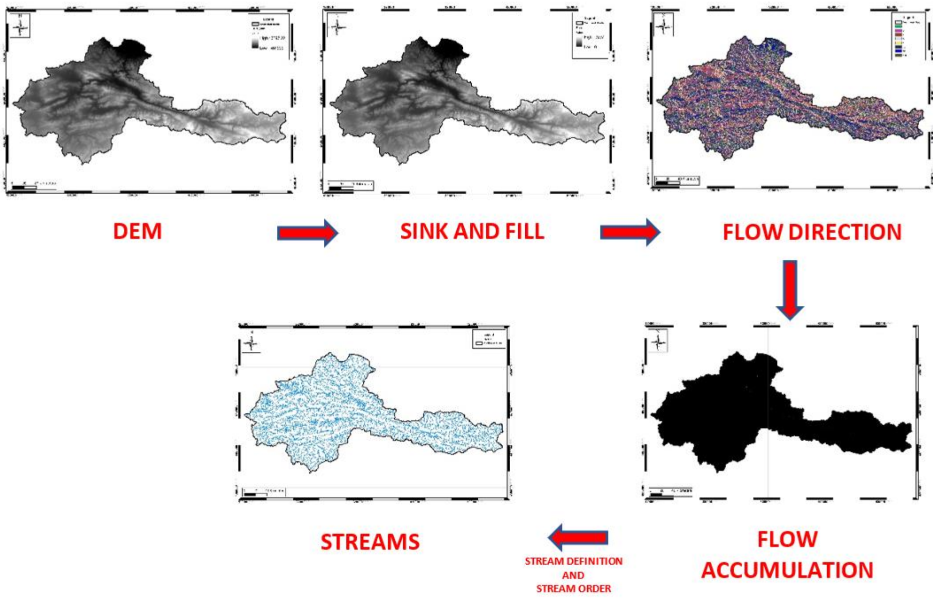

Figure 1.6. Stream Extraction from Digital Elevation Model

The geological boundaries in the basin were extracted from the 1/100 000 scale geological map provided by General Directorate of Mineral Research and Exploration

(MTA). 1990 version of Corine Land Cover was used in the study. This is the closest land cover data to the working year range. Soil maps created by ISRIC World Soil Information (Panagos et al., 2011) were used for soil data in the basin.

1.5. Previous Studies in Yeşilırmak Basin

Hydrological and hydrogeological studies were carried out by the Ministry of Environment and Forestry, General Directorate of Water Management and General Directorate of State Hydraulic Works (DSİ) covering all of the Yeşilırmak River Basin.

In 2008, the Yeşilırmak Basin Protection Action Plan was prepared by the Ministry of Environment and Forestry considering the views of the DSİ. In the scope of this report, it is aimed to determine the characteristics of the surface and groundwater and pollution status and the effects of urban, industrial, agricultural and economic activities. In addition, a detailed investigation of the sources of pollution detected in the basin, the determination of the environmental infrastructure of the basin, and the prevention of pollution in the basin were carried out. Finally, studies on the short, medium- and long-term measures have been made for the protection of the basin (Ministry of Environment and Forestry, 2008).

In 2015, the Yeşilırmak Basin Flood Management Plan report under the responsibility of the General Directorate of Water Management was prepared by Temelsu International Engineering Services Inc. The purpose of this report is to regulate the coordination of all activities and inter-agency coordination for the prevention and / or reduction of the physical and moral losses and damages that may occur in terms of human life, property, environment, natural, historical and cultural assets as a result of a possible flooding in the basin. Hydrological and hydraulic model studies were carried out to determine the regions to be affected in case of possible floods. Then, risk maps were created for possible areas that could be at risk and the measures to be taken for areas under risk were determined (Temelsu, 2015).

In 2016, the Yeşilırmak Basin Master Plan Report prepared by Temelsu International Engineering Services Inc. was submitted to the DSİ. Within the scope of this report; land classification and drainage, environment and water quality, basin water consumption, hydrology, hydrogeology, agricultural economy, flood and sedimentation control reports were prepared separately and submitted to the DSİ (Temelsu, 2016).

In this study, 1/100.000 and 1/25.000 geological maps were provided by the MTA. A detailed geological survey was not conducted in the study area during this study.

CHAPTER 2

CLIMATE

2.1. Climate of Yeşilırmak Basin

The study area is situated in both Central Anatolian Region and Central Black Sea Region and hence is characterized by both continental and Black Sea climate, respectively. Black Sea climate system is dominant near the coastline and shoreline. In Black Sea climate, winters are warm, and summers are cool and season transitions are soft. Towards the southern part of the basin, the basin is under the influence of high mountains. The northern part of the mountains receives orographic rainfall whereas the southern parts of the mountains are under the rain shadow and hence start to show the continental climate regime. Due to the influence of mountains in these regions, winters are cold, rainy and snowy, and summers are cool.

In this section, precipitation, temperature and potential evapotranspiration characteristics of the study area will be discussed at both regional and local (31 catchments) scales.

2.1.1. Precipitation

The meteorological stations belonging to DSİ and MGM in and around the basin were used to determine the precipitation distribution and precipitation characteristics of the basin. In the study area, 79 stations with the full data set covering the period 1973-1977 were used. The spatial distributions and information of the meteorological stations used for revealing the precipitation regime between 1973 and 1977 in Yeşilırmak basin are given in Figure 2.1 and Table 2.1. The annual precipitation values for the study catchments were obtained by constructing annual precipitation isohyets using the "Kriging" interpolation technique in the GIS environment and then taking the average precipitation within each catchment boundary. Figure 2.2 shows the mean annual precipitation isohyets in Yeşilırmak Basin for the period 1973-1977. As a result of these studies; the average annual precipitation in the northern part of the basin is in the range of 746-1697 mm, as can be understood from the observations of meteorological stations 1030, 1300 and 1760, 1840, 1970, 5100, 5180, 5320 from 1973 to 1977. This trend continues without too much variation between Samsun and Tokat. To the east of the Tokat, the precipitation values in the basin varies between 296 and 1224 mm as moving towards the Suşehri, Koyulhisar, Alucra and Kelkit regions respectively. This region receives less rainfall than the northern part of the basin. It is observed that the western and the southern parts of the basin have less rainfall (290-694 mm) than the northern and the eastern parts of the basin. Especially towards the east of Çorum and to the north of Yozgat, these precipitation values fall towards 290-384 mm. The amount of precipitation between 1973 and 1974 is less than 1975, 1976 and 1977 in Yeşilırmak Basin.

In brief, highest mean annual precipitation is observed in the central and northern parts of the basin. On the other hand, lower mean annual precipitation is observed in the west, south and easternmost of the basin as seen in Figure 2.2.

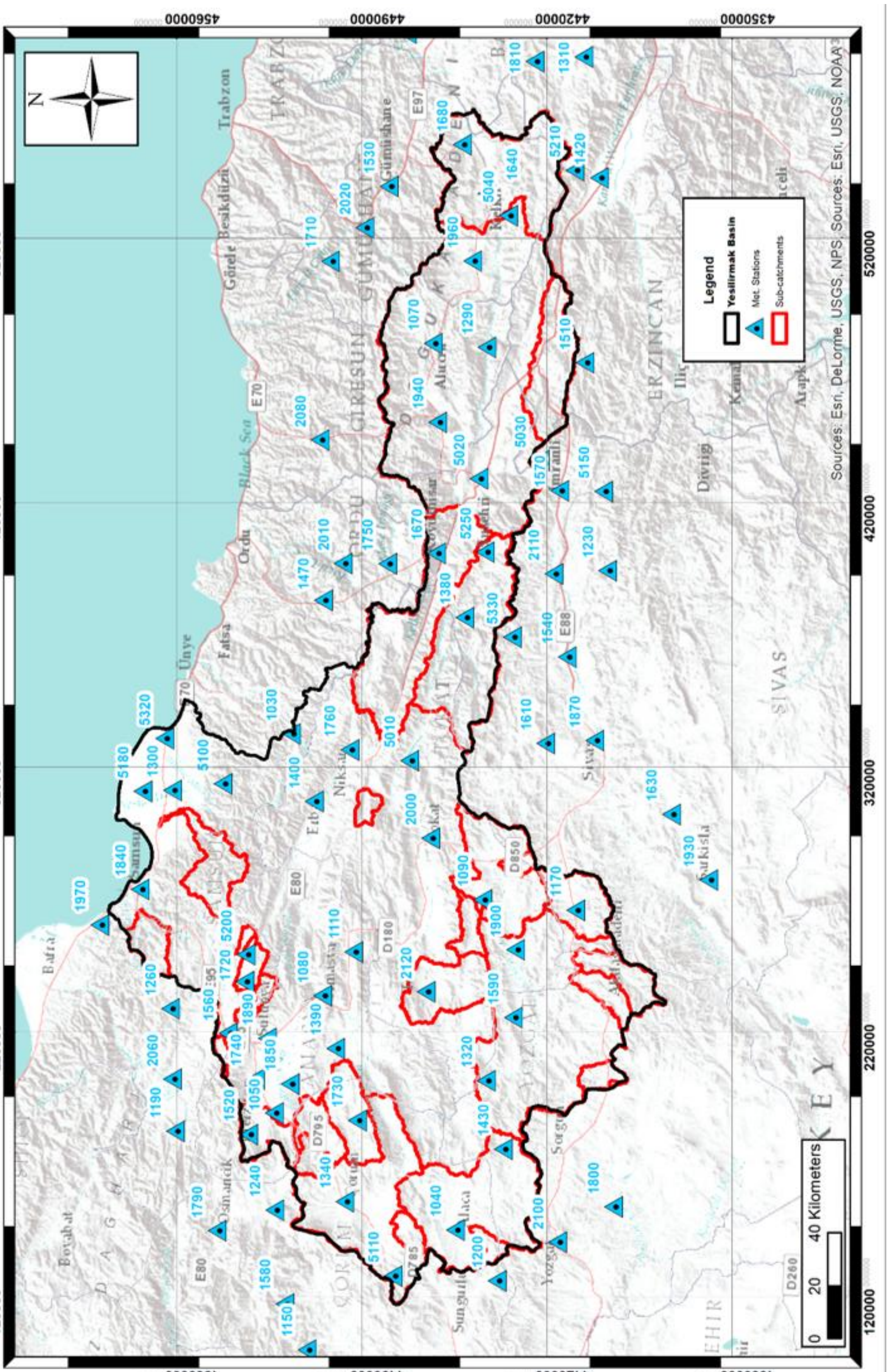

Figure 2.1. Meteorological Stations for Precipitation in Study Area

Table 2.1. Meteorological Stations and Precipitation Amounts for each Years

Station Number	Station Name	Organization	Coordinates		Mean Annual Precipitation (mm)					
			Latitude	Longitude	1973	1974	1975	1976	1977	1973-1977
1030	Akkuş	MGM	40.78	37.02	1108	885	949	1194	1180	1063
1040	Alaca	MGM	40.17	34.83	242	290	425	293	352	320
1050	Alicik	MGM	40.80	35.32	347	321	346	356	388	352
1070	Alucra	MGM	40.32	38.77	522	470	525	526	376	484
1080	Amasya	MGM	40.65	35.85	396	368	375	375	437	390
1090	Artova	MGM	40.12	36.30	404	365	441	483	547	448
1110	Aydınca	MGM	40.55	36.05	352	400	418	476	504	430
1130	Aydıntepe	MGM	40.40	40.15	362	328	376	500	469	407
1150	Bayat	MGM	40.65	34.27	417	403	613	442	326	440
1160	Bayburt	MGM	40.25	40.23	350	310	307	373	454	359
1170	Belcik (Yavu)	MGM	39.80	36.27	294	265	379	366	475	356
1190	Beşpınar	MGM	41.13	35.22	574	467	527	465	553	517
1200	Boğazkale	MGM	40.02	34.62	316	364	503	482	427	418
1230	Bulucan	MGM	39.72	37.77	518	529	565	558	551	544
1240	Büyüklaçin	MGM	40.78	34.88	437	285	428	418	416	397
1260	Çakıralan	MGM	41.17	35.77	594	567	523	513	658	571
1290	Çamoluk (Mindeval)	MGM	40.13	38.75	466	455	504	515	572	502
1300	Çarşamba	MGM	41.18	36.75	851	740	984	902	1485	992
1310	Çayırlık	MGM	39.80	40.03	322	356	373	416	434	380
1320	Çekerek	MGM	40.08	35.50	350	309	476	780	795	542
1340	Çorum	MGM	40.55	34.94	324	436	477	374	503	423
1380	Doğanşar	MGM	40.20	37.55	515	471	548	661	600	559
1390	Doğantepe	MGM	40.60	35.62	354	334	385	381	431	377
1400	Doğanyurt	MGM	40.70	36.72	458	458	516	622	580	527
1420	Erzincan	MGM	39.75	39.50	268	321	371	395	364	344
1430	Eymir	MGM	40.02	35.20	323	325	466	373	355	369
1470	Gölköy	MGM	40.68	37.62	916	998	943	1073	1176	1021
1510	Gümüşakar	MGM	39.80	38.68	517	515	569	807	602	602
1520	Gümüşhacıköy	MGM	40.88	35.22	394	309	378	349	473	381
1530	Gümüşhane	MGM	40.47	39.47	349	358	430	435	475	409
1540	Hafik	MGM	39.85	37.38	306	447	405	465	466	418
1560	Havza	MGM	40.97	35.67	428	408	483	434	576	466
1570	İmranlı	MGM	39.88	38.12	321	398	393	396	414	384
1580	İskilip	MGM	40.73	34.47	377	359	583	397	389	421
1590	Kadışehri	MGM	40.00	35.78	296	362	405	398	444	381
1610	Karaçayır	MGM	39.92	37.00	390	486	504	561	446	477
1630	Kayadibi	MGM	39.48	36.70	342	303	408	411	375	368
1640	Kelkit	MGM	40.13	39.43	283	276	249	345	346	300
1670	Koyulhisar	MGM	40.30	37.83	367	404	440	443	455	422
1680	Köse	MGM	40.22	39.65	366	267	304	377	381	339
1710	Kürtün	MGM	40.67	39.13	522	603	552	693	782	630
1720	Ladik	MGM	40.92	35.90	674	574	670	675	879	694
1730	Mecitözü	MGM	40.52	35.30	325	351	356	369	520	384
1740	Merzifon	MGM	40.87	35.47	384	351	349	326	496	381
1750	Mesudiye	MGM	40.47	37.78	451	534	646	512	752	579
1760	Niksar	MGM	40.58	36.95	475	489	548	625	643	556
1790	Osmancık	MGM	40.98	34.78	300	271	320	248	313	290
1800	Osmanpaşa	MGM	39.63	34.97	358	312	374	364	359	353
1810	Otlukbeli	MGM	39.97	40.02	397	388	366	433	443	405
1840	Samsun	MGM	41.28	36.30	614	544	689	538	716	620
1850	Sarıbuğday	MGM	40.75	35.45	316	307	348	260	433	333
1870	Sivas	MGM	39.75	37.02	285	397	410	441	472	401
1890	Suluova	MGM	40.83	35.65	296	308	289	294	461	330
1900	Sulusaray	MGM	40.00	36.08	319	372	513	428	539	434
1930	Şarkışla	MGM	39.35	36.42	515	238	364	373	375	373
1940	Şebinkarahisar	MGM	40.30	38.42	453	562	573	624	635	569
1960	Şiran	MGM	40.18	39.13	402	309	376	542	503	426
1970	Taflan	MGM	41.42	36.13	767	625	858	817	971	808
2000	Tokat	MGM	40.30	36.57	315	334	333	412	428	364
2010	Topçam	MGM	40.62	37.78	736	750	753	821	920	796
2020	Torul	MGM	40.55	39.28	519	542	491	577	628	551
2060	Vezirköprü	MGM	41.15	35.45	485	460	473	388	599	481
2080	Yavuzkemal	MGM	40.70	38.33	1156	1240	1088	1240	1399	1224
2100	Yozgat	MGM	39.82	34.80	391	444	634	550	481	500
2110	Zara	MGM	39.90	37.75	435	467	473	500	498	474
2120	Zile	DSI	40.30	35.88	292	325	461	399	440	383
5010	Almus Barajı	DSI	40.38	36.91	380	381	504	551	548	473
5020	Bostancık	DSI	40.16	38.17	224	324	298	285	349	296
5030	Çalıyurt	DSI	39.95	38.25	449	590	546	514	571	534
5040	Çambaşı	DSI	40.06	39.33	346	337	342	428	450	380
5100	Düzdağ	DSI	41.01	36.78	1566	1558	1557	1766	2043	1698
5110	Evciyenikışla	DSI	40.37	34.62	373	430	762	420	568	511
5150	Karacaören	DSI	39.73	38.12	507	621	588	726	592	607
5180	Kızılot	DSI	41.28	36.74	779	858	950	872	975	887
5200	Mazlumoğlu	DSI	40.92	36.02	506	469	647	510	777	582
5210	Mecidiyeköy	DSI	39.83	39.53	447	447	525	507	537	493
5250	Pazarbelen	DSI	40.13	37.84	455	585	480	552	519	518
5320	Terme	DSI	41.21	36.98	591	461	782	822	1076	746
5330	Yeniköy (Hafik)	DSI	40.04	37.47	397	506	591	611	563	534

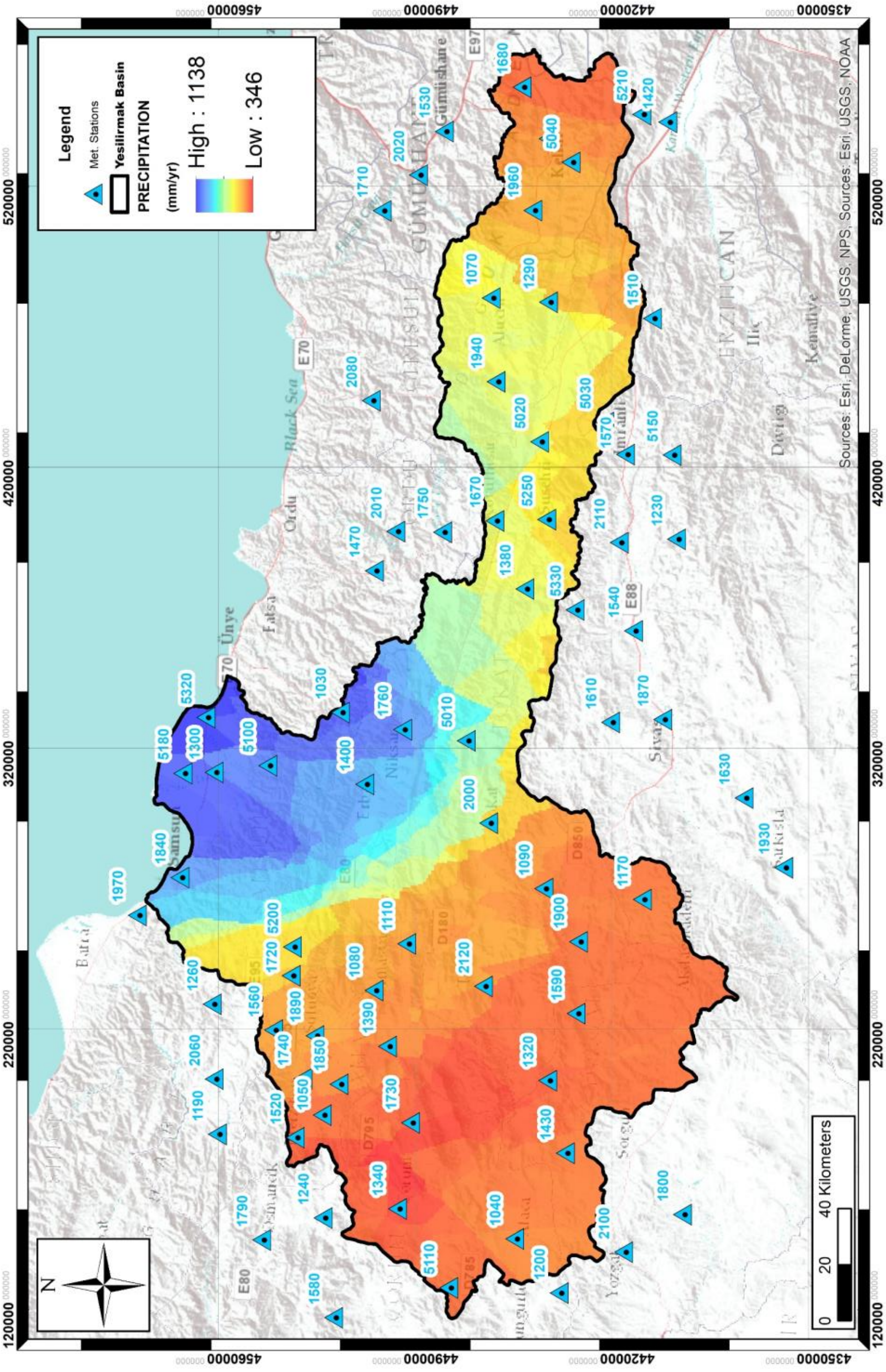

Figure 2.2. Mean Annual Precipitation of Yeşilırmak Basin

Precipitation of Study Area

Catchment precipitation information provided above was summarized in Table 2.2. Following these results, 25%, 50% and 75% percentiles of the mean annual precipitation values were used to classify the catchments into 4 precipitation classes. After comparing 25%, 50% and 75% percentiles of the mean annual precipitation values, low and moderate class have revised because the amount of precipitation difference between the classes was only 0.008 mm. Then, precipitation classes of catchments are named as low (between 386.27 mm and 395.93 mm), moderate (between 401.84 mm and 419.62 mm), high (between 420.05mm and 481.03 mm) and very high (between 488.79 mm and 766.40 mm). Geographically, precipitation conditions have been defined as high to very high in the north and east of the Yeşilırmak basin and moderate to low in the south and west of the Yeşilırmak basin (Table 2.2). As seen in Table 2.2, mean annual precipitation was low in 1974 and the mean annual precipitation was high in 1977. Although the study has a short period of time, it contains arid (1974) and wet years (1977).

Table 2.2. Precipitation Conditions of Study Catchments

Catchment No.	Mean Annual Precipitation (mm)	Years					Precipitation Conditions
	Mean	1973	1974	1975	1976	1977	
14-50	386.27	369.93	346.62	404.09	352.56	458.15	Low
14-26	390.81	374.81	350.62	400.86	359.21	468.50	
14-23	393.75	354.41	339.31	400.37	389.04	485.41	
14-88	395.93	385.29	356.97	397.96	360.93	478.66	
14-95	401.84	348.46	327.88	421.21	438.94	472.68	Moderate
14-80	401.89	346.42	328.67	420.58	440.26	473.51	
14-78	401.92	348.92	354.15	489.91	392.36	424.35	
14-29	403.82	336.75	333.20	442.00	431.62	475.46	
14-93	403.90	333.50	335.13	442.47	431.81	476.57	
1412	404.77	352.65	349.58	470.48	404.24	452.45	
14-46	407.94	348.42	353.13	428.91	442.42	466.81	
1409	408.41	345.59	343.72	429.22	442.16	481.35	
14-92	410.16	347.39	349.32	427.18	450.74	476.12	
1426	415.87	344.61	354.42	485.88	430.59	463.78	
1422	417.24	383.21	372.37	395.26	462.87	472.50	
14-62	419.62	353.73	346.70	430.28	465.59	501.80	
14-102	420.05	457.77	354.71	427.11	442.88	523.16	High
14-75	423.17	352.81	359.02	508.01	438.49	457.52	
1424	423.64	359.67	365.72	440.31	464.49	487.89	
14-83	436.63	364.92	366.70	447.26	472.05	531.70	
14-19	442.21	436.38	398.83	433.65	403.56	539.40	
14-20	449.47	426.49	405.23	444.85	416.32	554.36	
1419	476.72	455.24	424.00	475.46	443.31	585.28	
14-15	481.03	426.48	463.05	472.14	532.56	510.64	
14-11	488.79	463.44	432.29	492.43	455.89	599.84	Very High
1423	496.15	444.23	470.87	479.99	541.58	544.00	
1401	513.77	457.77	487.42	499.21	559.04	565.66	
1418	546.30	467.62	523.47	546.99	589.64	603.19	
14-14	593.05	556.59	521.15	597.12	555.49	733.29	
14-32	708.21	626.93	607.03	694.00	757.43	855.64	
14-42	766.40	701.01	652.19	765.05	770.15	944.09	

Spatial distribution of the Mean Annual Total Precipitation of the catchments is given Figure 2.3. The amount of the precipitation in catchments are also given in Figure 2.4 for each year.

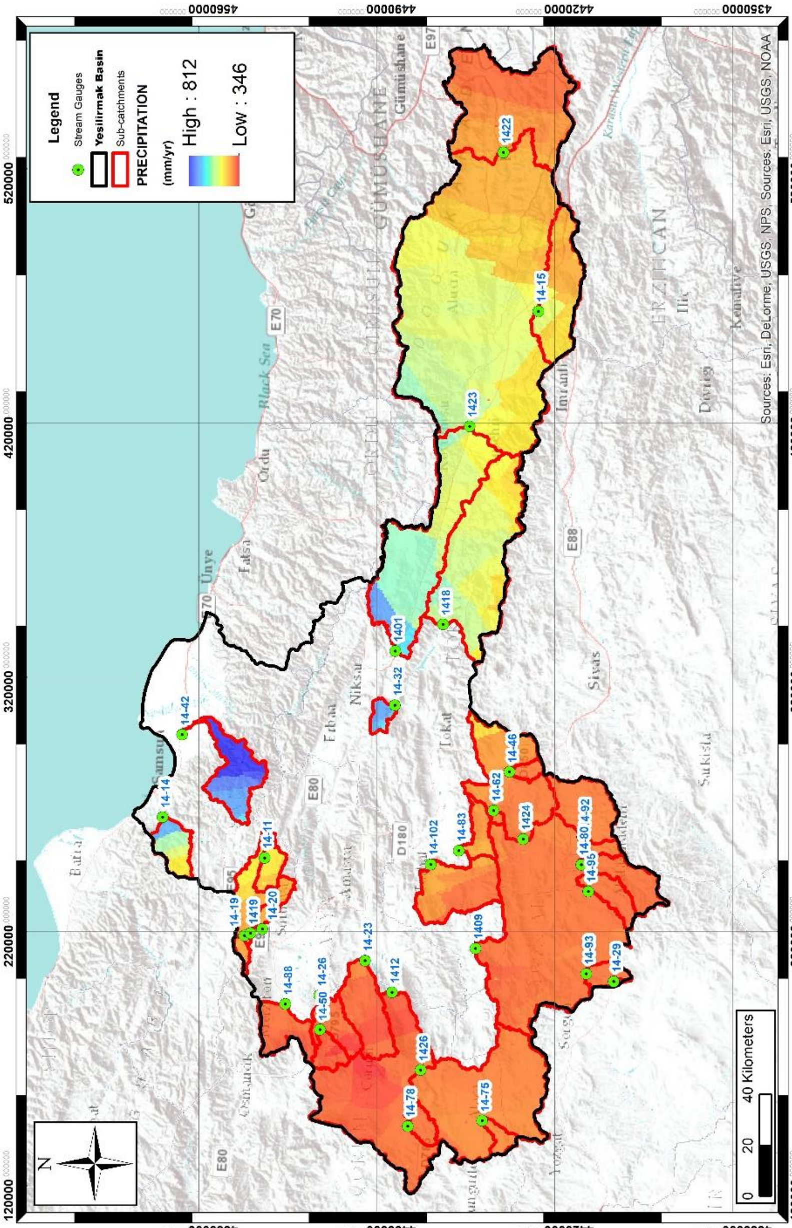

Figure 2.3. Mean Annual Precipitation of Study Catchments

2.1.2. Temperature

The meteorological stations belonging to DSİ and MGM in and around the basin were used to determine the temperature distribution and characteristics of the basin. In the study area, 30 stations with the full data set covering the period 1973-1977 were used. The spatial distributions and information of the meteorological stations used for revealing the temperature characteristics between 1973 and 1977 in Yeşilırmak basin are given in Figure 2.5 and Table 2.3. In this study, the annual average temperature isohyets were plotted using the "Kriging" interpolation technique in the ArcGIS environment.

As a result of these studies: the average annual temperature in the northern part of the basin is in the range of 10.8-14.2 °C as can be understood from the observations of meteorological stations of 1060, 1080, 1300, 1740, 1760 and 1840. This temperature regime is affecting Samsun, Suluova, Amasya, Erbaa, Niksar and Tokat regions. This part of the basin shows the highest temperatures between 1973 and 1977. As can be seen in the temperature data of stations 1750, 1830 and 1920, temperatures range from 8-12 °C in the east of Tokat to Koyulhisar and Suşehri region. In the Alucra and Kelkit regions, the temperature values range from 5.6 to 10 °C. This region represents the coldest part of the Yeşilırmak Basin. Temperatures in the western and southern parts are lower than the northern part of the basin and higher than the eastern part. Temperatures in Çorum, Alaca, Yozgat, Sorgun and Akdağmadeni regions vary between 7.8-11.3 °C. We can say that average temperatures are observed in this region compared to other parts of the basin. Mean annual temperature distribution in Yeşilırmak Basin between 1973 and 1977 is given in Figure 2.6.

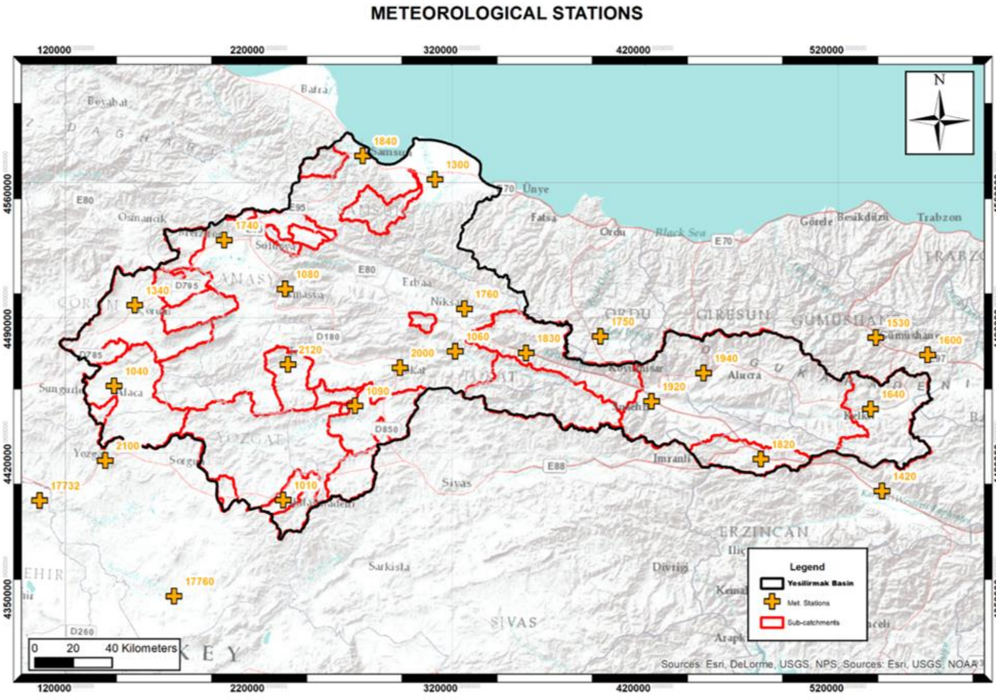

Figure 2.4. Meteorological Stations for Temperature

Table 2.3. Meteorological Stations and Mean Temperature Values for each Years

Station Number	Station Name	Organization	Coordinates		Annual Avarage Temperature (°C)					
			Latitude	Longitude	1973	1974	1975	1976	1977	1973-1977
1010	Akdağmadeni	MGM	39.67	35.88	7.7	8.0	7.6	8.3	7.6	7.8
1040	Alaca	MGM	40.17	34.83	10.3	7.4	8.7	8.7	9.3	8.9
1060	Almus	MGM	40.38	36.90	10.2	10.9	10.9	9.7	10.8	10.5
1080	Amasya	MGM	40.65	35.85	13.0	13.6	13.8	12.5	13.7	13.3
1090	Artova	MGM	40.12	36.30	8.1	8.1	8.0	7.2	8.6	8.0
1300	Çarşamba	MGM	41.18	36.75	13.9	14.3	14.9	13.4	14.6	14.2
1340	Çorum	MGM	40.55	34.94	9.8	10.0	10.4	9.2	10.3	10.0
1420	Erzincan	MGM	39.75	39.50	10.0	10.1	10.3	9.4	10.4	10.0
1530	Gümüşhane	MGM	40.47	39.47	9.1	9.5	9.4	8.6	9.6	9.3
1600	Kale	MGM	40.38	39.78	9.6	9.8	9.9	9.0	10.0	9.6
1640	Kelkit	MGM	40.13	39.43	6.0	5.8	5.3	5.0	5.7	5.6
1740	Merzifon	MGM	40.87	35.47	10.5	11.0	11.3	10.1	11.1	10.8
1750	Mesudiye	MGM	40.47	37.78	7.7	7.9	8.4	7.6	8.3	8.0
1760	Niksar	MGM	40.58	36.95	14.0	14.1	14.4	13.1	14.3	14.0
1820	Refahiye	MGM	39.90	38.77	6.1	5.9	5.6	5.6	5.8	5.8
1830	Tokat Resadıye	MGM	40.38	37.33	12.5	12.8	12.9	11.7	12.7	12.5
1840	Samsun	MGM	41.28	36.30	14.0	14.0	14.5	13.2	14.1	14.0
1920	Suşehri	MGM	40.17	38.10	10.1	10.2	10.4	9.8	10.3	10.2
1940	Şebinkarahisar	MGM	40.30	38.42	8.6	9.0	9.0	7.8	8.6	8.6
2000	Tokat	MGM	40.30	36.57	11.8	12.2	12.3	11.1	12.2	11.9
2100	Yozgat	MGM	39.82	34.80	8.2	8.3	8.3	7.5	8.6	8.2
2120	Zile	DSI	40.30	35.88	11.0	11.7	11.4	10.1	11.2	11.1
17160	Kırşehir	DSI	39.10	34.09	10.8	10.9	10.9	10.2	11.1	10.8
17193	Nevşehir	DSI	38.37	34.42	10.1	10.1	9.5	9.4	10.3	9.9
17196	Kayseri	DSI	38.45	35.29	9.6	9.6	9.0	9.0	9.8	9.4
17732	Çiçekdağı	DSI	39.37	34.25	11.2	11.3	11.4	10.5	11.9	11.3
17760	Boğazlıyan	DSI	39.12	35.15	9.5	9.1	9.0	8.2	9.3	9.0
17802	Pınarbaşı	DSI	38.43	36.24	7.5	8.0	7.1	7.1	7.6	7.5
17835	Ürgüp	DSI	38.38	34.35	10.3	10.4	10.1	9.7	10.4	10.2
17840	Sarız	DSI	38.29	36.30	7.6	7.5	6.4	6.2	7.0	6.9

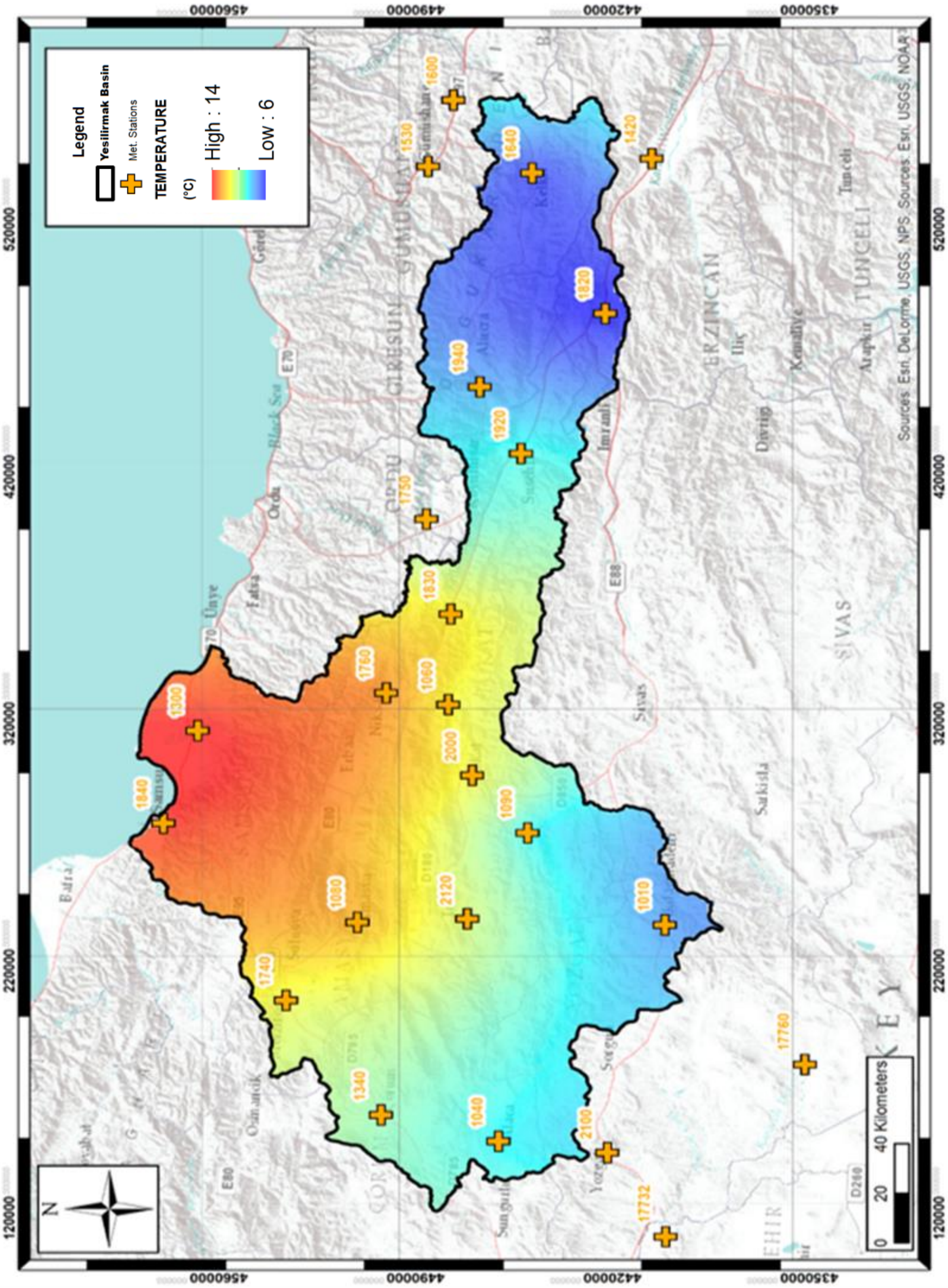

Figure 2.5. Mean Annual Temperatures in Yeşilırmak Basin

Temperatue of Study Area

Catchment temperature information provided above was summarized in Table 2.4. Following these results, 25%, 50% and 75% percentiles of the mean annual temperature values were used to classify the catchments into 4 temperature classes. Then, precipitation classes are named as low (between 7.39 °C and 8.75 °C), moderate (between 9.05 °C and 9.76 °C), high (between 10.35 °C and 10.75 °C) and very high (between 11.79 °C and 13.50 °C). Geographically, temperature conditions have been defined as high to very high in the north and middle of the Yeşilırmak basin and moderate to low in the south and west of the Yeşilırmak basin (Table 2.4). As seen in Table 2.4, temperatures were low in 1976 and temperatures were generally high in 1974 and 1975.

Table 2.4. Temperature Conditions of Study Catchments

Catchment No.	Annual Mean Temperature (°C)	Annual Mean Temperature (°C)					Temperature Conditions
		1973	1974	1975	1976	1977	
14-15	7.39	7.68	7.66	7.20	7.05	7.36	Low
1423	7.99	8.16	8.24	7.99	7.51	8.06	
1422	8.13	8.32	8.38	8.04	7.58	8.32	
14-80	8.32	8.43	8.62	8.04	8.27	8.26	
14-95	8.42	8.52	8.68	8.16	8.40	8.33	
1401	8.47	8.58	8.69	8.53	7.96	8.56	
14-92	8.68	8.81	9.04	8.42	8.36	8.76	
14-93	8.74	8.98	8.86	8.58	8.51	8.78	
14-29	8.75	8.99	8.86	8.61	8.50	8.81	
1409	9.05	9.18	9.30	8.93	8.72	9.14	Moderate
14-75	9.16	9.74	8.71	9.08	8.72	9.54	
1426	9.22	9.73	8.85	9.20	8.78	9.55	
14-62	9.36	9.49	9.72	9.23	8.78	9.60	
14-46	9.41	9.50	9.75	9.30	8.86	9.62	
14-78	9.50	9.99	9.04	9.59	9.02	9.88	
1412	9.55	9.92	9.24	9.65	9.04	9.88	
1424	9.58	9.66	9.92	9.53	9.00	9.81	
14-83	9.76	9.82	10.10	9.76	9.14	9.99	
14-50	10.35	10.36	10.31	10.73	9.69	10.68	High
14-102	10.37	10.31	10.66	10.61	9.69	10.56	
14-23	10.45	10.45	10.45	10.79	9.79	10.74	
14-26	10.45	10.44	10.45	10.83	9.78	10.77	
1418	10.58	10.47	10.75	10.93	9.93	10.82	
14-88	10.75	10.67	10.80	11.17	10.06	11.06	
14-19	11.79	11.57	11.95	12.33	11.02	12.11	Very High
14-32	12.28	12.07	12.44	12.81	11.40	12.66	
14-20	12.43	12.13	12.58	13.07	11.57	12.80	
1419	12.54	12.26	12.68	13.17	11.68	12.89	
14-11	12.75	12.45	12.90	13.42	11.86	13.13	
14-14	13.17	12.95	13.24	13.83	12.34	13.48	
14-42	13.50	13.24	13.55	14.21	12.60	13.88	

Spatial distribution of the Annual Mean Temperature of the catchments is given Figure 2.7. The amount of the temperature in catchments are also given in Figure 2.8 for each year.

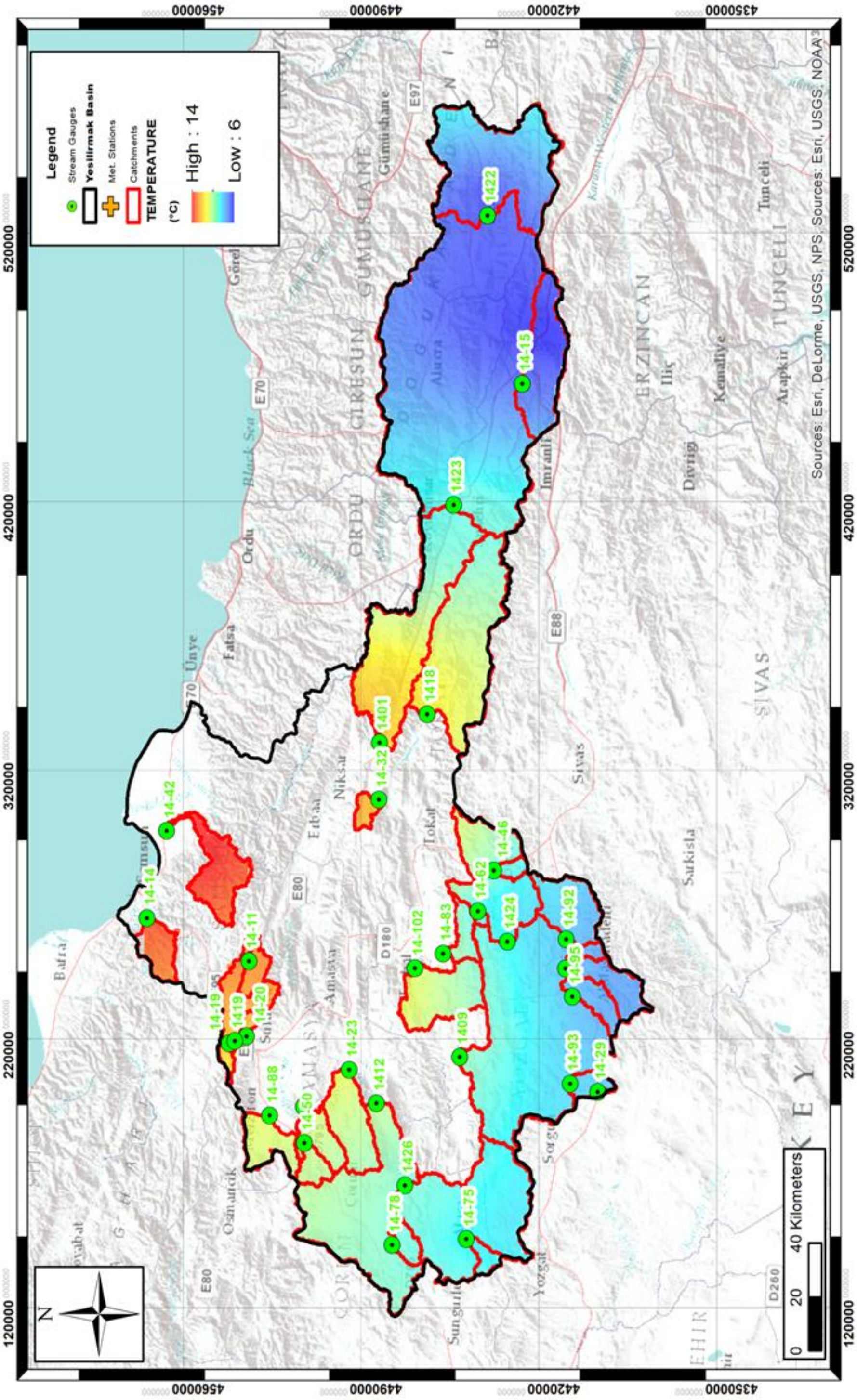

Figure 2.6. Mean Annual Temperature of Study Catchments

2.1.3. Potential Evapotranspiration

The meteorological stations belonging to DSİ and MGM in and around the basin were used to determine the potential evaporation distribution and characteristics of the basin. In the study area, 30 stations with the full data set covering the period 1973-1977 were used.

There are not enough pan evaporation data to calculate actual evaporation in meteorological stations in study area. Therefore, Thornthwaite Method (1948) was used to calculate potential evapotranspiration (PET) because only monthly temperature data available for study area:

$$PET=16*d\ (10T/I)^{a} \qquad (1)$$

Where;

T= Mean Temperature for the month (C°)

I= $\sum i$ Annual Thermal Index, $(i=(T/5)^{1.514}$

d=correction factor depends on latitude and month

$a=0.49+0.0179\ I - 0.0000771\ I^{2} + 0.000000675\ I^{3}$

The spatial distributions and information of the meteorological stations used for revealing the potential evapotranspiration characteristics between 1973 and 1977 in Yeşilırmak basin are given in the following Figure 2.9 and Table 2.5. In this study, the mean annual potential evapotranspiration isohyets were plotted using the "Kriging" interpolation technique in the ArcGIS environment.

As a result of these studies: at the northern part of the basin, potential evapotranspiration values vary from 1099.49 to 1112.83 mm, as can be seen from the meteorological station data of 1300 and 1840. The highest potential evapotranspiration values were observed in the part of basin bounded by the Samsun, Erbaa and western part of Ünye.

The potential evapotranspiration values in the Suluova, Amasya, Niksar Tokat and western parts of Koyulhisar vary between 929.39 - 1075.87 mm according to meteorological station data of 1740, 1080, 1760, 1060 and 1830. This region has the second highest potential evapotranspiration rate than the north of the basin.

The values of potential evapotranspiration in the basin are decreasing towards the Suşehri Koyulhisar, Alucra and Kelkit regions, respectively. Potential evapotranspiration values in this region vary from 726.66 to 925.51 mm as seen in the data of the stations 1750, 1920, 1940, 1820, 1530, 1640, 1420 and 1600. The lowest potential evapotranspiration values in the basin are observed in this region. Potential evapotranspiration values at 1010, 1040, 1090, 1340, 2100, 2120, 17160, 17193, 17196, 17732, 17760, 17835 and 17840 stations in the west and south of Basin vary from 758.34 to 974.08 mm. The lowest potential evapotranspiration values after north of the basin are observed in this region. Mean annual potential evapotranspiration distribution in Yeşilırmak Basin between 1973 and 1977 are given in Figure 2.10.

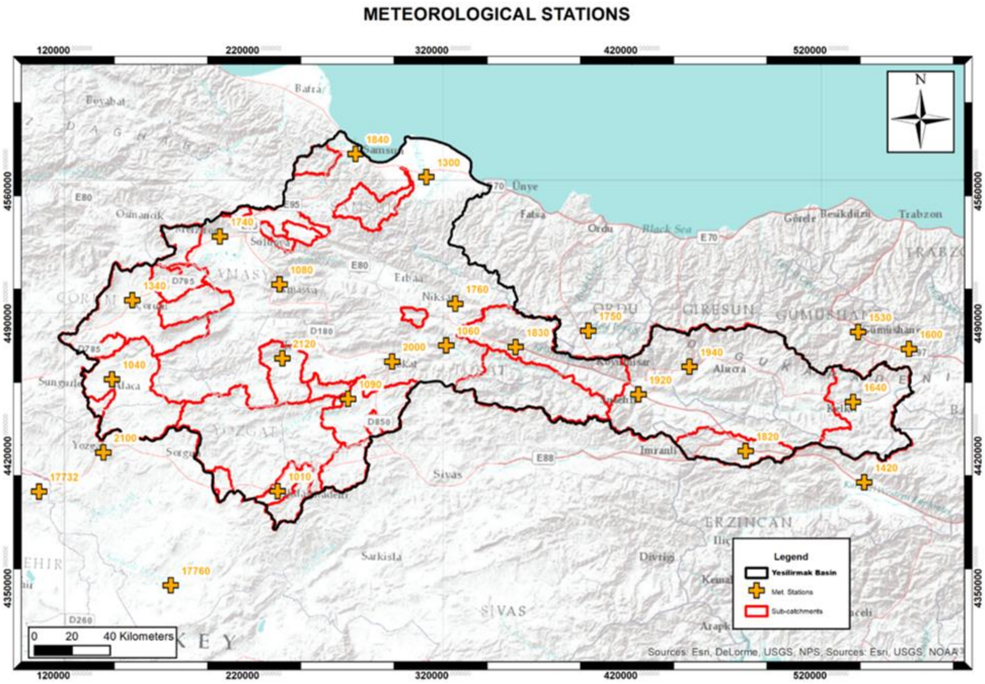

Figure 2.7. Meteorological Stations Meteorological Stations for Potential Evapotranspiration

Table 2.5. Meteorological Stations and Mean Potential Evapotranspiration Amounts for each Years

Station Number	Station Name	Organization	Coordinates		Mean Annual Potential Evapotranspiration (mm)					
			Latitude	Longitude	1973	1974	1975	1976	1977	1973-1977
1010	Akdağmadeni	MGM	39.67	35.88	808	825	779	829	819	812
1040	Alaca	MGM	40.17	34.83	973	774	829	874	865	863
1060	Almus	MGM	40.38	36.90	930	963	930	872	952	929
1080	Amasya	MGM	40.65	35.85	1045	1070	1127	1030	1107	1076
1090	Artova	MGM	40.12	36.30	827	799	807	719	837	798
1300	Çarşamba	MGM	41.18	36.75	1096	1115	1149	1080	1125	1113
1340	Çorum	MGM	40.55	34.94	925	937	924	872	937	919
1420	Erzincan	MGM	39.75	39.50	934	940	907	910	937	926
1530	Gümüşhane	MGM	40.47	39.47	868	890	860	857	883	872
1600	Kale	MGM	40.38	39.78	901	915	884	883	911	899
1640	Kelkit	MGM	40.13	39.43	714	759	723	700	737	727
1740	Merzifon	MGM	40.87	35.47	943	967	950	892	1001	951
1750	Mesudiye	MGM	40.47	37.78	805	812	802	801	828	810
1760	Niksar	MGM	40.58	36.95	1111	1122	1144	1078	1127	1117
1820	Refahiye	MGM	39.90	38.77	730	767	723	705	723	730
1830	Tokat Resadıye	MGM	40.38	37.33	1053	1038	1085	984	1063	1045
1840	Samsun	MGM	41.28	36.30	1101	1099	1131	1066	1101	1099
1920	Suşehri	MGM	40.17	38.10	900	912	889	895	916	902
1940	Şebinkarahisar	MGM	40.30	38.42	848	830	847	740	861	825
2000	Tokat	MGM	40.30	36.57	989	1014	1063	924	1042	1006
2100	Yozgat	MGM	39.82	34.80	832	804	815	783	848	816
2120	Zile	DSI	40.30	35.88	972	1004	961	903	934	955
17160	Kırşehir	DSI	39.10	34.09	971	946	905	914	938	935
17193	Nevşehir	DSI	38.37	34.42	933	911	854	873	903	895
17196	Kayseri	DSI	38.45	35.29	894	871	861	877	905	882
17732	Çiçekdağı	DSI	39.37	34.25	990	969	973	934	1005	974
17760	Boğazlıyan	DSI	39.12	35.15	881	843	844	845	875	858
17802	Pınarbaşı	DSI	38.43	36.24	816	802	789	775	837	804
17835	Ürgüp	DSI	38.38	34.35	946	964	876	889	911	917
17840	Sarız	DSI	38.29	36.30	777	782	775	698	759	758

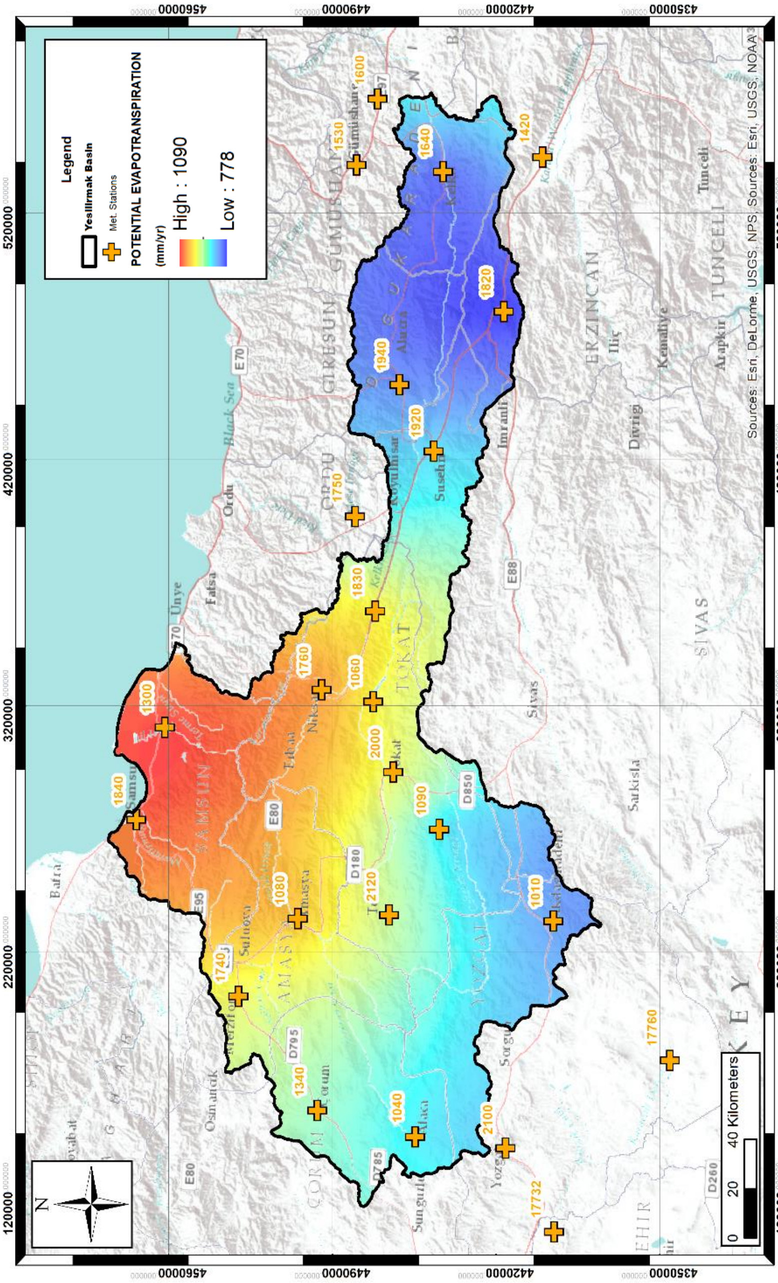

Figure 2.8. Potential Evapotranspiration in Yeşilırmak Basin

Potential Evapotranspiration of Study Area

Table 2.6 summarizes the catchment potential evapotranspiration information provided above. Following these results, 25%, 50% and 75% percentiles of the mean annual potential evapotranspiration values were used to classify the catchments into 4 evapotranspiration classes, namely, Low (between 797.62 mm and 852.39 mm), moderate (between 866.74mm and 894.12 mm), high (between 897.76 mm and 939.34 mm) and very high (between 951.46 mm and 1075.93 mm). Geographically, potential evapotranspiration conditions have been defined as generally high to very high in the north of the basin, moderate in the west and middle of the basin and moderate to low in the south and east of the Yeşilırmak basin.

Table 2.6. Potential Evapotranspiration of Conditions of Study Catchments

Catchment No.	Mean Annual Potential Evapotranspiration (mm)	Mean Annual Potential Evapotranspiration (mm)					Potential Evapotranspiration Conditions
		1973	1974	1975	1976	1977	
14-15	797.62	804.74	822.03	789.61	783.03	803.15	Low
1423	821.00	826.30	840.61	815.30	801.23	833.03	
14-80	834.10	845.99	842.71	811.45	827.19	846.32	
1422	837.74	837.18	861.37	825.80	821.93	847.28	
14-95	838.78	850.83	847.12	815.20	834.08	848.65	
1401	842.50	846.90	859.69	840.48	818.65	855.73	
14-92	850.33	865.14	860.65	841.07	830.99	869.05	
14-93	852.03	873.05	850.47	829.84	848.26	861.20	
14-29	852.39	872.80	849.21	831.77	847.22	862.60	
1409	866.74	882.19	874.84	856.68	848.04	880.12	Moderate
14-75	874.67	924.98	840.02	856.79	862.92	890.17	
1426	878.17	922.79	850.62	862.23	864.06	892.10	
14-62	878.95	895.04	891.82	882.15	849.96	899.58	
14-46	883.56	896.38	894.03	890.28	850.84	908.72	
1424	891.31	902.77	902.87	899.68	856.32	915.10	
14-78	893.41	939.50	864.98	879.50	872.74	908.45	
1412	894.12	931.75	874.35	882.94	872.64	910.34	
14-83	897.76	909.89	912.50	904.11	863.36	914.78	High
14-102	924.53	933.69	944.20	932.72	883.09	932.20	
14-50	932.93	948.22	934.15	933.23	895.05	957.08	
14-23	935.49	948.60	937.58	937.58	896.68	957.09	
14-26	937.13	950.15	939.60	938.39	898.02	961.85	
1418	939.34	939.85	947.05	954.41	894.01	958.70	
14-88	951.46	959.35	956.11	954.24	909.44	980.58	Very High
14-19	998.06	992.44	1006.52	1014.72	946.32	1030.87	
14-32	1019.85	1012.28	1031.74	1054.92	953.82	1042.35	
14-20	1025.39	1012.74	1033.73	1058.68	964.06	1054.02	
1419	1031.15	1018.98	1038.57	1062.99	970.41	1057.97	
14-11	1040.51	1026.14	1048.09	1078.10	976.27	1065.30	
14-14	1060.55	1051.51	1063.25	1092.89	1003.88	1079.84	
14-42	1075.93	1063.64	1080.02	1115.95	1012.69	1092.05	

Spatial distribution of the annual mean potential evapotranspiration of the catchments is given Figure 2.11. The amount of the annual mean potential evapotranspiration in catchments are also given in Figure 2.12 for each year.

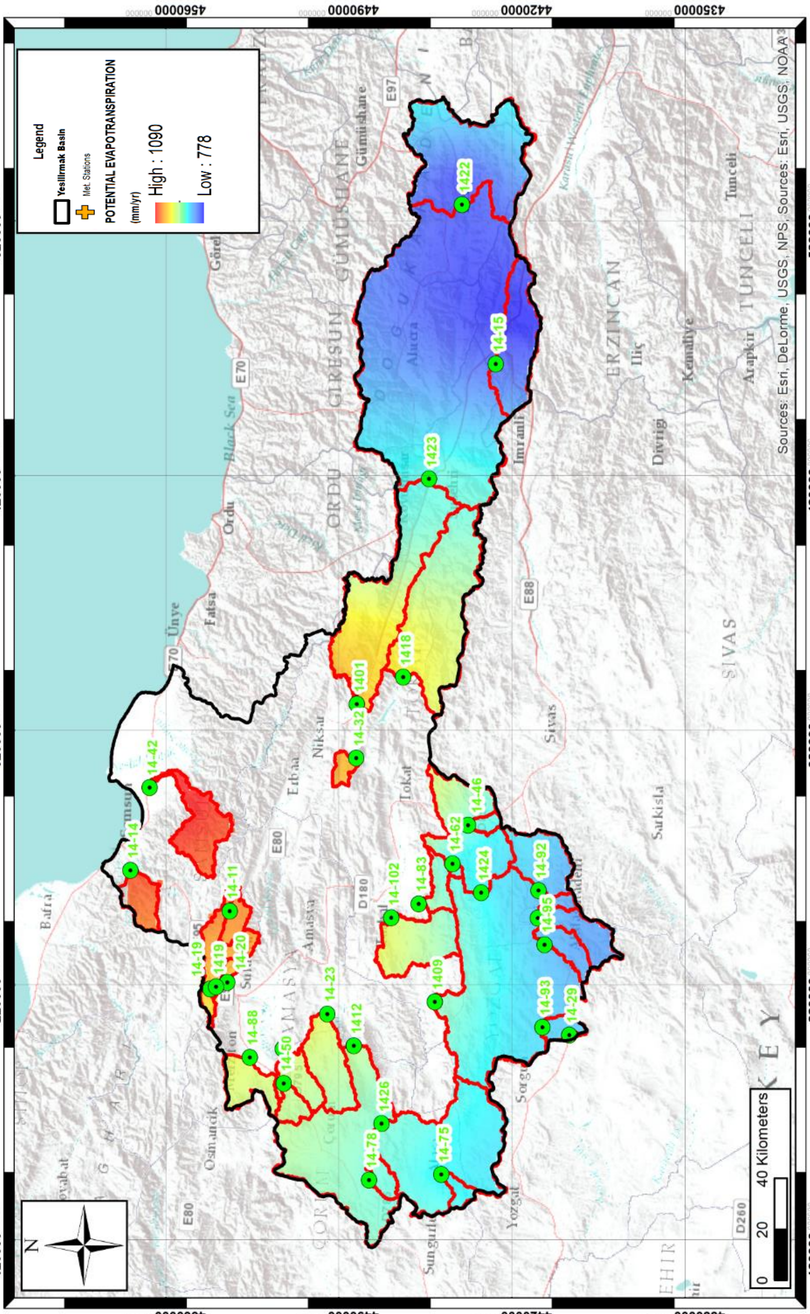

Figure 2.9. Mean Annual Potential Evapotranspiration (mm) in study area

CHAPTER 3

HYDROLOGY

3.1. Hydrology of Study Area

Yeşilırmak Basin covers an area of approximately 39,628 km^2 in the northern part of Anatolia and drains its waters to the Black Sea. This basin is surrounded by the Black Sea to the north and the basin divide is marked by the the Canik, Giresun, Gümüşhane, Pulur, Çimen, Kızıldağ, Köse, Tekeli, Yıldız, Çamlıbel, Akdağlar, Karababa, İnegöl and Kunduz Mountains. The Yeşilırmak Basin surrounded by Kızılırmak, Fırat-Dicle, Doğu Karadeniz and Çoruh basins.

Yeşilırmak River emerges from the Köse Mountains on the south-western side of the Susehri district in Sivas. It's length is about 519 km while draining lands in Tokat, Amasya and Samsun provinces. Yeşilırmak is mainly composed of 3 main branches. The Kelkit River is the largest branch of the Yeşilırmak River. Alluviums carried by the river formed the Çarşamba Plain at north of basin.

The number of dams in Yeşilırmak basin is very high and the most important structures are Hasan Ugurlu, Almus, Çakmak, Kılıçkaya, Süreyyabey and Koçhisar dams (Figure 3.1). In addition to hydropower production, these dams serve to meet irrigation, drinking and industrial water demand. Due to the derivation of its waters by the dams the flow regime is irregular, and the discharge is reduced. Another important issue that affects the outflows from the dams is evaporation losses that occur in dam reservoirs during hot summer periods. In this study, the time period (1973-1977) is selected so that the flow in the study catchments (31 sub-catchments) is not controlled by dams and represent natural flows.

3.1.1. Rivers

In this part of the thesis, the surface water resources of basin will be examined.

3.1.1.1. Yeşilırmak Main River

Yeşilırmak, born from the Köse Mountains on the southwest of Sivas Susehri District, is 519 km long. It enters the Amasya from the south and merges with the Çekerek River, 256 km, which is born from Yozgat territory in Kayabaşı district. Yeşilırmak, passes through the city center of Amasya, merges with Tersakan River coming from Ladik Lake and Kelkit River on the border of Taşova - Erbaa and is poured from Çarşamba to Karadeniz in Samsun province borders. There are Almus Dam (80 m height from thalweg), and Ataköy Dam on the Yeşilırmak, in Almus District. There are also Hasan Ugurlu Dam (175 m height from thalweg) at Ayvacık, 40 km south of Çarşamba District and Suat Ugurlu Dam in Balahor at its downstream (Figure 3.1).

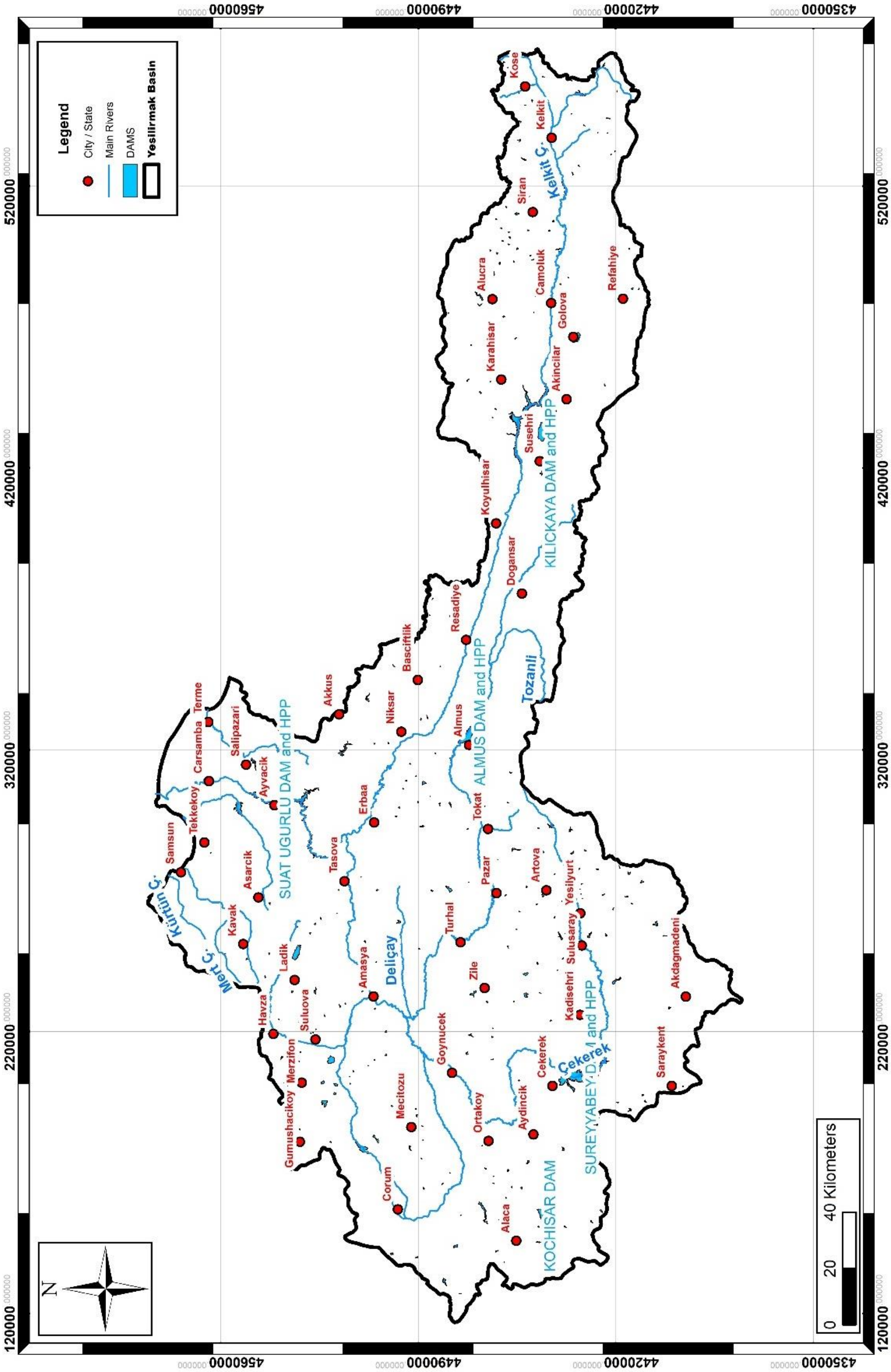

Figure 3.1. The boundaries of Yeşilırmak Basin and the Location of Most Important Dams

3.1.1.2. Çekerek River

Çekerek River is born from the Yıldız Mountains, 2500 m high, located 50 km north of Sivas Province. The length of Çekerek River is 200 km. It merges with Çorum Creek and joins with Yeşilırmak from 15 km south of Amasya. Çorum Çayı is formed by the merger of Derinçay and Alaca Stream.

3.1.1.3. Tersakan River

Tersakan River is born at the mountainside of Akdağ at an altitude of 1925 m. Tersakan takes the excess water of Lake Ladik and passes through Havza District. Finally, it merges with Yeşilırmak in Amasya. The length of the Tersakan River is 100 km. Şeyhsuyu, Gümüşsuyu, Derinöz and Salhan Brook are important branches of Tersakan. On these branches, there are Gümüşhacıköy Plain, Merzifon Plain and Suluova. Moreover, Derinöz Dam is also found on the Derinöz River.

3.1.1.4. Kelkit River

It originates from mountains at an altitude of 2600 m in the north-western part of Erzincan. The Kelkit Stream is born by the union of the mountains descending from the mountains between Gümüşhane and Erzincan. It flows from east to west between Gümüşhane Mountains. It passes from Kelkit to Şebinkarahisar and Koyulhisar and Niksar, joins with Yeşilırmak in Erbaa Plain. The length of river is 400 km.

3.1.1.5. Abdal River

Abdal River is located near Dikbıyık – Irmaksırtı region. The catchment area of river is about 502 km^2. The catchment area of that river starts from Asarcık with an altitude of 1200 m, and it is poured to Black Sea near Irmaksırtı after passing the Samsun – Ordu highway.

3.1.1.6. Kürtün River

Kürtün River begins at 1100 m elevations on the border of Kavak District and is poured into the Black Sea within the provincial center of Samsun. The length of the river is 47 km.

3.1.1.7. Engiz River

Catchment boundaries of Engiz River are starting from 1300 m elevation and it passes from Samsun – Sinop highway and is poured into the Black Sea.

3.1.1.8. Derinöz River

Catchment area of Derinöz River is about 120 km^2 and the altitude is 650 m. Derinöz River merges with Tersakan River downstream of Çatak Village.

3.1.2. Stream Gauges and Catchments

In this study, name of catchments was determined according to name of the stream gauges which are placed outlet of the catchments. General information about stream gauges is given Table 3.1. River network whose catchment area are above 2 km^2, spatial distribution of stream gauges and catchments were given in Figure 3.2.

Geographically, we divided stream gauges and catchments into 4 groups. The stream gauges and catchments 14-19, 14-20, 14-11, 14-14, 14-42 and 1419 are located at the north of the Yeşilırmak Basin. These catchments are on Havza, Derinöz, Ladik, Kürtün, Abdal and Çekerek River respectively. Area range of catchments changes between 52.60 and 513.20 km^2. At the middle and east of the Yeşilırmak Basin, there are 14-32, 14-15, 1418, 1422, 1423 and 1401. This stream gauges and catchments are generally on Yeşilırmak and Çekerek River. Area range of catchments changes between 94.10 and 1048.80 km^2. Stream gauges 14-78, 14-50, 14-88, 14-26, 14-23, 1426 and 1412 are found at the west of Yeşilırmak Basin. Catchment area of this stream gauges changes from 129.40 to 3668.80 km^2. At the south of Yeşilırmak Basin stream gauges 14-29, 14-62, 14-46, 14-75, 14-93, 14-83, 14-95, 14-80, 14-92, 14-102, 1424 and 1409 are found. Hydrograph and flow duration curves of these catchments are given in 3.3-3.6.

Table 3.1. General Information about Stream Gauges

Station No	Organisation	River	Station	Drainage Area (km^2)	Approximate Elevation	Coordinates
14-11	DSİ	Ladik Gölü	Regülatör Çıkışı	145.10	862	35°59'36.134"E 40°55'13.865"N
14-14	DSİ	Kürtün Çayı	Ahullu	259.00	140	36°11'43.394"E 41°17'7.541"N
14-15	DSİ	Çobanlı D.	Roski	725.50	1307	38°34'41.763"E 40°0'31.899"N
14-19	DSİ	Havza Çayı	Havza	52.60	615	35°39'15.405"E 40°58'51.19"N
14-20	DSİ	Derinöz Deresi	Çatak	102.40	653	35°39'42.428"E 40°54'37.497"N
14-23	DSİ	Mecitözü Çayı	Kaleboğazı	504.80	504	35°33'34.113"E 40°33'4.935"N
14-26	DSİ	Salhan Çayı	Çaybaşı	420.40	634	35°23'39.77"E 40°42'41.095"N
14-29	DSİ	Çelikpınar S	Karamağara Yay.	6.80	1155	35°30'30.124"E 39°40'7.821"N
14-32	DSİ	Çilkoru Deresi	Gökdere	94.10	734	36°44'55.282"E 40°28'29.708"N
14-42	DSİ	Aptal ırmağı	Dikbıyık	502.50	10	36°35'8.4"E 41°13'29.427"N
14-46	DSİ	Hazan Deresi	Bedirkale	72.50	1127	36°27'15.479"E 40°3'44.41"N
14-50	DSİ	Düvenci D.	Fidanlık	150.40	1031	35°13'50.135"E 40°42'2.82"N
14-62	DSİ	Sarsı Deresi	Artova	21.50	1242	36°16'25.794"E 40°6'53.912"N
14-75	DSİ	Söğütözü D.	B. Söğütözü	100.40	973	34°50'37.147"E 40°6'49.821"N
14-78	DSİ	Hatip Ç.	Babaoğlu	129.40	856	34°48'0.149"E 40°21'57.821"N
14-80	DSİ	Gündelen ç	Kızıllı	338.60	1193	36°2'18.107"E 39°47'51.82"N
14-83	DSİ	Bahçebaşı D.	Bahçebaşı	179.80	616	36°5'1.147"E 40°13'58.704"N
14-88	DSİ	Gümüşsuyu	Hanköy	317.70	622	35°20'35.789"E 40°49'36.682"N
14-92	DSİ	Germuga	Ekecik	477.70	1151	36°2'51.69"E 39°53'57.915"N
14-93	DSİ	Sarayözü d	Karamağara Yay.	138.00	1004	35°32'19.123"E 39°46'3.821"N
14-95	DSİ	Akdağmadeni S	İbrahimağa Ç.	212.40	1094	35°54'58.111"E 39°46'14.82"N
14-102	DSİ	Hotan Çayı	Bağlarpınarı	613.00	545	36°0'55.813"E 40°19'53.503"N
1401	EIE	Kelkit Ç.	Fatl•	10048.80	375	36°59'56"E 40°28'41.999"N
1409	EIE	Çekerek Ç.	Akcakecili	5267.60	730	35°38'8.999"E 40°9'46.001"N
1412	EIE	Çorum Çat	Seyhoglu Kop.	3668.80	530	35°25'3"E 40°27'6.001"N
1418	EIE	Yeşilırmak	Gömeleönü	1608.00	820	37°7'43"E 40°18'42.001"N
1419	EIE	Tersakan Ç.	Havza	513.20	630	35°39'59"E 40°57'37.001"N
1422	EIE	Kelkit Ç	Çiçekbükü	1714.00	1350	39°18'42.001"E 40°6'45"N
1423	EIE	Kelkit Ç.	Akcaagil kop.	8302.80	725	38°2'44.999"E 40°13'44"N
1424	EIE	Çekerek Ç.	Çardak Köp.	1032.80	1040	36°8'47"E 40°0'29.002"N
1426	EIE	Alata Ç.	Cemilbey Köp.	1817.20	650	35°3'51.001"E 40°20'21.001"N

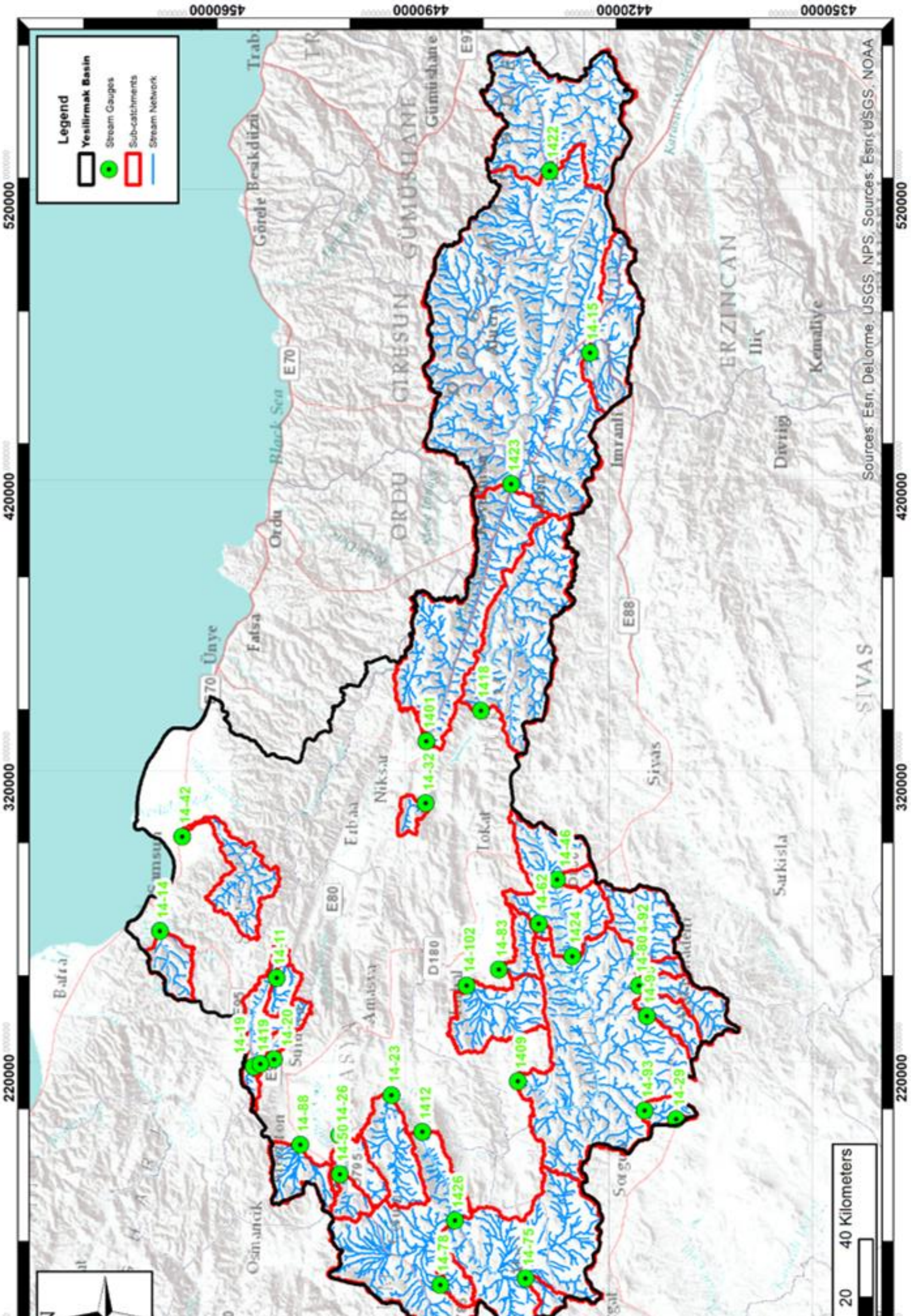

Figure 3.2. Stream Gauges and River Network Of Study Catchments

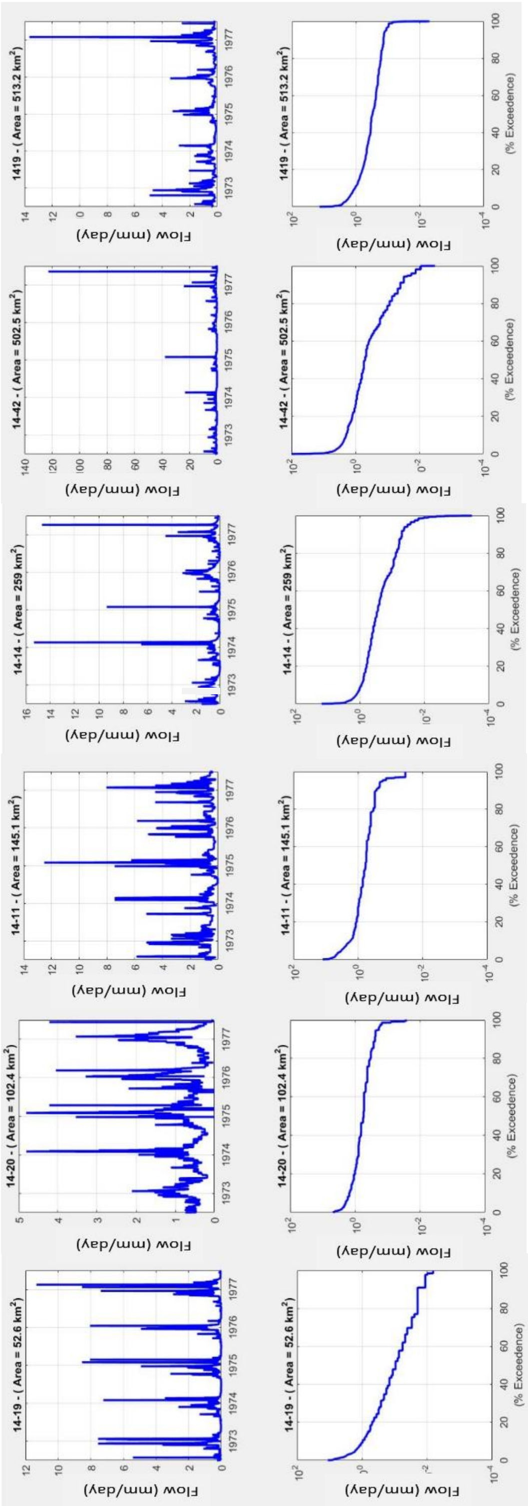

Figure 3.3. Hydrographs and Flow Duration Curves of Catchments Located at the North of Basin

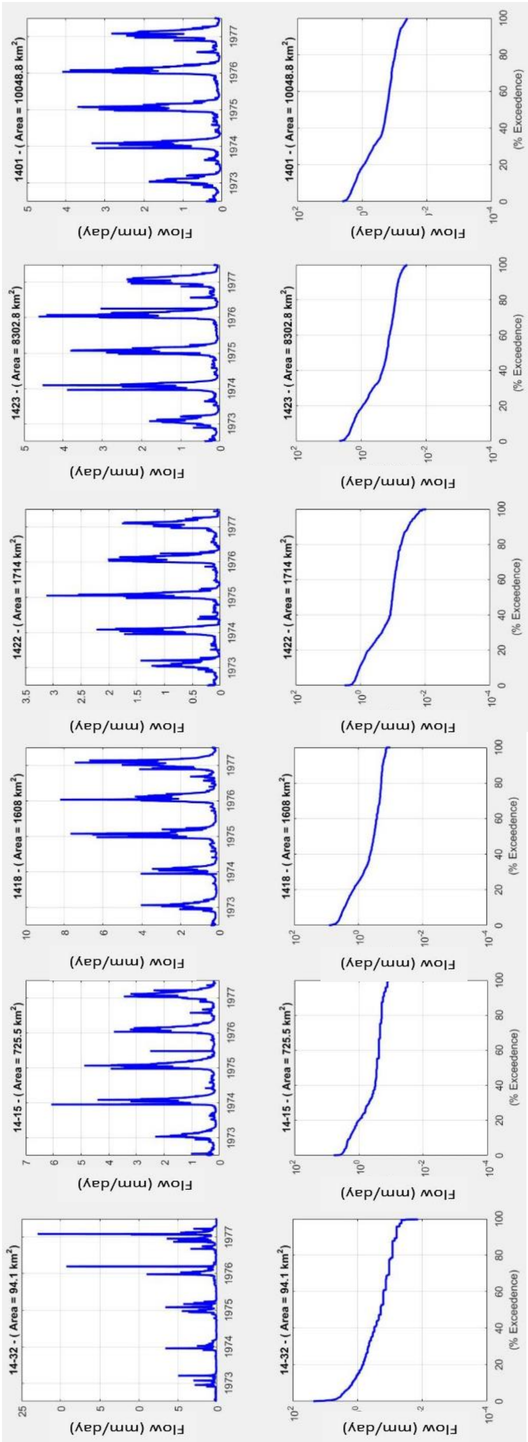

Figure 3.4. Hydrographs and Flow Duration Curves of Catchments Located at the Middle and North of Basin

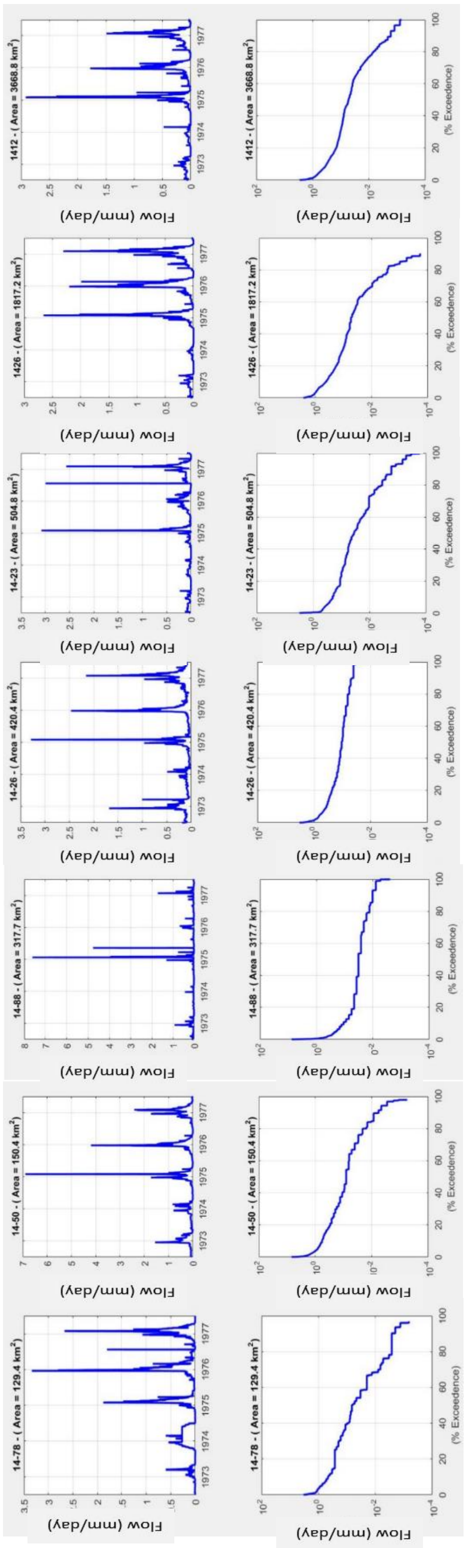

Figure 3.5. Hydrographs and Flow Duration Curves of Catchments Located at the West of Basin

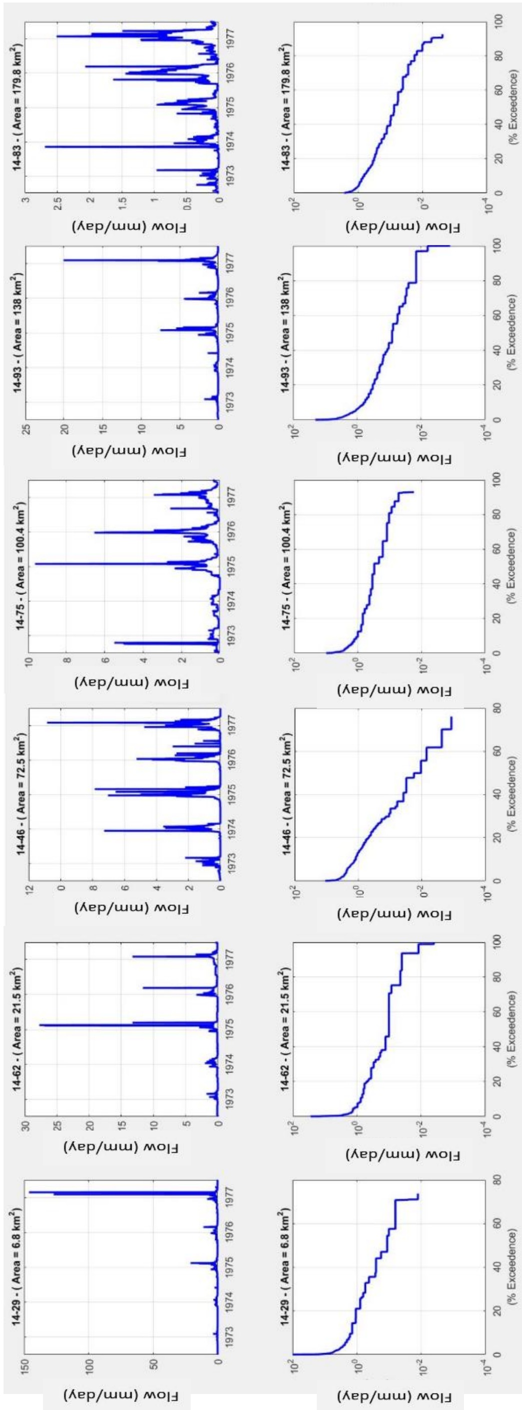

Figure 3.6. Hydrographs and Flow Duration Curves of Catchments Located at the South of Basin

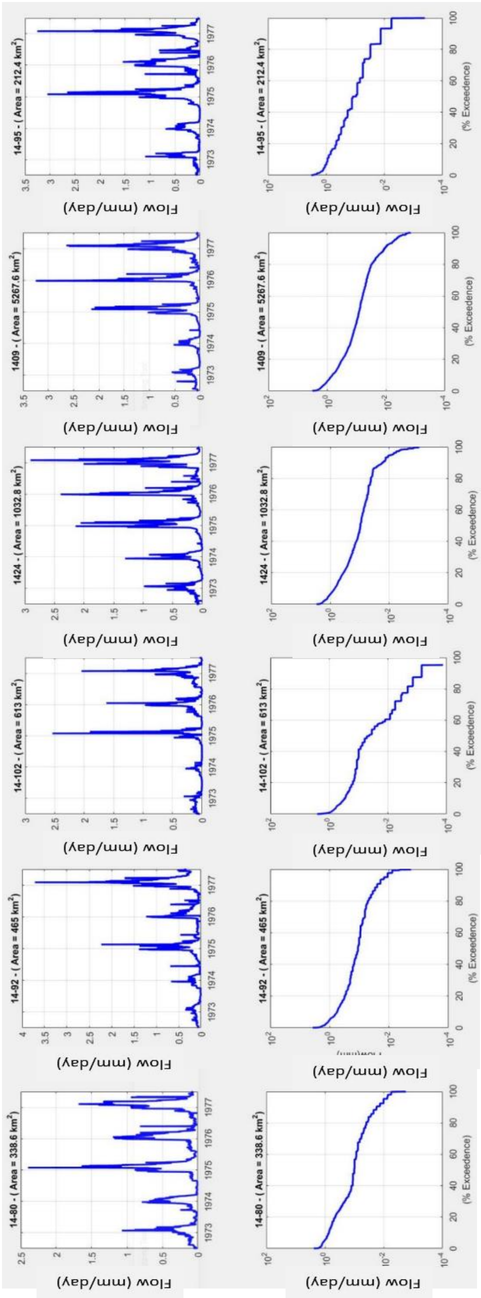

Figure 3.6 Cont’d

CHAPTER 4

GEOLOGY AND HYDROGEOLOGY

4.1. Regional Geology

The Yesilirmak Basin is spread over a very wide area and consists of very different geological formations depending on the tectonic evolution processes.

Therefore, presenting the definition of such a complex environment as a "geotectonic" model instead of stratigraphic geology seems to be a more understandable method for the reader. The geotectonical model works in this study are presented by compiling the works of (Okay, 2008) and (Yilmaz, 2004).

Turkey is divided into three major geological tectonic units, namely: (i) Pontides; (ii) Anatolid-Taurides and (iii) Arab Platform (Figure 4.1). The study area is located in the Sakarya Zone of the Pontides among these tectonic units. The Pontide continent is adjacent to the Anatolian-Taurid continental part through the Ankara-İzmir Suture Zone in the south. In the context of these tectonic relations, the following geological structures are present in the geotectonic model of the project area, mainly in a sequence from old to young: (Figure 4.2):

- Akdağmadeni Lithodem
- Tokat Massif (Karakaya Complex)
- Pontide Magmatic Belt
- Ankara-Erzincan Suture Belt

Along with the geologic products mentioned above of the paleo-tectonic evolution period, the following young units of the Neo-Tectonic period are included in the project area:

- Neogene Deposits

* Old and Young Alluviums

In the following sections, specific information about these geological structures that occurred during the tectonic evolution of Anatolia is presented by making quotations from previous studies.

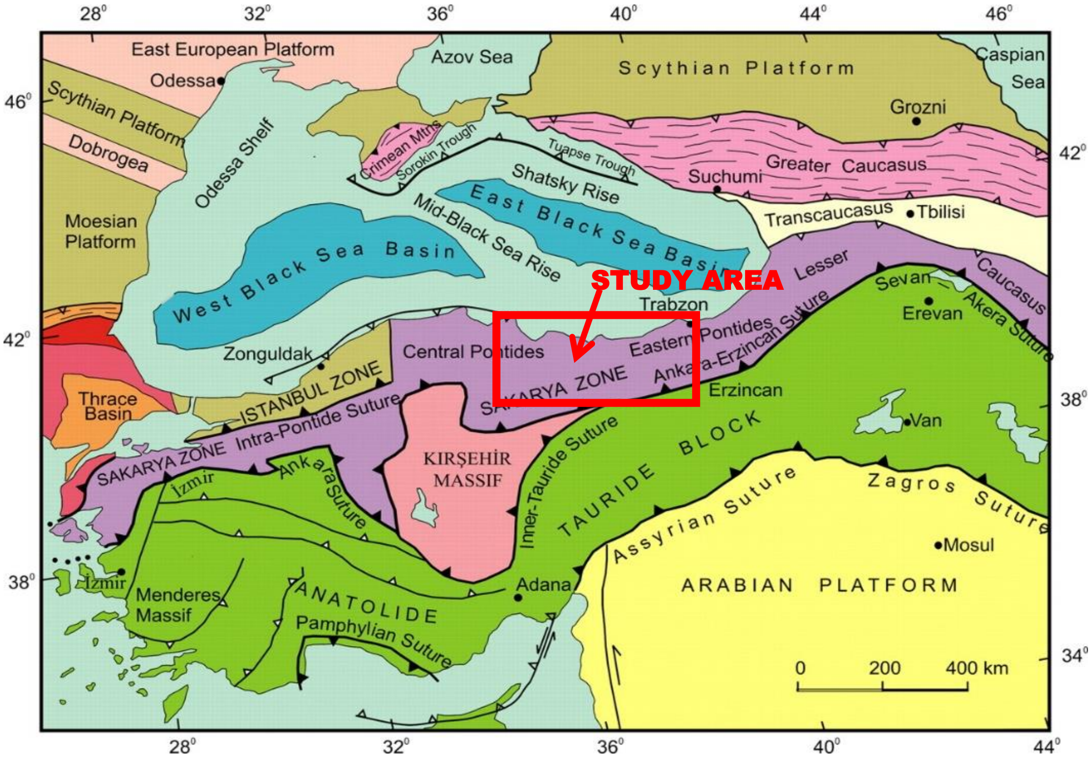

Figure 4.1. Tectonic map of northeastern mediterranean region showing the major sutures and continental blocks. Sutures are shown by heavy lines with the polarity of former subduction zones indicated by filled triangles. Heavy lines with open triangles represent active subduction zones (Okay and Tüysüz, 1999).

4.1.1. Akdağmadeni Lithodem

Akdağmadeni Lithodem is represented by metamorphic rocks is located at the south of Yesilirmak Basin near Akdağmadeni and Yıldızeli (Yilmaz et al., 1995). The formation is basement rock of Eocene units (Özcan et al., 1980). The unit consists mainly of gneiss, amphibolite and schist sequence; schist and marble, and intrusive rocks such as gabbro, granite, syenite, monzonite and tonalite which cut these rocks with metamorphic rocks such as marble and quartzite. It is also known that there is an Upper Cretaceous-Paleocene carbonate rocks located under the Eocene aged rocks and above the metamorphic rocks (Yilmaz and Özer, 1984).

4.1.2. Tokat Massif (Karakaya Complex)

The Tokat Massif is represented by metamorphic rocks in pre-Liassic age, which extends widely between Amasya and Reşadiye, in the western part of eastern Pontides. On the regional scale, the Tokat Massif can be correlated with the Karakaya Complex, which covers a very large area within the Sakarya Zone in the Western Pontides. Tokat Massif has been studied as Turhal Metamorphics and Devecidağı Complex in the study area (Yilmaz and Yilmaz, 2004).

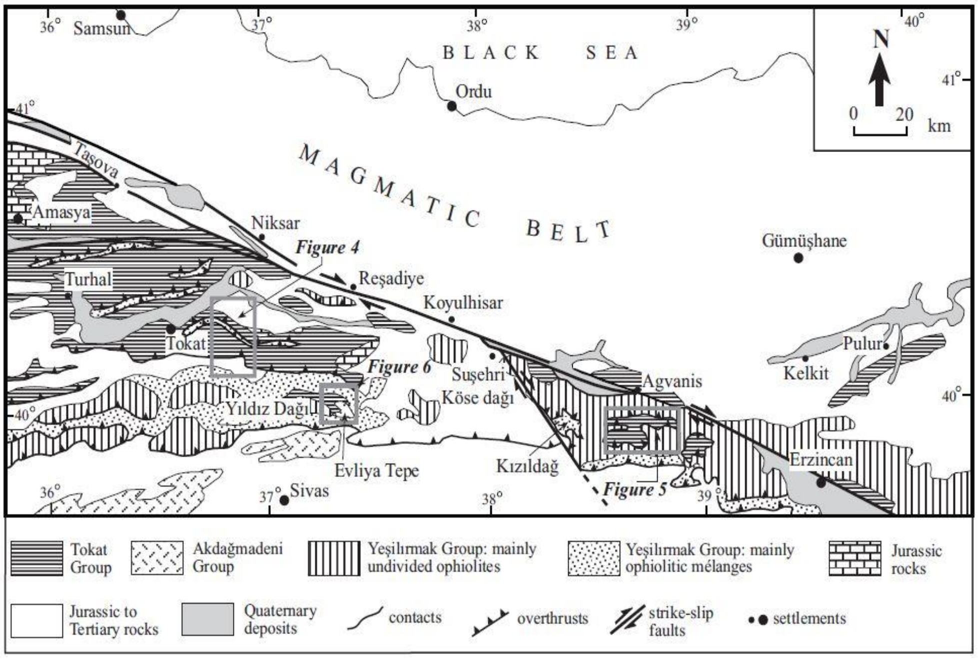

Figure 4.2. Simplified geological maps of the area between Tokat, Sivas and Erzincan (after Yilmaz 1980, 1982b; Özcan et al. 1980; Özcan and Aksay 1996; Yilmaz, 2004)

A: Turhal Metamorphics

The lower section of the unit consists of gneiss, amphibolite and mica schists; and the upper part consists of alternations of mica schist, phyllite, metaplastic, metabasic and marble levels. This alternation reflects the properties of an island-arc sequence (Yilmaz and Yilmaz, 2004).

B: Devecidağı Complex

This level which forms the southern part of the Tokat Massif, sometimes reflects the characteristics of the subduction, sometimes reflects the characteristics of fore-arc sequences. The metamorphic units forming the Tokat massif are also observed in the other parts of the eastern Pontides and along the North Anatolian Ophiolite Belt. These units were added as tectonic slices before the Late Campanian to the ophiolitic melange prism of the southern ophiolite belt. Some slices specific to the ophiolitic mélange prism of the Late Cretaceous age are located approximately D-B in the Tokat Massif (Yilmaz & Yilmaz, 2004).

Tectonic units called Tokat Massif in the study area are commonly called Karakaya Karmaşığı in the researches carried out in the Sakarya Zone in western Pontides since 1970's. The unit composed of rocks such as Triassic conglomerate, sandstone, quartzite, siltstone, slate, mudstone, radiolarite, spilitic basalt and diabase which had undergone low-grade metamorphism in Permo-Carboniferous limestone blocks by Bingöl et al. (1973) was named as Karakaya Formation.

In later studies, it was stated that the rock communities that were included in the definition of Karakaya Formation were scattered between the Tauride-Anatolid Platform and the Pontids in the Sakarya Zone mainly in the areas from the Biga Peninsula to Erzincan. This complex unit, which can be evaluated within the Kimmerid mountain ranges in terms of tectonic evolution, is divided into the formations which are named with different nomenclature in studies carried out by different researchers. The most well-known of these names are: (i) Emir formation, Ankara, Ortaköy Formation, Elmadağ Formation and Keçikaya Formation (Akyürek et al., 1984, 1996); (ii) Karakaya Complex's Nilüfer Unit, Hodul Unit, Çal Unit and Orhanlar Grovak Members (Okay et al., 1990, 1991; Levent and Okay, 1996).

4.1.3. Pontide Magmatic Suture

Kelkit Valley, which is extending in the direction of SE-NW between Suşehri and Taşova, flows in North Anatolian Fault Zone (NAFZ). The fault zone draws a sharp boundary between the Pontic Magmatic Belt and the Tokat Massif in this range. The contact of the Tokat Massif with the ophiolitic melange in the south is Ankara-Erzincan Suture Zone. In the north of NAFZ, there are volcanic rocks, all of which are the products of the "island-arc volcanism" of the Pontide Magmatic Belt, except in very limited areas. In the stagnation phase of volcanism, flysch rocks formed which are vertically-horizontally intercalated with that volcanic rocks. This Upper Cretaceous magmatic arc can be traced along the entire Black Sea coast from Georgia to Bulgaria. The most typical specimens are accompanied by calc-alkaline plutons in the magmatic island with a thickness of 2000 m, where deep marine lava and pyroclastics are observed in the Eastern Pontides. These geological formations are the backbone of the Eastern Black Sea Mountains (Bektaş et al., 1999).

According to the isotropic data obtained from the geological investigations carried out under the Plate Tectonics theory, in the Early Cretaceous northern subduction of İzmir-Ankara Ocean under the Pontides was continued. However, the development of the magmatic arc started from the Late Cretaceous to the late Paleocene and Eocene. Volcanic intercalated flysch sedimentary rocks were deposited in fore-arc (south) and back-arc (north) of this magmatic arc. The ages of volcanic, plutonic and flysch rocks, which are products of subduction zone tectonic activities, was determined from Upper Cretaceous to the Early Eocene. The geologic formations predominantly exhibiting flysch characteristics in the north and south parts of the magmatic arc have very complex structures at the regional scale; so, at this stage of the study, only the general descriptions showing typical characteristics are presented:

- Starting from the east of Samsun to the Niksar region in the SE and extending to the eastern parts of Tokat, Middle-Upper Eocene basalt, andesite, tuff, tuffite, agglomerate, sandstone and siltstone.
- Middle-Upper Eocene andesite, basalt and spilite lavas that show a very long interval east and west of Almus Dam.
- Upper Cretaceous sandstone, mudstone, clayey limestone in the SE-NW direction along the Kelkit Stream to the north of Reşadiye.

4.1.4. Ankara - Erzincan Suture

The ophiolites, which are the product of the subduction zones, are rock masses called "subduction zone complexes" that overlie the oceanic crust and upper mantle during subduction and are overlaid on the continental side. Within the ophiolite unit, mega-olistholith-bearing limestones, which come off from the carbonate platform during the closure of the oceans and / or during large-scale drifting faults, are frequently observed. The formation of olistoliths is related to the northward divergence of the Ankara-Erzincan Ocean beginning in the late Cretaceous. The northward displacement of this ocean collided with the Pontides of the Anatolide-Taurid continent and merged along the Ankara-Erzincan Kenet Zone. In the south of Tokat, there are ophiolitic masses which are containing E-W oriented limestone olistolithes. These masses are outcropped in Koyulhisar and in the narrow areas around Suşehri. Some slices specific to the ophiolitic melange prism of the Late Cretaceous age are located in the E-W direction in the Tokat Massif (Okay, 2008).

4.1.5. Neogene Deposits

According to Yilmaz and Yilmaz (2004) and Yilmaz et al. (1997) the areas where the neogene sediments are heavily exposed are listed below with their main headings, covering the study area from Çarşamba to downstream in study area.

A: Çarşamba Plain:

These young terrestrial sediments were deposited in the southwest of Terme and south of Çarşamba. The thickness of delta zone of the units composed of loose cemented conglomerate, sandstone, claystone and marl layers reaches 100-150 m. In most areas these units extend into the Black Sea with gentle inclination; while the plain is usually covered with old and young alluvium.

B: Erbaa – Tasova Region:

The thickest and widespread part of the Neogene sediments in the Yeşilırmak Basin is observed in the Erbaa-Tasova region. The young rocks formed by erosion from the mountains around these plains are composed of loose cemented conglomerate, sandstone and marl layers mainly of Pliocene age. According to previous studies, these units have lignite veins at some of these levels, reaching up to 500 m thick in the western part of the plains.

C: Almus Valley

In the previous studies, a Miocene formation, unconformably deposited on andesite and metamorphic schists, was found in the upper part of Yeşilırmak, in the south of Dünek Mountain in the east of Tokat, in Almus valley. Due to their tectonic relations, the Lower Tertiary age unit is mainly composed of red-green marl and marly sandstones and carbonated sandstones deposited on them.

D: Koyulhisar Region

Neogene deposits in this region are formed in a tectonic basin developing in andesites just like in Almus valley. According to some tectonically related interpretations of some researchers, these deposits may be temporally related to the Neogene units in the region of Almus and the Ağvanis region in the SE. Light colored carbonate layers are observed as the most prominent rock in these sediments.

1/100000 scale Geological Map of the Yeşilırmak basin is given in Figure 4.3.

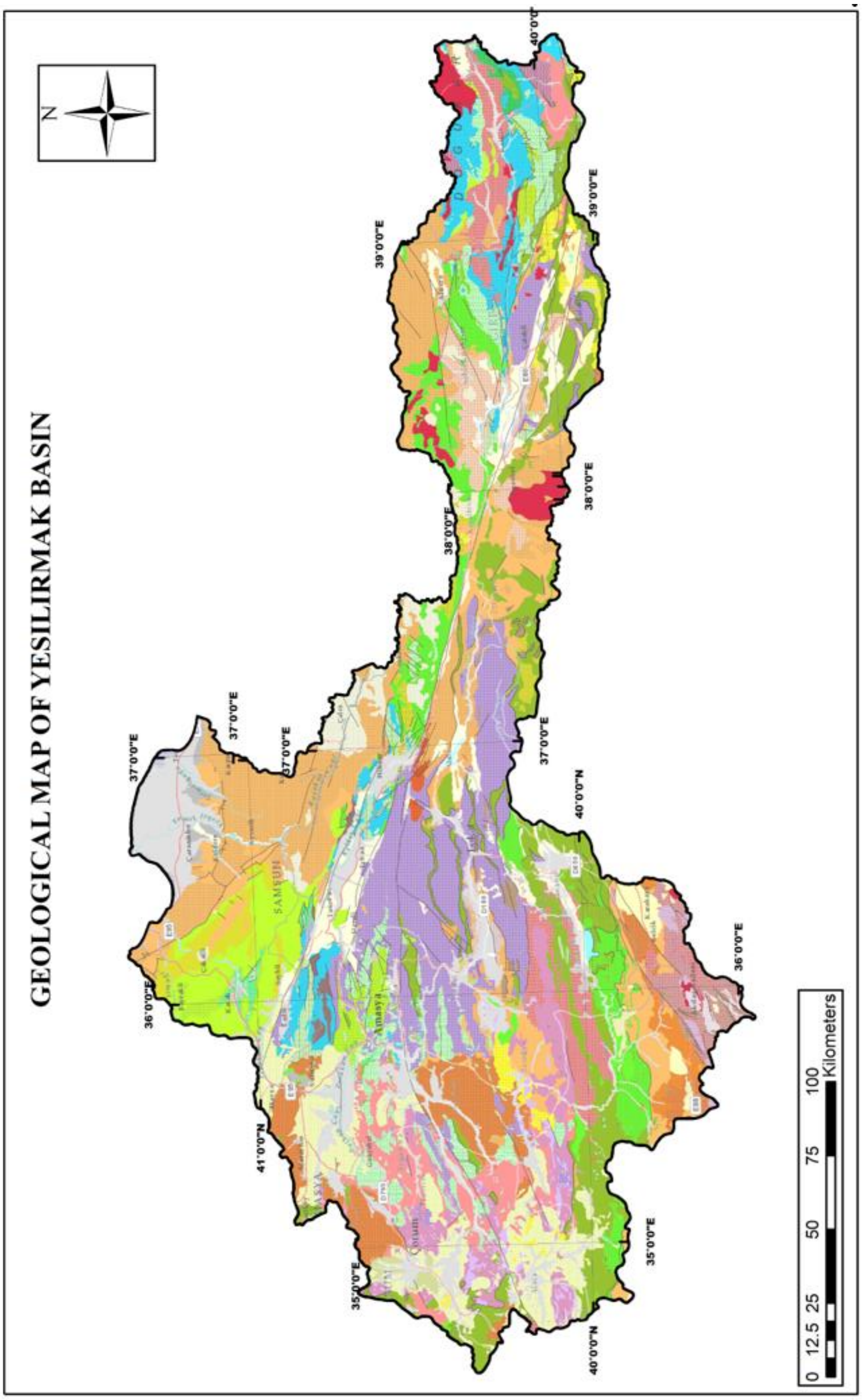

Figure 4.3. Geological Map of Yeşilırmak Basin (Akbaş et al., 2013).

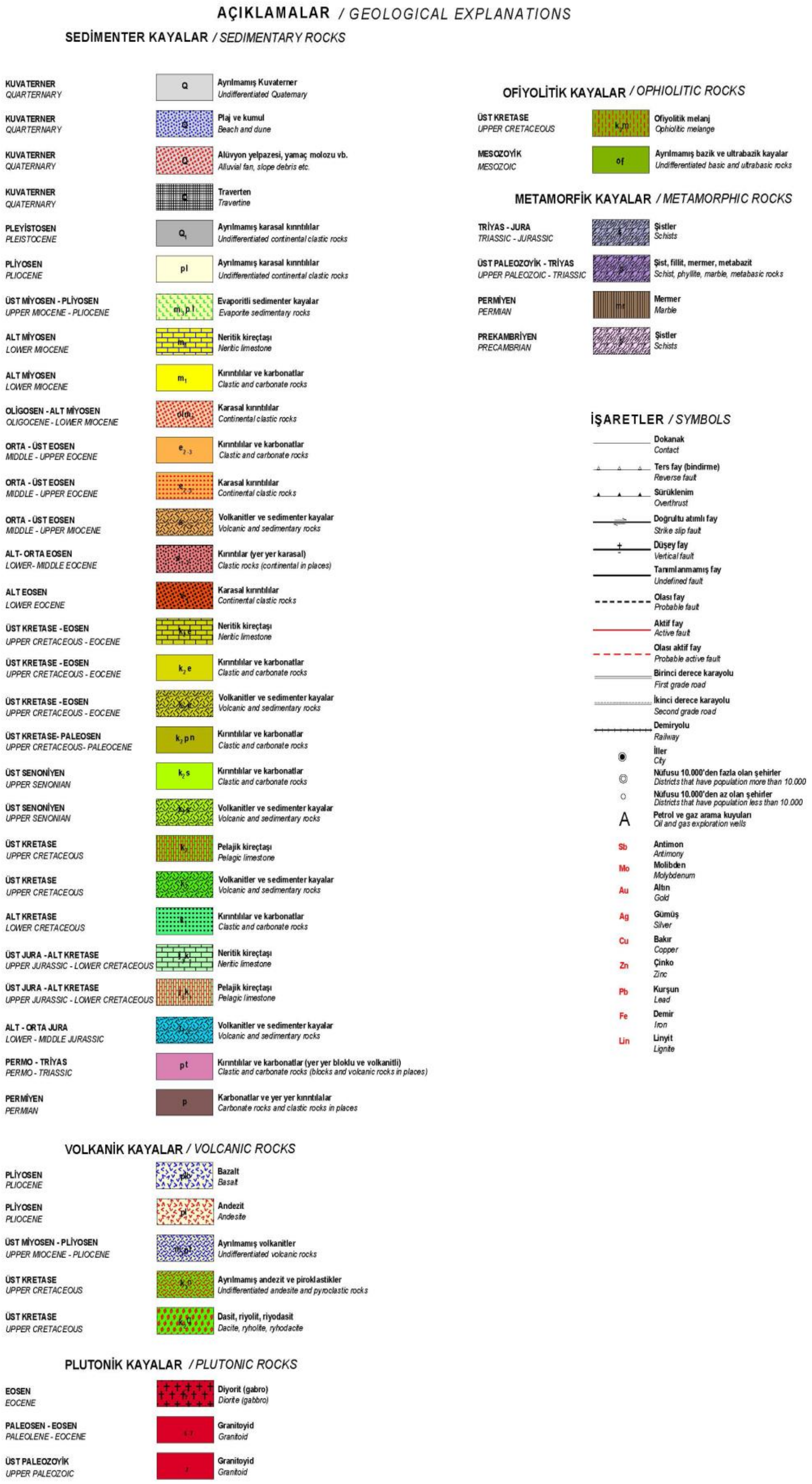

Figure 4.3 Cont'd

E: Eastern Part of Suşehri

In the wide plains between the Susahri and the east of Refahiye there are very gravelly loosely attached sandstone dominated by shallow marine sediments and young sediments of conglomerate-claystone intercalation.

F: Old and Young Alluvium

In the southern part of the Çarşamba and Terme plains, old and young alluviums of 20-25 m high, mainly consisting of sand-gravel, occupy large areas. These alluvial deposits are usually deposited in depressions formed by vertical (normal) and pull-apart faults in the Yesilirmak and Kelkit valleys. The most important of these depression basins are; The Tokat basin is known as the Erbaa-Niksar Depression and the Suşehri Basin. Apart from some swamp areas on Çarşamba, all the deltas and plains that are known form fertile agricultural areas.

4.2. Geology of Study Area

In this part of the thesis, local geology of the study catchments is given based on Geological Map of MTA (Scale: 1/25000). In the procedure, geological formations of 31 catchments are classified and grouped according to their lithological properties. These lithologies are divided into 10 main groups: Alluvium (ALV), Clastic Rocks (C), Limestone (L), Mélanges (ML), Marbles (MR), Metamorphic Rocks (MT), Ophiolitic Mélanges (OML), Plutonic Rocks (P), Pyroclastic Rocks (PY) and Volcanic Rocks (V). In the following sections, the lithological properties of geological formations for each catchment is summarized. Area percentage of each of these geological classes are listed in Table 4.1 for each studied catchment.

Table 4.1. Area percentage (%) of geological classes in study catchments

Area Percentage (%) of Geological Classes										
Color Code in Geological Map of Study Area										
Catchment No.	**Alluvium**	**Clastics**	**Limestone**	**Melange**	**Marbles**	**Metamorphic Rocks**	**Ophiolitic Melanges**	**Plutonic Rocks**	**Pyroclastic Rocks**	**Volcanic Rocks**
14-11	29.41	14.91	13.49	0.00	0.00	0.37	0.64	0.00	41.17	0.00
14-14	0.60	49.66	30.43	0.00	0.00	0.00	0.00	0.00	0.00	19.31
14-15	4.58	29.67	4.99	0.00	3.28	12.90	40.89	0.00	3.06	0.64
14-19	1.63	74.70	23.66	0.00	0.00	0.00	0.00	0.00	0.00	0.00
14-20	1.61	25.94	60.25	0.00	0.00	0.00	0.00	0.00	11.22	0.98
14-23	5.26	62.10	14.54	13.87	0.00	4.22	0.00	0.00	0.00	0.00
14-26	13.44	24.20	28.79	1.35	0.00	0.05	0.10	0.00	0.00	32.07
14-29	0.00	73.28	0.00	0.00	26.72	0.00	0.00	0.00	0.00	0.00
14-32	4.77	14.53	0.00	0.00	0.00	79.04	0.00	0.00	1.67	0.00
14-42	4.37	56.70	27.10	0.00	0.00	0.00	0.00	0.07	1.68	10.08
14-46	3.71	6.73	3.92	0.00	0.00	0.00	85.65	0.00	0.00	0.00
14-50	23.62	1.80	2.38	0.00	0.00	0.00	0.01	0.00	0.00	72.19
14-62	0.00	0.00	8.65	10.68	0.00	0.00	21.94	0.00	58.73	0.00
14-75	11.25	15.41	10.94	20.69	0.00	0.00	41.71	0.00	0.00	0.00
14-78	3.26	22.29	10.88	46.58	0.00	0.00	16.91	0.00	0.00	0.08
14-80	2.85	10.90	0.00	0.00	3.53	81.05	0.00	0.00	1.67	0.00
14-83	5.83	1.49	13.73	53.45	0.00	0.00	0.03	0.00	25.46	0.00
14-88	13.32	42.86	4.63	3.53	0.00	0.00	0.33	0.00	0.00	35.33
14-92	7.06	42.25	0.18	0.00	10.72	24.03	1.82	0.00	13.94	0.00
14-93	0.00	68.57	0.00	0.00	9.96	0.00	0.00	0.00	17.02	4.45
14-95	0.21	7.34	0.00	0.00	9.12	76.81	0.00	0.00	6.53	0.00
14-102	17.65	12.82	13.08	11.97	0.00	8.36	0.36	0.00	28.56	7.20
1401	3.53	23.46	16.44	0.00	0.67	4.46	9.46	5.48	14.65	21.86
1409	6.69	20.26	5.75	0.67	2.76	12.92	23.09	0.00	25.73	2.14
1412	13.21	37.69	7.20	13.83	0.00	1.49	17.79	0.00	3.38	5.40
1418	1.92	24.33	2.83	0.00	2.23	29.22	20.32	2.60	9.29	7.25
1419	13.14	50.66	9.41	0.00	0.00	0.11	0.18	0.00	15.81	10.68
1422	4.50	20.43	22.65	0.00	0.65	5.66	7.96	10.66	19.56	7.94
1423	3.90	26.62	15.44	0.00	0.80	5.19	9.59	6.32	12.21	19.93
1424	12.82	13.55	5.26	1.32	0.14	0.54	54.95	0.00	11.42	0.00
1426	10.16	41.83	4.34	13.24	0.00	0.40	21.82	0.00	6.23	2.00

14-11

The basement rock of catchment is composed of Lower-Upper Permian aged limestones. From older to younger: Upper Permian-Lower Triassic metamorphic rocks, Lower-Middle Jurassic pyroclastic rocks, Middle Jurassic-Lower Cretaceous limestones, Upper Cretaceous ophiolitic mélanges, and Upper Cretaceous-Quaternary age-varying clastic rocks are overlying this formation. The youngest unit of the catchment is alluvium. The most dominant geological units in the catchments are pyroclastic rocks and alluvium.

14-14

The basement rock of catchment is composed of Upper Cretaceous volcanic rocks. Upper Cretaceous-Upper Paleocene clastic rocks and Upper Cretaceous -Paleocene limestone units are dominant in the catchment. In addition, the Upper Cretaceous volcanic rocks are rarely found in the catchment. The youngest unit of the catchment is alluvium.

14-15

There are Upper Paleocene-Pliocene Clastic rocks, Middle-Jurassic-Lower Cretaceous and Lower Miocene limestones, Upper Permian-Lower Triassic metamorphic rocks and marbles, Upper Cretaceous ophiolitic mélanges, Lower-Middle Eocene pyroclastic rocks and Middle Eocene volcanic rocks in catchment 14-15. Ophiolitic mélanges and clastic rocks are the most dominant rock type in the catchment. Basement rocks of the catchment are composed of Upper Permian-Lower Triassic metamorphic rocks. The youngest unit of the catchment is alluvium.

14-19

In this catchment, Quaternary alluvial units are the youngest, Middle-Upper Eocene volcanic rocks are the oldest units. The most dominant rock types are the clastic rocks.

14-20

Quaternary alluviums, Lower Eocene-Quaternary clastic rocks, Lower Permian-Upper Cretaceous age limestones, Lower-Middle Jurassic pyroclastic rocks and Middle-Upper Eocene volcanic rocks are found in the catchment 14-20. The Upper and Lower Permian aged limestones are the main rocks of the catchment. The youngest unit of the catchment is alluvium. Limestones are the most dominant rock type in the catchment.

14-23

In catchment 14-23, there are Quaternary alluviums, Lower Eocene-Pliocene clastic rocks, Lower Triassic-Upper Cretaceous limestones, Lower-Upper Triassic Mélanges and Upper Permian-Lower Triassic metamorphic rocks. The basement rocks of the catchment are Permian-Lower Triassic metamorphic rocks. The youngest unit of the catchment is alluvium. The most dominant units in the catchment are clastic rocks.

14-26

Quaternary alluvium, Lower Eocene-Quaternary clastic rocks, Lower Triassic-Lower Cretaceous limestones, Lower-Upper Triassic mélanges, Upper Permian-Lower Triassic metamorphic rocks, Upper Cretaceous ophiolitic mélanges and Middle-Upper Eocene volcanic rocks are found in the catchment. Oldest units of the catchment are Upper Permian-Lower Triassic metamorphic rocks. The youngest unit of the catchment is alluvium. The most dominant units in the catchment are volcanic rocks and limestone.

14-29

In catchment 14-29, there are the youngest Upper-Middle Eocene clastic rocks and oldest Upper Permian-Lower Cretaceous marbles. The most dominant rock type of the catchment is clastic rocks.

14-32

Quaternary alluviums, Upper Paleocene-Pliocene clastic rocks, Upper Permian-Lower Triassic metamorphic rocks and Middle Eocene pyroclastic rocks are found in the catchment 14-32. The oldest units in the catchment are metamorphic rocks, youngest units in the catchment are alluviums. The most dominant rock type of the catchment are metamorphic rocks.

14-42

In catchment 14-42, there are Quaternary alluviums, Upper Cretaceous-Pliocene clastic rocks, Upper Cretaceous-Paleocene limestones, Lower Miocene plutonic rocks, Middle Eocene pyroclastic rocks, Upper Cretaceous - Middle Eocene volcanic rocks. Upper Cretaceous limestones and volcanic rocks are the oldest units in the catchment. The youngest unit of the catchment is alluvium. The most dominant rock type of the catchment are clastic rocks and limestones.

14-46

In the catchment 14-46, the most dominant rock type is Upper Cretaceous ophiolitic mélanges. Lower-Upper Triassic limestones are the oldest units of the catchment. The youngest unit of the catchment is alluvium. There are also Miocene-Pliocene clastic rocks in the catchment.

14-50

There are Quaternary alluviums, Lower-Middle Eocene clastic rocks, Lower Triassic-Lower Cretaceous Limestones, Upper Cretaceous ophiolitic mélanges and Middle-Upper Eocene volcanic rocks in the catchment 14-50. The most dominant rock type of the catchment is volcanic rocks.

14-62

In catchment 14-62, there are Middle Jurassic-Lower Cretaceous limestone, Lower-Upper Triassic mélanges, Upper Cretaceous ophiolitic mélanges and Middle Eocene pyroclastic rocks. The most dominant rock type of the catchment are pyroclastic rocks.

14-75

There are Quaternary alluviums, Upper Cretaceous-Pliocene clastics, Lower-Upper Triassic limestones and mélanges, and Upper Cretaceous ophiolitic mélanges in catchment 14-75. The most dominant unit of the catchment is ophiolitic mélanges.

14-78

Quaternary alluviums, Upper Miocene-Pliocene clastic rocks, Lower-Upper Triassic limestones and mélanges, Upper Cretaceous ophiolitic mélanges and Upper Eocene - Miocene volcanic rocks are found in catchment in 14-78. The oldest units of the catchment are Lower-Upper Triassic limestones and mélanges. The most dominant rock type of the catchment is mélanges.

14-80

There are Quaternary alluviums, Lower Miocene-Pliocene clastic rocks, Paleozoic marble and metamorphic rocks and Upper Cretaceous-Paleocene pyroclastic rocks in catchment 14-80. The most dominant rock type of the catchment are metamorphic rocks

14-83

In catchment 14-80, there are Quaternary alluviums, Middle-Upper Eocene clastic rocks, Lower-Upper Triassic limestones and mélanges, upper cretaceous ophiolitic mélanges and middle Eocene pyroclastic rocks. The youngest unit of the catchment is alluvium. The oldest unit of the catchment are limestones and mélanges. The most dominant rock type of the catchment is mélanges.

14-88

In catchment 14-88, the most dominant units are clastic rocks and volcanic rocks. There are also Quaternary alluviums, Lower Triassic-Upper Cretaceous limestone, Lower-Upper Triassic mélanges, Upper Cretaceous ophiolitic mélanges and Upper Cretaceous-Upper Eocene volcanic rocks in the catchment.

14-92

Quaternary alluviums, Upper Cretaceous-Quaternary clastic rocks, Upper Cretaceous limestones, Paleozoic marbles and metamorphic rocks, upper cretaceous ophiolitic mélanges and Upper Cretaceous-Paleocene pyroclastic rocks. The most dominant units of the catchment are clastic rocks.

14-93

The most dominant unit of the catchment 14-93 are clastic rocks. There are also Upper Permian-Lower Cretaceous marbles, Upper Cretaceous-Paleocene pyroclastic rocks and Pliocene volcanic rocks are found in catchment 14-93.

14-95

There are Quaternary alluviums, Lower-Middle Eocene clastic rocks, Paleozoic-Lower Cretaceous marbles and metamorphic rocks and Upper Cretaceous-Paleocene pyroclastic rocks are found in catchment 14-95. The most dominant unit of the catchment 14-95 are metamorphic rocks.

14-102

In catchment 14-102, there are Quaternary alluviums, Upper Cretaceous-Pliocene clastic rocks, Lower Permian-Lower Cretaceous limestones, Lower-Upper Triassic mélanges, Upper Permian-Lower Triassic metamorphic rocks, Upper Cretaceous ophiolitic mélanges, Middle Eocene pyroclastic rocks and Lower-Upper Triassic volcanic rocks. The most dominant unit of the catchment 14-102 are pyroclastic rocks.

1401

The most dominant rock types of the catchment are clastic and volcanic rocks. There are also Quaternary alluviums, Middle Jurassic-Lower Miocene limestones, Paleozoic-Lower Triassic marbles, Upper Permian-Lower Triassic metamorphic rocks, Upper Cretaceous ophiolitic mélanges, Upper Cretaceous-Upper Eocene plutonic rocks, Lower Jurassic-Middle Eocene pyroclastic rocks and -Upper Cretaceous-Pleistocene volcanic rocks.

1409

In catchment 1401, there are Quaternary alluviums, Upper Cretaceous-Pliocene clastic rocks, Lower Permian-Upper Cretaceous limestones, Lower-Upper Triassic mélanges, Paleozoic-Lower Cretaceous marbles and metamorphic rocks, Upper Cretaceous ophiolitic mélanges, Upper Cretaceous pyroclastic rocks, Lower Triassic-Pliocene volcanic rocks. The most dominant unit of the catchment are pyroclastic and clastic rocks.

1412

There are Quaternary alluviums, Upper Cretaceous-Pliocene clastic rocks, Lower Permian-Upper Cretaceous limestone, Lower-Upper Triassic mélanges, Lower Permian-Upper Triassic metamorphic rocks, Upper Cretaceous ophiolitic mélanges, Upper Cretaceous-Middle Eocene pyroclastic rocks and Lower Triassic-Miocene volcanic rocks. The most dominant units in the catchment are clastic rocks.

1418

The most dominant rock type of the catchment is metamorphic rocks. There are also Quaternary alluviums, Upper Cretaceous-Lower Miocene clastic rocks, Lower Permian-Paleocene limestones, Lower Permian-Lower Triassic metamorphic rocks and marbles, Upper Cretaceous ophiolitic mélanges, Upper Cretaceous-Upper Eocene plutonic rocks, Middle Eocene pyroclastic rocks and Lower Eocene-Upper Pliocene volcanic rocks in catchment 1418. The most dominant unit of the catchment are metamorphic rocks.

1419

There are Quaternary Alluviums, Upper Cretaceous-Quaternary clastic rocks, Lower Permian-Upper Cretaceous limestones, Upper Permian-Lower Triassic, Upper Cretaceous ophiolitic mélanges, Lower-Middle Jurassic, pyroclastic rocks and Middle Eocene-Miocene volcanic rocks in catchment 1419. The most dominant unit in the catchment are clastic rocks.

1422

The most dominant units in catchment 1422 are limestone and clastic rocks. There are also Quaternary alluviums, Paleozoic-Lower Triassic marbles and metamorphic rocks, Upper Cretaceous ophiolitic mélanges, Upper Cretaceous-Paleocene plutonic rocks, Lower-Middle Jurassic pyroclastic rocks and Upper Cretaceous-Miocene volcanic rocks in the catchment.

1423

In catchment 1423, there are Quaternary alluviums, Lower Permian-Quaternary clastic rocks, Upper Cretaceous-Lower Miocene limestones, Upper Permian-Lower Triassic marbles and metamorphic rocks. Upper Cretaceous ophiolitic mélanges, Upper Cretaceous-Paleocene plutonic rocks, Lower-Middle Jurassic pyroclastic rocks and Upper Cretaceous-Pleistocene volcanic rocks. The most dominant units in catchment 1423 are clastic rocks.

1424

The most dominant rock in catchment 1424 are ophiolitic mélanges. Quaternary alluviums, Lower Triassic-Upper Cretaceous limestones, Lower-Upper Triassic-mélanges, Paleozoic-Lower Triassic marbles and metamorphic rocks and Upper Cretaceous-Middle Eocene pyroclastic rocks are also found in catchment 1424.

1426

In catchment 1426, there are Quaternary alluviums, Upper Cretaceous-Pliocene clastic rocks, Lower-Upper Triassic melanges and metamorphic rocks, Upper Cretaceous ophiolitic melanges and pyroclastic rocks, and Lower-Upper traissic volcanic rocks. The most dominant rock unit in catchment is clastic rocks.

Spatial distribution of the geological units within catchments are given in Figure 4.4.

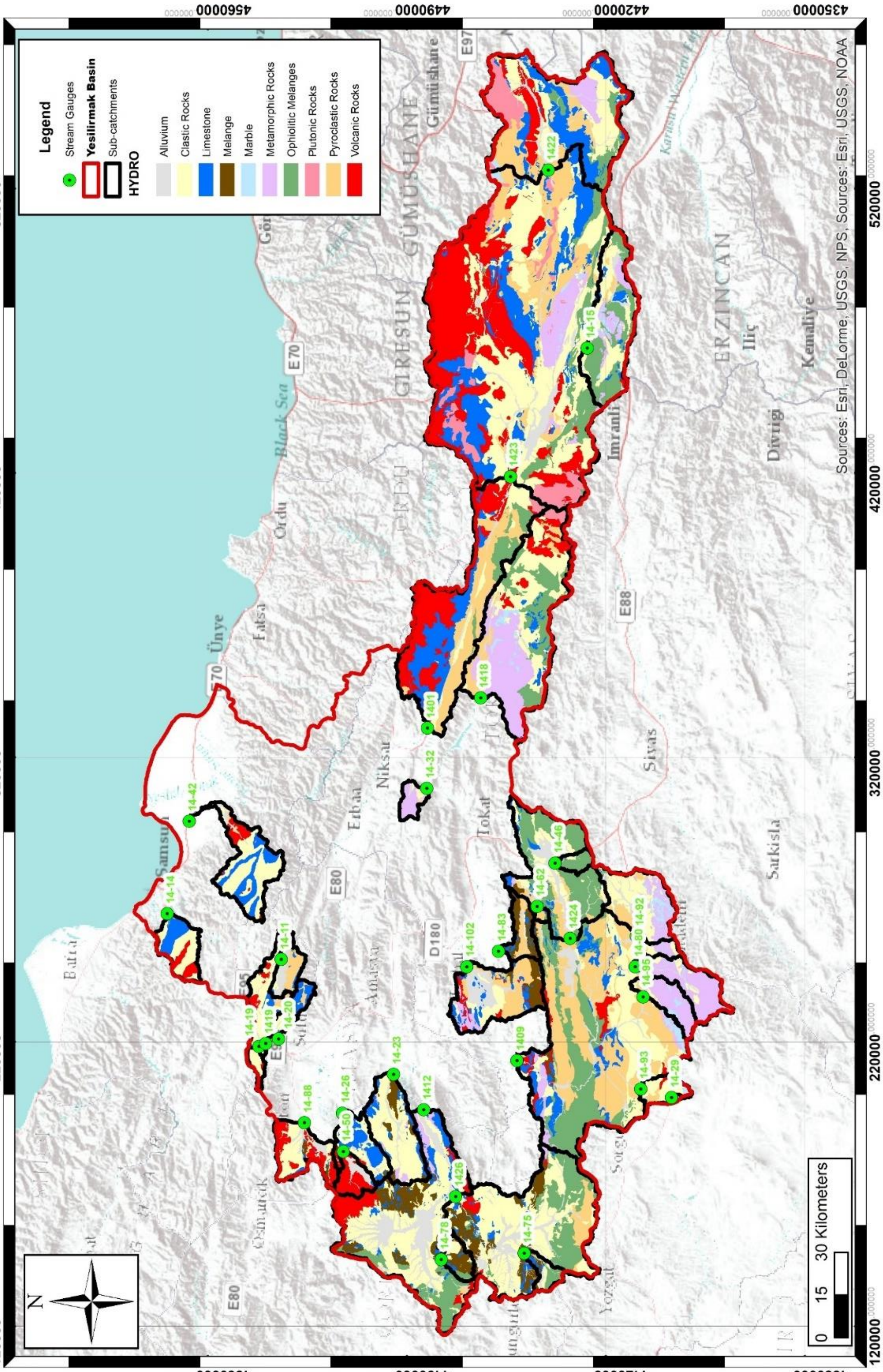

Figure 4.4. Geology of Study Catchments.

4.3. Regional Hydrogeology

At this stage of the study hydrogeological conditions is presented in a very general approach and under regional scale of geological formations.

Akdağmadeni Lithodem

As mentioned in Geology section above, Akdağmadeni Lithodem consists of gneiss, amphibolite and schist sequence; schist and marble, and intrusive rocks such as gabbro, granite, syenite, monzonite and tonalite. According to Aydın and Ekmekci (2005) marbles located near the Sızır (Sivas) are permeable units. Metamorphic rocks such as gneiss, amphibolite and schist are generally impermeable units. Similarly, intrusive rocks such as gabbro, granite, syenite etc. are also hydrogeologically impermeable units unless secondary porosity is developed through fracture system. However, these rocks can hold limited water related to secondary porosity.

Tokat Massif (Karakaya Complex)

Within the Tokat Massif are the units capable of carrying water: (i) olistolith limestone blocks of varying sizes within the complex; (ii) Jurassic limestone masses that represent a separate sedimentation level within the massif.

The age of the olistolith and karstic limestone blocks is generally determined as Permian. Depending on the tectonic activities on the continental margins, the size of these masses, which fall into the trench in the subduction zone and are transported by thrust faults, can vary. The units are covered by impermeable schist, so it contains limited water. These waters can only discharge in the topographic environment where the limestone is directly exposed.

Pontide Magmatic Belt

Basaltic, andesitic and rhyolitic lavas forming the backbone of the Pontide Magmatic Belt are practically impermeable. The sandstones, conglomerates and limestone levels of flysch unit, are permeable. Water discharges in these units are mostly through fountains. Apart from these geological occurrences, there are limestone masses that have been deposited in the prolonged stagnation phases of the volcanism and reaching large dimensions. These masses, which give their typical facies to the left bank of the Yeşilırmak valley in Amasya, do not have very pronounced karstic cavities because they are micritic.

Ankara - Erzincan Suture

The geological units in this belt are intertwined with each other due to compression tectonics and are accretionary complex. In the context of formation conditions, dominant rock types are peridotites, serpentines and ophiolitic complexes which are composed of volcanic and sedimentary rocks. These masses are impermeable. In the ophiolitic complex, there are also karstic limestones of different ages and sizes, separated from carbonate platforms and falling in mass and/or transported with mass; most of the springs can be discharged. In the ophiolitic complex, there are also karstic limestone blocks which breaks from the carbonate platform.

Neogene Deposits

A: Çarşamba Plain:

These units composed of loosly cemented conglomerate, sandstone, claystone and marl layers. Sandstone and conglomerate units are permeable, but claystone and marl layers can be described as impermeable in study area.

B: Erbaa – Tasova Region:

Similar to the Çarşamba Plain, Pliocene aged conglomerate, sandstone and marl units are dominant rocky types near the Erbaa – Taşova Region. Conglomerate and sandstone units are permeable units, but marl is impermeable in study area.

C: Almus Valley

In Almus Valley, red-green marl and marly sandstone and carbonated sandstones deposited. These units can be described as semi-pervious.

D: Koyulhisar Region

Light colored carbonate layers are observed as the most prominent rock in Koyulhisar Region. These rock units can be described as pervious.

E: Old and Young Alluvium

These units can be described as loosely cemented clay, silt, sand and gravel deposits in study area. They have been transported by rivers and accumulated in especially flat areas in the study area. Alluvial deposits are permeable and show aquifer properties.

4.4. Hydrogeology of Study Area

As mentioned in section 4.2, geological formations are divided into 10 main groups. In these groups alluvium, volcanic rocks and carbonate rocks (marbles and limestones) are important aquifers which can control the baseflow behavior of the catchments. For that reason, alluvium, volcanic and carbonate rocks area percentages were used in this study (Table 4.2 and Figure 4.5). Catchments with the highest area percentage of alluvium are 14-11 and 14-50. Moreover, carbonate rocks dominant catchments are 14-14, 14-20, 14-26, 14-29, 14-42 and 1422. On the other hand, Volcanic rocks dominant catchments are 14-14, 14-26, 14-72, 14-88 and 1401.

Table 4.2. Hydrogeologically Important Units in Study Catchments

Area Percentage (%) of Hydrogeologically Important Units			
Color Codes in Hydrogeological Map			
Catchment No.	Alluvium	Carbonate Rocks	Volcanic Rocks
14-11	29.41	13.49	0.00
14-14	0.60	30.43	19.31
14-15	4.58	8.27	0.64
14-19	1.63	23.66	0.00
14-20	1.61	60.25	0.98
14-23	5.26	14.54	0.00
14-26	13.44	28.79	32.07
14-29	0.00	26.72	0.00
14-32	4.77	0.00	0.00
14-42	4.37	27.10	10.08
14-46	3.71	3.92	0.00
14-50	23.62	2.38	72.19
14-62	0.00	8.65	0.00
14-75	11.25	10.94	0.00
14-78	3.26	10.88	0.08
14-80	2.85	3.53	0.00
14-83	5.83	13.73	0.00
14-88	13.32	4.63	35.33
14-92	7.06	10.90	0.00
14-93	0.00	9.96	4.45
14-95	0.21	9.12	0.00
14-102	17.65	13.08	7.20
1401	3.53	17.11	21.86
1409	6.69	8.51	2.14
1412	13.21	7.20	5.40
1418	1.92	5.06	7.25
1419	13.14	9.41	10.68
1422	4.50	23.29	7.94
1423	3.90	16.25	19.93
1424	12.82	5.39	0.00
1426	10.16	4.34	2.00

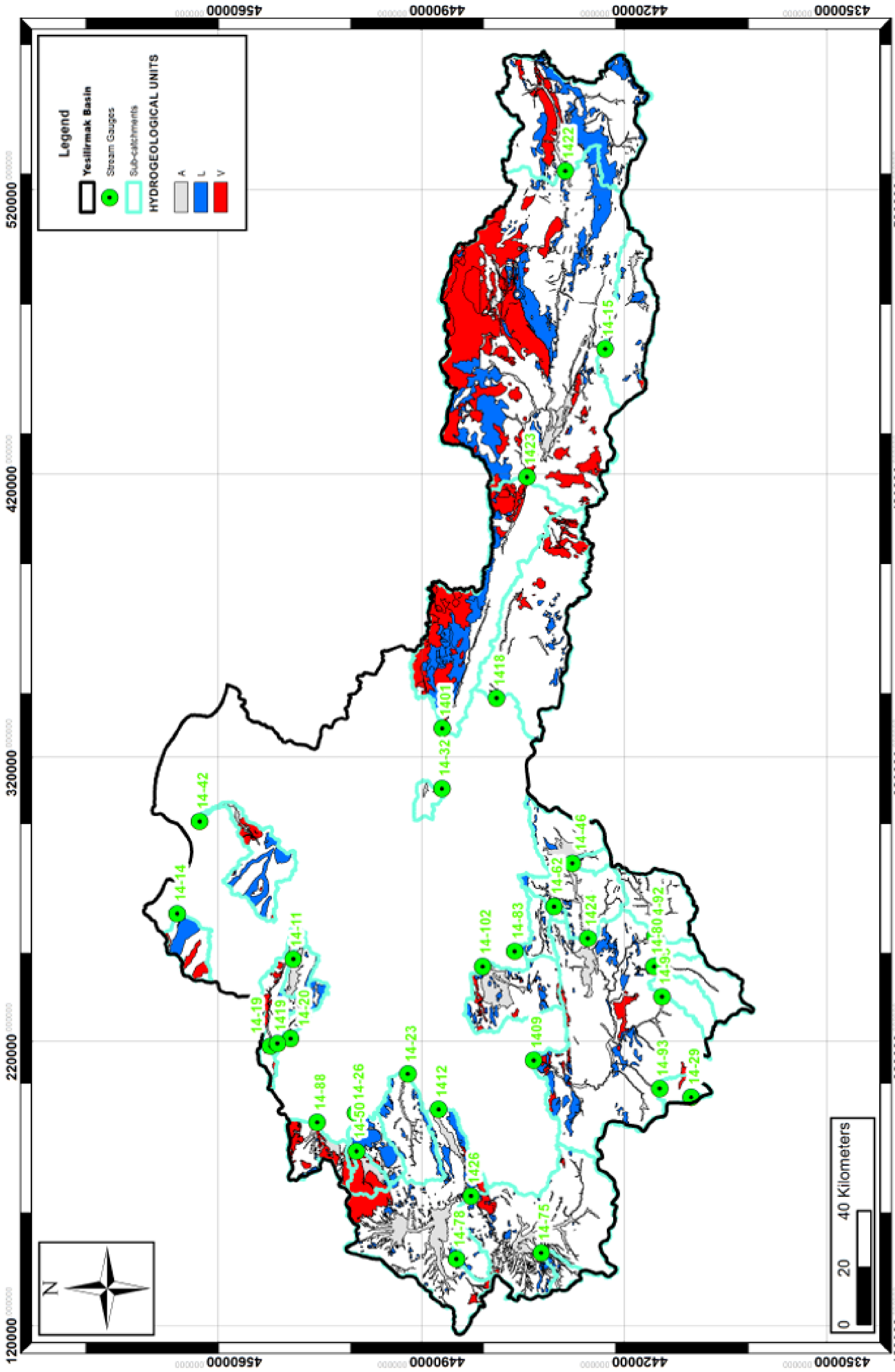

Figure 4.5. Spatial Distribution of Hydrogeologically Important Units Across Study Catchments.

CHAPTER 5

FLOW SIGNATURES

5.1. Flow Signatures

Flow signatures measure qualities of the dynamic response characteristics that give knowledge into the practical conduct of the catchment (Sawicz et al., 2013). It also helps us to distinguish specific response characteristics of catchments from others. In this study, the chosen signatures are flow duration curve signatures (Q_5, Q_{50}, Q_{95} and slope of flow duration curve (SFDC)), runoff ratio (RQP), baseflow index (BFI), streamflow elasticity (SFE) and day of half year flow (DHYF). These signatures were chosen from the combination of the indices available in the literature (Sawicz et al., 2013; Oudin et.al., 2010; Yilmaz et al., 2008; and Yadav et al., 2007) based on data availability in Yesilirmak Basin and it is aimed that there is no correlation between the signatures. Flow signatures which will be discussed in this section was derived from precipitation, streamflow and temperature records during study time period (1973-1977). Moreover, these signatures are not dependent on the size of the catchments. In this section, brief definition of each of signature will be explained.

5.1.1. Flow Duration Curve Signatures (Q5, Q50, Q95, SFDC)

Flow duration curve (FDC) (Figure 5.1) is described as a graphical illustration which reveal frequency distribution of the flow regime (Vogel and Fennessey, 1994). It is commonly used in hydrology to investigate the flow characteristics, hydrologic response of a drainage basin to various types and distributions of inputs by using exceedance percentages of flows (Croker et al., 2003). In other words, exceedance percentage flows help us to find flow signatures from low flow to high flow. High flow signatures (If Q_5 is high, catchment is surface flow dominated) are calculated by

5% of exceedance percentage on flow duration curve, medium flow signatures (it indicates average flow) are calculated by 50% of exceedance percentage on flow duration curve and low flow signatures (If Q_{95} is high, baseflow contribution of catchment is high) are calculated by 95% of exceedance percentage on flow duration curve. Moreover, slope of flow duration curve. SFDC, was calculated between 33% and 66% streamflow percentiles (Yadav et al., 2007). Yilmaz et al. (2008) noted that" a characteristic signature behavior for a watershed having ''flashy'' response is a steep slope of the midsegment FDC, while flatter midsegment slopes are associated with watersheds having slower and more sustained groundwater flow." All flow duration curve signatures have been calculated for each study catchment and were listed in Table 5.1. Figures 5.2, 5.3, 5.4 and 5.5 shows the spatial distribution of these flow signatures among study catchments.

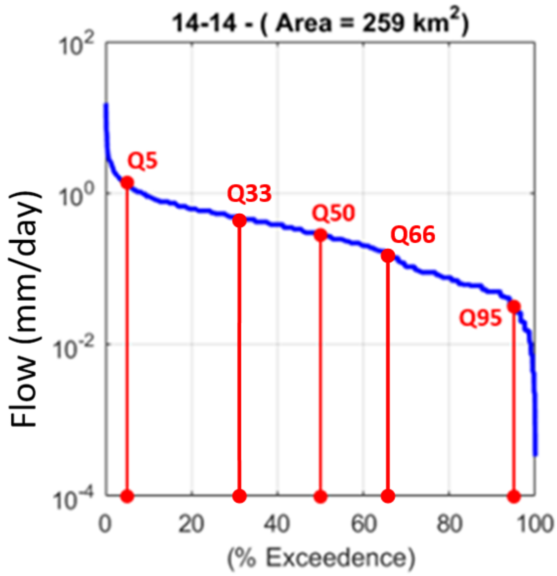

Figure 5.1. Example of Flow Duration Curve for Catchment 14-14

$$\text{SFDC} = \frac{ln\ (Q33\%) - \ln(Q66\%)}{(0.66 - 0.33)} \tag{2}$$

Table 5.1. Flow Duration Curve Signatures of Catchments

Catchment No.	Q5	Q33	Q50	Q66	Q95	SFDC	RQP	BFI	SFE	DHYF
14-11	3.275	0.953	0.589	0.441	0.173	0.771	0.708	0.826	0.422	209
14-14	1.268	0.484	0.274	0.107	0.033	1.511	0.270	0.844	-1.725	183
14-15	2.501	0.488	0.274	0.220	0.149	0.796	0.491	0.896	1.823	209
14-19	1.643	0.263	0.094	0.030	0.011	2.185	0.328	0.808	2.316	178
14-20	1.941	0.785	0.548	0.422	0.186	0.621	0.617	0.846	0.964	204
14-23	0.342	0.080	0.036	0.011	0.001	2.026	0.078	0.797	3.029	177
14-26	0.617	0.156	0.107	0.076	0.041	0.720	0.170	0.873	2.079	187
14-29	2.351	0.546	0.114	0.064	0.000	2.152	0.662	0.600	6.690	210
14-32	2.571	0.468	0.193	0.106	0.062	1.489	0.304	0.825	3.166	195
14-42	2.665	0.911	0.499	0.172	0.018	1.668	0.451	0.814	1.291	165
14-46	2.205	0.107	0.011	0.002	0.000	3.807	0.333	0.571	4.823	195
14-50	0.833	0.172	0.080	0.040	0.003	1.455	0.207	0.810	1.892	188
14-62	1.165	0.301	0.100	0.100	0.012	1.099	0.303	0.866	-1.062	208
14-75	1.635	0.430	0.301	0.120	0.000	1.273	0.404	0.804	-6.348	178
14-78	0.768	0.187	0.067	0.007	0.001	3.332	0.159	0.795	-1.522	225
14-80	1.021	0.214	0.102	0.059	0.010	1.295	0.230	0.822	1.842	209
14-83	0.937	0.187	0.077	0.028	0.000	1.906	0.179	0.686	7.388	193
14-88	0.201	0.038	0.033	0.021	0.008	0.585	0.061	0.848	9.220	183
14-92	1.003	0.204	0.111	0.065	0.015	1.145	0.211	0.837	1.160	204
14-93	1.127	0.200	0.081	0.031	0.014	1.856	0.266	0.834	9.749	209
14-95	1.098	0.305	0.122	0.055	0.006	1.715	0.263	0.819	0.532	211
14-102	0.536	0.113	0.044	0.006	0.001	2.996	0.102	0.735	3.618	182
1401	2.218	0.445	0.176	0.123	0.058	1.285	0.375	0.862	2.362	205
1409	1.104	0.164	0.084	0.046	0.005	1.262	0.211	0.842	4.293	190
1412	0.560	0.105	0.054	0.020	0.001	1.653	0.116	0.821	-0.593	182
1418	3.600	0.672	0.330	0.218	0.148	1.125	0.592	0.885	6.283	205
1419	1.645	0.461	0.303	0.205	0.115	0.809	0.383	0.842	1.577	179
1422	1.346	0.215	0.104	0.074	0.021	1.064	0.275	0.839	-3.227	211
1423	2.248	0.434	0.161	0.103	0.060	1.436	0.396	0.870	3.151	208
1424	1.146	0.201	0.095	0.052	0.008	1.345	0.217	0.842	2.518	189
1426	0.832	0.105	0.054	0.010	0.000	2.398	0.137	0.736	-1.615	190

Higher Q5 values are observed in catchments 1418, 14-11, 14-42 and 14-32 respectively, lower values are observed in catchments 14-88, 14-102, 1412. While higher Q50 are observed in catchments 14-11, 14-20 and 14-42, catchments 14-46, 14-88 and 14-102 shows lower medium flows. Higher Q95, was observed in catchments 14-20, 14-15 and 14-11 while catchments 14-29, 14-46, 14-75, 14-83 and 1426 has no baseflow contribution. Steep SFDC was observed in catchments 14-46, 14-78 and 14-102. On the other hand, flatter slopes are observed in 14-88, 14-20 and 14-26.

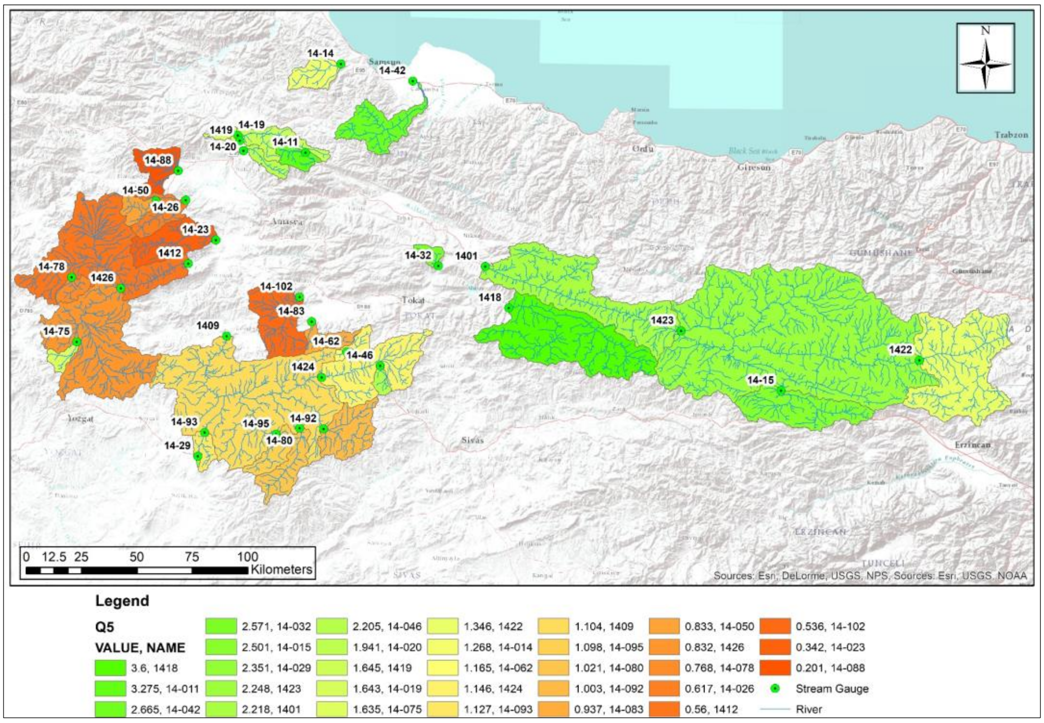

Figure 5.2. Q5 Distribution Across Study Catchments

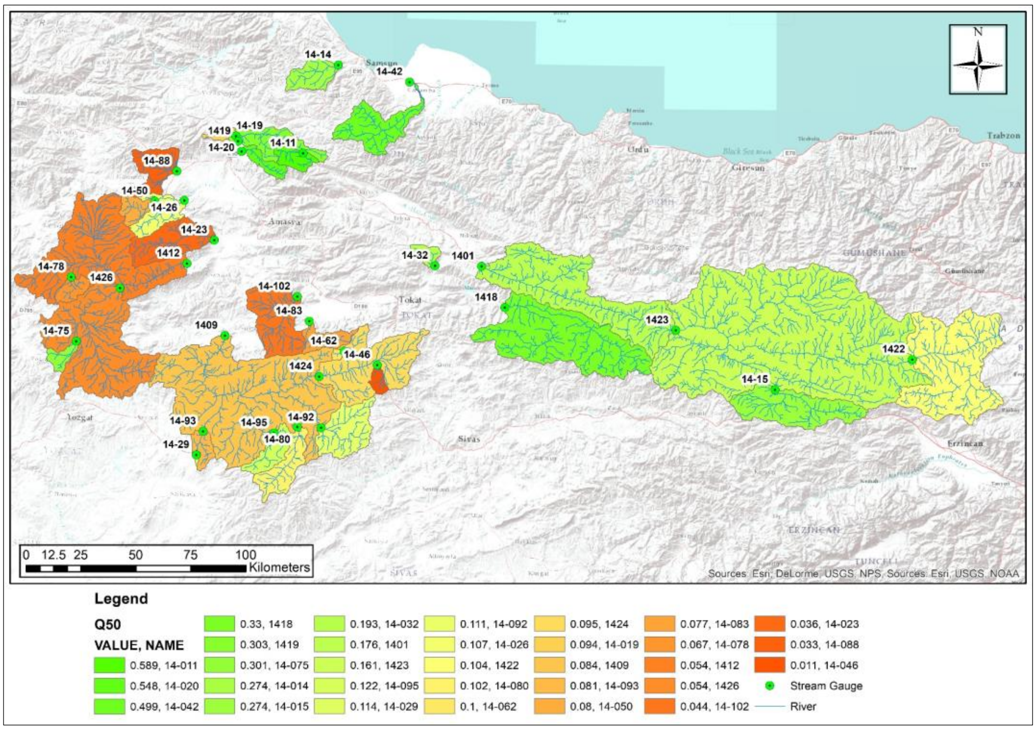

Figure 5.3 Q50 Distribution Across Study Catchments

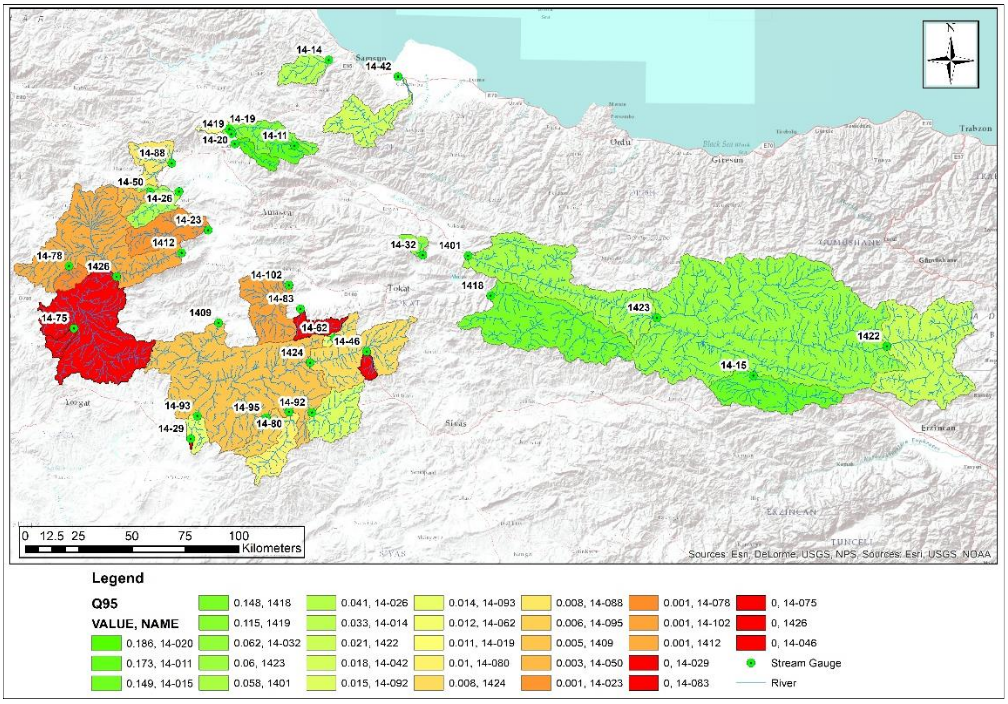

Figure 5.4 Q95 Distribution Across Study Catchments

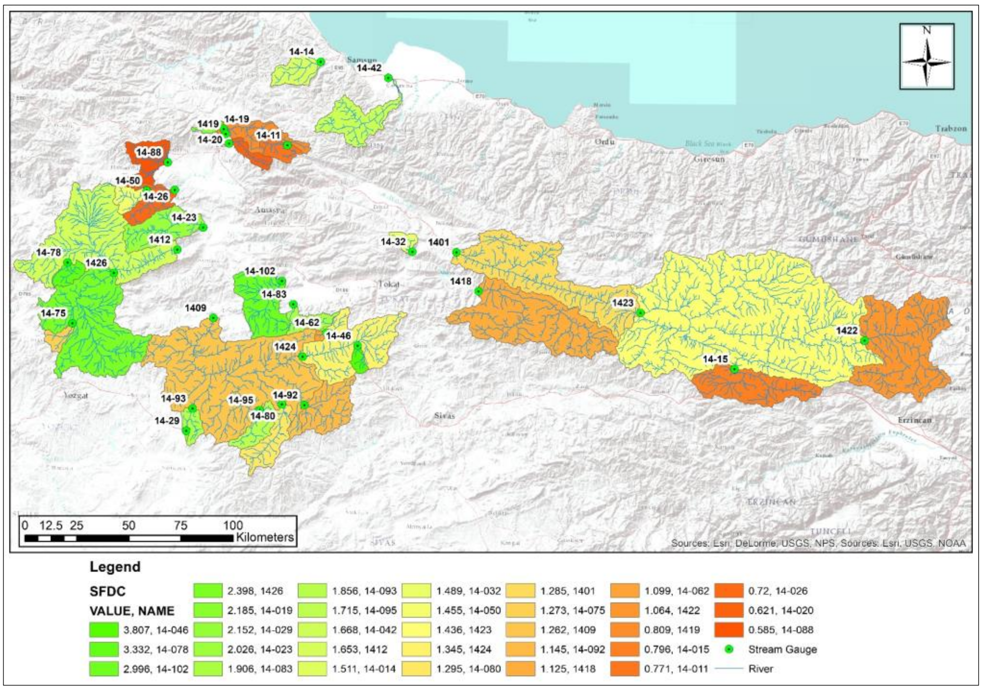

Figure 5.5 Slope of Flow Duration Curve Distribution Across Study Catchments

5.1.2. Runoff Ratio (RQP)

Runoff Ratio is defined as the ratio of average annual runoff, Q, to average annual precipitation, P (Yadav et al.,2007) and it is unitless:

$$RQP = \frac{Q}{P} \tag{3}$$

Runoff ratio simply summarizes how effectively the input precipitation is converted to streamflow in the long timescales. If the runoff ratio in the catchment is high, significant portion of the input precipitation is converted to streamflow. However, if the flow ratio in the catchment is low, significant portion of the input precipitation is either lost through evapotranspiration or lost through deep recharge (does not feed streamflow at annual timescale). If we assume that the catchment storage does not change at the annual time scale, this signature than summarizes the degree to which water balance is dominated by streamflow vs. evapotranspiration in the long run.

As seen in Figure 5.6 and Table 5.1, highest runoff ratio values were seen in catchment 14-11 (0.708), 14-20 (0.517) and 1418 (0.592). Lowest runoff ratio values were observed in catchments 14-23 (0.078), 14-88 (0.061), 14-102 and 1412 (0.102, 0.116). Thus, we expect that water more dominantly exits these catchments in the form of streamflow. However, in catchments 14-23, 14-88, 14-102 and 1412, it is expected that water exits these catchments in the form of evapotranspiration in long term (assuming no change in storage).

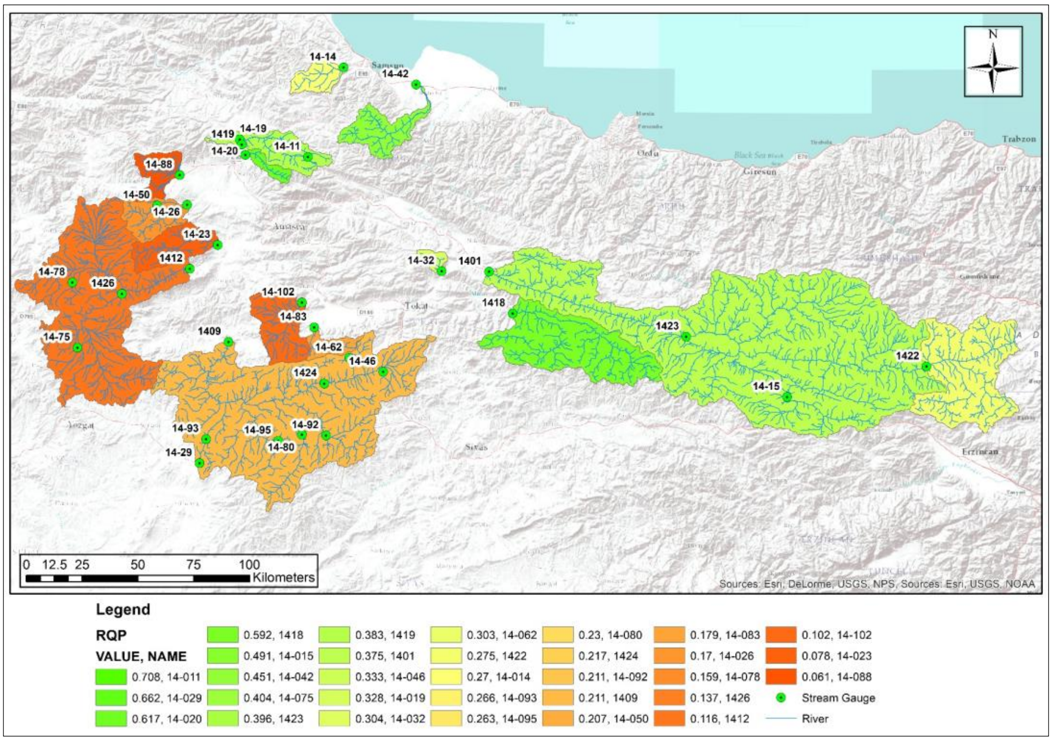

Figure 5.6 Runoff Ratio Distribution Across Study Catchments

5.1.3. Baseflow Index (BFI)

Baseflow index is calculated by dividing long-term baseflow to total streamflow. Higher value of baseflow index indicates higher baseflow contribution in catchment response. Numerous analytical methods have been developed to separate baseflow from total streamflow (McCuen,1989). In this study, single-pass filter method of Arnold et al. (1995) was used to calculate baseflow. The parameter *c* was set as 0.925 according to Eckhardt (2007). Moreover, we focused on the relative baseflow contribution of the catchments to compare the results. After that step, to calculate baseflow index, ratio of streamflow to daily baseflow was found for each catchment and average value was selected for each catchment in study time period (1973-1977).

$$Q_{Dt} = cQ_{Dt-1} + \frac{1+c}{2}(Q_t - Q_{t-1}) \tag{4}$$

Where;

Q_{Dt} is the direct flow value at time-step t

Qt is the total flow at time step t

c is a parameter

As seen in Figure 5.7, higher baseflow index values were observed in catchments 14-15, 1418, 14-26 and 1423 while lower baseflow index values were observed in catchments 14-46, 14-49, 14-83 and 14-102.

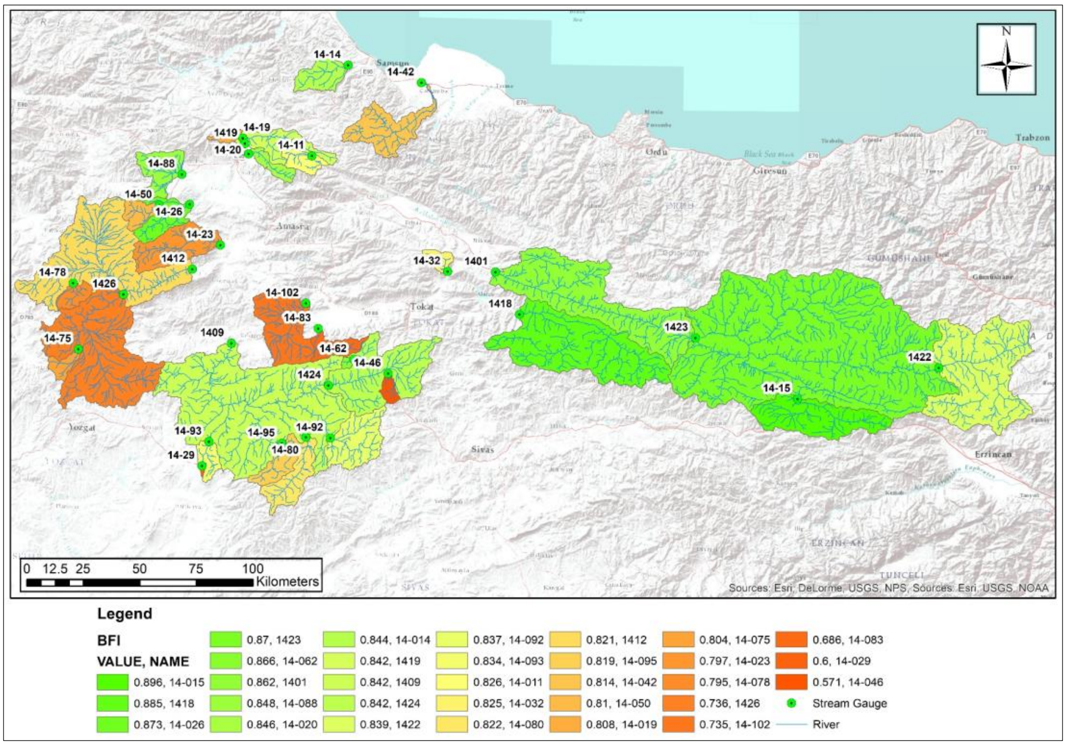

Figure 5.7 Baseflow Index Distribution Across Study Catchments

5.1.4. Streamflow Elasticity (SFE)

Streamflow elasticity can be described as ratio of inter-annual difference between annual streamflow to the inter-annual difference between annual precipitation. After this calculation, the result was normalized by runoff ratio and median value of results was used in our study. Normalization step helps reduce the effect of outliers in the data (Schaake, 1990; Dooge, 1992; Sankarasubramanian et al., 2001)).

$$\text{SFE}=\frac{dQ}{dP}*\frac{P}{Q} \tag{5}$$

As seen in Figure 5.8, higher streamflow elasticity values were observed in catchments 1-83, 14-88 and 14-93. On the other hand, lower elasticity values were observed in catchments 14-75, 1422 and 14-14. Thus, we can expect that catchments whose streamflow elasticity values greater than 1 would, susceptible to change of precipitation and lower than 1 would insusceptible to change of precipitation.

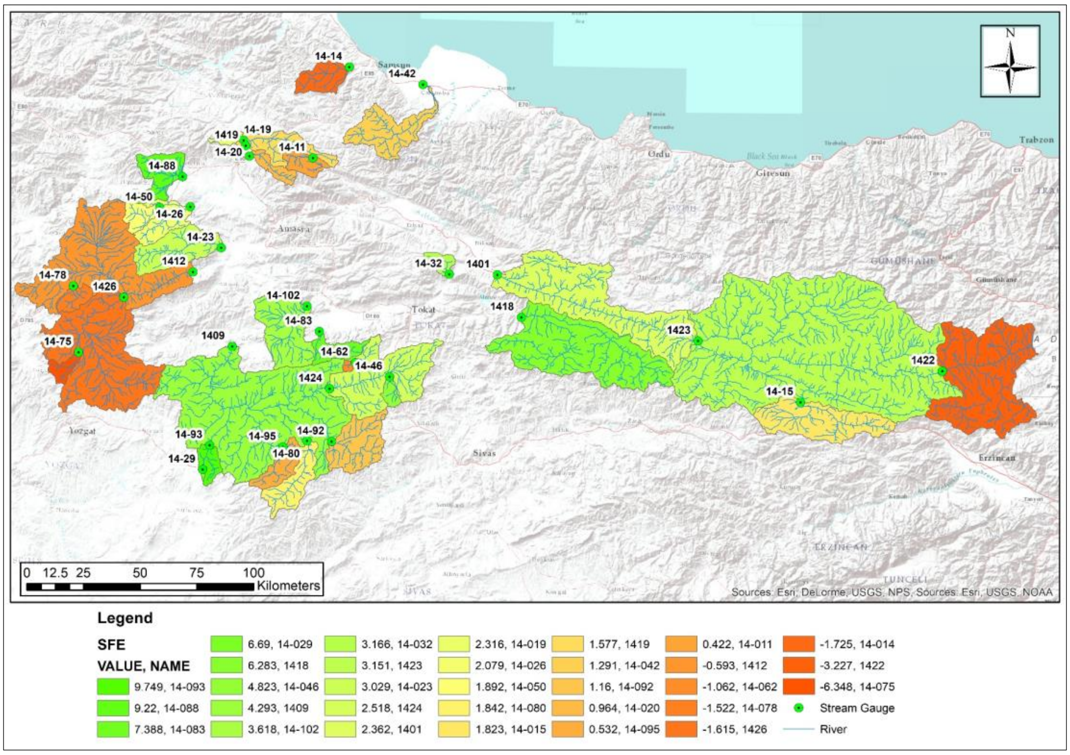

Figure 5.8 Streamflow Elasticity Distribution Across Study Catchments

5.1.5. Day of Half Year Flow (DHYF)

In snowmelt-dominated catchments, the majority of streamflow occurs during the spring-summer snowmelt period (Clow, 2010). Thus, if the 50% or more of annual flow occurs during spring-early summer period (April-July period for northern hemisphere corresponding today of year values 121-213), then we can expect that snowmelt contribution to streamflow is dominant.

In this study, we calculated day of half year flow parameters for each year from the daily streamflow records. Then, we used the median value for 5 years interval (Table 5.2). For example, based on the values of this signature, half of the annual flow occurred later (in late July) in catchments 14-78, 14-95 and 1422, while half of the annual flow occurred earlier (in early June) in catchments 14-42, 14-23, 14-19 and 14-

75 etc. Therefore, it can be said that the streamflow of the latter catchments is more dominated by snowmelt.

Table 5.2 Day of Half Year Flow values of catchments (1973-1977)

Catchment No.	YEARS					
	1973	1974	1975	1976	1977	Day of Half Year Flow
14-11	169	214	213	185	209	209
14-14	153	209	183	175	208	183
14-15	200	205	209	218	213	209
14-19	168	168	178	178	205	178
14-20	191	205	215	192	204	204
14-23	109	125	215	177	193	177
14-26	176	168	209	187	206	187
14-29	210	193	215	185	214	210
14-32	189	174	198	195	207	195
14-42	162	162	205	165	205	165
14-46	202	195	189	193	197	195
14-50	188	169	211	179	201	188
14-62	208	202	225	209	207	208
14-75	111	166	209	178	193	178
14-78	256	231	225	190	207	225
14-80	209	191	220	205	220	209
14-83	178	172	217	193	212	193
14-88	166	169	213	183	207	183
14-92	182	189	204	207	222	204
14-93	209	194	214	178	211	209
14-95	220	187	225	204	211	211
14-102	118	167	219	182	202	182
1401	205	205	208	211	204	205
1409	190	189	221	189	210	190
1412	154	159	215	182	197	182
1418	205	206	204	212	203	205
1419	169	163	207	179	206	179
1422	211	203	208	216	211	211
1423	208	205	209	212	204	208
1424	187	187	201	189	195	189
1426	159	162	215	190	205	190

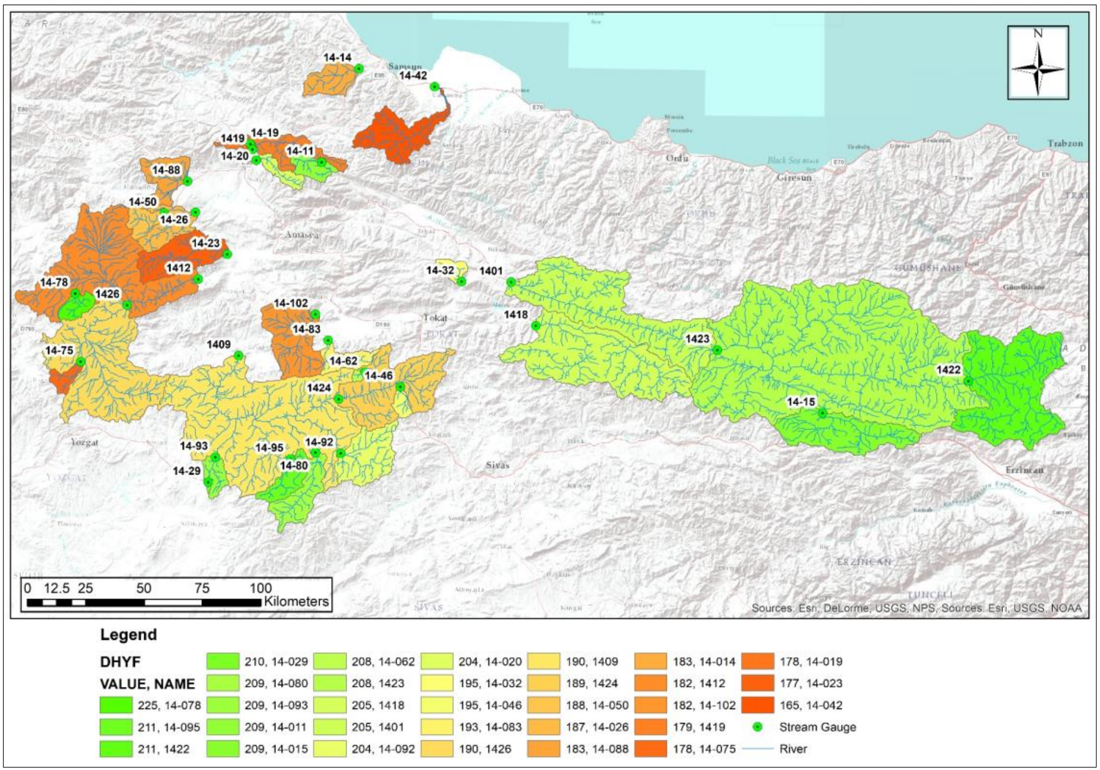

Figure 5.9 Day of Half Year Flow Distribution Across Study Catchments

CHAPTER 6

CATCHMENT PROPERTIES

6.1. Geological Properties

As mentioned in Chapter 4, carbonate rocks, volcanic rocks and alluvium units are hydrogeologically important geologic units bearing groundwater in the study catchments. The flow of groundwater is largely dependent on the interaction between permeable rocks and geological structures.

Alluvial deposits generally consist of clay, silt, sand and gravel size loose sediments, generally with high permeability. Such deposits are generally located on flood plains and river benches and can be considered as units that enable groundwater recharge.

One of the other aquifer rock types is volcanic rocks. Pyroclastic rocks or silicic rocks usually have low permeability except where they are fractured. Porous textures and columnar joints can be observed in rapidly cooling rocks such as basalt. Volcanic rocks with this type of geological structures have water storage and transmission properties as aquifers (Miller, 1999).

According to Legrand and Stringfield (1966), there are 4 hydrological zones in which the aquifer characteristics of carbonate rocks are evaluated:

Zone 1: Carbonates on the surface or near the surface: Groundwater is at the level of these rocks. The flow from the rain infiltrates vertically towards the water table and contributes directly to the surface water.

Zone 2: Carbonates buried beneath an impermeable unit: The water moves under the artesian pressure through the rocks to a lower discharge.

Zone 3: Carbonates without significant discharge are: a) carbonates buried under impermeable deposits where water will never escape b) carbonates that are not in control of the flow of water.

Zone4: Carbonates elevated above adjacent impervious valleys: Water discharge does not occur beneath surface.

In the light of the above-mentioned definitions, the percentage distributions of alluvium (ALV), carbonate (CAR) and volcanic rocks (VOR) in the catchment are given in Figure 6.1 to 6.3. Accordingly, the catchments estimated to have a higher groundwater potential are as follows:

The catchments with an alluvium ratio above 20% are 14-11 and 14-50. Catchments with an alluvium ratio between 10 and 20% are 14-102, 14-26, 14-88, 1412, 1419, 1424, 14-75 and 1426. (Figure 6.1).

The catchments with a carbonate rock ratio of over 50% is only 14-50. The catchments with carbonate rock ratios between 20 and 30% are 14-14, 14-26 14-42, 14-29, 14-19 (Figure 6.2).

The catchments with a volcanic rock ratio of over 50 is only 14-50. The catchments with volcanic rock ratios between 30 and 50% are 14-88 and 14-26 (Figure 6.3).

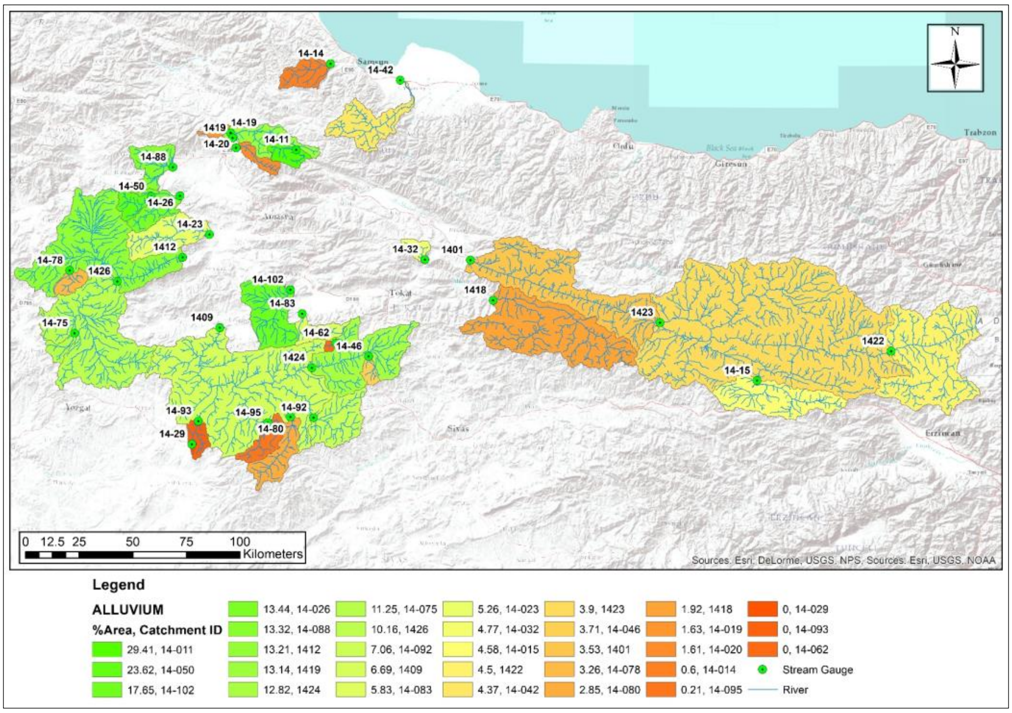

Figure 6.1. Alluvium (%) Distribution Across Study Catchments.

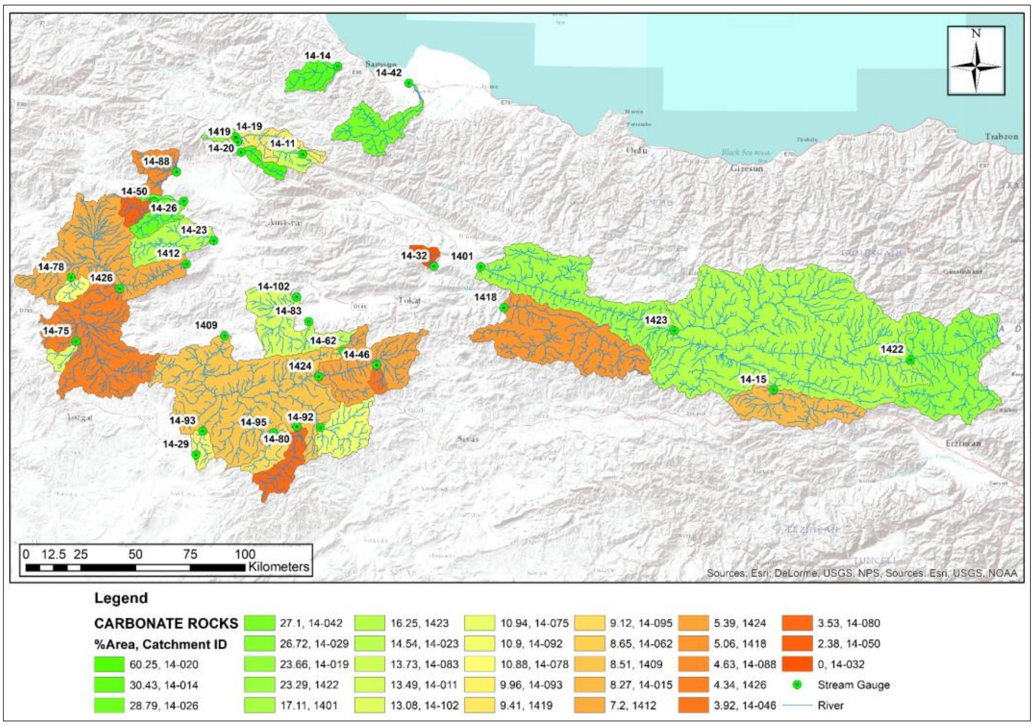

Figure 6.2. Carbonate Rocks (%) Distribution Across Study Catchments.

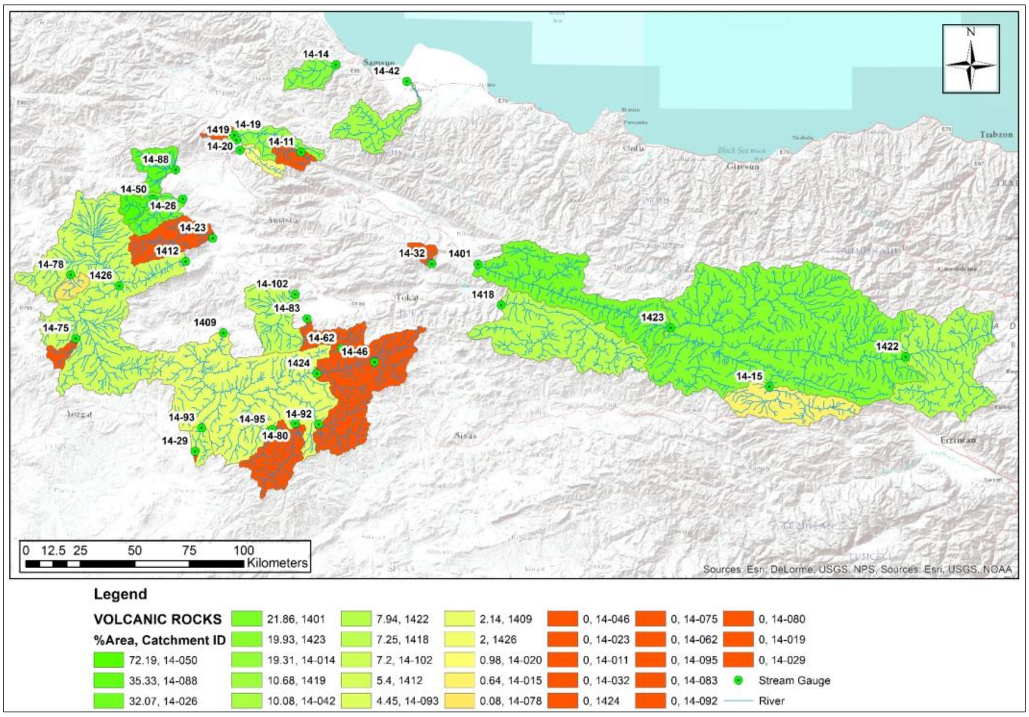

Figure 6.3. Volcanic Rocks (%) Distribution Across Study Catchments.

6.2. Soil Properties

Soils are one of the important elements of the water cycle on a global scale. The soil type can provide important information about the hydrologic response of rainfall, infiltration and groundwater recharge, surface flows and horizontal movement of water. Therefore, knowing the hydraulic behavior of soils in a catchment is critical to understand the catchment hydrologic response characteristics (Ross et al., 2018).

Physical structure, storage properties and permeability of the soil are the components that affect the hydrological response characteristics. Soils can be classified as permeable, semi-permeable and impermeable. According to ASTM standards, soils passing through the sieve #200 (silt and clay) are generally classified as impermeable, while the soils passing through the sieve 4 and remaining on the sieve #200 (sandy soils) are classified as permeable.

When the soil structures in a catchment are examined, one of the factors affecting the measured surface water is the soil type. For example, in a catchment with a high percentage of silt and clay, surface water is effective, and infiltration and groundwater recharge is almost negligible. On the other hand, in a catchment with a semi-permeable or permeable soil type, it can be concluded that the groundwater level is close to the surface and the groundwater supply is higher, the surface waters may be relatively lower than a catchment which impermeable soil type is dominant (Wolock et al., 2004).

In this study, 250 m resolution raster soil maps provided by ISRIC World Soil Information (Hengl et.al., 2017) database were used. The average clay, silt and sand ratios in each study catchments was calculated as a percentage using these raster maps. The clay and silt-bearing soils in the catchment are considered impervious and the sand-bearing soils are considered permeable.

Raster maps containing clay, silt and sand ratios separately in the study catchments are shown in Figures 6.4, 6.5 and 6.6. When the percent area of soils are examined for each catchment, the following results are revealed:

- In the catchments 14-62, 14-93, 1426, 14-29, 14-23, 1412, 14-19 and 14-75 respectively, the clay + silt ratios are above 70 percent and the sand ratio are below 30 percent. In these catchments, groundwater recharge is expected to be relatively low and surface runoff is expected to be higher.
- In the catchments 14-102, 14-26, 1424, 14-50, 1419, 14-88, 14-42, 14-78, 1409, 14-92, 14-46, 14-14, 14-83, 14-11 and 14-20 respectively, the clay + silt ratios are above 65 percent and the sand ratio is below 35 percent. According to the previous catchment group, groundwater recharges are expected to be relatively low and their surface flows are higher.
- In the catchments, 1422, 14-32, 1401, 1418, 14-95, 1423 and 14-15 respectively, the clay + silt ratios are above 60 percent and the sand ratio are below 40 percent. In these catchments, groundwater recharges and surface

flows are expected to be close to the same rate compared to the other two catchment groups described above.

- In the catchment 14-80, the clay + silt ratios are above 55 percent and the sand ratio is below 45 percent. In this catchment, groundwater recharge is expected to be higher than other catchments.

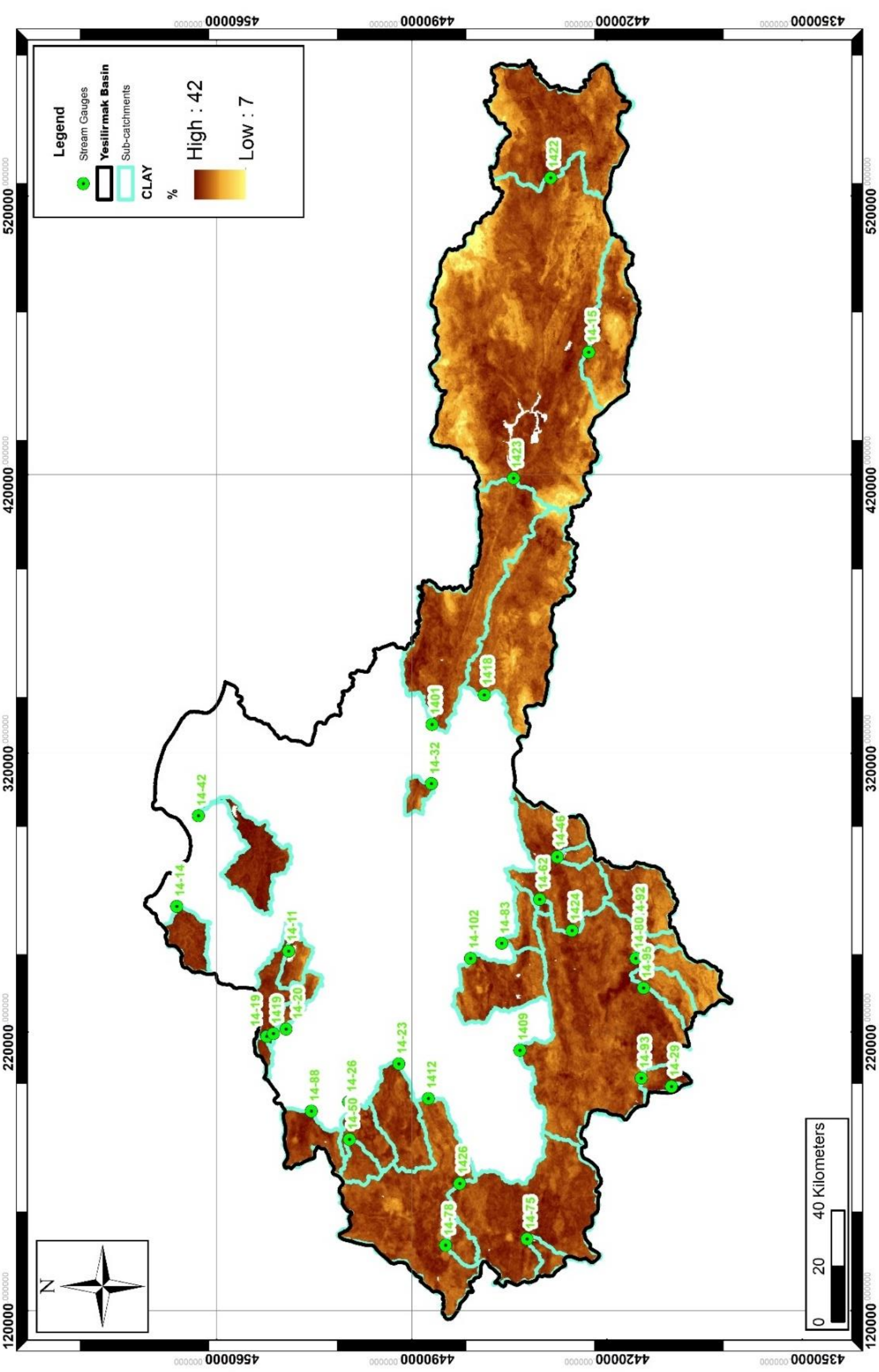

Figure 6.4. Clay (%) Distribution Across Study Catchments

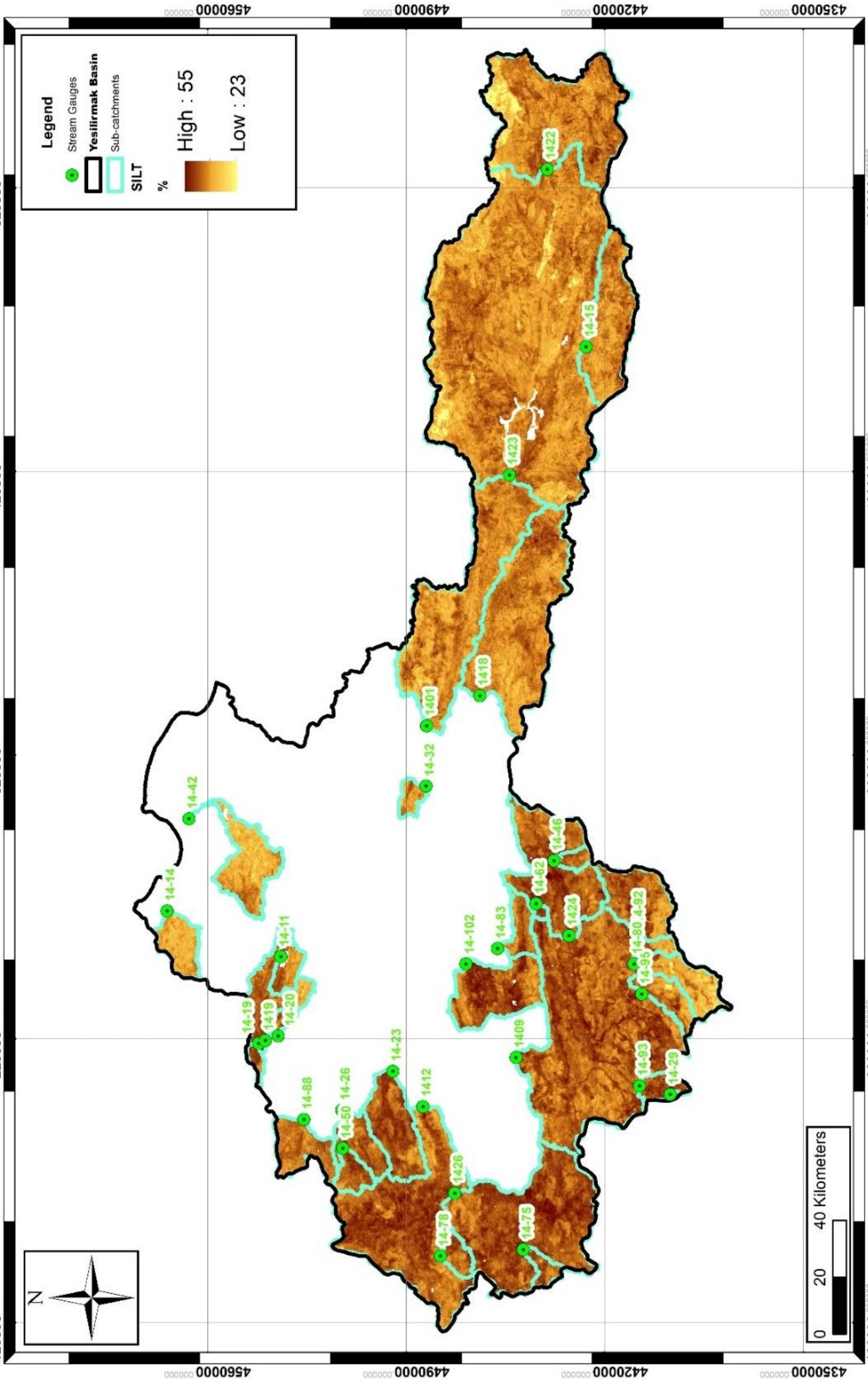

Figure 6.5. Silt (%) Distribution Across Study Catchments

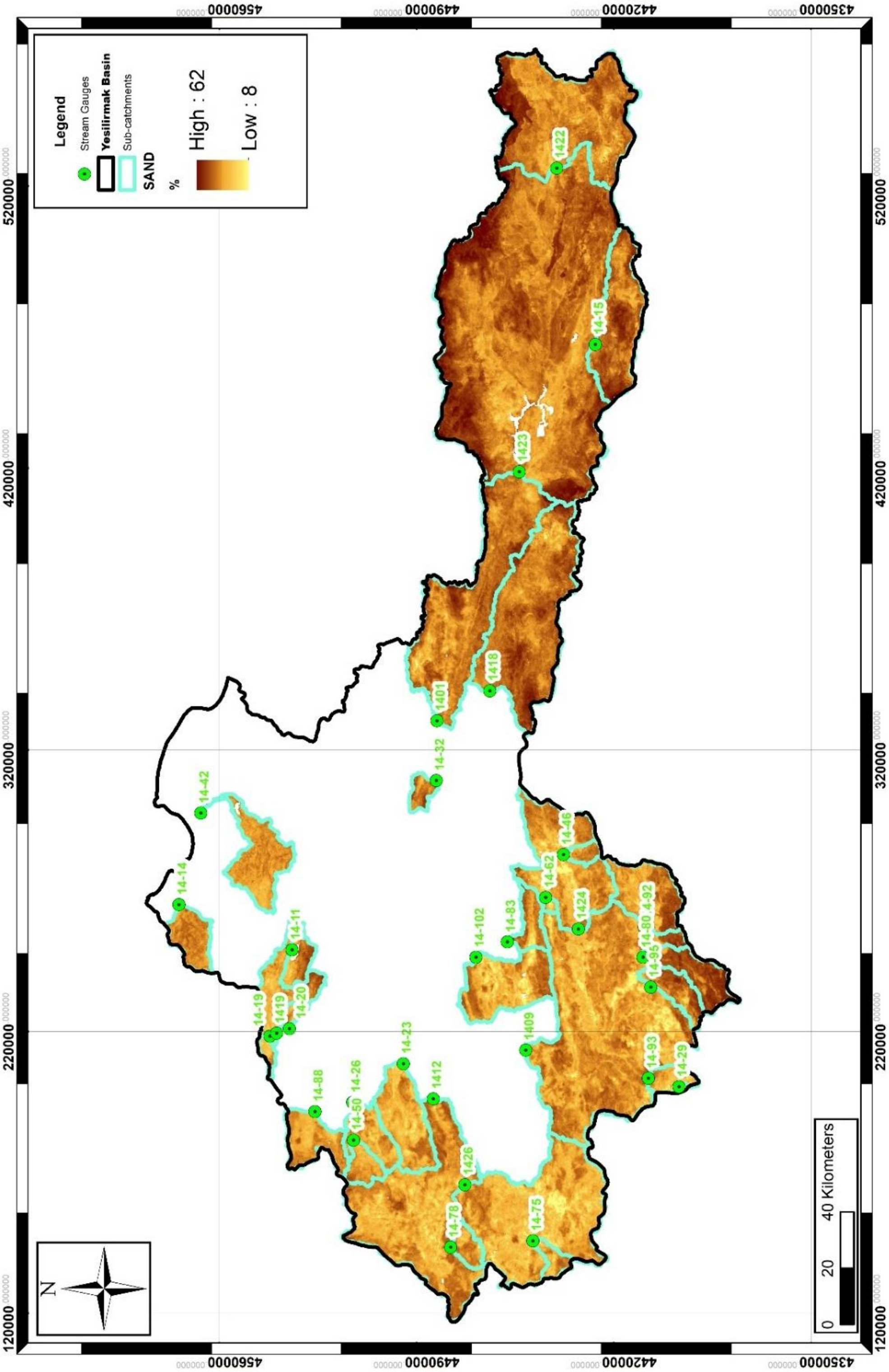

Figure 6.6. Sand (%) Distribution Across Study Catchments

6.3. Land Cover Properties

6.3.1. Runoff Curve Number (CN)

The soil structure of the study area was obtained from the 250 m resolution raster maps, which gives the sand, silt and clay contents obtained from ISRIC World Soil Information (Hengl et.al, 2017) as percentage.

Soil structure classification by United States Department of Agriculture (USDA) according to sand, silt and clay ratios is given in Figure 6.7. Based on this classification, the soil structure of the studied catchments is classified.

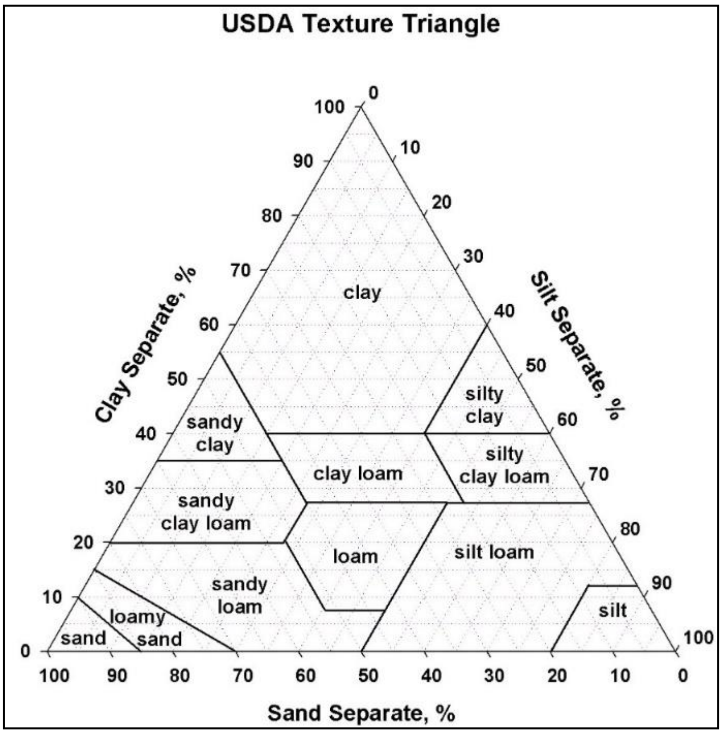

Figure 6.7. USDA Texture Triangle (USDA, 1986)

According to this classification, hydrological soil groups A, B, C and D were obtained by adhering to the general infiltration capacity of the soil structure properties of the catchments. General characteristics of hydrological soil groups are given below.

Group A soils are typically in gravel or sandy texture, containing less than 10% clay and more than 90% sand or gravel (High Infiltration-Low Runoff).

Group B generally has a texture of silt loam, loam, or loamy sand and contains 10-20% clay and 50-90% sand (Moderate Infiltration-Moderate Runoff).

Group C has generally loam, sandy clay loam, clay loam and silty clay loam texture and it contains 20-40% clay and less than 50% sand (Low Infiltration-Moderate to High Runoff).

Group D has high flow potential in fully saturated state. The transmission of water in the soil is prevented or very limited. The soil group D has generally clayey texture and contains more than 40% clay and less than 50% sand (Very Low Infiltration-High Runoff).

Then the hydrological soil group map obtained is evaluated together with Corine Land Cover map layer; sub-areas were obtained for each land use and hydrological soil group.

Based on the classification made by the USDA Soil Conservation Service (SCS) in 1986, the CN values assigned to these subdomains are given in the Table 6.1 and the weighted CN values for each catchment area are calculated as given Figure 6.8.

Table 6.1 Runoff Curve Numbers for Urban Areas (USDA, 1986)

Description of land use	Hydrologic soil groups			
	A	B	C	D
Paved parking lots, roofs, driveways	98	98	98	98
Streets and roads				
Paved with curbs an storm sewers	98	98	98	98
Gravel	76	85	89	91
Dirt	72	82	87	89
Cultivated (agriculture crop) land*				
Without conservation treatment (no terraces)	72	81	88	91
With conservation treatment (terraces, conlours)	62	71	78	81
Pasture or range land				
Poor (<50% ground cover or heavily grazed)	68	79	86	89
Good (<50-75% ground cover, not heavily grazed)	39	61	74	80
Meadow (grass, no grazing, mowed for hay)	30	58	71	78
Brush (good, >75% ground cover)	30	48	65	73
Wood and Forests				
Poor (small trees/brush destroyed by overgrazing/burning)	45	66	77	83
Fair (grazing but not burned, some brush)	36	60	73	79
Good (no grazing, brush covers >75% impervious)	30	55	70	77
Open spaces (lawns, parks, golf courses, cemetries)				
Gras covers 50% of ground	49	69	79	84
Good (gras covers 50% of area)	39	61	74	80
Commercial & business districts (85% impervious)	89	92	94	95
Industrial districts (72% impervious)	81	88	91	99
Residental areas				
0.05 ha piots, about 65% impervious	77	85	90	92
0.1 ha plots, about 38% impervious	61	75	83	87
0.2 ha piots, about 25% impervious	54	70	80	85
0.4 ha piots, about 20% impervious	51	68	79	84

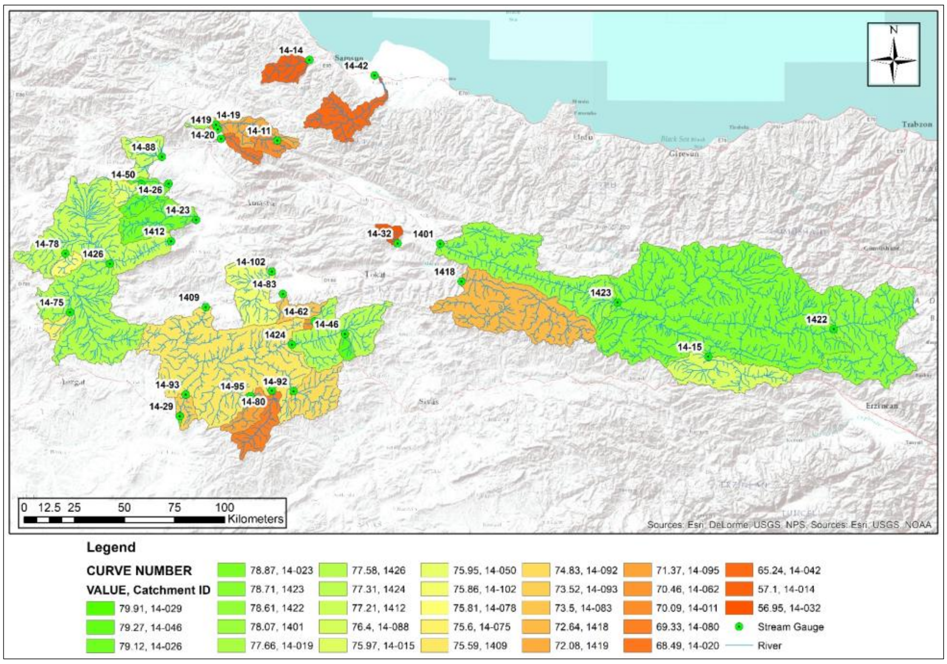

Figure 6.8. Runoff Curve Number Distribution Across Study Catchments

6.3.2. Corine Land Cover (IAL)

Maps of land use are based on CORINE Land Classification System. The CORINE Land Cover Classification System was created under the Coordination of Information on the Environment Project and is the common classification system used in all EU Member States since 1990.

In our country, the implementation of the project was initiated by the Ministry of Environment and Forestry in 1998; The CORINE System serves four main purposes:

- Collecting information on the state of the environment according to the priority issues determined for all member states of the European Union,
- Acquisition of data and harmonization of information at the international level,
- Ensuring the consistency of information and data compatibility
- Establishment of Land Use Maps according to European Environment Agency criteria.

In addition, with the CORINE System, it is possible to monitor the environmental change over a number of years in different levels (International, Union, National and Regional).

The most available land cover data close to the study period is the 1990 Corine Land Cover data. In this study, irrigated areas parameter (IAL) is used although there are many land cover types in Corine Land Cover data. Merchán et al. (2013) and Kuentz et al. (2017), found significant relationship between the irrigation volumes and flow. Implementation of irrigation in the study area increase the flow both monthly and annually in this study. IAL values for each study catchment are given in Figure 6.9.

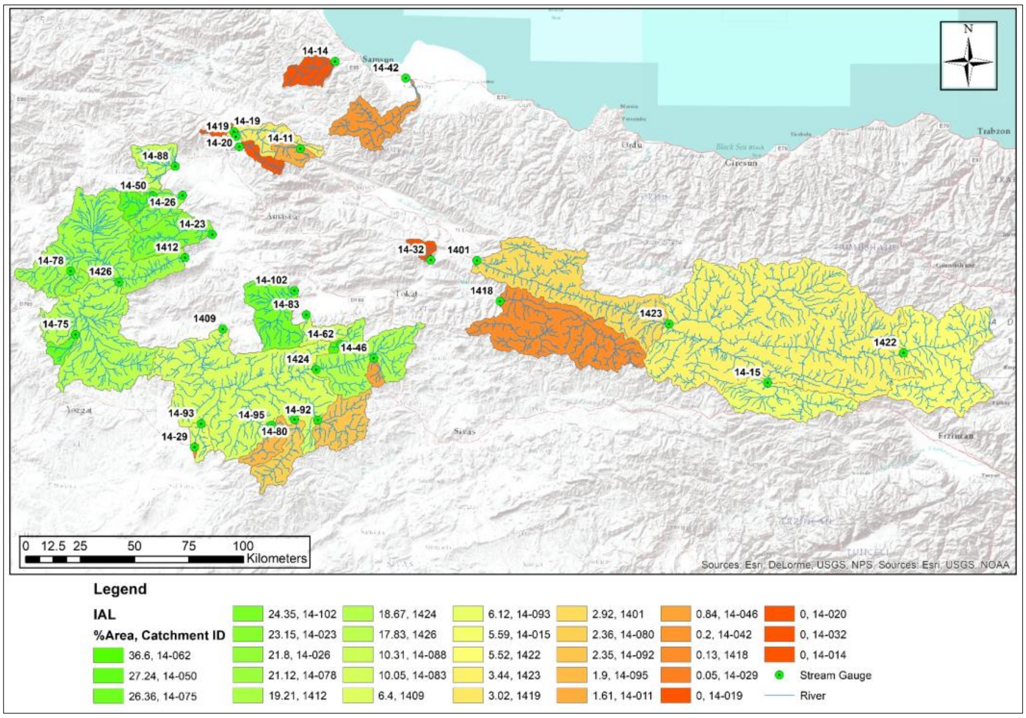

Figure 6.9. Irrigated Arable Lands Distribution Across Study Catchments

6.4. Physical Properties

6.4.1. Hypsometry Integral (HI)

The hypsometric curve defines the height / area distribution of drainage areas of different sizes (from a single valley to the continental scale) (Langbein et al. 1947; Strahler, 1952). Hypsometric integral (HI) expresses the area under this curve numerically. These are the important indicators of the catchment conditions (Ritter et al. 2002). According to Strahler (1952) shape of the hypsometric curve reveals the maturity of the catchments (Figure 6.10). Catchments which have convex upward hypsometric curves are classified as young. On the other hand, catchments having hypsometric curves concave upwards at high elevations and convex downwards at low elevations are classified as mature which means the catchment was subjected to more erosion.

Strahler (1952) and Sarangi et al. (2001) indicates that catchments with an integral value of hypsometry less than 0.3 were characterized as old or fully stabilized. When HI is between 0.3 and 0.6, the catchments was described as mature or inequlibrium stage. It is finally described as young when HI greater than 0.6 which means it is highly susceptible to erosion.

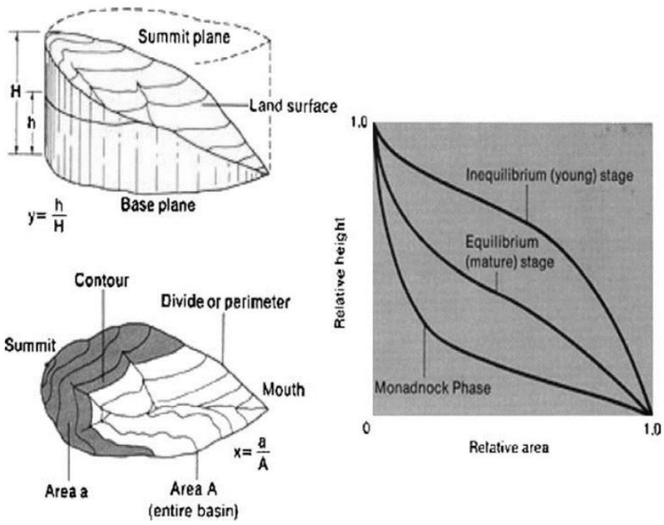

Figure 6.10. Hypsometry Curve and Hypsometry Integral Concept (Ritter et al. 2002)

The hypsometry curve can also give us hints about the snow cover in the catchments. It can be thought that the snow cover may remain longer in the catchments with high cumulative areas at higher elevations. For this reason, considering the water year, the flow will occur later in the higher elevations and in the catchments with high snow cover. It will also affect hydrological response of the catchments.

In study catchments, 14-78, 14-83 and 14-42 show highest hypsometry integral values (Figure 6.11). It indicates that 14-78, 14-83 and 14-42 is very young catchments compared to other study catchments.

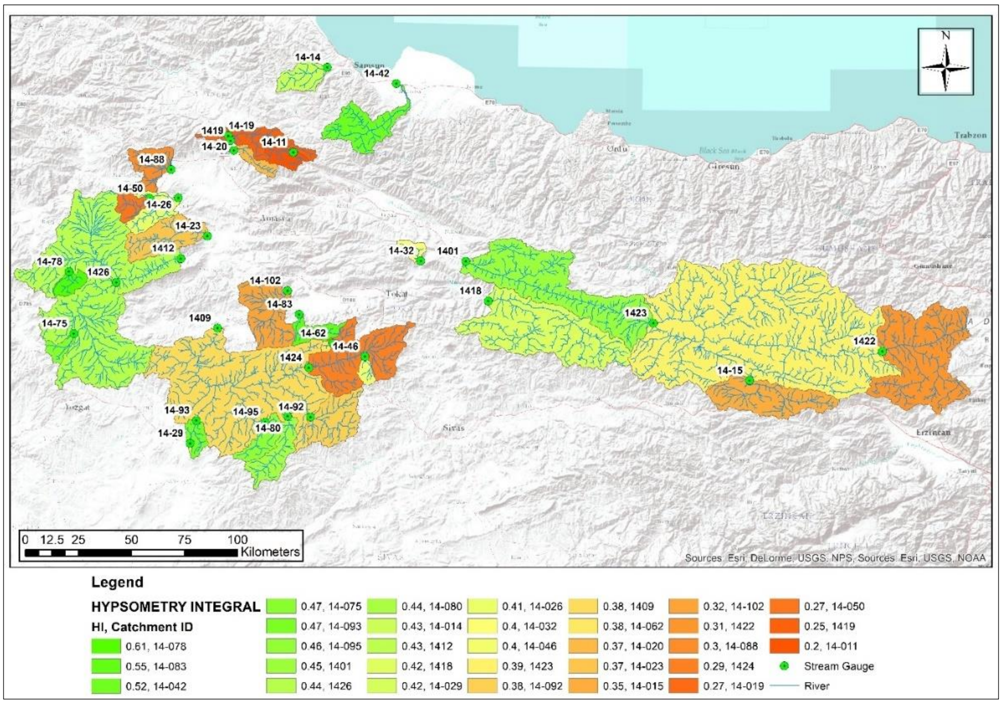

Figure 6.11. Hypsometry Integral Distribution Across Study Catchments

6.4.2. Longest Flow Path (LFP)

Longest flow path can be described as the path required for a “water particle” to travel from the catchment boundary along the longest watercourse to the catchment outlet (Kirpich 1940, McCuen et al. 1984, McCuen 2005, USDA NRCS 2010, SANRAL 2013). Longest flow paths are often associated with time of concentration in the catchment. Accordingly, the longer the flow path in the catchment, the greater the concentration and distribution in the catchment. Distribution of longest flow path in study catchments is given in Figure 6.12.

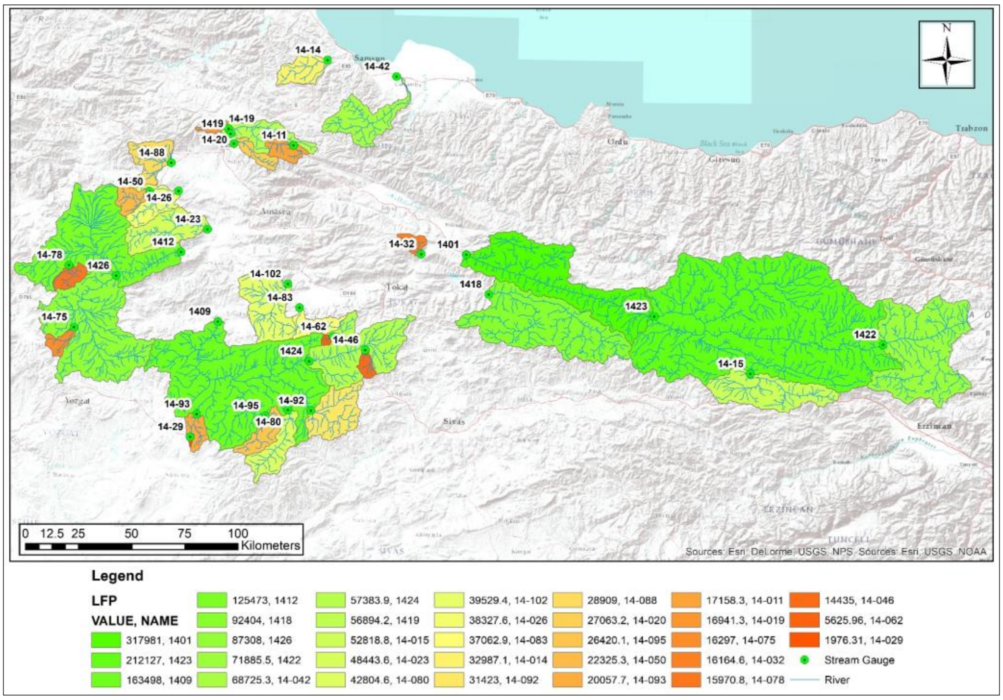

Figure 6.12. Distribution of Longest Flow Path Across Study Catchments

6.4.3. Drainage Density (DRD)

Drainage density is calculated by dividing the total length of streams in a catchment by catchment’s total drainage area. Although Enthekhabi (2001) and Dingman (1978) indicated that there is not any relationship between drainage density and hydrology response, according to Harlin (1984) there is a relation between drainage density and time to hydrograph peak. Higher values of drainage density show that the rivers in the catchment are denser. On the other hand, low drainage density value indicates that sparse river network is present in the catchment. The greater the drainage density in the catchment, the greater the water collecting capacity of the catchment. In addition, travel time will be longer in catchments with high drainage density. Thus, it will likely affect the surface flows. Catchments with high drainage density are expected to have more surface flows. Figure 6.13 shows distribution of drainage density across studied catchments.

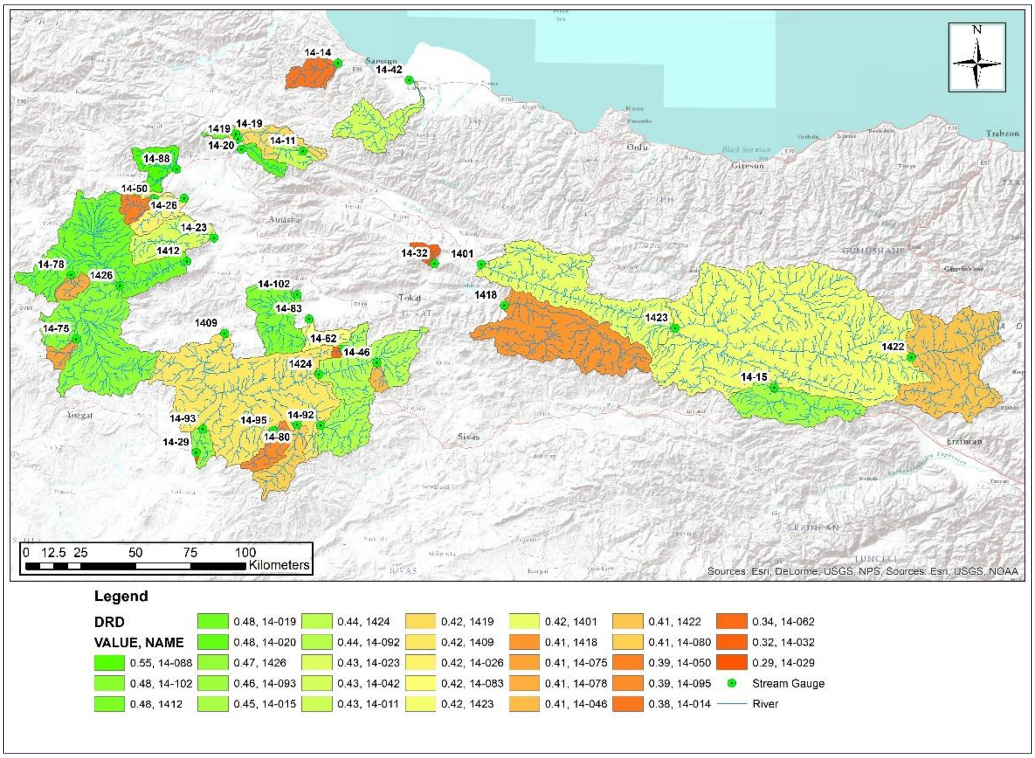

Figure 6.13. Drainage Density Distribution Across Study Catchments

6.4.4. Elevation (ELV)

One of the major role of the catchments is to store and release water. In catchments, water is stored in lakes, rivers, plants and unconsolidated sediment deposits. Catchments usually have less chance of storing water, with an increase in height and a decrease in surface area. However, water can be stored more in flat catchments than in higher catchments with increasing surface area (Staudinger et al.,2017). In addition, elevation affects evapotranspiration and streamflow due to its effect on temperature and rainfall (Dingman, 1981; Boyer, 1984). Precipitation, which is seen as snow in higher elevations, can be seen as rainfall in lower elevations. Moreover, snow can be easily stored due to temperature difference at higher elevations; In lower elevations, snow storage at relatively higher temperatures is quite difficult. Therefore, the flows of the catchments at relatively high elevations may increase later than the flows of the catchments at lower elevations. Elevation Map was created for the 31 study catchments using a 30 m resolution Digital Elevation Model. Table 6.2 and Figure 6.14 shows elevation statistics and distribution in study catchments.

Table 6.2 Elevations Statistics of Studied Catchments

	Elevation (m)			
Catchment No.	**Minimum**	**Maximum**	**Mean**	**Standart Deviation**
14-11	868.14	1976.31	1086.52	244.17
14-14	159.19	1304.21	656.74	167.56
14-15	1300.84	3006.57	1900.12	241.70
14-19	638.32	1628.71	902.95	199.05
14-20	654.48	2059.49	1172.98	304.65
14-23	510.44	1709.71	958.68	194.05
14-26	633.16	1770.43	1094.58	178.61
14-29	1155.50	1425.59	1270.15	56.06
14-32	735.95	1672.57	1112.16	186.17
14-42	4.67	1243.10	644.37	258.67
14-46	1126.38	1819.62	1404.52	153.36
14-50	1024.25	1770.43	1226.78	156.81
14-62	1238.12	1591.57	1370.91	78.59
14-75	977.07	1524.00	1235.02	109.44
14-78	859.59	1386.84	1181.58	90.76
14-80	1190.99	2140.90	1608.43	179.65
14-83	616.44	1786.38	1262.78	155.96
14-88	622.70	1831.34	986.98	238.63
14-92	1151.01	1931.21	1449.46	163.30
14-93	1002.88	1496.96	1236.26	86.62
14-95	1086.51	1860.09	1440.10	145.70
14-102	575.48	1897.50	993.09	246.53
1401	314.80	3297.22	1643.46	425.05
1409	737.94	2140.90	1273.43	213.63
1412	533.33	1810.19	1076.64	200.28
1418	815.04	2703.12	1599.61	325.85
1419	604.44	1976.31	941.24	200.96
1422	1346.42	2916.33	1836.13	248.96
1423	719.64	3297.22	1723.57	386.61
1424	1044.13	2038.41	1333.56	173.78
1426	657.36	1757.03	1143.81	149.00

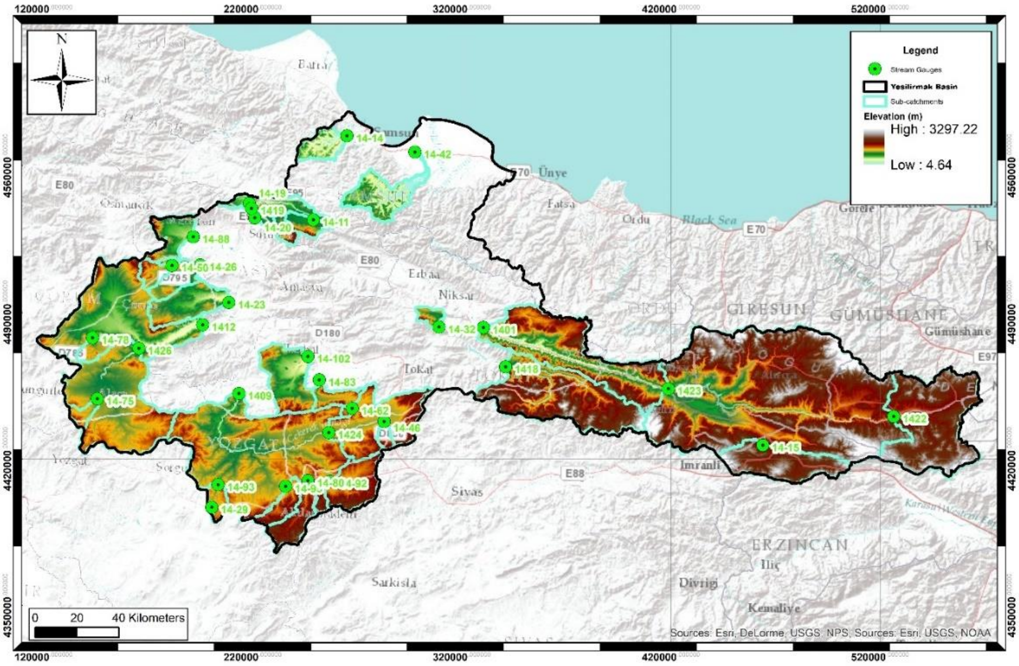

Figure 6.14. Elevation Distribution Across Study Catchments

6.4.5. Area (ARE)

One of the physical descriptors which affects hydrological response of a catchment is the surface area. Although there are numerous physical descriptors affecting the hydrological response, the scale also play an important role. Because, the increase of scale in the catchment causes an increase in heterogeneity. For example, when the area of the catchment increases, soil type, geology, land use and topographic characteristics may vary more. This means that we will expect a different hydrologic response as the catchment area increases. Unlike large catchments, small watersheds reveal a homogeneity in physical features as mentioned above such as simple geological features, topographic characteristics etc. In addition, precipitation in small catchments will generally show a more uniform spread compared to large catchments. Thus, catchment which is small reflects climatic conditions uniformly. On the other hand, catchment which is large will likely show uneven rainfall distribution (Singh, 1997).

When comparing the hydrological responses of the catchments with different rainfall areas, normalization should be done to prevent the variability of the scale and to distinguish the hydrological responses more effectively. Therefore, in this study, daily flows were normalized with the catchment area. Area distributions of study catchments is given in Figure 6.15.

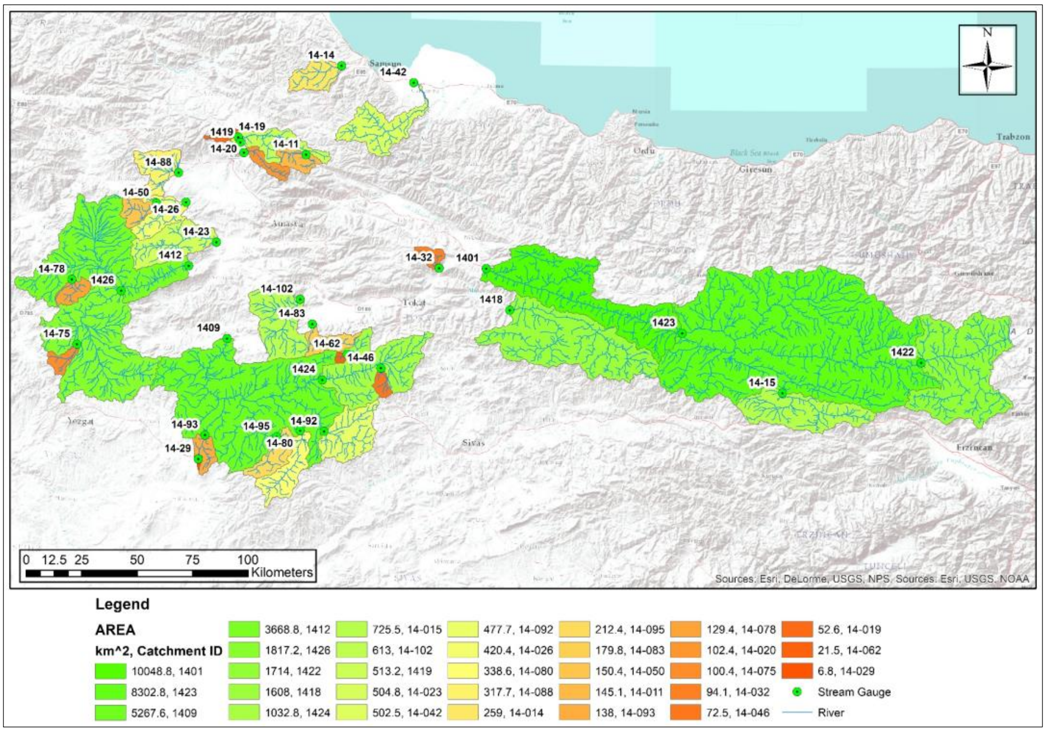

Figure 6.15. Area Distributions of Study Catchments

6.4.6. Aspect (ASP)

Aspect can be defined as the location and directions of the slopes relative to the sun. It is an essential topographic factor as it controls the direct solar radiation and wind exposure, and thus on snow and ice accumulation and ablation (Gao et al., 2017). Aspect parameter plays a decisive role in snow dominated catchments. Slopes facing in different directions are exposed to different amounts of sunlight. Accordingly, the snow-covered slopes facing south and west, respectively, are under the influence of more sunlight. It can be said that these slopes are freed from the snow cover more quickly. However, on the slopes facing north and east, the snow cover generally melts later than the south and west facing slopes. In the hydrological sense, in the catchments where the south-facing slopes are more dense, it is expected that the snow waters will melt immediately after the winter season. On the other hand, it is estimated that the snow on the slopes facing the north will melt later (Edwards et al., 2015).

Aspect Map (Table 6.3 and Figure 6.16) was created for the 31 study catchments using a 30 m resolution Digital Elevation Model.

Table 6.3 Aspect Statistics of Catchments

Catchment No.	Mean Aspect (°)	Mean Aspect
14-11	150	Southeast
14-14	172	South
14-15	179	South
14-19	134	Southeast
14-20	203	Southwest
14-23	162	South
14-26	154	Southeast
14-29	193	South
14-32	165	Southeast
14-42	179	South
14-46	136	Southeast
14-50	143	Southeast
14-62	159	South
14-75	151	Southeast
14-78	220	Southwest
14-80	184	South
14-83	194	South
14-88	144	Southeast
14-92	206	Southwest
14-93	203	Southwest
14-95	199	South
14-102	158	South
1401	181	South
1409	187	South
1412	183	South
1418	182	South
1419	186	South
1422	181	South
1423	181	South
1424	194	South
1426	183	South

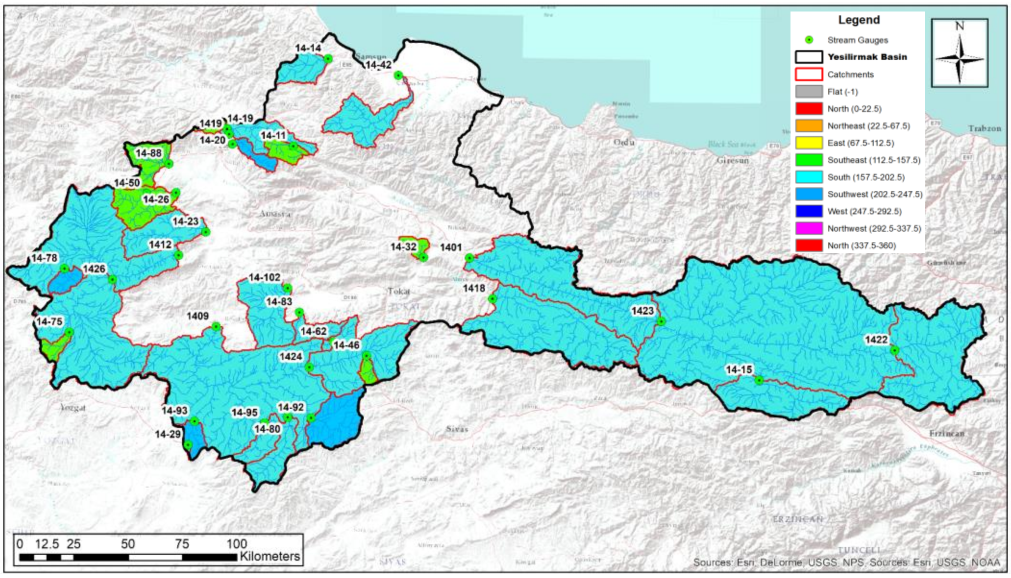

Figure 6.16. Aspect Map of Study Catchments

6.4.7. Slope (SLP)

Slope is the one of the widely used landscape descriptors in hydrology. Surface water, which is controlled by the slopes and permeability of the landsurface. The runoff flow more rapidly from the steep slopes onto the flatter slopes. Moreover, rate of runoff also depends on soil and geological features of catchments. Thus, relation between geological and soil characteristics and slope affects the hydrological response of catchments. For instance, if a catchment has flatter land slope, it will take longer time while water run off the surface. This will increase the chances of groundwater recharge in the catchment if the surface material is permeable (Winter, 2001).

In this study, slope map was prepared from a 30m resolution DEM of the study area by using 3D Analyst tool of ArcGIS software (Figure 6.17). After this step, Slope Map was classified as horizontal (0°-2°), very flat (2°-5°), flat (5°-10°), moderate (10°-25°) and steep (>25°) (Brouwer et al., 1985).

Table 6.4 Slope Statistics of Catchments

Catchment No.	Mean Slope (°)	Slope Conditions
14-11	10	Moderate
14-14	15	Moderate
14-15	13	Moderate
14-19	8	Flat
14-20	21	Moderate
14-23	12	Moderate
14-26	4	Very Flat
14-29	6	Flat
14-32	14	Moderate
14-42	17	Moderate
14-46	11	Moderate
14-50	4	Very Flat
14-62	10	Moderate
14-75	12	Moderate
14-78	5	Flat
14-80	14	Moderate
14-83	13	Moderate
14-88	16	Moderate
14-92	14	Moderate
14-93	6	Flat
14-95	11	Moderate
14-102	18	Moderate
1401	15	Moderate
1409	10	Moderate
1412	8	Flat
1418	18	Moderate
1419	9	Flat
1422	13	Moderate
1423	14	Moderate
1424	9	Flat
1426	7	Flat

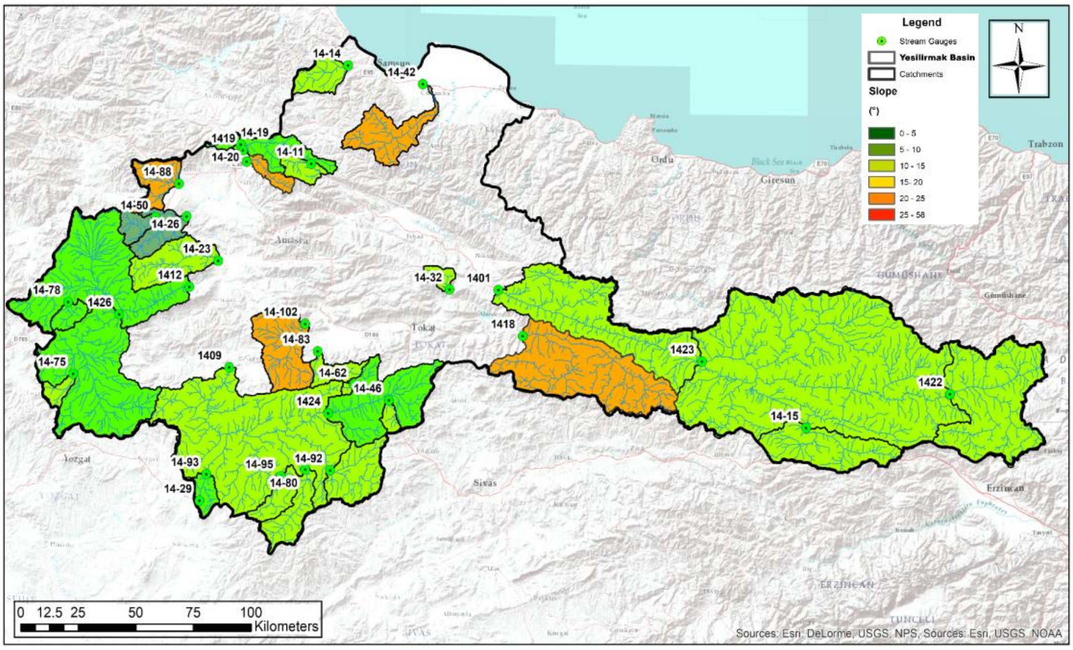

Figure 6.17. Slope Map of Study Catchments

6.5. Climatic Properties

Climatic conditions are another factor affecting the hydrological response. In this section of the report, the general information referred to in Chapter 2 will be reassessed with comments specific to the hydrological response.

Time-series data of monthly precipitation, and temperature for all studied catchments were provided by the DSI and MGM (Temelsu, 2015).

6.5.1. Precipitation (PPT)

Rainfall is one of the most important components of the hydrological cycle. The amount and density of the rainfall is a component that is proportional to the flow in a cycle from rain to flow. Under low rainfall conditions, groundwater feeds streams (effluent system).

On the other hand, in the case of high precipitation, surface water and groundwater are increasing throughout the year. This increases the hydraulic pressure in the lower flow reach and contributes to the groundwater through the riverbanks. Thus, the system returns to an influent system from effluent. Therefore, rainfall is one of the important factors affecting groundwater recharge or discharge (Brunke and Gonser, 1997). According to Gabellani et al. (2007), significant changes are observed in surface waters (especially increases in high discharges up to 25%) in storm event conditions in different size catchments. According to Segond et al. (2007), the dominant source of runoff production was characterized as rainfall according to many numerical experiments in medium size catchments. In areas exposed to intense rainfalls, infiltration capacity is also important in determining the hydrological response. Therefore, more accurate results can be obtained when the flow data and the precipitation and soil characteristics of the catchments are evaluated together (Nicotina et al., 2008).

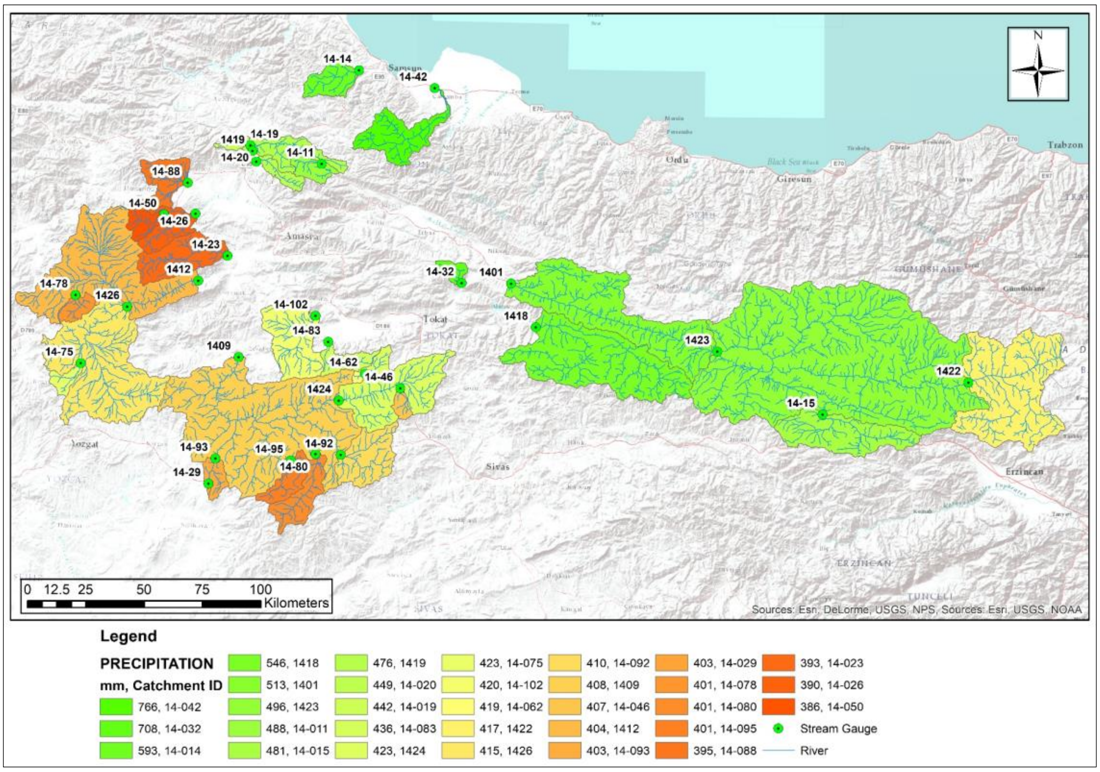

Figure 6.18. Precipitation Distribution Across Study Catchments

6.5.2. Potential Evapotranspiration (PET)

One of the key components of the hydrological cycle is potential evapotranspiration. Hagan et al. (1967) describes the potential evapotranspiration as “the idealized quantity of water evaporated per -unit area, per unit time from an idealized, extensive free water surface under existing atmospheric conditions.” Evapotranspiration, which represents a bond between soil and the atmosphere, is an important variable to consider in analyzing the impact of climate changes on water resources. According to Dooge (1992), the impact of climate change on water resources can be estimated by precipitation and potential evapotranspiration variables. As mentioned in Chapter 2, according to the availability of data, evapotranspiration values of the study catchments were calculated by Thornthwaite (1948), a Temperature-Based method. In the study conducted in the Yeşilırmak Basin, it is expected that evapotranspiration will increase, and runoff will decrease as the temperature increases. Figure 6.19 shows potential evapotranspiration distribution across study catchments.

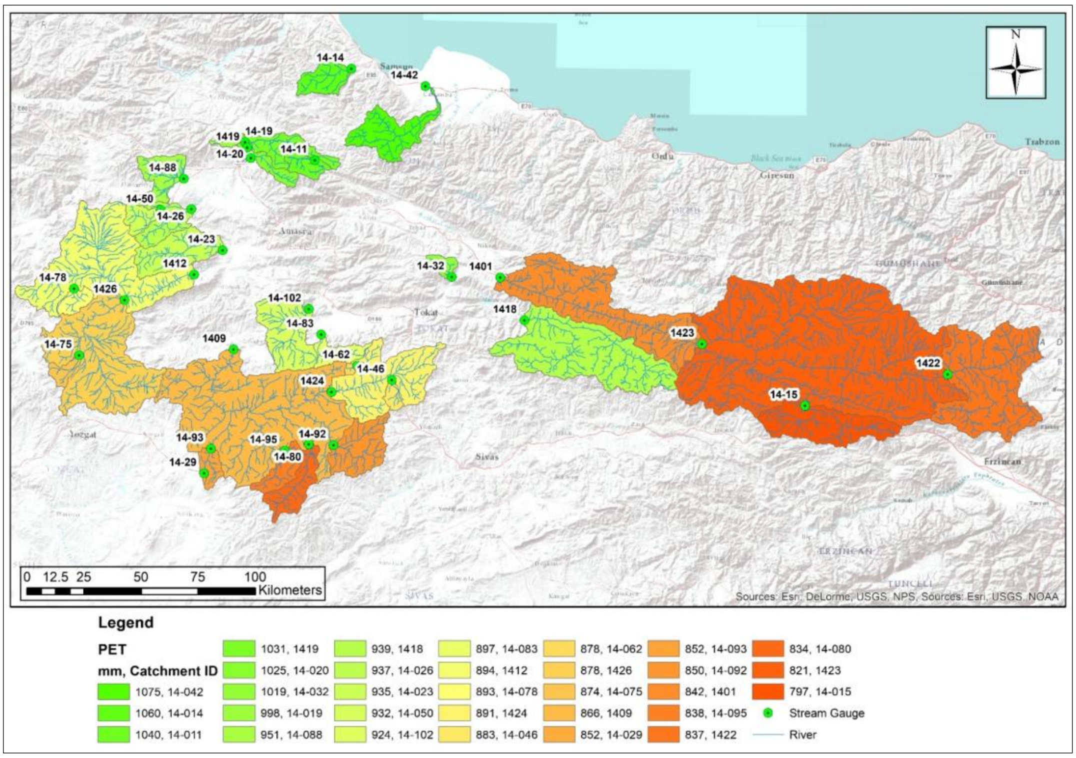

Figure 6.19. Potential Evapotranspiration Distribution Across Study Catchments

6.5.3. Aridity Index (ARI)

Aridity index is defined as the annual average rate of precipitation per year to the average potential evapotranspiration. It was first used by UNESCO (1979) to identify arid areas. In 1992, these definitions were modified. It has also been used by (Arora, 2002) and (Sawicz et al., 2014) to determine the hydrological responses of the catchments in variable climatic conditions. As the Aridity index reaches 1, the humidity of the measured area increases, so that surface water in the region is expected to be higher than in arid areas. According to Tsakiris, and Vangelis (2005), aridity index values are defined in 5 intervals (Table 6.4).

Table 6.5 Aridity Index Intervals (Tsakiris and Vangelis, 2005)

Zone	UNESCO (1979) P/PET (Penman method)	UNEP (1992) P/PET (Thornthwaite method)
Hyper-arid	< 0.03	< 0.05
Arid	0.03 – 0.20	0.05 – 0.20
Semi-arid	0.20 – 0.50	0.20 – 0.50
Sub-humid	0.50 – 0.75	0.50 – 0.65
Humid	> 0.75	> 0.65

Aridity index values were calculated to cover the years 1973-1977 in the study catchments within the Yeşilırmak basin (Table 6.5 and Figure 6.20). According to this figure, catchments 14-32 and 14-42 are classified as humid, catchments 14-14, 14-15, 1401, 1418, and 1423 are classified as sub-humid. The remaining catchments were defined as semi-arid.

Table 6.6 Aridity Index of Study Catchments

Catchment No.	Aridity Index (ARI)	ARI Interval
14-11	0.47	Semi Arid
14-14	0.56	Sub-Humid
14-15	0.60	Sub-Humid
14-19	0.44	Semi Arid
14-20	0.44	Semi Arid
14-23	0.42	Semi Arid
14-26	0.42	Semi Arid
14-29	0.47	Semi Arid
14-32	0.69	Humid
14-42	0.71	Humid
14-46	0.46	Semi Arid
14-50	0.41	Semi Arid
14-62	0.48	Semi Arid
14-75	0.48	Semi Arid
14-78	0.45	Semi Arid
14-80	0.48	Semi Arid
14-83	0.49	Semi Arid
14-88	0.42	Semi Arid
14-92	0.48	Semi Arid
14-93	0.47	Semi Arid
14-95	0.48	Semi Arid
14-102	0.45	Semi Arid
1401	0.61	Sub-Humid
1409	0.47	Semi Arid
1412	0.45	Semi Arid
1418	0.58	Sub-Humid
1419	0.46	Semi Arid
1422	0.50	Semi Arid
1423	0.60	Sub-Humid
1424	0.48	Semi Arid
1426	0.47	Semi Arid

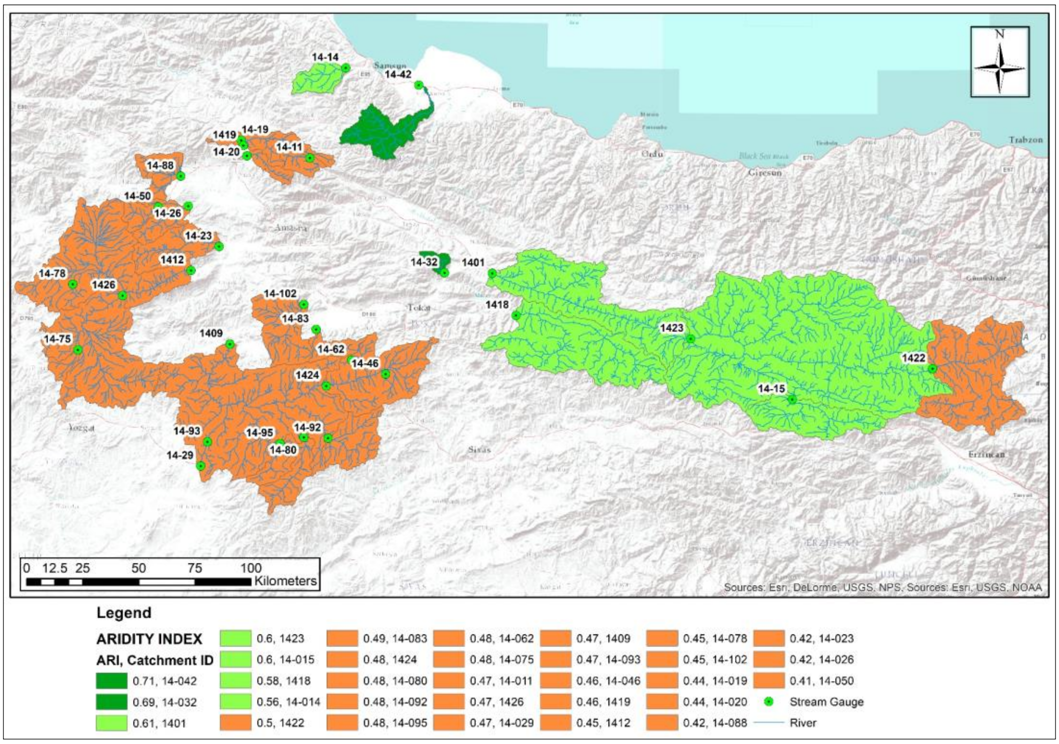

Figure 6.20. Aridity Index Distribution Across Study Catchments

CHAPTER 7

AFFINITY PROPAGATION CLUSTERING ALGORITHM

7.1. Affinity Propagation

Clustering algorithms are unsupervised machine learning algorithms that are used to explore multi-dimensional heterogeneous datasets. Clustering is defined as grouping and dividing heterogeneous data into meaningful groups. To create a meaningful group from vector data with a heterogeneous structure, the nearest distances from each center of the clusters to each other are calculated. The data sets that are closest to each other form a cluster. These clusters can be elliptical or circular. There are many types of clustering algorithms used in hydrology to find meaningful groups from heterogenous data as mentioned in background section (Section 1.1). K-means, Ward’s method, hierarchical clustering and spectral clustering are commonly used algorithms for clustering objects. However, unreasonable results can emerge according to type of algorithms for certain types of data. For example, Brusco et al. (2017) indicates that according to results of Adjusted Rand Index values, K-median clustering provides better solution than K-means clustering. Moreover, choosing appropriate number of clusters is a challenging problem for clustering algorithms like K-means, Ward’s (Milligan & Cooper, 1985) and K-median methods although they are easy to implement. In addition, initial seeds and order of data have a strong impact on clustering results for both K-means and hierarchical clustering algorithms. If the initial solution is close to the final solution, this method of solution yields effective results. Furthermore, these clustering algorithms are very sensitive to outliers and scaling used for the input data (such as Z-score normalization). Spectral clustering is another algorithm which also uses K-means clustering algorithm at the final step so beforementioned problems related to K-means clustering is also valid for spectral clustering (Brusco et al., 2019). On the other hand, affinity propagation algorithm

(Frey and Dueck, 2007) simultaneously identifies all data points as potential exemplars and exchanges real-time messages between data points until high-quality clusters occur. As a result, clustering of data by identifying sample data points rather than parametric methods, such as K-means, allows for domain-specific models that can achieve superior results. Affinity propagation is an innovative and easily expandable clustering algorithm that quickly and successfully identifies exemplars. It continually finds better solutions than standard sample-based clustering algorithms such as k-medoids and provides comparable or better results in a much shorter time for large datasets (Frey and Dueck, 2007).

Exemplar is defined as the best representative of a clustered data group. Unlike most of the clustering algorithms, such as K-means algorithm (Figure 6.1), affinity propagation simultaneously accepts all data points as potential exemplars. By examining all the points in the data network, it transmits real-time messages into the data network until the clusters occur (Figure 6.2). Affinity propagation sends 2 types of messages between two data points, responsibilities (r) and availabilities (a). Responsibilities are sent to candidate exemplar from data points. It reflects whether the sent message is evaluated as exemplar for the point receiving the message. Availabilities are sent to data points from the candidate samples and reflects the suitability of being the exemplar for the point receiving the message. All data points of affinity propagation along with the results of responsibility and availability messages are evaluated as a cluster member or exemplar. The affinity propagation algorithm is summarized in the box given in Table 6.1. At any time, a valid estimate can be obtained for cluster assignments by bringing together the messages of responsibility and availability (Dueck, 2009).

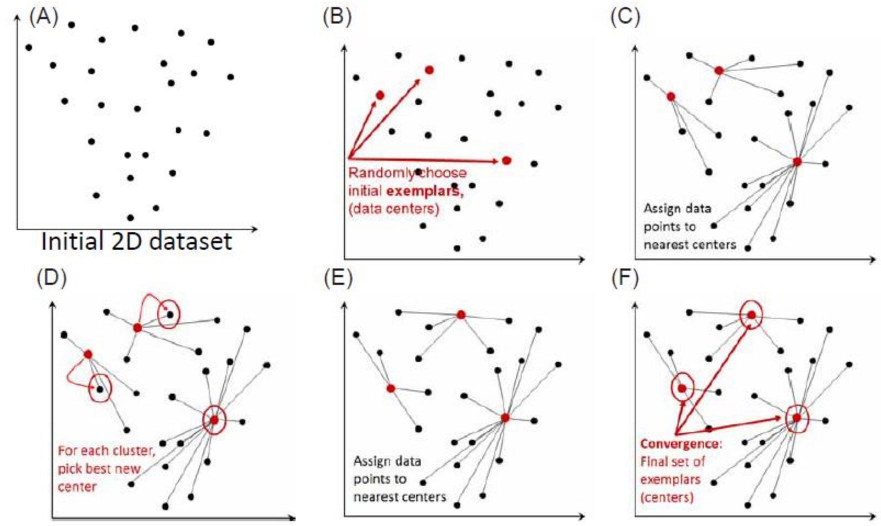

Figure 7.1. K-Means Clustering Algorithm Scheme (Dueck, 2009)

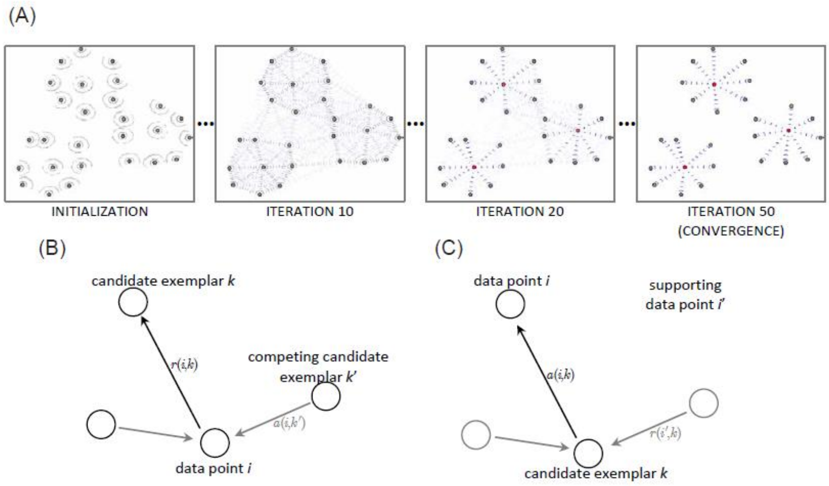

Figure 7.2. Affinity Propagation Clustering Algorithm Scheme (Dueck, 2009)

Table 7.1. Affinity Propagation Algorithm (Dueck, 2009)

AFFINITY PROPAGATION

INPUT: a set of pairwise similarities, $\{s(i,k)\}_{(i,k)\in\{1,\ldots,N\}^2, i\neq k}$ where $s(i,k)\in\mathbb{R}$ indicates how well-suited data point k is as an exemplar for data point i.

$$e.g.,\ s(i,k) = -\left\|\mathbf{x}_i - \mathbf{x}_k\right\|^2,\ i\neq k \text{ (squared Euclidean distance)}$$

For each data point k, a real number $s(k,k)$ indicating the *a priori* preference (negative cost of adding a cluster) that it be chosen as an exemplar.

$$e.g.\ s(k,k) = p \quad \forall k \in \{1,\ldots,N\} \text{ (global preference)}$$

INITIALIZATION: set availabilities to zero, $\forall i,k\colon a(i,k)=0$.

REPEAT: responsibility and availability updates until convergence

$$\forall i,k\colon\ r(i,k) = s(i,k) - \max_{k':k'\neq k}\left[s(i,k') + a(i,k')\right]$$

$$\forall i,k\colon\ a(i,k) = \begin{cases} \sum_{i':i'\neq i} \max[0,\ r(i',k)], & \text{for } k=i \\ \min\left[0,\ r(k,k)+\sum_{i':i'\notin\{i,k\}} \max[0,\ r(i',k)]\right], & \text{for } k\neq i \end{cases} \tag{1.1}$$

OUTPUT: assignments $\hat{\mathbf{c}} = (\hat{c}_1,\ldots,\hat{c}_N)$, where $\hat{c}_i = \operatorname{argmax}_k\left[a(i,k)+r(i,k)\right]$ and $\hat{c}_i$ indexes the cluster's exemplar to which point i is assigned. Specifically, if point i is in a cluster with point k serving as the exemplar, then $\hat{c}_i=k$ and $\hat{c}_k=k$. Note: one run of k-medoids may be needed to resolve contradictory solutions.

7.2. Cluster Analysis Validation

After clustering analysis, the correctness of clustering algorithm results is verified using appropriate criteria and techniques. Various validation methods are used for this task. These validation methods are divided into two groups as internal and external methods. Internal validation can be described as evaluating results of a clustering algorithm in terms of quantities that involve the vectors of the data set themselves (Halkidi et al., 2002). Silhouette Index values were used in this study for internal validation of the cluster analysis. On the other hand, External validation implies that we evaluate the results of clustering algorithm based on a pre-specified structure, which is imposed on a data set and reflects our intuition about clustering structure of the data set. Normalized Mutual Information, Cramer's V Coefficient and Adjusted Rand Index were used for external validation indices. Internal and external validation methods used in this thesis are described in sections below.

7.2.1. Silhouette Index

Silhouette Index shows how similar the sample *i* is in its own set, compared to other elements. The Silhouette index value can take values between -1 and +1. As a cluster's silhouette index becomes closer to 1, the result of the clustering analysis become more accurate. Silhouette index value is calculated from the following formula (Rousseeuw, 1987):

$$x = \frac{b(i) - a\ (i)}{\max\{a(i), b(i)\}} \tag{6}$$

Where;

s(i)= silhouette index

i= object i belong to cluster A.

a(i) = avarage dissimilarity of i to all other objects of A.

d(i, C)= average dissimilarity of i to all objects of C.

b(i)= minimum d(i, C), where C ≠ A

7.2.2. Cramer’s V Coefficient

Cramer's V coefficient measures the strength of the relationship between two variables, *IxJ,* independent of the number of rows and columns. It takes values from 0 to 1; where 0 indicates that there is no relationship. 1 shows the exact relationship between the two variables (Cramér, 1946). Cramer’s V coefficient value is calculated using the following formula:

$$\phi_c = \sqrt{\frac{X^2}{N\,(k-1)}} \tag{7}$$

$$X^2 = \sum \frac{(O_i - E_i)^2}{E_i} \tag{8}$$

Where;

ϕ_c denotes Cramér's V

χ^2 is the Pearson chi-square statistic

(O is observed value; E is expected value)

N is the sample size involved in the test, and

k is the minimum of (rows-1) or (columns-1).

7.2.3. Adjusted Rand Index

Adjusted rand index (Hubert and Arabie, 1985) is the modification of the Rand Index (Rand, 1971). Upper boundary of the index is 1. Unlike Rand Index, it can take negative values. 1 indicates that similarities between the two cluster is perfect. If we have two groups X= {X_1, X_2, …, X_r} and Y= {Y_1, Y_2, …, Y_s}, overlap between the X and Y can be given by Table 7.2 [n_{ij}], where each entry n_{ij} represents the number of objects common in X and Y (Singh et al., 2016). In this study, X and Y are two clusters sets based on flow signatures and/or catchment properties obtained by affinity propagation clustering algorithm.

Table 7.2. Contingency Table

$X \backslash Y$	Y_1	Y_2	$\ldots$	Y_s	Sums
X_1	n_{11}	n_{12}	$\ldots$	n_{1s}	a_1
X_2	n_{21}	n_{22}	$\ldots$	n_{2s}	a_2
$\vdots$	$\vdots$	$\vdots$	$\ddots$	$\vdots$	$\vdots$
X_r	n_{r1}	n_{r2}	$\ldots$	n_{rs}	a_r
Sums	b_1	b_2	$\ldots$	b_s	

Adjusted Rand Index is calculated as below:

$$\text{ARI} = \frac{\sum_{ij}\binom{n_{ij}}{2} - [\sum_i \binom{a_i}{2} \sum_j \binom{b_j}{2}]/\binom{n}{2}}{\frac{1}{2}\left[\sum_i \binom{a_i}{2} + \sum_i \binom{b_j}{2}\right] - [\sum_i \binom{a_i}{2} \sum_j \binom{b_j}{2}]/\binom{n}{2}} \tag{9}$$

7.2.4. Normalized Mutual Information

Normalized mutual information (NMI) measures shared information between two clusters (Strehl and Ghosh, 2002). The maximum value of the NMI is 1 if two sets of elements fit one to one. Normalized mutual information is calculated from the following formula:

$$X^2 = \frac{2 \text{ x } I\ (Y; C)}{[H(Y) + H\ (C)]} \tag{10}$$

$$H\ (X) = \sum_{i=1}^{n} p(x_i) \log_2(\frac{1}{p(x_i)} \tag{11}$$

Where

Y: Class labels

C: Cluster labels

I (Y;C): mutual information between two random variable Y and C

H(X): entropy of X, X will be consensus clustering while Y will be the true labels

$p(x_i)$= *probability of the* i^{th} *outcome of X*

CHAPTER 8

RESULTS AND DISCUSSIONS

In this part of the thesis, i) the relationships between the flow signatures, ii) the results of the cluster analysis for flow signatures and catchment properties using affinity propagation algorithm, and iii) the degree of agreement between clusters of flow signatures and catchment properties are investigated. Two cases were considered in clustering 31 catchments:

- CASE 1: Only 8 flow signatures were input to the clustering algorithm, namely, Flow Duration Statistics (Q5, Q50, Q95, SFDC), Runoff Ratio (RQP), Baseflow Index (BFI), Streamflow Elasticity (SFE) and Day of Half Year Flow (DHYF). The results of the cluster analysis for this case is called FLOW.

- CASE 2: For individual groups of climatic, geological, land cover and soil properties, separately; and for each variable within flow signatures, physical, climatic, geological, land cover and soil parameters, separately. Affinity propagation clustering analysis results of individual groups of climatic, geological, land cover, topography and soil properties are called as CLIM, GEO, LCOV, TOPO and SOIL respectively. Abbreviations of each flow signature and catchment properties is given in Table 8.1

Table 8.1. Abbreviations for Each Flow Signatures

Group Abbreviations	Variable Abbreviations	Description	Minimum Value	Maximum Value
Flow Signatures (FLOW)	Q5	5th Percentile Exceedance Flow	0.201	3.600
	Q50	50th Percentile Exceedance Flow	0.011	0.589
	Q95	95th Percentile Exceedance Flow	0.000	0.186
	SFDC	Slope of Flow Duration Curve	0.585	3.807
	RQP	Runoff Ratio	0.0002	0.0019
	BFI	Baseflow Index	0.571	0.896
	SFE	Streamflow Elasticity	-6.35	9.22
	DHYF	Day of Half Year Flow	165	225
Geological Properties (GEO)	ALV	Percentage of Alluvium (%)	0.00	29.41
	CAR	Percentage of Carbonate Rocks (%)	0.00	60.25
	VOR	Percentage of Volcanic Rocks (%)	0.00	72.19
Soil Properties (SOIL)	CLSL	Percentage of Clay and Silt (%)	58.38	71.80
	SND	Percentage of Sand (%)	27.89	41.62
Landcover Properties (LCOV)	IAL	Permanently Irrigated Arable Land (%)	0.00	36.60
	CN	Runoff Curve Number	56.95	79.91
Topographic Properties (TOPO)	HI	Hypsometry Integral	0.20	0.61
	LFP	Longest Flow Path (m)	1976.31	317980.90
	DRD	Drainage Density (km^{-1})	0.29	0.55
	ELV	Elevation (m), Mean	644.37	1900.12
	ARE	Area (km^2), Mean	6.80	10048.80
	ASP	Mean Aspect (°)	134	220
	SLP	Mean Slope (°)	4.25	21.44
Climatic Properties (CLIM)	PPT	Mean Annual Precipitation (mm)	386.27	766.40
	PET	Mean Annual Potential Evapotranspiration (mm)	797.62	1075.93
	ARI	Aridity Index	0.41	0.71

In the analysis, the Silhouette values - an internal cluster validation technique - were used to investigate the quality and cohesion of the clustering (Böse et al., 2011) (Figure 8.1). Since each variable have different units, Z-Score Normalization (Montgomery and Runger, 2007, p.164) was performed before Affinity Propagation clustering analysis was applied. In the individual groupings, the actual values of each variable were used. Results and relation of each and individual groups of flow signatures and catchment properties will be discussed with the help of the external cluster validation techniques in Section 8.3.

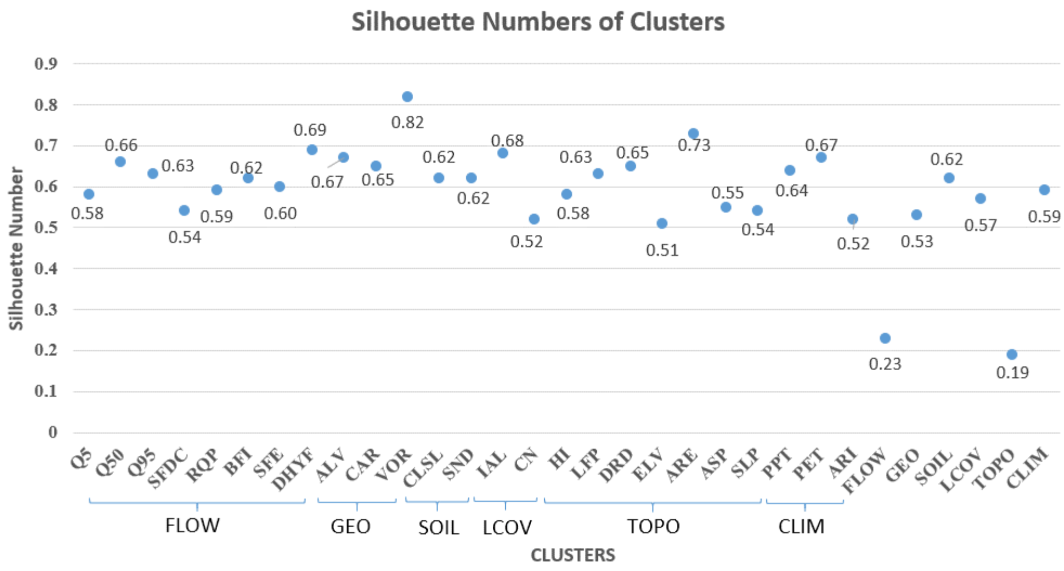

Figure 8.1. Silhouette Numbers of Clusters (see Table 8.1 for abbreviations).

8.1. Relationships between Flow Signatures

This section investigates possible relationships between eight flow signatures used in this study. Figure 8.2 and Table 8.2 show the relationships between eight flow signatures based on Pearson (1896) and Spearman (1904) methods to enable investigation of both linear and nonlinear relationships between these signatures. Focusing on the flow signatures, the highest correlation values were obtained between SFDC and BFI (negative correlation) and between RQP and Q5, Q50 and Q95 values obtained from the Flow Duration Curve (positive correlation).

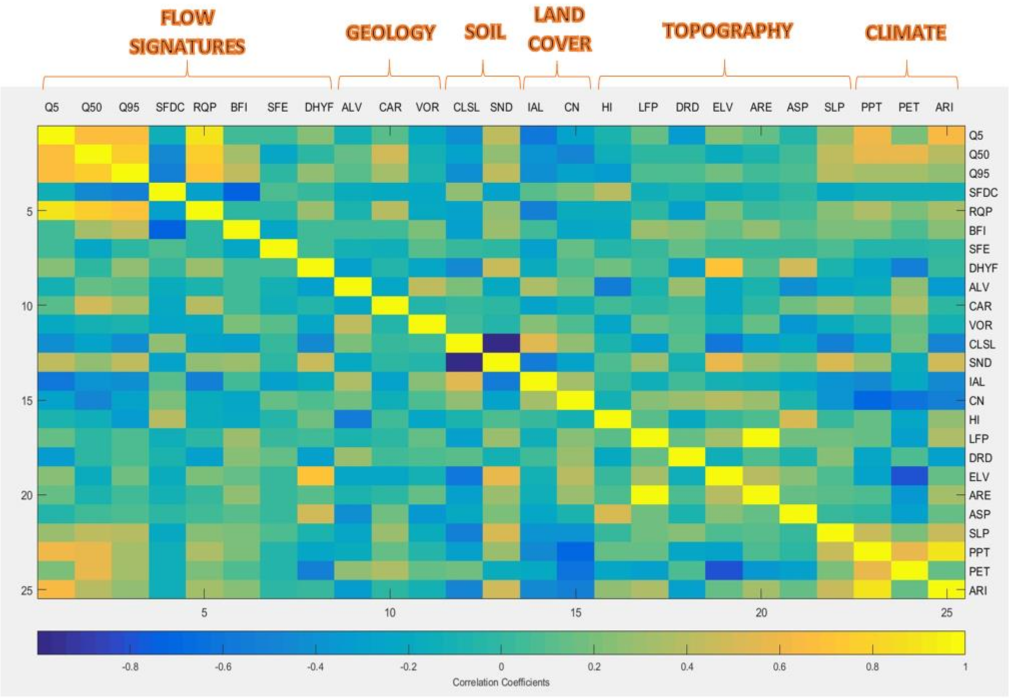

Figure 8.2. Signature Relationship Matrix (see Table 8.1 for abbreviations).

Table 8.2. Flow Signatures Correlation Coefficients

Flow Signatures	Q_5	Q_{50}	Q_{95}	SFDC	RQP	BFI	SFE	DHYF	Correlation Coefficient
Q_5	1	0.69	0.66	-0.16	0.88	0.08	-0.19	0.23	Pearson
		0.76	0.56	-0.20	0.94	0.25	-0.06	0.26	Spearman
	Q_{50}	1	0.78	-0.47	0.77	0.32	-0.29	-0.20	Pearson
			0.73	-0.52	0.80	0.46	-0.32	-0.15	Spearman
		Q_{95}	1	-0.52	0.71	0.47	-0.15	0.25	Pearson
				-0.67	0.53	0.76	-0.13	0.20	Spearman
			SFDC	1	-0.29	-0.78	0.03	0.00	Pearson
					-0.29	-0.83	0.15	-0.09	Spearman
				RQP	1	0.07	-0.20	0.30	Pearson
						0.27	-0.13	0.29	Spearman
					BFI	1	-0.11	0.13	Pearson
							-0.17	0.20	Spearman
						SFE	1	-0.05	Pearson
								-0.21	Spearman
							DHYF	1	Pearson
									Spearman

The spatial distributions of the clusters for each of the flow signatures are given in Figure 8.3, whereas the distribution of the signature values within each cluster are listed in Table 8.3. The results of the cluster analysis show that, the catchments with high Q5 value, which is one of the flow signatures that symbolize the high surface flows in the basin, are seen along Samsun and

Kelkit Valley, north of Amasya. As moving from the northern part of the basin towards the east, the catchments 14-11, 14-42, 14-32, 1401, 1418, 1423 and 14-15 are marked by high Q5 values. Q5 values are low in the south and south west of the basin. The Q50 and Q95 values are higher to the north and east of the basin, as in the case of Q5 values, with generally low values in the west and south. SFDC values show a heterogeneous spread in the basin. The catchments having high SFDC are characterized by flashy flow response. Thus, in the event of a precipitation, a rapid flow increase is observed immediately after the rainfall and when the precipitation is reduced the flow conditions return back to the normal conditions in a short time (Gordon et al., 2004). 14-46, 14-78, 14-102, 1426, 14-19, 14-29 and 14-26 are the catchments where SFDC values are high. RQP flow signature shows a similar spatial pattern with the Q5, Q50 and Q95 flow signatures. According to this; The RQP values are high in the catchments 14-11, 14-20, 14-19 located to the north of the study area except for 14-29 and 14-75. In addition, RQP values are high in the catchments with high-elevation and humid catchments, namely 1401, 1418, 1423 and 14-15 located in the Kelkit Valley in the east of the basin. This finding is in line with Sankarasubramanian and Vogel (2003) and Sawicz (2013). The SFE and baseflow index BFI values show the most heterogeneous spatial distribution. As expected, the value of DHYF -indicating snow potential - is generally correlated with the elevation of the catchments.

Table 8.3. Clustering results for individual flow signatures

Cluster No.	Catchment No.	Q5	Cluster No.	Catchment No.	Q50	Cluster No.	Catchment No.	Q95	Cluster No.	Catchment No.	SFDC	Cluster No.	Catchment No.	RQP	Cluster No.	Catchment No.	BFI	Cluster No.	Catchment No.	SFE	Cluster No.	Catchment No.	DHYF
CL1	14-11	3.275	CL1	14-11	0.589	CL1	14-11	0.173	CL1	14-11	0.771	CL1	14-19	0.328	CL1	14-15	0.896	CL1	14-29	6.690	CL1	14-11	209
	1418	3.600		14-20	0.548		14-20	0.186		14-15	0.796		14-32	0.304		14-26	0.873		14-83	7.388		14-15	209
CL2	14-19	1.643		14-42	0.499	CL2	14-15	0.149		14-20	0.621		14-46	0.333		14-62	0.866		1418	6.283		14-20	204
	14-20	1.941	CL2	14-19	0.094		1418	0.148		14-26	0.720		14-62	0.303		1401	0.862	CL2	14-75	-6.348		14-29	210
	14-75	1.635		14-26	0.107	CL3	14-14	0.033		14-88	0.585		1401	0.375		1418	0.885	CL3	14-88	9.220		14-62	208
	1419	1.645		14-29	0.114		14-19	0.011		1419	0.809		1419	0.383		1423	0.870		14-93	9.749		14-80	209
	1422	1.346		14-50	0.080		14-42	0.018	CL2	14-19	2.185		1422	0.275	CL2	14-11	0.826	CL4	14-23	3.029		14-92	204
CL3	14-15	2.501		14-62	0.100		14-62	0.012		14-23	2.026	CL2	14-11	0.708		14-19	0.808		14-32	3.166		14-93	209
	14-29	2.351		14-80	0.102		14-92	0.015		14-29	2.152		14-20	0.617		14-23	0.797		14-46	4.823		14-95	211
	14-32	2.571		14-83	0.077		14-93	0.014		14-83	1.906		14-29	0.662		14-32	0.825		14-102	3.618		1401	205
	14-42	2.665		14-92	0.111		1422	0.021		1426	2.398		1418	0.592		14-42	0.814		1409	4.293		1418	205
	14-46	2.205		14-93	0.081	CL4	14-23	0.001	CL3	14-46	3.807	CL3	14-15	0.491		14-50	0.810		1423	3.151		1422	211
	1401	2.218		14-95	0.122		14-29	0.000		14-78	3.332		14-42	0.451		14-75	0.804	CL5	14-11	0.422		1423	208
	1423	2.248		1409	0.084		14-46	0.000		14-102	2.996		14-75	0.404		14-78	0.795		14-15	1.823	CL2	14-78	225
CL4	14-14	1.268		1422	0.104		14-50	0.003	CL4	14-50	1.455		1423	0.396		14-80	0.822		14-19	2.316	CL3	14-26	187
	14-50	0.833		1424	0.095		14-75	0.000		14-62	1.099	CL4	14-14	0.270		14-95	0.819		14-20	0.964		14-32	195
	14-62	1.165	CL3	14-14	0.274		14-78	0.001		14-75	1.273		14-26	0.170		1412	0.821		14-26	2.079		14-46	195
	14-80	1.021		14-15	0.274		14-80	0.010		14-80	1.295		14-50	0.207	CL3	14-29	0.600		14-42	1.291		14-50	188
	14-83	0.937		14-75	0.301		14-83	0.000		14-92	1.145		14-80	0.230		14-46	0.571		14-50	1.892		14-83	193
	14-92	1.003		1418	0.330		14-88	0.008		1401	1.285		14-83	0.179	CL4	14-83	0.686		14-80	1.842		1409	190
	14-93	1.127		1419	0.303		14-95	0.006		1409	1.262		14-92	0.211		14-102	0.735		14-92	1.160		1424	189
	14-95	1.098	CL4	14-23	0.036		14-102	0.001		1418	1.125		14-93	0.266		1426	0.736		14-95	0.532		1426	190
	1409	1.104		14-46	0.011		1409	0.005		1422	1.064		14-95	0.263	CL5	14-14	0.844		1401	2.362	CL4	14-14	183
	1424	1.146		14-78	0.067		1412	0.001		1423	1.436		1409	0.211		14-20	0.846		1419	1.577		14-19	178
	1426	0.832		14-88	0.033		1424	0.008		1424	1.345		1424	0.217		14-88	0.848		1424	2.518		14-23	177
CL5	14-23	0.342		14-102	0.044		1426	0.000	CL5	14-14	1.511	CL5	14-23	0.078		14-92	0.837	CL6	14-14	-1.725		14-42	165
	14-26	0.617		1412	0.054	CL5	14-26	0.041		14-32	1.489		14-78	0.159		14-93	0.834		14-62	-1.062		14-75	178
	14-78	0.768		1426	0.054		14-32	0.062		14-42	1.668		14-88	0.061		1409	0.842		14-78	-1.522		14-88	183
	14-88	0.201	CL5	14-32	0.193		1401	0.058		14-93	1.856		14-102	0.102		1419	0.842		1412	-0.593		14-102	182
	14-102	0.536		1401	0.176		1423	0.060		14-95	1.715		1412	0.116		1422	0.839		1422	-3.227		1412	182
	1412	0.560		1423	0.161	CL6	1419	0.115		1412	1.653		1426	0.137		1424	0.842		1426	-1.615		1419	179

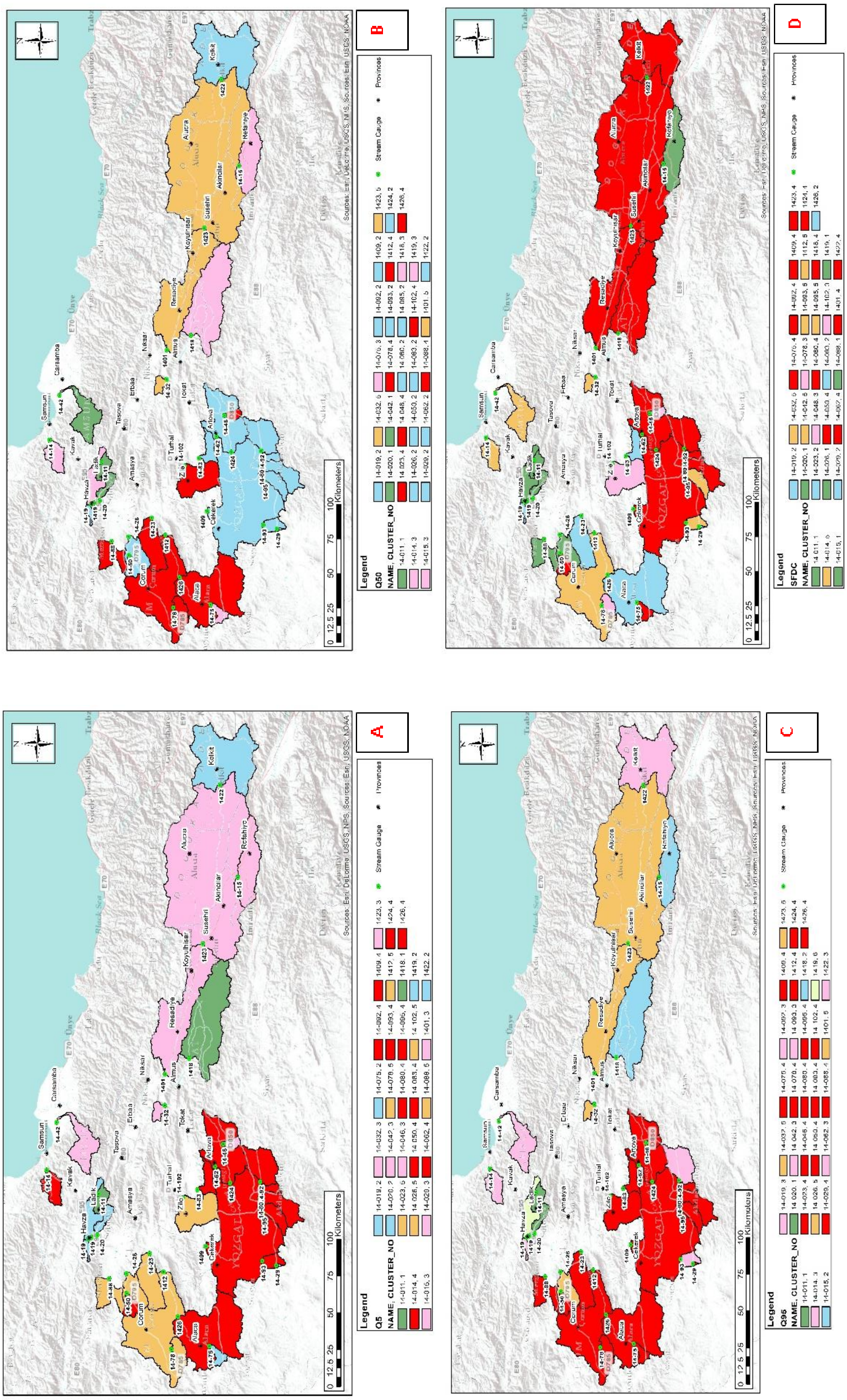

Figure 8.3. Cluster Maps based on Flow Signatures, (a) Q5, (b) Q50, (c) Q95, (d) SFDC

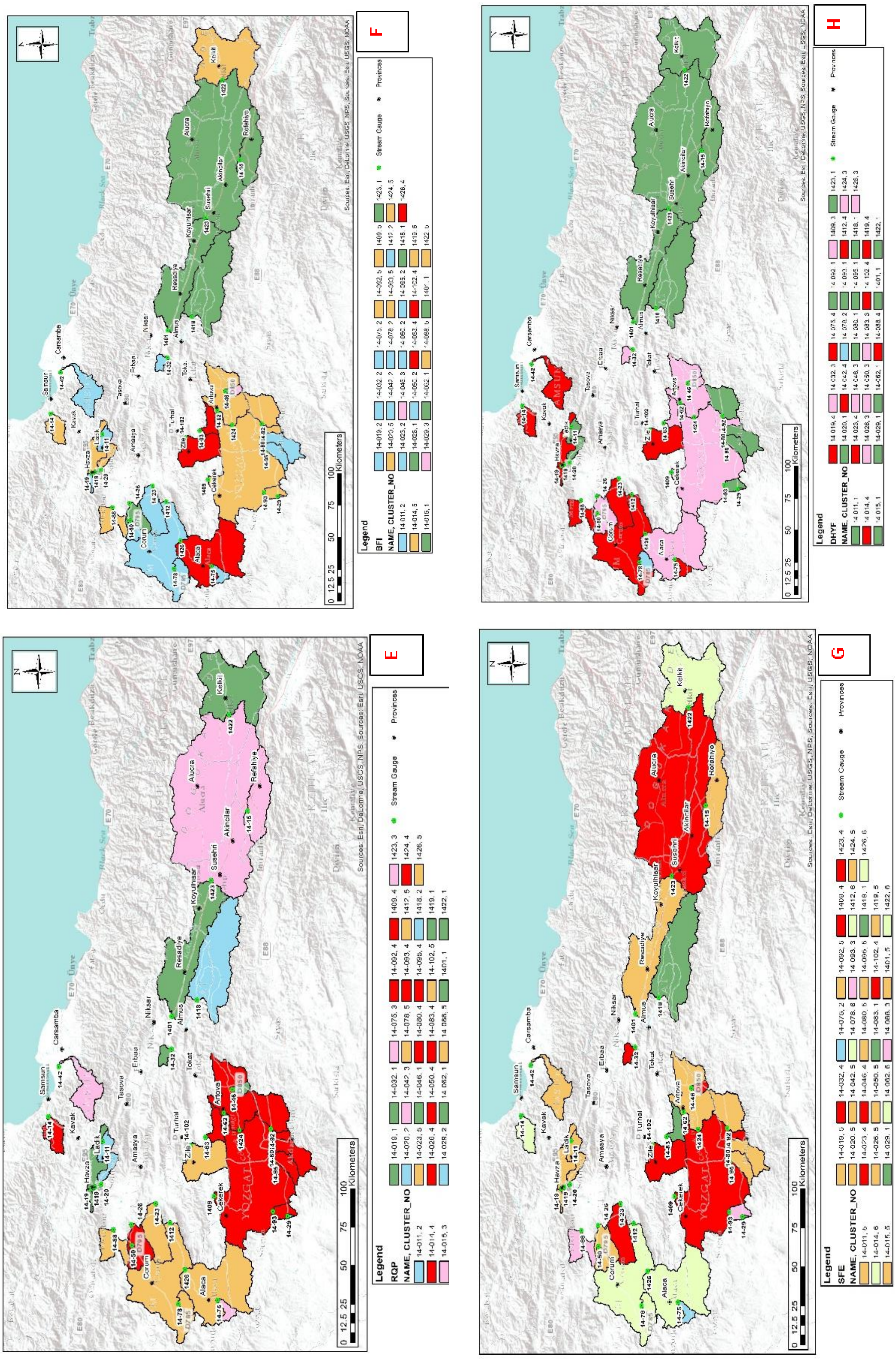

Figure 8.3 Cont'd, (e) RQP, (f) BFI, (g) SFE, (d) DHYF

8.2. Results

The results of Affinity Propagation clustering analysis are provided below for the two cases described above and the clusters were further interpreted to deduce hydrologically meaningful information. Note that in Case 1, clustering algorithm is run using all flow signatures and resulting clusters are then linked to their climatic and physical properties via interpretation. In Case 2, climatic, geologic, soil, topography and landcover descriptors were grouped separately and input to the clustering algorithm (5 algorithm runs). The clusters obtained in this case were then validated with the clusters obtained in Case 1 (flow signatures only) using external validation metrics. To help in the evaluation process, the clusters were also obtained for all the individual descriptors separately (25 algorithm runs).

Case 1

In the first case, affinity propagation clustering analysis was performed for 31 catchments using a group of 8 flow signatures as input, namely Flow Duration Statistics (Q5, Q50, Q95, SFDC), RQP, BFI, SFE and DHYF. The results of the cluster analysis for this case is called FLOW.

The spatial distribution of the clusters is given in Figure 8.4 and flow signature values of each cluster are listed in Table 8.4. In Case 1, 31 study catchments are grouped into six clusters according to Affinity Propagation clustering results. The Table 8.4 shows the distribution of the catchment properties in the basins that are clustered based on FLOW (Case 1). The results are discussed below with the help of geographical location and catchment properties.

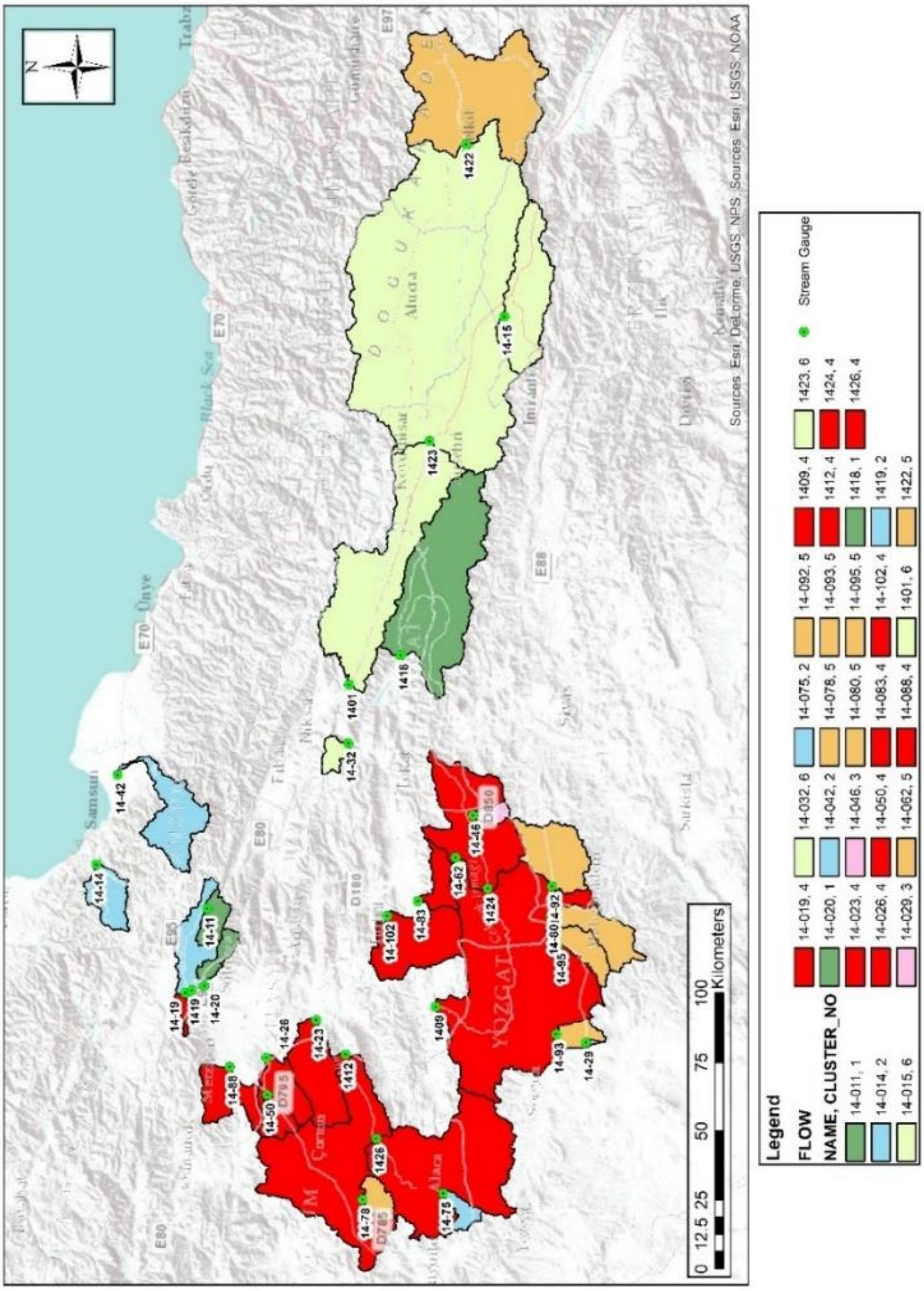

Figure 8.4. Cluster Maps of Catchments (FLOW)

Table 8.4. Catchment Properties of Each Cluster

Cluster No.	Catchment No.	Q5	Q50	Q95	SFDC	RQP	BFI	SFE	DHYF	ALV	CAR	VOR	CLSL	SND	IAL	CN	HI	LFP	DRD	ELV	ARE	ASP	SLP	PPT	PET	ARI
CL1	14-11	3.275	0.589	0.173	0.771	0.708	0.826	0.422	209	29.41	13.49	0.00	65.84	34.16	1.61	70.09	0.20	17158.35	0.43	1086.52	145.10	150.02	9.91	488.79	1040.51	0.47
	14-20	1.941	0.548	0.186	0.621	0.617	0.846	0.964	204	1.61	60.25	0.98	65.20	34.80	0.00	68.49	0.37	27063.20	0.48	1172.98	102.40	203.47	21.44	449.47	1025.39	0.44
	1418	3.600	0.330	0.148	1.125	0.592	0.885	6.283	205	1.92	5.06	7.25	62.53	37.47	0.13	72.64	0.42	92403.96	0.41	1599.61	1608.00	181.90	17.80	546.30	939.34	0.58
CL2	14-14	1.268	0.274	0.033	1.511	0.270	0.844	-1.725	183	0.60	30.43	19.31	66.26	33.74	0.00	57.10	0.43	32987.08	0.38	656.74	259.00	172.08	15.22	593.05	1060.55	0.56
	14-42	2.665	0.499	0.018	1.668	0.451	0.814	1.291	165	4.37	27.10	10.08	68.17	31.83	0.20	65.24	0.52	68725.28	0.43	644.37	502.50	179.23	17.18	766.40	1075.93	0.71
	14-75	1.635	0.301	0.000	1.273	0.404	0.804	-6.348	178	11.25	10.94	0.00	70.10	29.90	26.36	75.60	0.47	16297.05	0.41	1235.02	100.40	150.81	11.92	423.17	874.67	0.48
	1419	1.645	0.303	0.115	0.809	0.383	0.842	1.577	179	13.14	9.41	10.68	68.72	31.28	3.02	72.08	0.25	56894.20	0.42	941.24	513.20	186.36	8.75	476.72	1031.15	0.46
CL3	14-29	2.351	0.114	0.000	2.152	0.662	0.600	6.690	210	0.00	26.72	0.00	71.60	28.40	0.05	79.91	0.42	1976.31	0.29	1270.15	6.80	193.14	5.70	403.82	852.39	0.47
	14-46	2.205	0.011	0.000	3.807	0.333	0.571	4.823	195	3.71	3.92	0.00	66.70	33.30	0.84	79.27	0.40	14435.01	0.41	1404.52	72.50	136.34	11.27	407.94	883.56	0.46
CL4	14-19	1.643	0.094	0.011	2.185	0.328	0.808	2.316	178	1.63	23.66	0.00	70.15	29.85	0.00	77.66	0.27	16941.34	0.48	902.95	52.60	134.38	8.32	442.21	998.06	0.44
	14-23	0.342	0.036	0.001	2.026	0.078	0.797	3.029	177	5.26	14.54	0.00	70.89	29.11	23.15	78.87	0.37	48443.64	0.43	958.68	504.80	162.43	11.91	393.75	935.49	0.42
	14-26	0.617	0.107	0.041	0.720	0.170	0.873	2.079	187	13.44	28.79	32.07	69.60	30.40	21.80	79.12	0.41	38327.64	0.42	1094.58	420.40	154.11	4.25	390.81	937.13	0.42
	14-50	0.833	0.080	0.003	1.455	0.207	0.810	1.892	188	23.62	2.38	72.19	68.81	31.19	27.24	75.95	0.27	22325.33	0.39	1226.78	150.40	143.40	4.18	386.27	932.93	0.41
	14-83	0.937	0.077	0.000	1.906	0.179	0.686	7.388	193	5.83	13.73	0.00	65.90	34.10	10.05	73.50	0.55	37062.90	0.42	1262.78	179.80	194.15	13.06	436.63	897.76	0.49
	14-88	0.201	0.033	0.008	0.585	0.061	0.848	9.220	183	13.32	4.63	35.33	68.40	31.60	10.31	76.40	0.30	28908.96	0.55	986.98	317.70	143.94	16.26	395.93	951.46	0.42
	14-102	0.536	0.044	0.001	2.996	0.102	0.735	3.618	182	17.65	13.08	7.20	69.99	30.01	24.35	75.86	0.32	39529.39	0.48	993.09	613.00	157.74	18.49	420.05	924.53	0.45
	1409	1.104	0.084	0.005	1.262	0.211	0.842	4.293	190	6.69	8.51	2.14	67.83	32.17	6.40	75.59	0.38	163498.29	0.42	1273.43	5267.60	187.35	9.58	408.41	866.74	0.47
	1412	0.560	0.054	0.001	1.653	0.116	0.821	-0.593	182	13.21	7.20	5.40	70.37	29.63	19.21	77.21	0.43	125472.68	0.48	1076.64	3668.80	183.10	7.71	404.77	894.12	0.45
	1424	1.146	0.095	0.008	1.345	0.217	0.842	2.518	189	12.82	5.39	0.00	68.91	31.09	18.67	77.31	0.29	57383.89	0.44	1333.56	1032.80	193.61	8.98	423.64	891.31	0.48
	1426	0.832	0.054	0.000	2.398	0.137	0.736	-1.615	190	10.16	4.34	2.00	71.79	28.21	17.83	77.58	0.44	87308.01	0.47	1143.81	1817.20	182.94	6.82	415.87	878.17	0.47
CL5	14-62	1.165	0.100	0.012	1.099	0.303	0.866	-1.062	208	0.00	8.65	0.00	72.11	27.89	36.60	70.46	0.38	5625.96	0.34	1370.91	21.50	158.85	9.90	419.62	878.95	0.48
	14-78	0.768	0.067	0.001	3.332	0.159	0.795	-1.522	225	3.26	10.88	0.08	67.84	32.16	21.12	75.81	0.61	15970.78	0.41	1181.58	129.40	220.42	5.16	401.92	893.41	0.45
	14-80	1.021	0.102	0.010	1.295	0.230	0.822	1.842	209	2.85	3.53	0.00	58.38	41.62	2.36	69.33	0.44	42804.55	0.41	1608.43	338.60	184.00	14.26	401.89	834.10	0.48
	14-92	1.003	0.111	0.015	1.145	0.211	0.837	1.160	204	7.06	10.90	0.00	66.75	33.25	2.35	74.83	0.38	31422.96	0.44	1449.46	477.70	205.80	14.09	410.16	850.33	0.48
	14-93	1.127	0.081	0.014	1.856	0.266	0.834	9.749	209	0.00	9.96	4.45	71.80	28.20	6.12	73.52	0.47	20057.65	0.46	1236.26	138.00	203.09	6.39	403.90	852.03	0.47
	14-95	1.098	0.122	0.006	1.715	0.263	0.819	0.532	211	0.21	9.12	0.00	62.52	37.48	1.90	71.37	0.46	26420.12	0.39	1440.10	212.40	199.07	11.18	401.84	838.78	0.48
	1422	1.346	0.104	0.021	1.064	0.275	0.839	-3.227	211	4.50	23.29	7.94	64.02	36.00	5.52	78.61	0.31	71885.55	0.41	1836.13	1714.00	180.95	12.90	417.24	837.74	0.50
CL6	14-15	2.501	0.274	0.149	0.796	0.491	0.896	1.823	209	4.58	8.27	0.64	61.50	38.50	5.59	75.97	0.35	52818.79	0.45	1900.12	725.50	178.71	13.40	481.03	797.62	0.60
	14-32	2.571	0.193	0.062	1.489	0.304	0.825	3.166	195	4.77	0.00	0.00	63.71	36.29	0.00	56.95	0.40	16164.60	0.32	1112.16	94.10	164.73	14.23	708.21	1019.85	0.69
	1401	2.218	0.176	0.058	1.285	0.375	0.862	2.362	205	3.53	17.11	21.86	62.71	37.29	2.92	78.07	0.45	317980.90	0.42	1643.46	10048.80	181.13	14.73	513.77	842.50	0.61
	1423	2.248	0.161	0.060	1.436	0.396	0.870	3.151	208	3.90	16.25	19.93	62.44	37.56	3.44	78.71	0.39	212127.10	0.42	1723.57	8302.80	181.12	14.49	496.15	821.00	0.60

The catchments in the CL1 class are 14-11 and 14-20 located in the north of Yeşilırmak Basin and 1418 located between Tokat and Susehri (Figure 8.4). Class CL1 is represented by high Q5, Q50, Q95, RQP, BFI, DHYF and low SFDC values. SFE values in the catchments showed a heterogeneous distribution. Geologically, the ALV in the 14-11 catchment and the CAR ratios in the 14-20 catchment have the highest values in the studied catchments (Table 8.4). When Q95 values are examined; the highest two Q95 values are observed in this class (CL1). High Q95 values indicate more sustained baseflow conditions (groundwater) which are then related to high ALV and CAR percentages. In the catchment 1418, no geologically distinct distribution was observed. However, 1418 is situated at higher elevations than 14-11 and 14-20. In addition, the catchment area of 1418 is approximately 10 times larger than these catchments. Therefore, PPT and water collected in 1418 is higher than 14-11 and 14-20. In addition, SND and ARI values of the 1418 were higher than the other two catchments. These characteristics indicate why the groundwater and surface water signatures of 1418 are close to the other two catchments in this class. High Baseflow index value for catchment 1418 also indicates the contribution from groundwater. Apart from these distinguishing characteristics, no other characteristic was different in CL1 class compared to other classes.

The catchments in cluster CL2 (1419, 14-14 and 14-42) are located to the north, in the vicinity of Samsun, except catchment 14-75, located towards the south west of the Yeşilırmak basin (Figure 8.4). These catchments are characterized by high Q5, Q50, RQP and low DHYF values (Table 8.4). These flow signature characteristics could be related to high precipitation and evapotranspiration and low elevation as shown in Table 8.4.

The two catchments in CL3 class (14-29 and 14-46) are characterized by very low Q95 values (actually streams dry out), and relatively high Q5, SFDC and SFE values. These flow signatures characterize catchments with flashy streamflow response (rapid flow response to rain events). These flow signature values are also supported by catchment physical properties including smallest area values and highest curve number values among the 31 study catchments. Note that high curve number values indicate that precipitation dominantly converts into direct flow and hence groundwater recharge is low.

Eleven catchments in CL4 cluster are very distinct in terms of low values of all the flow signatures. These catchments are located towards the southwest of the Yeşilırmak basin, characterized by low precipitation and arid conditions (low aridity index values). These catchments are located on the wide alluviums of the rivers (high alluvium percentage) with low slopes and high permanent irrigated arable land.

Seven catchments in cluster CL5 are located to the south (14-93, 14-95, 14-80, 14-92, 14-62), southwest (14-78), and to the west end (1422) of the Yeşilırmak basin (Figure 8.4). These catchments are characterized by moderate flow signature values, except DHYF being high (indicating snowmelt). Their climatic characteristics are represented by low to moderate precipitation and low evapotranspiration. Physical characteristics are distinct in terms of high elevations – explaining high day of half year flow signature. Being situated in high elevations alluvium percentage is also low in these catchments.

Four catchments in cluster CL6 (14-15, 14-32, 1401, 1423) are located to the east of Yeşilırmak Basin. These catchments are characterized by high to moderate flow signatures, except SFDC being low. In terms of climate, these catchments have the highest aridity index values, indicating humid conditions with high precipitation and low potential evapotranspiration. In terms of physical characteristics, these catchments are situated at highest elevations with moderate slope values. Their sand percentage is also high. Note that the catchment 14-32 differs from other catchments in the CL6 cluster with low area and low elevation values. However, humid climatic characteristics compensates for this fact and reflected in the moderate to high flow signatures.

Case 2

As mentioned earlier, in Case 2 affinity propagation clustering algorithm is first applied for individual groups of climatic, topographic, geological, land cover and soil properties, separately and hence clustering algorithm was run 5 times. Next, the algorithm was run for each of the descriptors in flow signatures, physical, climatic, geological, land cover and soil characteristics, separately, thus having a total of 25 runs. Affinity propagation clustering analysis results of each flow signatures and catchment properties are given in Appendix A and B. The results of the clustering algorithm for individual groups of climatic, geological, land cover, topography and soil properties are called as CLIM, GEO, LCOV, TOPO and SOIL respectively and given in Table 8.5. In this section, cluster results of CLIM, GEO, LCOV, TOPO and SOIL is discussed.

Table 8.5. Cluster Analysis Result of GEO, SOIL, LCOV, TOPO and CLIM

GEO					SOIL				LCOV				TOPO									CLIM				
Cluster No.	Catchment No.	ALV	CAR	VOR	Cluster No.	Catchment No.	CLSL	SND	Cluster No.	Catchment No.	IAL	CN	Cluster No.	Catchment No.	HI	LFP	DRD	ELV	ARE	ASP	SLP	Cluster No.	Catchment No.	PPT	PET	ARI
CL1	14-11	29.41	13.49	0.00	CL1	14-11	65.84	34.16	CL1	14-14	0.00	57.10	CL1	14-11	0.20	17158.35	0.43	1086.52	145.10	150.02	9.91	CL1	14-14	593.05	1060.55	0.56
CL2	14-15	4.58	8.27	0.64		14-14	66.26	33.74		14-32	0.00	56.95		14-14	0.43	32987.08	0.38	656.74	259.00	172.08	15.22	CL2	14-23	393.75	935.49	0.42
	14-23	5.26	14.54	0.00		14-20	65.20	34.80	CL2	14-62	36.60	70.46		14-19	0.27	16941.34	0.48	902.95	52.60	134.38	8.32		14-26	390.81	937.13	0.42
	14-32	4.77	0.00	0.00		14-46	66.70	33.30	CL3	14-23	23.15	78.87		14-23	0.37	48443.64	0.43	958.68	504.80	162.43	11.91		14-50	386.27	932.93	0.41
	14-46	3.71	3.92	0.00		14-83	65.90	34.10		14-26	21.80	79.12		14-26	0.41	38327.64	0.42	1094.58	420.40	154.11	4.25		14-88	395.93	951.46	0.42
	14-62	0.00	8.65	0.00		14-92	66.75	33.25		14-50	27.24	75.95		14-42	0.52	68725.28	0.43	644.37	502.50	179.23	17.18		14-102	420.05	924.53	0.45
	14-78	3.26	10.88	0.08	CL2	14-19	70.15	29.85		14-75	26.36	75.60		14-75	0.47	16297.05	0.41	1235.02	100.40	150.81	11.92	CL3	14-32	708.21	1019.85	0.69
	14-80	2.85	3.53	0.00		14-23	70.89	29.11		14-78	21.12	75.81		1419	0.25	56894.20	0.42	941.24	513.20	186.36	8.75		14-42	766.40	1075.93	0.71
	14-83	5.83	13.73	0.00		14-29	71.60	28.40		14-102	24.35	75.86	CL2	14-29	0.42	1976.31	0.29	1270.15	6.80	193.14	5.70	CL4	14-15	481.03	797.62	0.60
	14-92	7.06	10.90	0.00		14-62	72.11	27.89		1412	19.21	77.21		14-32	0.40	16164.60	0.32	1112.16	94.10	164.73	14.23		1401	513.77	842.50	0.61
	14-93	0.00	9.96	4.45		14-75	70.10	29.90		1424	18.67	77.31		14-46	0.40	14435.01	0.41	1404.52	72.50	136.34	11.27		1418	546.30	939.34	0.58
	14-95	0.21	9.12	0.00		14-93	71.80	28.20		1426	17.83	77.58		14-50	0.27	22325.33	0.39	1226.78	150.40	143.40	4.18		1423	496.15	821.00	0.60
	1409	6.69	8.51	2.14		14-102	69.99	30.01	CL4	14-11	1.61	70.09		14-62	0.38	5625.96	0.34	1370.91	21.50	158.85	9.90	CL5	14-29	403.82	852.39	0.47
	1418	1.92	5.06	7.25		1412	70.37	29.63		14-20	0.00	68.49	CL3	14-15	0.35	52818.79	0.45	1900.12	725.50	178.71	13.40		14-46	407.94	883.56	0.46
CL3	14-20	1.61	60.25	0.98		1426	71.79	28.21		14-42	0.20	65.24		14-80	0.44	42804.55	0.41	1608.43	338.60	184.00	14.26		14-62	419.62	878.95	0.48
CL4	14-26	13.44	28.79	32.07	CL3	14-80	58.38	41.62		14-80	2.36	69.33		14-83	0.55	37062.90	0.42	1262.78	179.80	194.15	13.06		14-75	423.17	874.67	0.48
CL5	14-50	23.62	2.38	72.19	CL4	14-26	69.60	30.40		14-83	10.05	73.50		14-92	0.38	31422.96	0.44	1449.46	477.70	205.80	14.09		14-78	401.92	893.41	0.45
CL6	14-88	13.32	4.63	35.33		14-42	68.17	31.83		14-93	6.12	73.52		14-95	0.46	26420.12	0.39	1440.10	212.40	199.07	11.18		14-80	401.89	834.10	0.48
CL7	14-75	11.25	10.94	0.00		14-50	68.81	31.19		14-95	1.90	71.37		1418	0.42	92403.96	0.41	1599.61	1608.00	181.90	17.80		14-83	436.63	897.76	0.49
	14-102	17.65	13.08	7.20		14-78	67.84	32.16		1418	0.13	72.64		1422	0.31	71885.55	0.41	1836.13	1714.00	180.95	12.90		14-92	410.16	850.33	0.48
	1412	13.21	7.20	5.40		14-88	68.40	31.60		1419	3.02	72.08	CL4	14-20	0.37	27063.20	0.48	1172.98	102.40	203.47	21.44		14-93	403.90	852.03	0.47
	1419	13.14	9.41	10.68		1409	67.83	32.17	CL5	14-15	5.59	75.97		14-88	0.30	28908.96	0.55	986.98	317.70	143.94	16.26		14-95	401.84	838.78	0.48
	1424	12.82	5.39	0.00		1419	68.72	31.28		14-19	0.00	77.66		14-102	0.32	39529.39	0.48	993.09	613.00	157.74	18.49		1409	408.41	866.74	0.47
	1426	10.16	4.34	2.00		1424	68.91	31.09		14-29	0.05	79.91	CL5	1401	0.45	317980.90	0.42	1643.46	10048.80	181.13	14.73		1412	404.77	894.12	0.45
CL8	14-14	0.60	30.43	19.31	CL5	14-15	61.50	38.50		14-46	0.84	79.27		1423	0.39	212127.10	0.42	1723.57	8302.80	181.12	14.49		1422	417.24	837.74	0.50
	14-19	1.63	23.66	0.00		14-32	63.71	36.29		14-88	10.31	76.40	CL6	14-78	0.61	15970.78	0.41	1181.58	129.40	220.42	5.16		1424	423.64	891.31	0.48
	14-29	0.00	26.72	0.00		14-95	62.52	37.48		14-92	2.35	74.83		14-93	0.47	20057.65	0.46	1236.26	138.00	203.09	6.39		1426	415.87	878.17	0.47
	14-42	4.37	27.10	10.08		1401	62.71	37.29		1401	2.92	78.07		1409	0.38	163498.29	0.42	1273.43	5267.60	187.35	9.58	CL6	14-11	488.79	1040.51	0.47
	1401	3.53	17.11	21.86		1418	62.53	37.47		1409	6.40	75.59		1412	0.43	125472.68	0.48	1076.64	3668.80	183.10	7.71		14-19	442.21	998.06	0.44
	1422	4.50	23.29	7.94		1422	64.02	36.00		1422	5.52	78.61		1424	0.29	57383.89	0.44	1333.56	1032.80	193.61	8.98		14-20	449.47	1025.39	0.44
	1423	3.90	16.25	19.93		1423	62.44	37.56		1423	3.44	78.71		1426	0.44	87308.01	0.47	1143.81	1817.20	182.94	6.82		1419	476.72	1031.15	0.46

CLIM

As a result of the clustering analysis performed according to the group consisting of only climate descriptors, 6 classes emerged (Figure 8.5 and Table 8.5). CL1 cluster contains only one catchment (14-14) situated close to the Black Sea and characterized by very high potential evapotranspiration and high precipitation and aridity index values. CL2 cluster represents driest catchments with lowest precipitation and aridity index values and moderate to high evapotranspiration. These catchments are grouped at the mid-southwest of the Yeşilırmak basin. CL3 cluster represents the most humid catchments (14-32 and 14-42) towards the north of the Yeşilırmak basin. CL4 class is represented by relatively high precipitation and low potential evapotranspiration values. Therefore, CL4 is the cluster with second highest aridity index values. CL5 cluster contains 15 catchments (largest cluster) which are characterized by moderate to low precipitation and potential evapotranspiration values. Therefore, the aridity index values are moderate to low. CL6 cluster is characterized by very high evapotranspiration values followed by relatively high precipitation values, resulting in moderate to low aridity index (dry conditions).

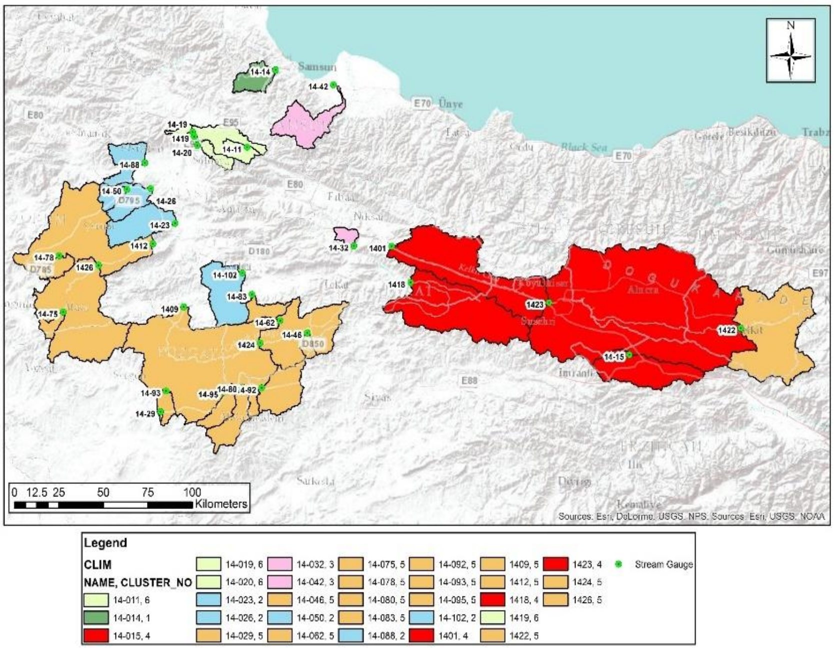

Figure 8.5. Cluster Analysis Results of CLIM

GEO

As a result of the cluster analysis performed according to the group consisting of only geological descriptors (%Alluvium, %Carbonate Rocks, %Volcanic rocks) 8 classes emerged (Figure 8.6 and Table 8.5). CL1 and CL3 clusters are composed of single catchments that are represented by highest values of alluvium and carbonate rock percentages, respectively. CL5 on the other hand, is a catchment characterized by highest volcanic rock and high alluvium percentage values. CL4 cluster is another single catchment relatively high percentages of all three geologic units. CL6 cluster is a single catchment with moderate volcanic rocks and alluvium percentages while carbonate percentage is low. Catchments in CL2 cluster are characterized by low percentages of alluvium, carbonate rocks and volcanic rocks and hence represent less permeable catchments with low aquifer yield potential. CL7 cluster contains six catchments with moderate to high alluvium percentage while carbonate rock and volcanic rock percentages show heterogeneity. The catchments in CL8 class are represented by low alluvium percentage and high carbonate rock percentage.

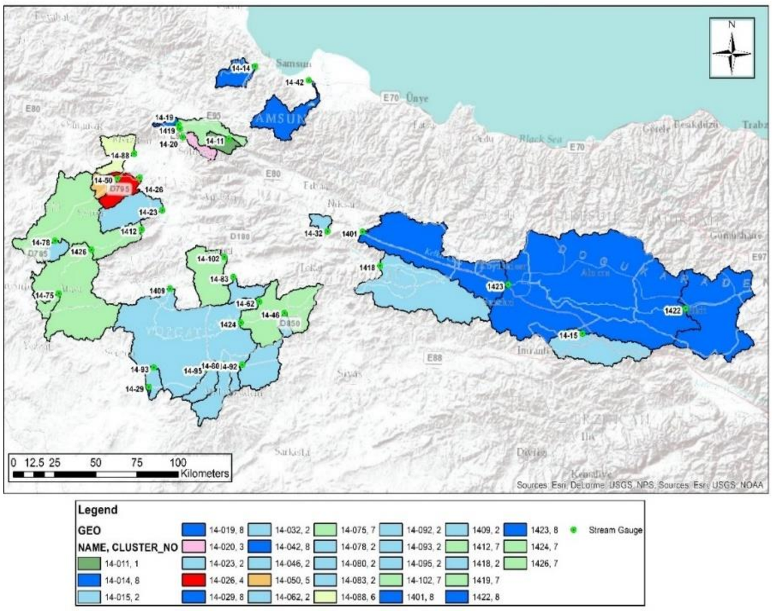

Figure 8.6. Cluster Analysis Results of GEO

LCOV

Affinity propagation analysis was performed by using landcover descriptors, namely irrigated arable land and curve number. According to the results five clusters are formed (Figure 8.7 and Table 8.5). CL1 cluster contains two catchments with no irrigated arable land and lowest Curve number values compared to other clusters. Single catchment (14-62) in CL2 cluster is characterized by the highest irrigated arable land and moderate curve number values. CL3 cluster, contains nine catchments with high irrigated arable land and curve number values. Nine catchments in CL4 class is represented by low irrigated arable land and moderate curve number values. Finally, CL5 cluster contains ten catchment represented by the low irrigated arable land and high curve number values.

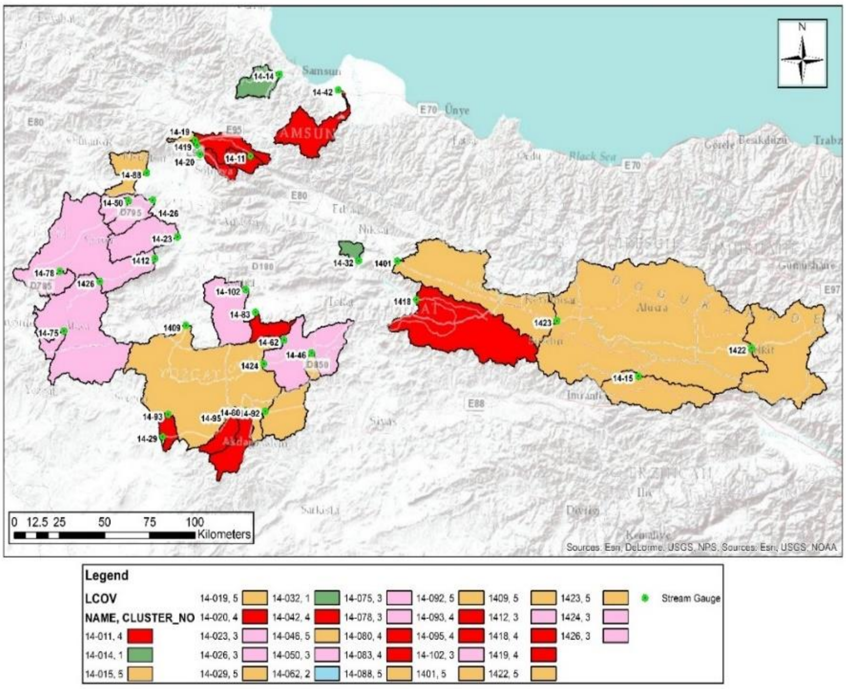

Figure 8.7. Cluster Analysis Results of LCOV

TOPO

According to the results of cluster analysis performed according to the group of topographical characteristics (seven in total), six clusters emerged (Figure 8.8 and Table 8.5). Starting with CL5 cluster, two catchments are represented by high elevation and highest values of area and longest flow path descriptors. CL2 cluster contains five catchments that are characterized by moderate to high elevation and low area values. CL1 cluster with eight catchments represents moderate to low values for all the topographic descriptors. CL3 cluster is characterized by high elevation and moderate values of the remaining descriptors. CL4 cluster contains three catchments with high slope and drainage density values and low hypsometric integral values. CL6 cluster is mainly represented by catchments having very low slope values together with moderate to high values for the remaining descriptors. Only exceptions are catchments 14-78 and 14-93 having lower area and longest flow path values in addition to the higher hypsometric integral values compared to other catchments in this cluster.

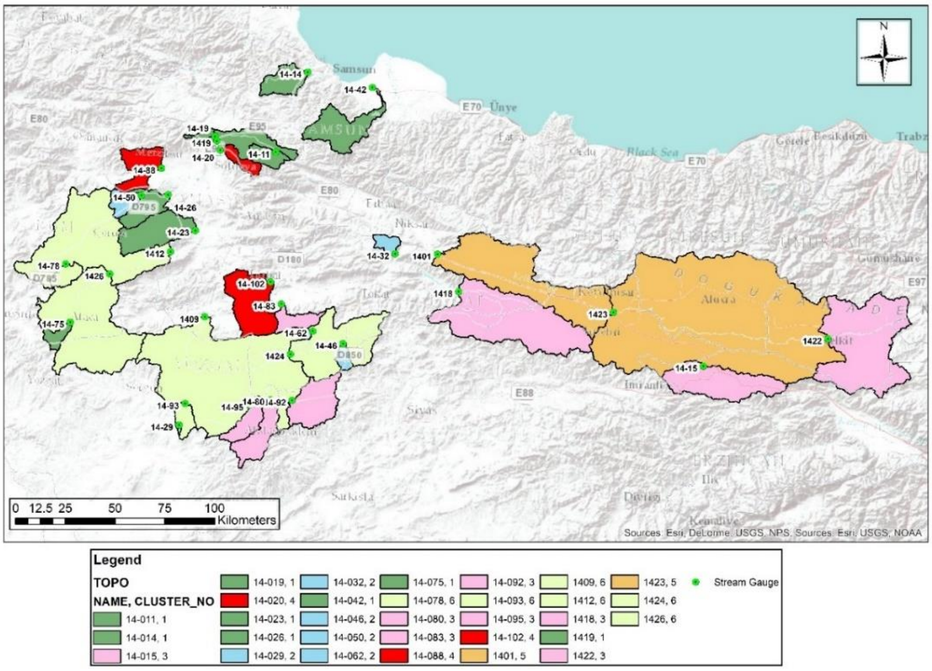

Figure 8.8. Cluster Analysis Results of TOPO

SOIL

Upon running the affinity propagation algorithm for the soil descriptors as a group (percentage of silt and clay, percentage of sand) a total of 5 clusters are revealed (Figure 8.9 and Table 8.5). Note however that, percentages of these two soil descriptors add to 100, therefore the clustering can also be treated as single input. As such, the percentage of silt and clay increases and the percentage of sand decreases as moving from CL3 cluster towards CL5, CL1, CL4 and CL2.

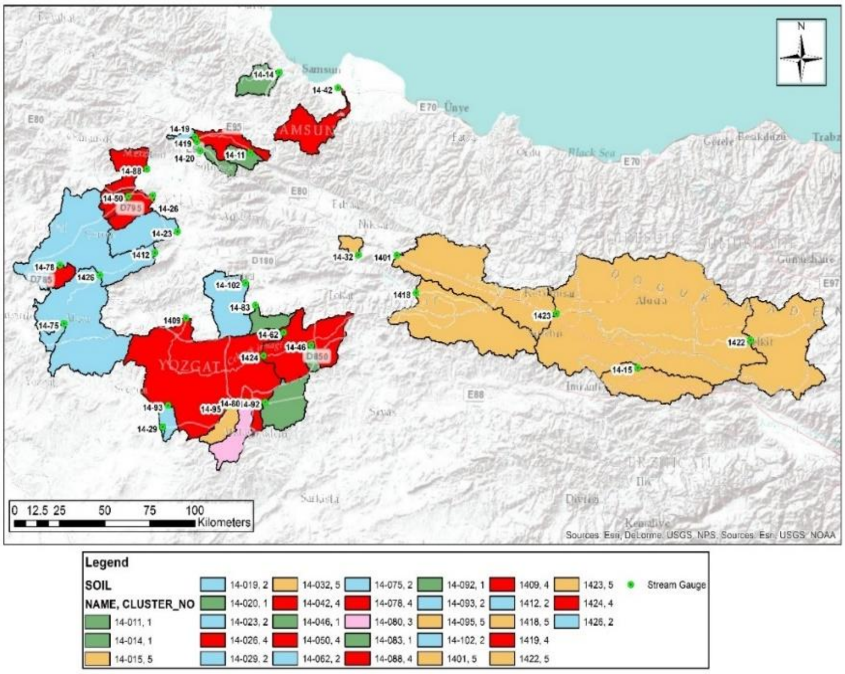

Figure 8.9. Cluster Analysis Results of SOIL

8.3. Validation of the Clusters

In this section of thesis, clustering based on group of flow signatures (Case 1) will be compared to the clusters obtained from groups of climate properties and catchment physical characteristics (Case 2). The validation will be performed by external cluster validation indices, namely, Cramer's V, Adjusted Rand Index and Normalized Mutual Index (see Section 7.2). The purpose of external validation is to investigate the degree to which the clusters based on flow signatures agree with those clusters obtained by groups of climate properties and catchment physical properties. To further help the evaluation process, the external validation was also performed for each of the descriptors within all the groups described above (a total of 25 descriptors).

Validation indices were calculated between clusters obtained from the group of flow signatures and group of climate properties, group of catchment physical properties as well as between individual descriptors (Table 8.5). SPSS® software was used to calculate Cramer's V coefficient and Matlab® was used to calculate the remaining indices. Based on the index values the following conclusions can be made:

- For Case 1, the values of the validation indices between FLOW group and individual descriptors were analyzed. Focusing on the Cramer's V Coefficient values, it can be seen from Table 8.6 that the highest coefficient values were obtained between the FLOW group and aridity index, potential evapotranspiration and precipitation in climate properties, followed by elevation in topographic properties, in a decreasing order (varying between 0.62 and 0.57). Upon considering the Adjusted Rand Index (Table 8.7), climate properties, PET, PPT and ARI have the highest index values, followed by the soil type and elevation. The results based on Normalized Mutual Index (Table 8.8) puts the emphasis on the climate properties with highest values for PPT, PET, ARI followed by elevation topographic property. These results indicate that climate properties are the main driver of hydrologic response in the study catchments followed by elevation topographic property and soil type.

- For Case 2, the values of the validation indices between FLOW group and groups of climate and catchment physical descriptors (CLIM, GEO, TOPO, LCOV, SOIL) were analyzed. According to Cramer's V Coefficient values it can be seen from Table 8.6 that the highest coefficient values were obtained between FLOW and group of climate properties followed by group of topographic properties. It can be seen that the coefficient values obtained from group of climate variables were similar to those obtained by coefficient values for individual climate descriptors (ARI, PET and PPT). Similarly, the coefficient values obtained from group of topographic variables were similar to those obtained by coefficient values for elevation only. After CLIM and TOPO groups, GEO and LCOV groups have the highest coefficient values. When Adjusted Rand Index values in Table 8.7 are considered, similar results are obtained however grouping of descriptors in CLIM, TOPO, LCOV and

SOIL provides higher index value, in other words, more correspondence between clusters of FLOW and the former groups compared to individual descriptors in those groups. Normalized Mutual Index values (Table 8.8) provide similar results with Adjusted Rand Index, both for the order of importance of groups as well as importance of grouping compared to individual descriptors.

Table 8.6. Cramer’s V Coefficients

	CRAMER'S V COEFFICENT																													
	Q5	Q50	Q95	SFDC	RQP	BFI	SFE	DHYF	ALV	CAR	VOR	SND	IAL	CN	HI	LFP	DRD	ELV	ARE	ASP	SLP	PPT	PET	ARI	FLOW	GEO	SOIL	LCOV	TOPO	CLIM
Q5	1.00	0.57	0.55	0.36	0.68	0.41	0.41	0.46	0.50	0.35	0.38	0.35	0.44	0.45	0.45	0.48	0.36	0.46	0.45	0.37	0.34	0.60	0.51	0.53	0.68	0.60	0.35	0.44	0.50	0.63
	Q50	1.00	0.73	0.46	0.63	0.35	0.46	0.43	0.43	0.44	0.39	0.42	0.41	0.49	0.38	0.50	0.31	0.48	0.48	0.33	0.46	0.62	0.51	0.57	0.70	0.54	0.42	0.45	0.59	0.61
		Q95	1.00	0.44	0.54	0.49	0.35	0.42	0.49	0.53	0.42	0.49	0.42	0.45	0.46	0.45	0.25	0.51	0.42	0.36	0.41	0.57	0.52	0.52	0.63	0.61	0.49	0.43	0.47	0.61
			SFDC	1.00	0.35	0.46	0.43	0.42	0.32	0.32	0.39	0.36	0.25	0.46	0.37	0.37	0.38	0.43	0.40	0.25	0.25	0.45	0.41	0.50	0.43	0.44	0.36	0.39	0.41	0.51
				RQP	1.00	0.37	0.48	0.47	0.44	0.32	0.25	0.38	0.47	0.40	0.35	0.52	0.40	0.44	0.47	0.35	0.39	0.51	0.40	0.45	0.63	0.51	0.38	0.43	0.46	0.49
					BFI	1.00	0.39	0.37	0.27	0.33	0.32	0.39	0.43	0.30	0.34	0.50	0.32	0.40	0.43	0.37	0.30	0.46	0.33	0.39	0.62	0.40	0.39	0.38	0.50	0.48
						SFE	1.00	0.36	0.35	0.34	0.32	0.30	0.47	0.33	0.40	0.40	0.45	0.31	0.43	0.43	0.32	0.43	0.41	0.34	0.41	0.43	0.30	0.40	0.40	0.37
							DHYF	1.00	0.44	0.35	0.35	0.45	0.36	0.32	0.45	0.37	0.25	0.63	0.43	0.33	0.36	0.39	0.51	0.26	0.63	0.50	0.45	0.40	0.56	0.44
								ALV	1.00	0.35	0.57	0.42	0.46	0.39	0.63	0.38	0.47	0.37	0.42	0.39	0.40	0.39	0.43	0.37	0.50	0.88	0.42	0.43	0.42	0.46
									CAR	1.00	0.33	0.31	0.25	0.52	0.30	0.43	0.28	0.35	0.41	0.36	0.38	0.45	0.41	0.34	0.47	0.73	0.31	0.26	0.53	0.44
										VOR	1.00	0.37	0.31	0.31	0.33	0.54	0.50	0.44	0.54	0.44	0.47	0.48	0.46	0.58	0.40	0.79	0.37	0.33	0.52	0.56
											SND	1.00	0.41	0.33	0.41	0.46	0.37	0.48	0.47	0.39	0.42	0.45	0.44	0.49	0.51	0.46	1.00	0.39	0.47	0.49
												IAL	1.00	0.42	0.25	0.38	0.43	0.37	0.38	0.35	0.38	0.36	0.50	0.33	0.48	0.54	0.41	0.83	0.48	0.44
													CN	1.00	0.32	0.39	0.30	0.46	0.43	0.19	0.32	0.55	0.45	0.36	0.52	0.57	0.33	0.69	0.42	0.57
														HI	1.00	0.39	0.31	0.37	0.39	0.46	0.25	0.45	0.37	0.31	0.42	0.66	0.41	0.32	0.31	0.46
															LFP	1.00	0.39	0.49	0.87	0.46	0.50	0.47	0.42	0.47	0.45	0.35	0.46	0.34	0.65	0.43
																DRD	1.00	0.39	0.37	0.36	0.27	0.47	0.27	0.38	0.33	0.63	0.37	0.43	0.55	0.44
																	ELV	1.00	0.53	0.48	0.53	0.61	0.56	0.58	0.57	0.51	0.48	0.44	0.57	0.68
																		ARE	1.00	0.46	0.41	0.43	0.48	0.43	0.42	0.35	0.47	0.35	0.61	0.44
																			ASP	1.00	0.22	0.41	0.37	0.43	0.42	0.60	0.39	0.44	0.48	0.52
																				SLP	1.00	0.53	0.43	0.47	0.50	0.52	0.42	0.46	0.56	0.46
																					PPT	1.00	0.54	0.56	0.59	0.40	0.45	0.59	0.45	0.77
																						PET	1.00	0.51	0.61	0.60	0.44	0.54	0.61	0.82
																							ARI	1.00	0.62	0.60	0.49	0.40	0.57	0.76
																								FLOW	1.00	0.52	0.51	0.52	0.57	0.60
																									GEO	1.00	0.46	0.49	0.58	0.52
																										SOIL	1.00	0.39	0.47	0.49
																											LCOV	1.00	0.43	0.56
																												TOPO	1.00	0.54
																													CLIM	1.00

Table 8.7. Adjusted Rand Indices

	ADJUSTED RAND INDEX																													
	Q5	Q50	Q95	SFDC	RQP	BFI	SFE	DHYF	ALV	CAR	VOR	SND	IAL	CN	HI	LFP	DRD	ELV	ARE	ASP	SLP	PPT	PET	ARI	FLOW	GEO	SOIL	LCOV	TOPO	CLIM
Q5	1.00	0.31	0.14	0.04	0.46	0.02	-0.01	0.08	0.09	0.01	0.03	0.00	0.07	0.06	0.01	0.01	-0.06	0.13	0.01	0.03	-0.01	0.16	0.11	0.14	0.24	0.12	0.00	0.08	0.08	0.28
Q50		1.00	0.26	0.11	0.42	-0.03	0.07	0.10	0.02	0.03	0.04	0.02	-0.01	0.09	-0.04	0.00	-0.05	0.14	-0.01	-0.03	0.02	0.23	0.11	0.19	0.30	0.06	0.02	0.07	0.10	0.29
Q95			1.00	0.00	0.13	0.08	-0.08	0.00	0.05	0.09	0.12	0.07	0.03	0.08	-0.02	-0.02	-0.08	0.06	-0.03	-0.07	0.02	0.26	0.15	0.11	0.28	0.10	0.07	0.10	0.02	0.35
SFDC				1.00	0.01	0.06	0.03	0.05	-0.01	-0.02	-0.02	0.01	-0.06	0.05	0.02	-0.10	0.11	0.07	-0.06	-0.03	-0.04	-0.01	0.05	0.10	0.01	-0.04	0.01	0.00	-0.01	0.10
RQP					1.00	0.00	0.06	0.07	0.04	-0.05	-0.06	0.03	0.08	0.04	-0.03	0.09	0.00	0.08	0.00	-0.01	0.01	0.11	0.02	0.06	0.20	0.04	0.03	0.08	0.05	0.10
BFI						1.00	0.02	0.02	-0.06	-0.03	0.00	0.03	0.05	-0.06	-0.01	0.06	-0.04	0.03	0.01	0.00	0.00	0.03	-0.03	-0.01	0.03	-0.06	0.03	0.02	0.05	0.02
SFE							1.00	0.00	-0.03	-0.05	-0.03	-0.04	0.11	-0.05	0.02	-0.03	0.02	-0.07	0.01	0.00	-0.05	-0.03	0.04	-0.05	-0.03	-0.09	-0.04	0.04	0.03	-0.04
DHYF								1.00	0.10	0.01	0.02	0.12	0.11	0.02	0.07	-0.06	-0.06	0.26	-0.02	0.03	0.02	-0.04	0.27	-0.03	0.27	0.09	0.12	0.10	0.18	0.05
ALV									1.00	-0.02	0.04	0.08	0.13	0.02	0.13	-0.03	0.22	0.03	0.06	0.01	0.09	-0.02	0.07	-0.01	0.10	0.36	0.08	0.14	0.02	0.04
CAR										1.00	0.01	-0.04	-0.07	0.14	-0.04	-0.06	-0.04	-0.04	-0.05	-0.01	0.01	0.03	0.05	-0.02	0.05	0.21	-0.04	-0.07	0.08	0.11
VOR											1.00	0.00	-0.03	-0.03	0.03	0.08	0.01	0.14	0.16	0.00	0.09	0.06	0.08	0.11	-0.02	0.23	0.00	-0.02	0.02	0.24
SND												1.00	0.07	-0.02	0.05	0.03	0.04	0.11	0.02	0.02	0.08	0.05	0.07	0.13	0.13	-0.01	1.00	0.06	0.07	0.06
IAL													1.00	0.08	-0.03	-0.05	0.01	0.00	-0.02	0.04	0.06	-0.05	0.21	0.02	0.08	0.09	0.07	0.41	0.08	-0.01
CN														1.00	-0.03	-0.06	0.01	-0.02	-0.05	-0.06	-0.02	0.04	0.05	0.01	0.10	0.10	-0.02	0.35	0.00	0.06
HI															1.00	-0.06	-0.06	0.00	-0.04	0.07	-0.05	0.00	-0.01	-0.03	-0.01	0.12	0.05	-0.01	-0.07	0.05
LFP																1.00	-0.06	0.07	0.47	-0.01	0.07	0.03	-0.04	0.04	-0.04	-0.05	0.03	-0.08	0.16	-0.01
DRD																	1.00	0.01	-0.09	0.00	-0.01	-0.02	-0.04	0.02	-0.06	0.02	0.04	0.04	0.09	0.01
ELV																		1.00	0.14	0.09	0.16	0.04	0.16	0.17	0.11	0.07	0.11	0.08	0.14	0.24
ARE																			1.00	-0.03	-0.02	0.03	0.03	-0.03	-0.07	-0.01	0.02	-0.08	0.09	0.03
ASP																				1.00	-0.04	-0.04	0.05	0.10	-0.02	0.09	0.02	0.07	0.05	0.09
SLP																					1.00	0.03	0.13	0.17	0.04	0.04	0.08	0.08	0.12	0.07
PPT																						1.00	0.09	0.12	0.19	0.07	0.05	0.04	-0.02	0.30
PET																							1.00	0.14	0.21	0.11	0.07	0.17	0.21	0.47
ARI																								1.00	0.17	0.06	0.13	-0.01	0.13	0.38
FLOW																									1.00	0.07	0.13	0.14	0.15	0.24
GEO																										1.00	-0.01	0.09	0.13	0.15
SOIL																											1.00	0.06	0.07	0.06
LCOV																												1.00	0.04	0.06
TOPO																													1.00	0.17
CLIM																														1.00

Table 8.8. Normalized Mutual Information

NORMALIZED MUTUAL INDEX																														
	Q5	Q50	Q95	SFDC	RQP	BFI	SFE	DHYF	ALV	CAR	VOR	SND	IAL	CN	HI	LFP	DRD	ELV	ARE	ASP	SLP	PPT	PET	ARI	FLOW	GEO	SOIL	LCOV	TOPO	CLIM
Q5	1.00	0.41	0.38	0.23	0.57	0.25	0.23	0.27	0.29	0.18	0.20	0.19	0.27	0.24	0.20	0.28	0.20	0.33	0.26	0.16	0.15	0.43	0.30	0.33	0.50	0.38	0.19	0.29	0.35	0.49
Q50		1.00	0.53	0.31	0.52	0.19	0.31	0.27	0.25	0.25	0.20	0.24	0.21	0.32	0.17	0.24	0.17	0.32	0.23	0.15	0.24	0.46	0.31	0.39	0.56	0.32	0.24	0.30	0.40	0.47
Q95			1.00	0.27	0.35	0.35	0.24	0.26	0.29	0.34	0.27	0.31	0.25	0.27	0.21	0.26	0.12	0.32	0.25	0.17	0.20	0.45	0.34	0.35	0.51	0.42	0.31	0.30	0.31	0.55
SFDC				1.00	0.19	0.31	0.26	0.16	0.14	0.16	0.22	0.21	0.08	0.25	0.23	0.17	0.24	0.28	0.22	0.09	0.08	0.27	0.23	0.28	0.26	0.23	0.21	0.21	0.24	0.37
RQP					1.00	0.20	0.30	0.28	0.28	0.14	0.11	0.22	0.29	0.22	0.16	0.33	0.23	0.29	0.27	0.16	0.20	0.32	0.21	0.26	0.46	0.28	0.22	0.28	0.30	0.34
BFI						1.00	0.23	0.18	0.12	0.17	0.17	0.22	0.24	0.12	0.20	0.31	0.15	0.22	0.24	0.20	0.11	0.28	0.15	0.19	0.32	0.22	0.22	0.22	0.31	0.30
SFE							1.00	0.15	0.20	0.19	0.15	0.15	0.24	0.15	0.25	0.24	0.23	0.14	0.31	0.22	0.15	0.26	0.20	0.16	0.28	0.22	0.15	0.27	0.26	0.26
DHYF								1.00	0.29	0.14	0.20	0.28	0.22	0.12	0.21	0.16	0.09	0.49	0.22	0.15	0.17	0.19	0.34	0.08	0.52	0.33	0.28	0.24	0.35	0.28
ALV									1.00	0.18	0.25	0.31	0.29	0.21	0.32	0.23	0.33	0.21	0.29	0.14	0.18	0.22	0.22	0.16	0.34	0.61	0.31	0.29	0.26	0.30
CAR										1.00	0.18	0.31	0.29	0.21	0.32	0.23	0.33	0.21	0.29	0.14	0.18	0.22	0.22	0.16	0.28	0.47	0.14	0.11	0.33	0.26
VOR											1.00	0.24	0.15	0.14	0.22	0.32	0.27	0.32	0.34	0.24	0.25	0.30	0.24	0.34	0.24	0.45	0.24	0.19	0.29	0.35
SND												1.00	0.24	0.12	0.26	0.27	0.24	0.33	0.28	0.18	0.25	0.27	0.24	0.27	0.36	0.28	1.00	0.25	0.33	0.33
IAL													1.00	0.27	0.08	0.16	0.19	0.18	0.17	0.15	0.22	0.18	0.36	0.15	0.29	0.34	0.24	0.61	0.31	0.29
CN														1.00	0.13	0.17	0.13	0.19	0.21	0.05	0.14	0.25	0.23	0.17	0.31	0.35	0.12	0.57	0.20	0.31
HI															1.00	0.22	0.17	0.18	0.22	0.21	0.08	0.21	0.15	0.15	0.21	0.38	0.26	0.17	0.14	0.30
LFP																1.00	0.22	0.31	0.72	0.25	0.30	0.33	0.18	0.23	0.26	0.26	0.27	0.17	0.49	0.26
DRD																	1.00	0.23	0.23	0.13	0.09	0.24	0.09	0.18	0.17	0.28	0.24	0.24	0.35	0.21
ELV																		1.00	0.37	0.29	0.32	0.31	0.37	0.40	0.40	0.34	0.33	0.29	0.45	0.49
ARE																			1.00	0.25	0.20	0.32	0.27	0.19	0.25	0.26	0.28	0.19	0.42	0.30
ASP																				1.00	0.06	0.21	0.20	0.26	0.21	0.34	0.18	0.24	0.31	0.33
SLP																					1.00	0.28	0.24	0.35	0.27	0.26	0.25	0.27	0.33	0.29
PPT																						1.00	0.33	0.37	0.47	0.30	0.27	0.31	0.27	0.58
PET																							1.00	0.33	0.44	0.37	0.24	0.34	0.39	0.69
ARI																								1.00	0.41	0.33	0.27	0.18	0.34	0.61
FLOW																									1.00	0.36	0.36	0.38	0.43	0.53
GEO																										1.00	0.28	0.35	0.43	0.36
SOIL																											1.00	0.25	0.33	0.33
LCOV																												1.00	0.26	0.34
TOPO																													1.00	0.46
CLIM																														1.00

The results of the external validation indices calculated between FLOW group clusters and other groups of catchment climate and physical properties are summarized in Table 8.9. The results of these indices indicate that climate properties are the most important input when classifying flow signatures in the catchments. It is followed by the topographic properties of catchments which have second highest correspondence with FLOW clusters (high index values). After CLIM and TOPO group of descriptors, the index values decrease as going from LCOV to GEO and SOIL group, respectively. The results of different clustering combinations show that climate is primary, topography is secondary catchment properties while classifying study catchments according to flow signatures. This information can help us to estimate flow signature values in ungauged catchments when climatic and topographical features of the catchments are known.

Table 8.9. Summary Table of Cluster Analysis Validation

CLUSTER ANALYSIS VALIDATION - FLOW			
Group	**Cramer's V Coefficient**	**Adjusted Rand Index**	**Normalized Mutual Information**
CLIM	0.60	0.24	0.53
TOPO	0.57	0.15	0.43
LCOV	0.52	0.14	0.38
GEO	0.52	0.07	0.36
SOIL	0.51	0.13	0.36

CHAPTER 9

CONCLUSIONS AND RECOMMENDATIONS

Within the scope of this thesis, the hydrological responses in 31 catchments in Yeşilırmak Basin having natural flow conditions and continuous streamflow and meteorological data were studied using flow signatures, catchment climatic properties and physiographic descriptors. The study time period was selected as the 5-year period between 1973 and 1977 based on data availability and natural flow conditions. Catchment climatic properties and physiographic descriptors controlling catchment flow responses were investigated using cluster analysis. Catchment flow responses were characterized using flow signatures including Flow Duration Curve Parameters (Q5, Q50, Q95, Slope of Flow Duration Curve), Runoff Ratio, Baseflow Index, Streamflow Elasticity and Day of Half Year Flow. Catchment climatic and physiographic descriptors were defined using climatic, topographic, geologic, soil and landcover properties.

Affinity Propagation Clustering Algorithm was used to cluster study catchments based on flow signatures. Next, catchment clusters were obtained for individual as well as groups of climatic and physical descriptors. The correspondence between clusters obtained from flow signatures and clusters obtained from catchment properties (climatic and physical) were than validated (compared) by using External Cluster Validation indices including Cramer's V Coefficient, Adjusted Rand Index and Normalized Mutual Information. When the results of the clustering analysis for each and individual flow signatures and catchment properties were compared, it was seen that climate properties are the most important descriptors when clustering flow signatures in the catchments. Secondarily, the topographic descriptors, specifically elevation, has the second correspondence with the flow signature clusters. It should be noted that the validation index values did not indicate one-to-one correspondence but correspondence to a certain degree. In other words, catchments' climatic and topographic descriptors are generally the most important factors affecting the hydrological responses in the study catchments. Geographically, the catchments in the same cluster were generally close to each other. Our results suggest that first climate then topographic properties modify the impacts landcover, soil and geology on hydrologic regimes, which means that changes in climatic and topographic conditions will impact the streamflow response.

According to these results, the following recommendations can be given:

- Increasing the number of catchments in clustering analysis would enable more heterogeneity in flow and catchment descriptors and better clustering performance (high silhouette values). In this way, descriptors controlling flow response could be better identified.
- This study was performed with only 5-year of daily flow and monthly meteorological datasets based on data availability and ensuring natural flow conditions. It is recommended that the time period should be expanded to include more variability in catchment response and climatic properties to better capture seasonal and interannual variability.
- Performing this study in the different basins of Turkey can help to find relationship between hydrologic response and catchment properties. For example, Eastern Black Sea Basin is represented by humid climatic conditions, high elevation and slope values and high area percentage of igneous rocks. Thus, it is expected that surface water is dominant than baseflow contribution in the basin. Thus, the impacts of climatic and topographic on flow signatures can be interpreted more distinctly.
- Expanding limited data using larger and global dataset and then applying different combinations of supervised and/or unsupervised machine learning

algorithms can help to find out relationship between flow signatures and catchment properties in further studies.

REFERENCES

Akbaş, B., Akdeniz, N., Aksay, A., Altun, İ., Balcı, V., Bilginer, E., Bilgiç, T., Duru, M., Ercan, T., Gedik, İ., Günay, Y., Güven, İ.H., Hakyemez, H. Y., Konak, N., Papak, İ., Pehlivan, Ş., Sevin, M., Şenel, M., Tarhan, N.,Turhan, N., Türkecan, A., Ulu, Ü., Uğuz, M.F., Yurtsever, A. ve diğerleri. (2013). Türkiye Jeoloji Haritası Maden Tetkik ve Arama Genel Müdürlüğü Yayını. Ankara Türkiye

Ali, G., Tetzlaff, D., Soulsby, C., McDonnell, J. J., & Capell, R. (2012). A comparison of similarity indices for catchment classification using a cross-regional dataset. Advances in Water Resources, 40, 11-22.

Bektaş, O., Şen, C., Atici, Y., & Köprübaşi, N. (1999). Migration of the Upper Cretaceous subduction-related volcanism towards the back-arc basin of the eastern Pontide magmatic arc (NE Turkey). Geological Journal, 34(1-2), 95-106.

Bingöl, E., Akyürek, B., and Korkmazer, B., 1973. Biga yarımadasının jeolojisi ve Karakaya Formasyonunun bazı özellikleri. Proceedings of the 50th Anniversary of the Turkish Republic Earth Science Congress. Mineral Research and Exploration Institute of Turkey (MTA) Publications, 70-77.

Beven, K. J. (2000). Uniqueness of place and process representations in hydrological modelling. Hydrology and Earth System Sciences Discussions, 4(2), 203-213.

Bower, D., Hannah, D. M., & McGregor, G. R. (2004). Techniques for assessing the climatic sensitivity of river flow regimes. Hydrological processes, 18(13), 2515-2543.

Boyer, D. G. (1984). Estimation Of Daily Temperature Means Using Elevation And Latitude In Mountainous Terrain 1.*JAWRA Journal of the American Water Resources Association*,*20*(4), 583-588.

Brekke LD, Miller NL, Bashford KE, Quinn NWT, Dracup JA (2004) Climate change impacts uncertainty for water resources in the San Joaquin River Basin, California. Journal of the American Water Resources Association 40: 149–164.

Brouwer, C., Goffeau, A., & Heibloem, M. (1985). Irrigation Water Management: Training Manual No. 1-Introduction to Irrigation.*Food and Agriculture Organization of the United Nations, Rome, Italy*, 102-103.

Brunke M, Gonser T (1997) The ecological significance of exchange processes between rivers and groundwater. Freshwater Biol 37:1–33.

Brusco, M. J., Shireman, E., & Steinley, D. (2017). A comparison of latent class, K-means, and K-median methods for clustering dichotomous data. Psychological methods, 22(3), 563.

Brusco, M. J., Steinley, D., Stevens, J., & Cradit, J. D. (2019). Affinity propagation: An exemplar-based tool for clustering in psychological research. British Journal of Mathematical and Statistical Psychology, 72(1), 155-182.

Buttle, J. (2006). Mapping first-order controls on streamflow from drainage basins: the T3 template. Hydrological Processes: An International Journal, 20(15), 3415-3422.

Chiverton, A., Hannaford, J., Holman, I., Corstanje, R., Prudhomme, C., Bloomfield, J., & Hess, T. M. (2015). Which catchment characteristics control the temporal dependence structure of daily river flows?. Hydrological Processes, 29(6), 1353-1369.

Clow, D. W. (2010). Changes in the timing of snowmelt and streamflow in Colorado: a response to recent warming.*Journal of Climate*,*23*(9), 2293-2306.

Croker, K. M., Young, A. R., Zaidman, M. D., & Rees, H. G. (2003). Flow duration curve estimation in ephemeral catchments in Portugal. Hydrological sciences journal, 48(3), 427-439.

Dingman, S.L. 1978. Drainage density and streamflow: A Closer Look. Water Resources Research 30: 1183-1187.

Dingman, S. L. (1981). Elevation: a major influence on the hydrology of New Hampshire and Vermont, USA/L'altitude exerce une influence importante sur l'hydrologie du New Hampshire et du Vermont, Etats-Unis.*Hydrological Sciences Journal*,*26*(4), 399-413.

Dooge, J.C.I. (1992), Hydrologic Models and climate change, Journal of Geophysical Research, 97(D3): 2677-2686.

Dueck, D. (2009). Affinity propagation: clustering data by passing messages. Toronto: University of Toronto.

Eckhardt, K. (2008). A comparison of baseflow indices, which were calculated with seven different baseflow separation methods. Journal of Hydrology, 352 (1-2), 168-173.

Edwards, P. J., Williard, K. W., & Schoonover, J. E. (2015). Fundamentals of watershed hydrology.Journal of contemporary water research & education, 154(1), 3-20.

Frey, B. J., & Dueck, D. (2007). Clustering by passing messages between data points.science,315(5814), 972-976.

Gabellani, I., G. Boni, L. Ferraris, J. von Hardenberg, and A. Provenzale (2007), Propagation of uncertainty from rainfall to runoff: A case study with a stochastic rainfall generator, Adv. Water Resour., 30, 2061 – 2071, doi: 10.1016/j.advwatres.2006.11.015.

Gao, H., Ding, Y., Zhao, Q., Hrachowitz, M., & Savenije, H. H. (2017). The importance of aspect for modelling the hydrological response in a glacier catchment in Central Asia.*Hydrological processes*,*31*(16), 2842-2859.

Gerrits, A. M. J., Savenije, H. H. G., Veling, E. J. M., and Pfister, L.: Analytical derivation of the Budyko curve based on rainfall characteristics and a simple evaporation model, Water Resour. Res., 45, W04403, doi:10.1029/2008WR007308, 2009.

Hagan, R., Haise, H., and Edrninster, T. (1967), Irrigation of Agricultural Lands American Society of Agronomy Inc., Madison Wisconsin No. 11.

Harlin, J.M. 1984. Watershed morphometry and time to hydrograph peak. Journal of Hydrology Vol. 67, No. 1-4, p 141-154.

Hengl, T., de Jesus, J. M., Heuvelink, G. B., Gonzalez, M. R., Kilibarda, M., Blagotić, A., ... & Guevara, M. A. (2017). SoilGrids250m: Global gridded soil information based on machine learning. *PLoS one*, *12*(2), e0169748.

Holmes, M. G. R., Young, A. R., Gustard, A., & Grew, R. (2002). A region of influence approach to predicting flow duration curves within ungauged catchments. Hydrology and Earth System Sciences, 6(4), 721-731.

Kirpich, Z. P., (1940). Time of concentration of small agricultural watersheds. Civil Engineering, vol. 6, p. 362.

Kuentz, A., Arheimer, B., Hundecha, Y., & Wagener, T. (2017). Understanding hydrologic variability across Europe through catchment classification. *Hydrology and Earth System Sciences*, *21*(6), 2863-2879.

Laizé, C. L., & Hannah, D. M. (2010). Modification of climate–river flow associations by basin properties. Journal of Hydrology, 389(1-2), 186-204.

Langbein, W. B. (1947). Topographic characteristics of drainage basins.

Lemann, T., Roth, V., & Zeleke, G. (2017). Impact of precipitation and temperature changes on hydrological responses of small-scale catchments in the Ethiopian Highlands. *Hydrological sciences journal*, *62*(2), 270-282.

Lettenmaier DP, Gan TY (1990) Hydrologic Sensitivities of the Sacramento-San Joaquin River Basin, California, to Global Warming. Water Resources Research 26: 69–86.

Ley, R., Casper, M. C., Hellebrand, H., & Merz, R. (2011). Catchment classification by runoff behaviour with self-organizing maps (SOM). Hydrology and Earth System Sciences, 15(9), 2947-2962.

McCuen, R. H., Wong, S. L., and Rawls, W. J. 1984. "Estimating urban time of concentration." J. Hydraul. Eng., 110(7), 887–904.

McCuen, R. H., 1989. Hydrologic Analysis and Design. Prentice Hall, pp. 355-360.

McCuen, R. H. 2005. Hydrologic analysis and design, 3rd Ed., Prentice-Hall, Englewood Cliffs, N.J.

Merchán, D., Causapé, J., & Abrahao, R. (2013). Impact of irrigation implementation on hydrology and water quality in a small agricultural basin in Spain. *Hydrological sciences journal*, *58*(7), 1400-1413.

Merz, R., & Blöschl, G. (2009). A regional analysis of event runoff coefficients with respect to climate and catchment characteristics in Austria. Water Resources Research, 45(1).

Miller, J. A. (1999). *Ground water atlas of the United States: Introduction and national summary* (No. 730-A, pp. A1-A15). US Geological Survey.

Miller NL, Bashford KE, Strem E (2003) Potential Impacts of Climate Change on California Hydrology. J of the American Water Resources Association 39: 771–784.

Ministry of Environment and Forestry. (2008). Yeşilırmak Basin Protection Action Plan.

Montgomery, D. C., Runger, G.C. (2007). Applied statistics and probability for engineers. Hoboken, NJ: Wiley, 164.

Nicótina, L., Alessi Celegon, E., Rinaldo, A., & Marani, M. (2008). On the impact of rainfall patterns on the hydrologic response. *Water Resources Research*, *44*(12).

Null, S. E., Viers, J. H., & Mount, J. F. (2010). Hydrologic response and watershed sensitivity to climate warming in California's Sierra Nevada. *PLoS One*, *5*(4), e9932.

Okay, A. I., & Tüysüz, O. (1999). Tethyan sutures of northern Turkey. *Geological Society, London, Special Publications*, *156*(1), 475-515.

Okay, A. I. (2008). Geology of Turkey: a synopsis. Anschnitt, 21, 19-42.

Oudin, L., Kay, A., Andréassian, V., & Perrin, C. (2010). Are seemingly physically similar catchments truly hydrologically similar? Water Resources Research, 46(11).

Özcan, A., Erkan, A., Keskin, E., Oral, A., Özer, S., Sümengen, M., & Tekeli, O. (1980). Kuzey Anadolu fayı-Kırşehir masifi arasının temel jeolojisi. Maden Tetkik ve Arama Enstitüsü Rapor, (6722).

Panagos, P., Jones, A., Bosco, C., & Kumar, P. S. (2011). European digital archive on soil maps (EuDASM): preserving important soil data for public free access. International Journal of Digital Earth, 4(5), 434-443.

Parmenter, B., & Melcher, J. (2012). Watershed and Drainage Delineation by Pour Point in ArcMap 10: http://sites.tufts.edu/gis/files/2013/11. Watershed-and-Drainage-Delineation-by-Pour-Point. pdf

Pike, J. G.: The estimation of annual runoff from meteorological data in a tropical climate, J. Hydrol., 2, 116–123, 1964.

Rao, A. R., & Srinivas, V. V. (2006). Regionalization of watersheds by fuzzy cluster analysis. Journal of Hydrology, 318(1-4), 57-79.

Rice, J. S., Emanuel, R. E., Vose, J. M., & Nelson, S. A. (2015). Continental US streamflow trends from 1940 to 2009 and their relationships with watershed spatial characteristics. Water Resources Research, 51(8), 6262-6275.

Ritter, D. F., Kochel, R. C., & Miller, J. R. (2006). Process Geomorphology. Long Grove.

Sarangi, A., Bhattacharaya, A.K., Singh, A. and Singh, A.K. (2001) Use of Geographical Information System (GIS) in assessing the erosion status of watersheds. Indian Jour. Soil. Cons., v.29(3), pp.190–195.

Shaake, J. C. (1990). From Climate to Flow, in Climate Change and US Water Resources. Waggoner, PE (ed.), 177-206.

Sankarasubramanian, A., Vogel, R. M., & Limbrunner, J. F. (2001). Climate elasticity of streamflow in the United States. Water Resources Research, 37(6), 1771-1781.

SANRAL (South African National Roads Agency Limited), 2013. Drainage manual. 6th ed. Pretoria: South African National Roads Agency Limited

Sawicz, K., Wagener, T., Sivapalan, M., Troch, P. A., & Carrillo, G. (2011). Catchment classification: empirical analysis of hydrologic similarity based on catchment function in the eastern USA. Hydrology and Earth System Sciences, 15(9), 2895-2911.

Sawicz, K. A. (2013). Catchment classification-Understanding hydrologic similarity through catchment function.

Sawicz, K. A., Kelleher, C., Wagener, T., Troch, P., Sivapalan, M., & Carrillo, G. (2014). Characterizing hydrologic change through catchment classification. Hydrology and Earth System Sciences, 18(1), 273-285.

Segond, M., H. Wheater, and C. Onof (2007), The significance of spatial rainfall representation for flood runoff estimation: A numerical evaluation based on the Lee catchment, UK, J. Hydrol., 347, 116 – 131, doi: 10.1016/j.jhydrol.2007.09.040.

Safeeq, M.; Fares, A. Hydrologic response of a Hawaiian watershed to future climate change scenarios. Hydrological processes. 26(18):2745-2764, 2012.

Singh, V.P. 1997. Effect of spatial and temporal variability in rainfall and watershed characteristics on stream flow hydrograph. Hydrologic Processes. Vol. 11, no. 12, pp. 1649-1669.

Singh, S. K., McMillan, H., Bárdossy, A., & Fateh, C. (2016). Nonparametric catchment clustering using the data depth function. Hydrological Sciences Journal, 61(15), 2649-2667.

Sivakumar, B. (2008). Dominant processes concept, model simplification and classification framework in catchment hydrology. Stochastic Environmental Research and Risk Assessment, 22(6), 737-748.

Sivapalan, M. (2003). Prediction in ungauged basins: a grand challenge for theoretical hydrology. Hydrological Processes, 17(15), 3163-3170.

Sivapalan, M., Blöschl, G., Merz, R., & Gutknecht, D. (2005). Linking flood frequency to long-term water balance: Incorporating effects of seasonality. Water Resources Research, 41(6).

Staudinger, M., Stoelzle, M., Seeger, S., Seibert, J., Weiler, M., & Stahl, K. (2017). Catchment water storage variation with elevation. *Hydrological Processes*, *31*(11), 2000-2015.

Strahler, A. N. (1952). Hypsometric (area-altitude) analysis of erosional topography. Geological Society of America Bulletin, 63(11), 1117-1142.

Stringfield, V. T., & LeGrand, H. E. (1966). Hydrology of limestone terranes in the coastal plain of the southeastern United States (Vol. 93). Geological Society of America.

Strassberg, G., Jones, N. L., & Maidment, D. R. (2011). ARC hydro groundwater: GIS for hydrogeology. Esri Press.

Stringfield, V. T., & LeGrand, H. E. (1969). Hydrology of carbonate rock terranes—A review: With special reference to the United States. *Journal of Hydrology*, *8*(3), 349-376.

Temelsu International Engineering Services Inc. (2015). Yeşilırmak Basin Flood Management Plan.

Temelsu International Engineering Services Inc. (2016). Yeşilırmak Basin Master Plan Report.

Thornthwaite CW (1948) An approach toward a rational classification of climate. Geogr Rev 38:55–94

Tsakiris, G., & Vangelis, H. (2005). Establishing a drought index incorporating evapotranspiration. *European Water*, *9*(10), 3-11.

USDA Soil Conservation Service (1986), Urban hydrology for small watersheds. Technical Release 55, U.S. Department of Agriculture, Washington, DC.

U.S. Department of Agriculture, Natural Resources Conservation Service. 2010. National Engineering Handbook, Part 630, Chapter 14, Stage discharge relations (draft), Washington, DC.

Vogel, R. M., & Fennessey, N. M. (1994). Flow-duration curves. I: New interpretation and confidence intervals. *Journal of Water Resources Planning and Management*, *120*(4), 485-504.

Wagener, T., Sivapalan, M., Troch, P., & Woods, R. (2007). Catchment classification and hydrologic similarity. Geography compass, 1(4), 901-931.

Wagener, T., Wheater, H., & Gupta, H. V. (2004). Rainfall-runoff modelling in gauged and ungauged catchments. World Scientific.

Winter, T. C. (2001). The concept of hydrologic landscapes 1. *JAWRA Journal of the American Water Resources Association*, *37*(2), 335-349.

Yadav, M., Wagener, T., & Gupta, H. (2007). Regionalization of constraints on expected watershed response behavior for improved predictions in ungauged basins. *Advances in Water Resources*, *30*(8), 1756-1774.

Yates, D., & Strzepek, K. M. (1994). Potential evapotranspiration methods and their impact on the assessment of river basin runoff under climate change.

Yilmaz, K. K., Gupta, H. V., & Wagener, T. (2008). A process-based diagnostic approach to model evaluation: Application to the NWS distributed hydrologic model. Water Resources Research, 44(9).

Yllmaz, Y., Serdar, H. S., Genc, C., Yigitbas, E., Gürer, Ö. F., Elmas, A., ... & Gürpinar, O. (1997). The geology and evolution of the Tokat Massif, south-central Pontides, Turkey. International Geology Review, 39(4), 365-382.

Yilmaz, A and Özer, S., 1984, Kuzey Anadolu Bindirme Kuşağı'nın Akdağmadeni (Yozgat) ile Karaçayır (Sivas) arasındaki bölümünün temel jeoloji incelemesi ve Tersiyer havzasının yapısal evrimi: Ketin Simpozyum, TJK Yayını, 163-174, Ankara.

Yilmaz, A., Uysal, Ş., Bedi, Y., Göç, H., & Aydın, N. (1995). Akdağ Masıfi ve Dolayının Jeolojisi. *Maden Tetkik ve Arama Dergisi*, *117*(117).

Yilmaz, A., & Yilmaz, H. (2004). Geology and structural evolution of the tokat massif (Eastern Pontides, Turkey). Turkish Journal of Earth Sciences, 13(2), 231-246

APPENDICES

A. APPENDIX A

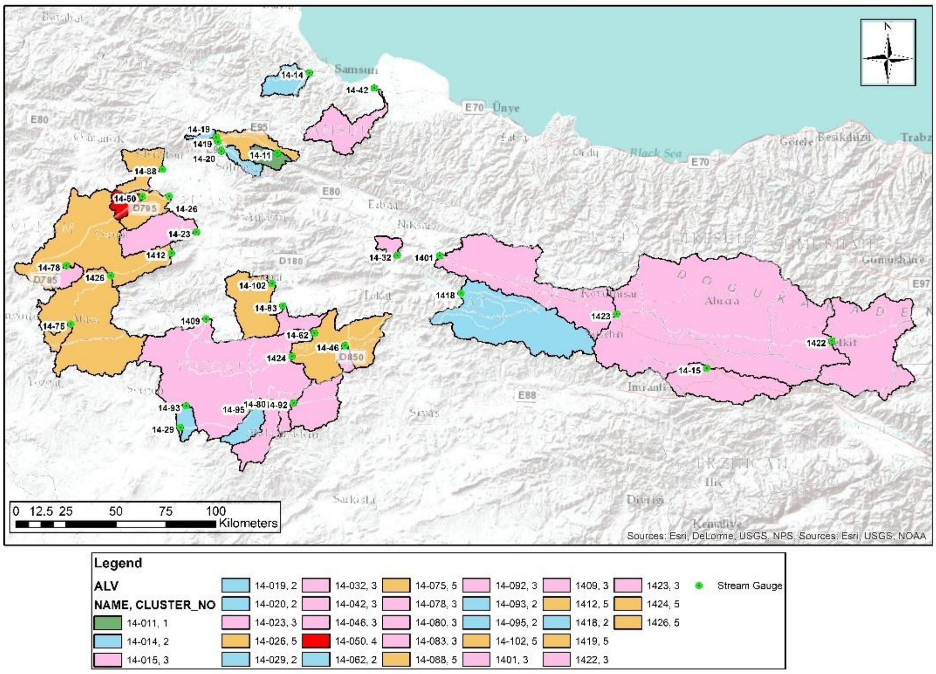

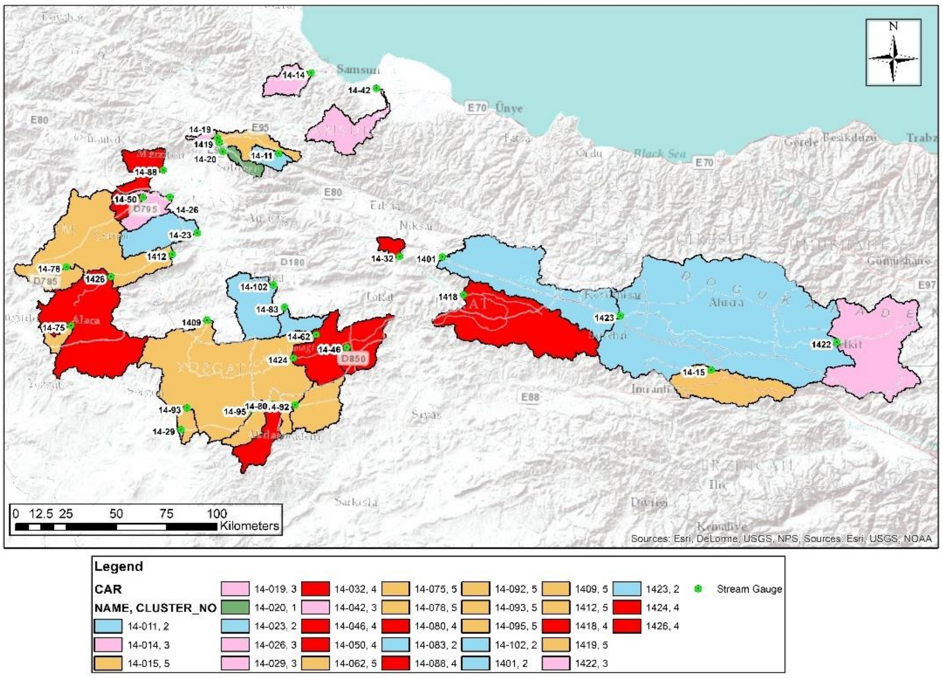
Legend
CAR
NAME, CLUSTER_NO
14-011, 2
14-014, 3
14-015, 5
14-019, 3
14-020, 1
14-023, 2
14-026, 3
14-029, 3
14-032, 4
14-042, 3
14-046, 4
14-050, 4
14-062, 5
14-075, 5
14-078, 5
14-080, 4
14-083, 2
14-088, 4
14-092, 5
14-093, 5
14-095, 5
14-102, 2
1401, 2
1409, 5
1412, 5
1418, 4
1419, 5
1422, 3
1423, 2
1424, 4
1426, 4
Stream Gauge
Sources: Esri, DeLorme, USGS, NPS, Sources: Esri, USGS, NOAA
0 12.5 25 50 75 100 Kilometers

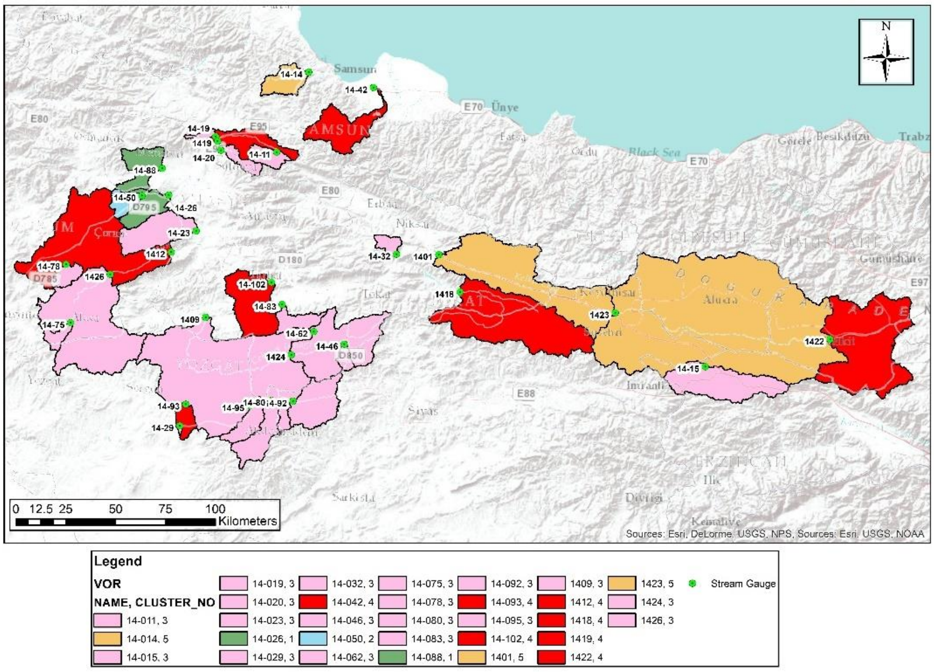
Legend
VOR
NAME, CLUSTER_NO
14-011, 3
14-014, 5
14-015, 3
14-019, 3
14-020, 3
14-023, 3
14-026, 1
14-029, 3
14-032, 3
14-042, 4
14-046, 3
14-050, 2
14-062, 3
14-075, 3
14-078, 3
14-080, 3
14-083, 3
14-088, 1
14-092, 3
14-093, 4
14-095, 3
14-102, 4
1401, 5
1409, 3
1412, 4
1418, 4
1419, 4
1422, 4
1423, 5
1424, 3
1426, 3
Stream Gauge
Sources: Esri, DeLorme, USGS, NPS, Sources: Esri, USGS, NOAA
0 12.5 25 50 75 100 Kilometers

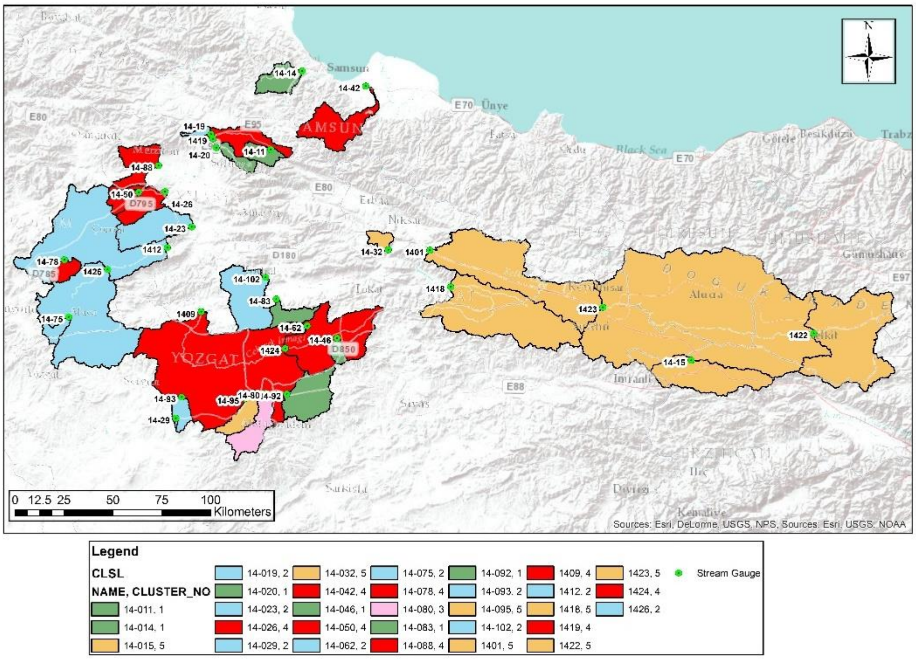

Samsun
Black Sea
E70 Ünye
E80
E95
D795
D180
D850
E88
YOZGAT
Sivas
0 12.5 25 50 75 100 Kilometers
Sources: Esri, DeLorme, USGS, NPS, Sources: Esri, USGS, NOAA
Legend
CLSL
NAME, CLUSTER_NO
14-011, 1
14-014, 1
14-015, 5
14-019, 2
14-020, 1
14-023, 2
14-026, 4
14-029, 2
14-032, 5
14-042, 4
14-046, 1
14-050, 4
14-062, 2
14-075, 2
14-078, 4
14-080, 3
14-083, 1
14-088, 4
14-092, 1
14-093, 2
14-095, 5
14-102, 2
1401, 5
1409, 4
1412, 2
1418, 5
1419, 4
1422, 5
1423, 5
1424, 4
1426, 2
Stream Gauge

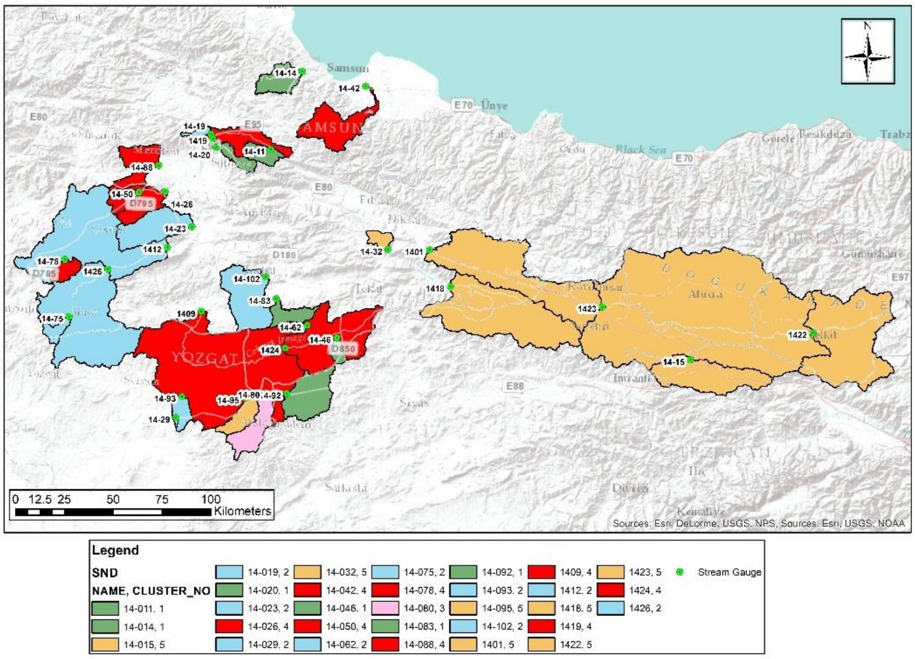

Samsun
Black Sea
E70 Ünye
E80
E95
D795
D180
D850
E88
YOZGAT
Sivas
0 12.5 25 50 75 100 Kilometers
Sources: Esri, DeLorme, USGS, NPS, Sources: Esri, USGS, NOAA
Legend
SND
NAME, CLUSTER_NO
14-011, 1
14-014, 1
14-015, 5
14-019, 2
14-020, 1
14-023, 2
14-026, 4
14-029, 2
14-032, 5
14-042, 4
14-046, 1
14-050, 4
14-062, 2
14-075, 2
14-078, 4
14-080, 3
14-083, 1
14-088, 4
14-092, 1
14-093, 2
14-095, 5
14-102, 2
1401, 5
1409, 4
1412, 2
1418, 5
1419, 4
1422, 5
1423, 5
1424, 4
1426, 2
Stream Gauge

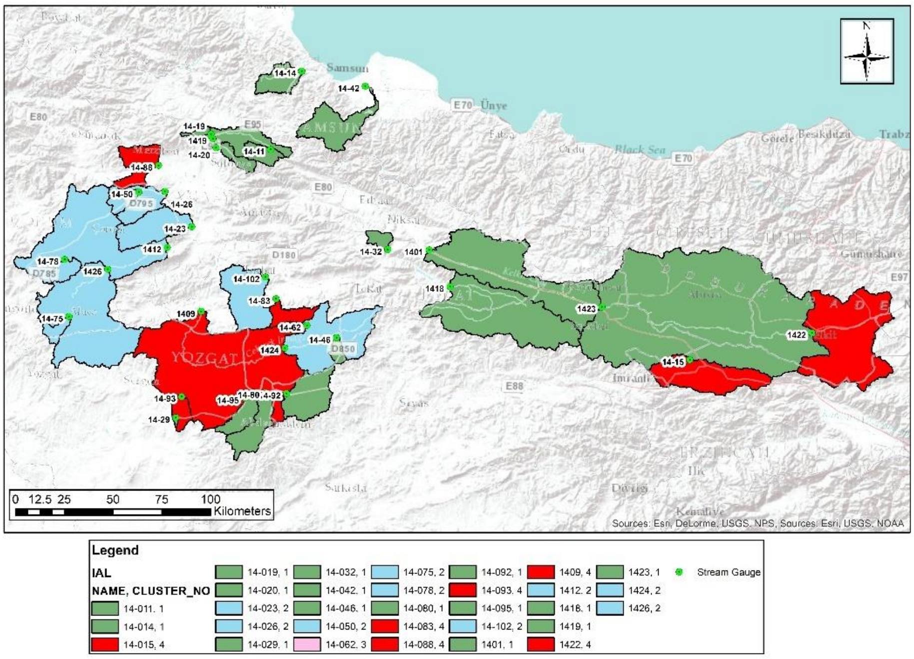
0 12.5 25 50 75 100
Kilometers
Sources: Esri, DeLorme, USGS, NPS, Sources: Esri, USGS, NOAA
Legend
IAL
NAME, CLUSTER_NO
14-011, 1
14-014, 1
14-015, 4
14-019, 1
14-020, 1
14-023, 2
14-026, 2
14-029, 1
14-032, 1
14-042, 1
14-046, 1
14-050, 2
14-062, 3
14-075, 2
14-078, 2
14-080, 1
14-083, 4
14-088, 4
14-092, 1
14-093, 4
14-095, 1
14-102, 2
1401, 1
1409, 4
1412, 2
1418, 1
1419, 1
1422, 4
1423, 1
1424, 2
1426, 2
Stream Gauge

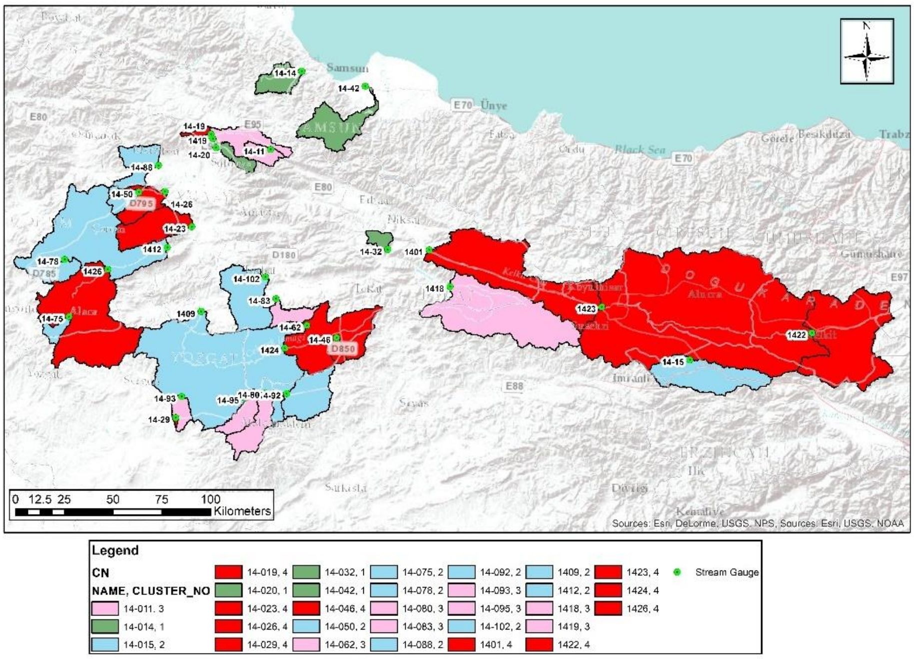
0 12.5 25 50 75 100
Kilometers
Sources: Esri, DeLorme, USGS, NPS, Sources: Esri, USGS, NOAA
Legend
CN
NAME, CLUSTER_NO
14-011, 3
14-014, 1
14-015, 2
14-019, 4
14-020, 1
14-023, 4
14-026, 4
14-029, 4
14-032, 1
14-042, 1
14-046, 4
14-050, 2
14-062, 3
14-075, 2
14-078, 2
14-080, 3
14-083, 3
14-088, 2
14-092, 2
14-093, 3
14-095, 3
14-102, 2
1401, 4
1409, 2
1412, 2
1418, 3
1419, 3
1422, 4
1423, 4
1424, 4
1426, 4
Stream Gauge

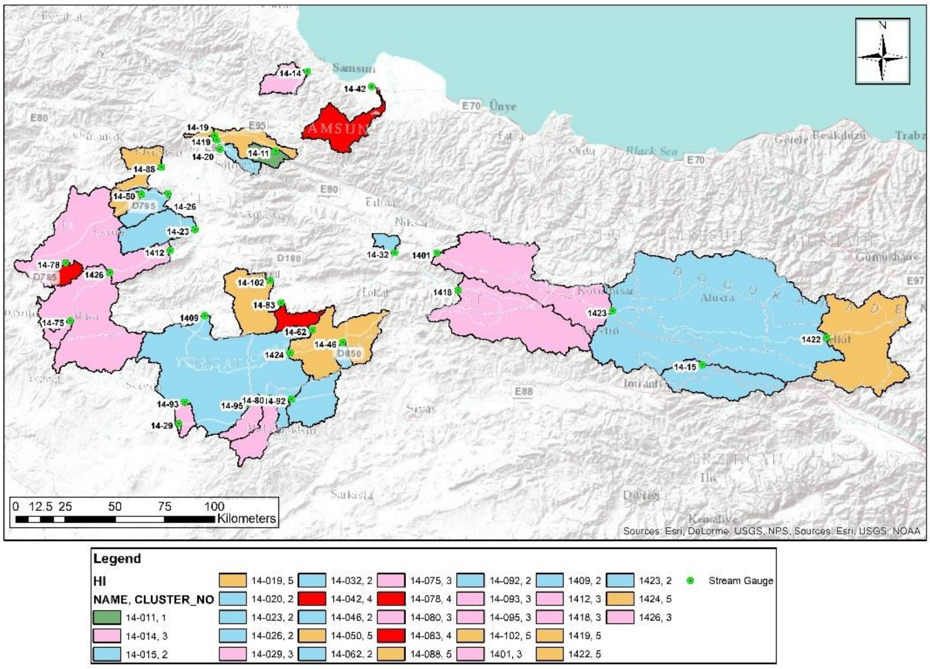
Legend
HI
NAME, CLUSTER_NO
14-011, 1
14-014, 3
14-015, 2
14-019, 5
14-020, 2
14-023, 2
14-026, 2
14-029, 3
14-032, 2
14-042, 4
14-046, 2
14-050, 5
14-062, 2
14-075, 3
14-078, 4
14-080, 3
14-083, 4
14-088, 5
14-092, 2
14-093, 3
14-095, 3
14-102, 5
1401, 3
1409, 2
1412, 3
1418, 3
1419, 5
1422, 5
1423, 2
1424, 5
1426, 3
Stream Gauge
0 12.5 25 50 75 100 Kilometers
Sources: Esri, DeLorme, USGS, NPS, Sources: Esri, USGS, NOAA

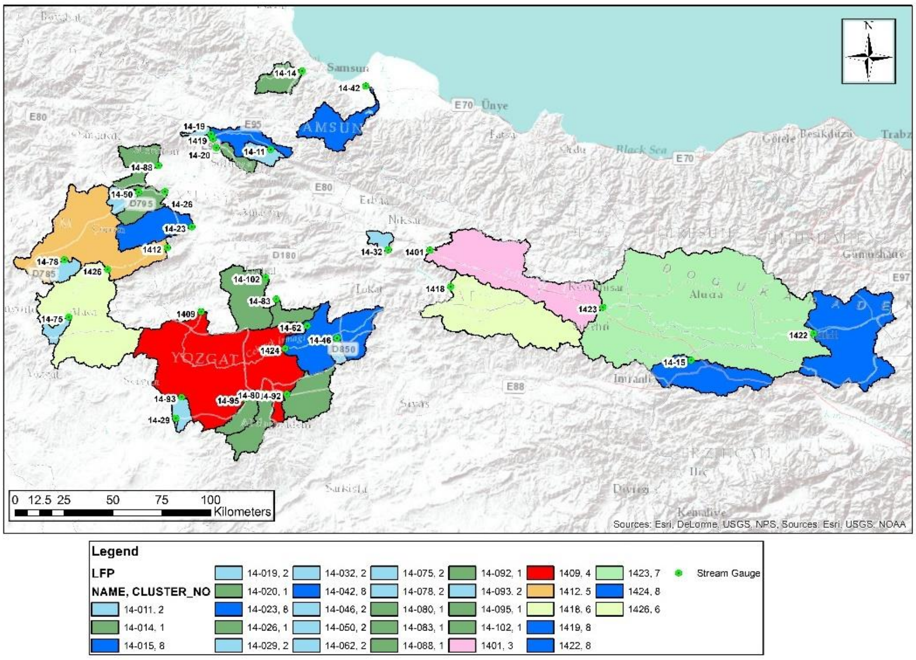
Legend
LFP
NAME, CLUSTER_NO
14-011, 2
14-014, 1
14-015, 8
14-019, 2
14-020, 1
14-023, 8
14-026, 1
14-029, 2
14-032, 2
14-042, 8
14-046, 2
14-050, 2
14-062, 2
14-075, 2
14-078, 2
14-080, 1
14-083, 1
14-088, 1
14-092, 1
14-093, 2
14-095, 1
14-102, 1
1401, 3
1409, 4
1412, 5
1418, 6
1419, 8
1422, 8
1423, 7
1424, 8
1426, 6
Stream Gauge
0 12.5 25 50 75 100 Kilometers
Sources: Esri, DeLorme, USGS, NPS, Sources: Esri, USGS, NOAA

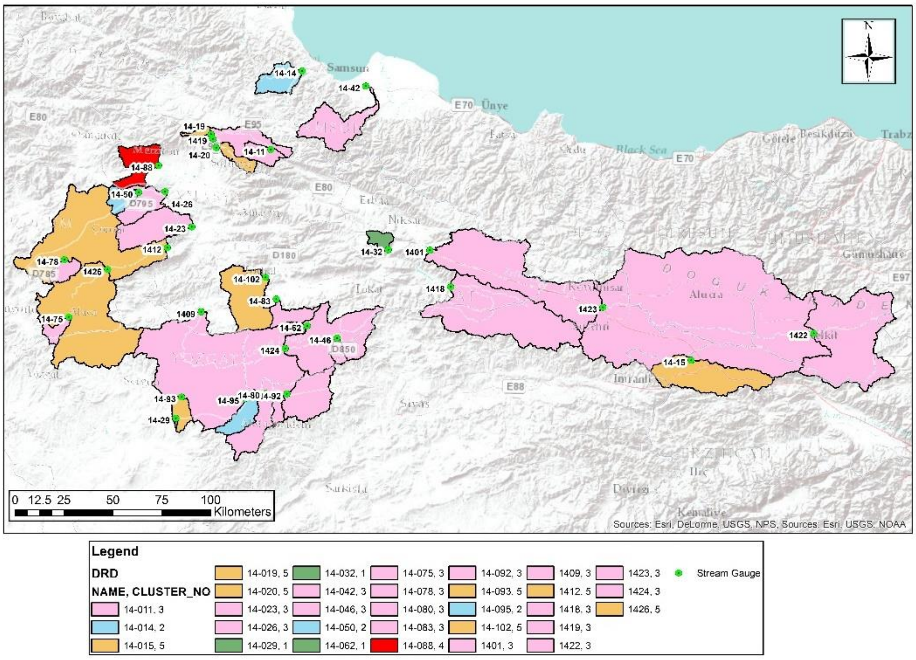
0 12.5 25 50 75 100
Kilometers
Sources: Esri, DeLorme, USGS, NPS, Sources: Esri, USGS, NOAA
Legend
DRD
NAME, CLUSTER_NO
14-011, 3
14-014, 2
14-015, 5
14-019, 5
14-020, 5
14-023, 3
14-026, 3
14-029, 1
14-032, 1
14-042, 3
14-046, 3
14-050, 2
14-062, 1
14-075, 3
14-078, 3
14-080, 3
14-083, 3
14-088, 4
14-092, 3
14-093, 5
14-095, 2
14-102, 5
1401, 3
1409, 3
1412, 5
1418, 3
1419, 3
1422, 3
1423, 3
1424, 3
1426, 5
Stream Gauge

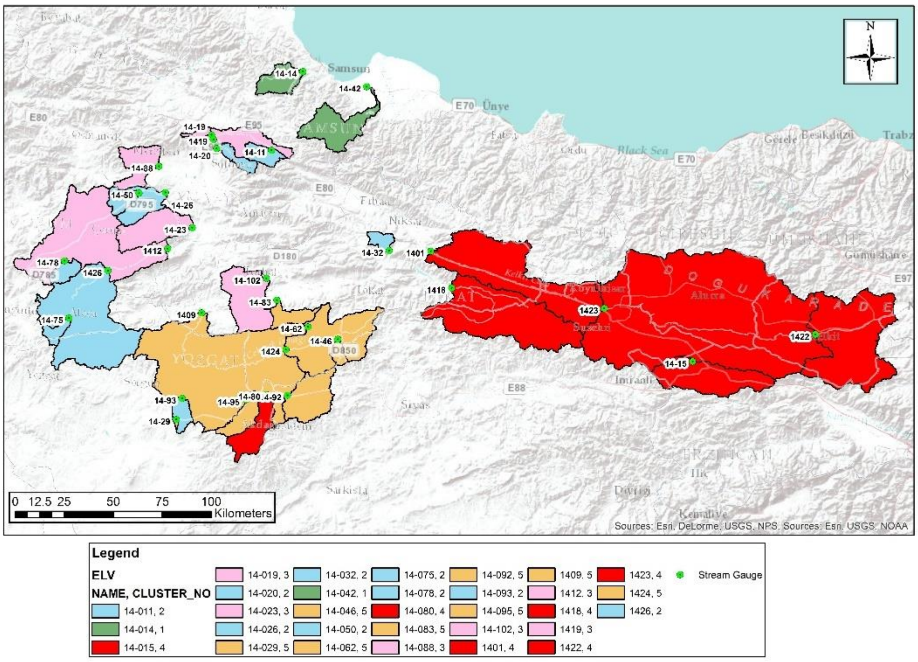
0 12.5 25 50 75 100
Kilometers
Sources: Esri, DeLorme, USGS, NPS, Sources: Esri, USGS, NOAA
Legend
ELV
NAME, CLUSTER_NO
14-011, 2
14-014, 1
14-015, 4
14-019, 3
14-020, 2
14-023, 3
14-026, 2
14-029, 5
14-032, 2
14-042, 1
14-046, 5
14-050, 2
14-062, 5
14-075, 2
14-078, 2
14-080, 4
14-083, 5
14-088, 3
14-092, 5
14-093, 2
14-095, 5
14-102, 3
1401, 4
1409, 5
1412, 3
1418, 4
1419, 3
1422, 4
1423, 4
1424, 5
1426, 2
Stream Gauge

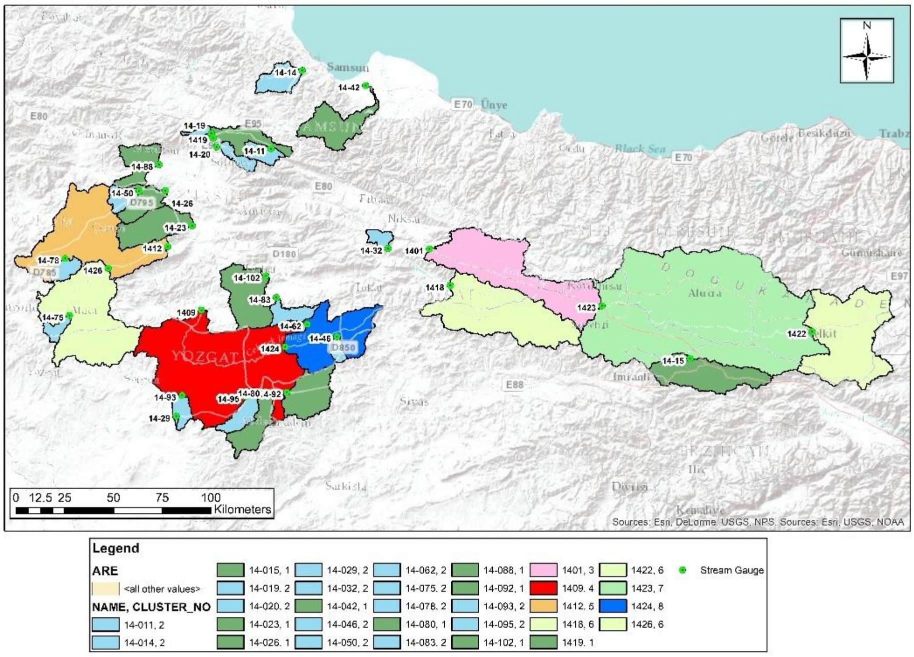
Legend
ARE
<all other values>
NAME, CLUSTER_NO
14-011, 2
14-014, 2
14-015, 1
14-019, 2
14-020, 2
14-023, 1
14-026, 1
14-029, 2
14-032, 2
14-042, 1
14-046, 2
14-050, 2
14-062, 2
14-075, 2
14-078, 2
14-080, 1
14-083, 2
14-088, 1
14-092, 1
14-093, 2
14-095, 2
14-102, 1
1401, 3
1409, 4
1412, 5
1418, 6
1419, 1
1422, 6
1423, 7
1424, 8
1426, 6
Stream Gauge
Kilometers
Sources: Esri, DeLorme, USGS, NPS, Sources: Esri, USGS, NOAA

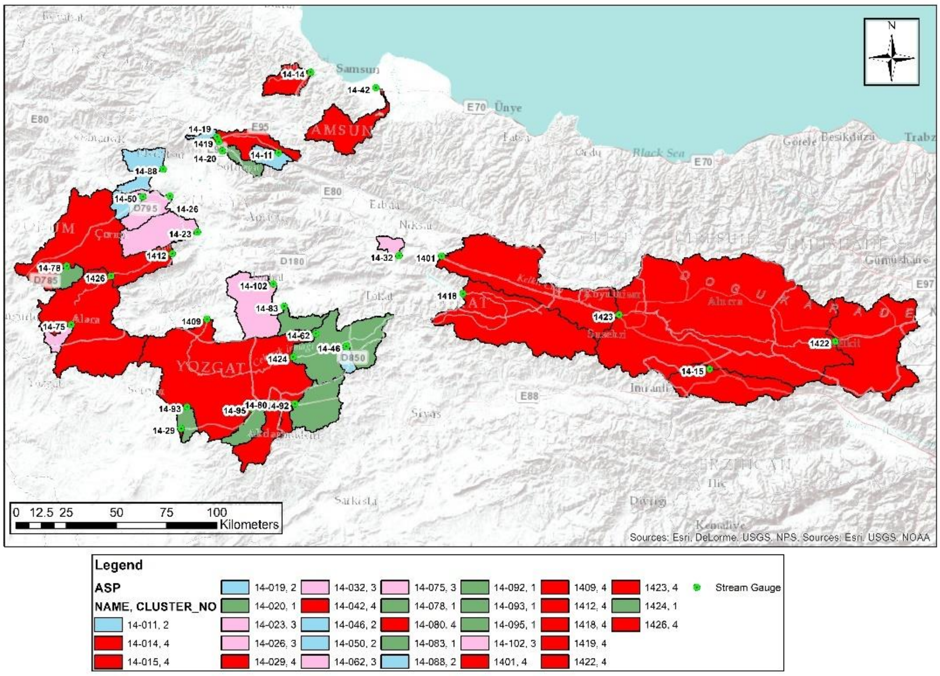
Legend
ASP
NAME, CLUSTER_NO
14-011, 2
14-014, 4
14-015, 4
14-019, 2
14-020, 1
14-023, 3
14-026, 3
14-029, 4
14-032, 3
14-042, 4
14-046, 2
14-050, 2
14-062, 3
14-075, 3
14-078, 1
14-080, 4
14-083, 1
14-088, 2
14-092, 1
14-093, 1
14-095, 1
14-102, 3
1401, 4
1409, 4
1412, 4
1418, 4
1419, 4
1422, 4
1423, 4
1424, 1
1426, 4
Stream Gauge
Kilometers
Sources: Esri, DeLorme, USGS, NPS, Sources: Esri, USGS, NOAA

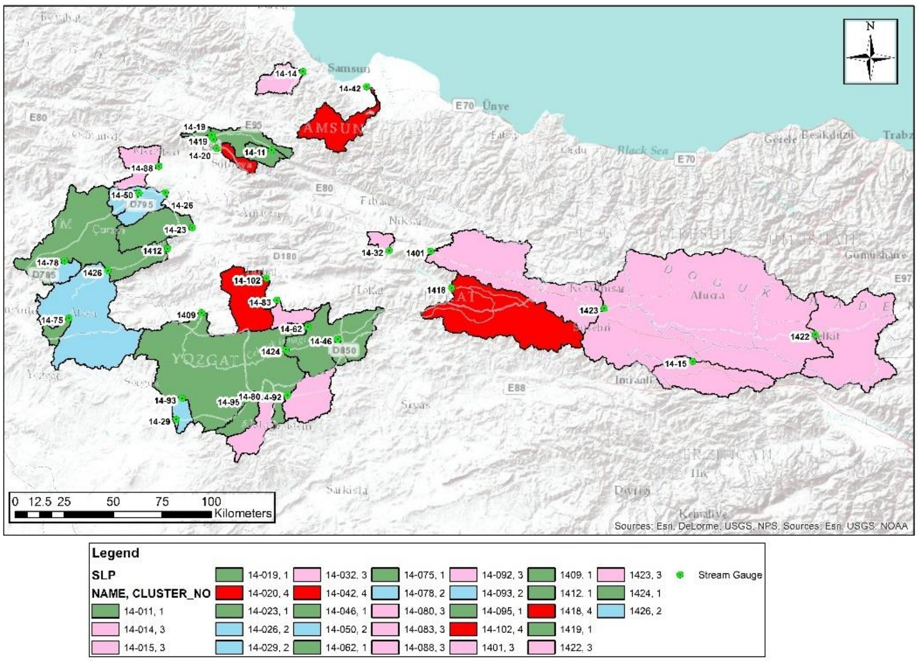
Legend
SLP
NAME, CLUSTER_NO
14-011, 1
14-014, 3
14-015, 3
14-019, 1
14-020, 4
14-023, 1
14-026, 2
14-029, 2
14-032, 3
14-042, 4
14-046, 1
14-050, 2
14-062, 1
14-075, 1
14-078, 2
14-080, 3
14-083, 3
14-088, 3
14-092, 3
14-093, 2
14-095, 1
14-102, 4
1401, 3
1409, 1
1412, 1
1418, 4
1419, 1
1422, 3
1423, 3
1424, 1
1426, 2
Stream Gauge
0 12.5 25 50 75 100
Kilometers
Sources: Esri, DeLorme, USGS, NPS, Sources: Esri, USGS, NOAA

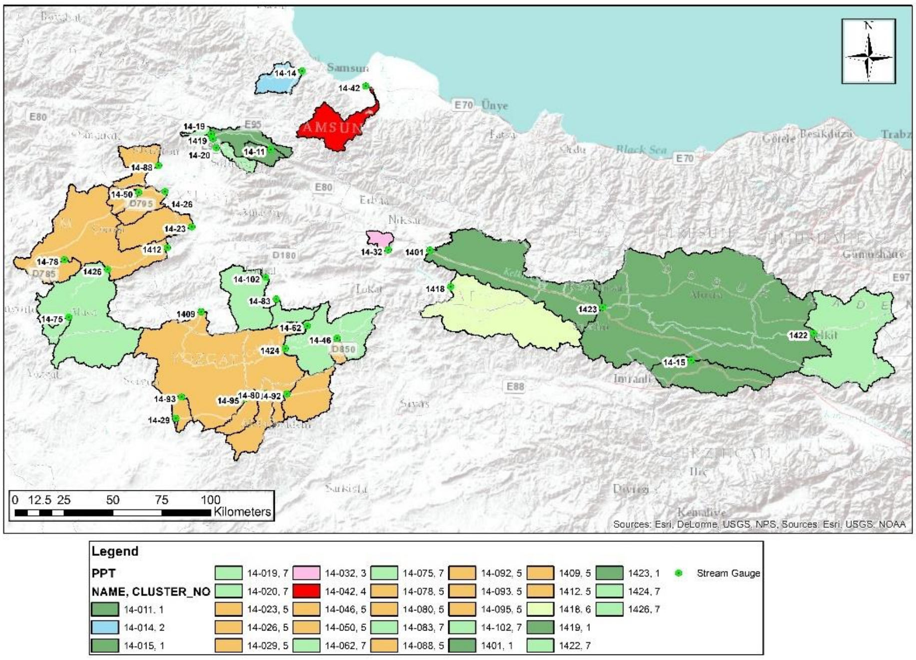
Legend
PPT
NAME, CLUSTER_NO
14-011, 1
14-014, 2
14-015, 1
14-019, 7
14-020, 7
14-023, 5
14-026, 5
14-029, 5
14-032, 3
14-042, 4
14-046, 5
14-050, 5
14-062, 7
14-075, 7
14-078, 5
14-080, 5
14-083, 7
14-088, 5
14-092, 5
14-093, 5
14-095, 5
14-102, 7
1401, 1
1409, 5
1412, 5
1418, 6
1419, 1
1422, 7
1423, 1
1424, 7
1426, 7
Stream Gauge
0 12.5 25 50 75 100
Kilometers
Sources: Esri, DeLorme, USGS, NPS, Sources: Esri, USGS, NOAA

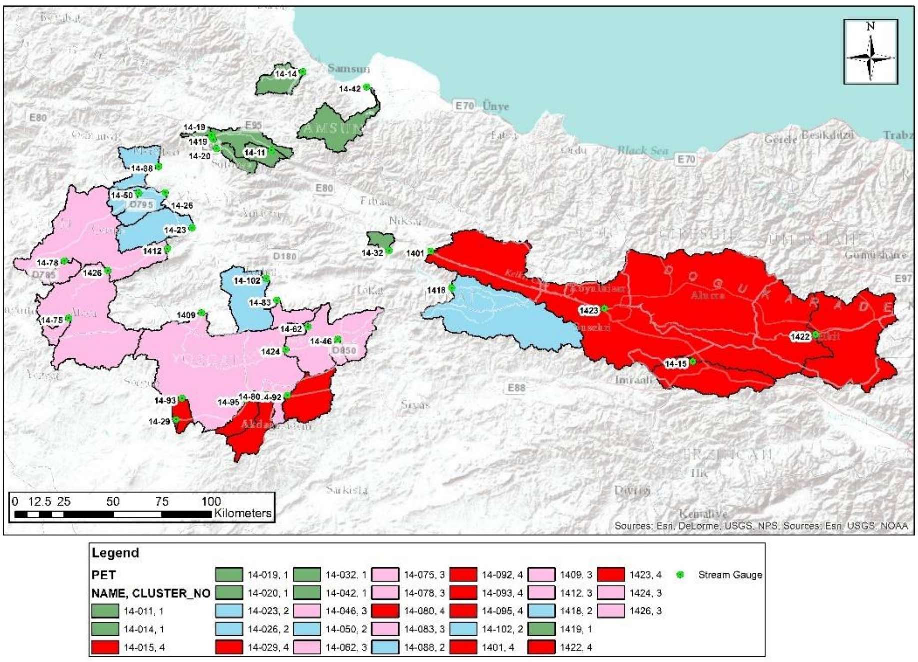
Legend
PET
NAME, CLUSTER_NO
14-011, 1
14-014, 1
14-015, 4
14-019, 1
14-020, 1
14-023, 2
14-026, 2
14-029, 4
14-032, 1
14-042, 1
14-046, 3
14-050, 2
14-062, 3
14-075, 3
14-078, 3
14-080, 4
14-083, 3
14-088, 2
14-092, 4
14-093, 4
14-095, 4
14-102, 2
1401, 4
1409, 3
1412, 3
1418, 2
1419, 1
1422, 4
1423, 4
1424, 3
1426, 3
Stream Gauge
0 12.5 25 50 75 100
Kilometers
Sources: Esri, DeLorme, USGS, NPS, Sources: Esri, USGS, NOAA

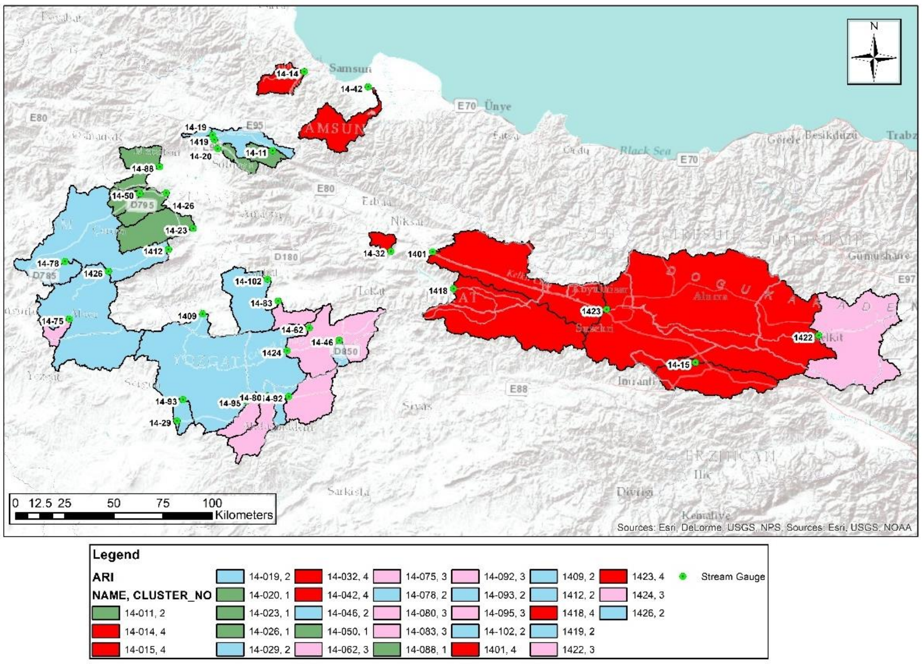
Legend
ARI
NAME, CLUSTER_NO
14-011, 2
14-014, 4
14-015, 4
14-019, 2
14-020, 1
14-023, 1
14-026, 1
14-029, 2
14-032, 4
14-042, 4
14-046, 2
14-050, 1
14-062, 3
14-075, 3
14-078, 2
14-080, 3
14-083, 3
14-088, 1
14-092, 3
14-093, 2
14-095, 3
14-102, 2
1401, 4
1409, 2
1412, 2
1418, 4
1419, 2
1422, 3
1423, 4
1424, 3
1426, 2
Stream Gauge
0 12.5 25 50 75 100
Kilometers
Sources: Esri, DeLorme, USGS, NPS, Sources: Esri, USGS, NOAA

B. APPENDIX B

Cluster No.	Catchment No.	Q5	Cluster No.	Catchment No.	Q50	Cluster No.	Catchment No.	Q95	Cluster No.	Catchment No.	SFDC	Cluster No.	Catchment No.	RQP	Cluster No.	Catchment No.	BFI	Cluster No.	Catchment No.	SFE	Cluster No.	Catchment No.	DHYF
CL1	14-11	3.275	CL1	14-11	0.589	CL1	14-11	0.173	CL1	14-11	0.771	CL1	14-19	0.328	CL1	14-15	0.896	CL1	14-29	6.690	CL1	14-11	209
	1418	3.600		14-20	0.548		14-20	0.186		14-15	0.796		14-32	0.304		14-26	0.873		14-83	7.388		14-15	209
CL2	14-19	1.643		14-42	0.499	CL2	14-15	0.149		14-20	0.621		14-46	0.333		14-62	0.866		1418	6.283		14-20	204
	14-20	1.941	CL2	14-19	0.094		1418	0.148		14-26	0.720		14-62	0.303		1401	0.862	CL2	14-75	-6.348		14-29	210
	14-75	1.635		14-26	0.107	CL3	14-14	0.033		14-88	0.585		1401	0.375		1418	0.885	CL3	14-88	9.220		14-62	208
	1419	1.645		14-29	0.114		14-19	0.011		1419	0.809		1419	0.383		1423	0.870		14-93	9.749		14-80	209
	1422	1.346		14-50	0.080		14-42	0.018	CL2	14-19	2.185		1422	0.275	CL2	14-11	0.826	CL4	14-23	3.029		14-92	204
CL3	14-15	2.501		14-62	0.100		14-62	0.012		14-23	2.026	CL2	14-11	0.708		14-19	0.808		14-32	3.166		14-93	209
	14-29	2.351		14-80	0.102		14-92	0.015		14-29	2.152		14-20	0.617		14-23	0.797		14-46	4.823		14-95	211
	14-32	2.571		14-83	0.077		14-93	0.014		14-83	1.906		14-29	0.662		14-32	0.825		14-102	3.618		1401	205
	14-42	2.665		14-92	0.111		1422	0.021		1426	2.398		1418	0.592		14-42	0.814		1409	4.293		1418	205
	14-46	2.205		14-93	0.081	CL4	14-23	0.001	CL3	14-46	3.807	CL3	14-15	0.491		14-50	0.810		1423	3.151		1422	211
	1401	2.218		14-95	0.122		14-29	0.000		14-78	3.332		14-42	0.451		14-75	0.804	CL5	14-11	0.422		1423	208
	1423	2.248		1409	0.084		14-46	0.000		14-102	2.996		14-75	0.404		14-78	0.795		14-15	1.823	CL2	14-78	225
CL4	14-14	1.268		1422	0.104		14-50	0.003	CL4	14-50	1.455		1423	0.396		14-80	0.822		14-19	2.316	CL3	14-26	187
	14-50	0.833		1424	0.095		14-75	0.000		14-62	1.099	CL4	14-14	0.270		14-95	0.819		14-20	0.964		14-32	195
	14-62	1.165	CL3	14-14	0.274		14-78	0.001		14-75	1.273		14-26	0.170		1412	0.821		14-26	2.079		14-46	195
	14-80	1.021		14-15	0.274		14-80	0.010		14-80	1.295		14-50	0.207	CL3	14-29	0.600		14-42	1.291		14-50	188
	14-83	0.937		14-75	0.301		14-83	0.000		14-92	1.145		14-80	0.230		14-46	0.571		14-50	1.892		14-83	193
	14-92	1.003		1418	0.330		14-88	0.008		1401	1.285		14-83	0.179	CL4	14-83	0.686		14-80	1.842		1409	190
	14-93	1.127		1419	0.303		14-95	0.006		1409	1.262		14-92	0.211		14-102	0.735		14-92	1.160		1424	189
	14-95	1.098	CL4	14-23	0.036		14-102	0.001		1418	1.125		14-93	0.266		1426	0.736		14-95	0.532		1426	190
	1409	1.104		14-46	0.011		1409	0.005		1422	1.064		14-95	0.263	CL5	14-14	0.844		1401	2.362	CL4	14-14	183
	1424	1.146		14-78	0.067		1412	0.001		1423	1.436		1409	0.211		14-20	0.846		1419	1.577		14-19	178
	1426	0.832		14-88	0.033		1424	0.008		1424	1.345		1424	0.217		14-88	0.848		1424	2.518		14-23	177
CL5	14-23	0.342		14-102	0.044		1426	0.000	CL5	14-14	1.511	CL5	14-23	0.078		14-92	0.837	CL6	14-14	-1.725		14-42	165
	14-26	0.617		1412	0.054	CL5	14-26	0.041		14-32	1.489		14-78	0.159		14-93	0.834		14-62	-1.062		14-75	178
	14-78	0.768		1426	0.054		14-32	0.062		14-42	1.668		14-88	0.061		1409	0.842		14-78	-1.522		14-88	183
	14-88	0.201	CL5	14-32	0.193		1401	0.058		14-93	1.856		14-102	0.102		1419	0.842		1412	-0.593		14-102	182
	14-102	0.536		1401	0.176		1423	0.060		14-95	1.715		1412	0.116		1422	0.839		1422	-3.227		1412	182
	1412	0.560		1423	0.161	CL6	1419	0.115		1412	1.653		1426	0.137		1424	0.842		1426	-1.615		1419	179

Cluster No.	Catchment No.	ALV	Cluster No.	Catchment No.	CAR	Cluster No.	Catchment No.	VOR	Cluster No.	Catchment No.	CLSL	Cluster No.	Catchment No.	SND	Cluster No.	Catchment No.	IAL	Cluster No.	Catchment No.	CN	Cluster No.	Catchment No.	HI
CL1	14-11	29.41	CL1	14-20	60.25	CL1	14-26	32.07	CL1	14-11	65.84	CL1	14-11	34.16	CL1	14-11	1.61	CL1	14-14	57.10	CL1	14-11	0.20
CL2	14-14	0.60	CL2	14-11	13.49		14-88	35.33		14-14	66.26		14-14	33.74		14-14	0.00		14-20	68.49	CL2	14-15	0.35
	14-19	1.63		14-23	14.54	CL2	14-50	72.19		14-20	65.20		14-20	34.80		14-19	0.00		14-32	56.95		14-20	0.37
	14-20	1.61		14-83	13.73	CL3	14-11	0.00		14-46	66.70		14-46	33.30		14-20	0.00		14-42	65.24		14-23	0.37
	14-29	0.00		14-102	13.08		14-15	0.64		14-83	65.90		14-83	34.10		14-29	0.05	CL2	14-15	75.97		14-26	0.41
	14-62	0.00		1401	17.11		14-19	0.00		14-92	66.75		14-92	33.25		14-32	0.00		14-50	75.95		14-32	0.40
	14-93	0.00		1423	16.25		14-20	0.98	CL2	14-19	70.15	CL2	14-19	29.85		14-42	0.20		14-75	75.60		14-46	0.40
	14-95	0.21	CL3	14-14	30.43		14-23	0.00		14-23	70.89		14-23	29.11		14-46	0.84		14-78	75.81		14-62	0.38
	1418	1.92		14-19	23.66		14-29	0.00		14-29	71.60		14-29	28.40		14-80	2.36		14-88	76.40		14-92	0.38
CL3	14-15	4.58		14-26	28.79		14-32	0.00		14-62	72.11		14-62	27.89		14-92	2.35		14-92	74.83		1409	0.38
	14-23	5.26		14-29	26.72		14-46	0.00		14-75	70.10		14-75	29.90		14-95	1.90		14-102	75.86		1423	0.39
	14-32	4.77		14-42	27.10		14-62	0.00		14-93	71.80		14-93	28.20		1401	2.92		1409	75.59	CL3	14-14	0.43
	14-42	4.37		1422	23.29		14-75	0.00		14-102	69.99		14-102	30.01		1418	0.13		1412	77.21		14-29	0.42
	14-46	3.71	CL4	14-32	0.00		14-78	0.08		1412	70.37		1412	29.63		1419	3.02	CL3	14-11	70.09		14-75	0.47
	14-78	3.26		14-46	3.92		14-80	0.00		1426	71.79		1426	28.21		1423	3.44		14-62	70.46		14-80	0.44
	14-80	2.85		14-50	2.38		14-83	0.00	CL3	14-80	58.38	CL3	14-80	41.62	CL2	14-23	23.15		14-80	69.33		14-93	0.47
	14-83	5.83		14-80	3.53		14-92	0.00	CL4	14-26	69.60	CL4	14-26	30.40		14-26	21.80		14-83	73.50		14-95	0.46
	14-92	7.06		14-88	4.63		14-95	0.00		14-42	68.17		14-42	31.83		14-50	27.24		14-93	73.52		1401	0.45
	1401	3.53		1418	5.06		1409	2.14		14-50	68.81		14-50	31.19		14-75	26.36		14-95	71.37		1412	0.43
	1409	6.69		1424	5.39		1424	0.00		14-78	67.84		14-78	32.16		14-78	21.12		1418	72.64		1418	0.42
	1422	4.50		1426	4.34		1426	2.00		14-88	68.40		14-88	31.60		14-102	24.35		1419	72.08		1426	0.44
	1423	3.90	CL5	14-15	8.27	CL4	14-42	10.08		1409	67.83		1409	32.17		1412	19.21	CL4	14-19	77.66	CL4	14-42	0.52
CL4	14-50	23.62		14-62	8.65		14-93	4.45		1419	68.72		1419	31.28		1424	18.67		14-23	78.87		14-78	0.61
CL5	14-26	13.44		14-75	10.94		14-102	7.20		1424	68.91		1424	31.09		1426	17.83		14-26	79.12		14-83	0.55
	14-75	11.25		14-78	10.88		1412	5.40	CL5	14-15	61.50	CL5	14-15	38.50	CL3	14-62	36.60		14-29	79.91	CL5	14-19	0.27
	14-88	13.32		14-92	10.90		1418	7.25		14-32	63.71		14-32	36.29	CL4	14-15	5.59		14-46	79.27		14-50	0.27
	14-102	17.65		14-93	9.96		1419	10.68		14-95	62.52		14-95	37.48		14-83	10.05		1401	78.07		14-88	0.30
	1412	13.21		14-95	9.12		1422	7.94		1401	62.71		1401	37.29		14-88	10.31		1422	78.61		14-102	0.32
	1419	13.14		1409	8.51	CL5	14-14	19.31		1418	62.53		1418	37.47		14-93	6.12		1423	78.71		1419	0.25
	1424	12.82		1412	7.20		1401	21.86		1422	64.02		1422	36.00		1409	6.40		1424	77.31		1422	0.31
	1426	10.16		1419	9.41		1423	19.93		1423	62.44		1423	37.56		1422	5.52		1426	77.58		1424	0.29

Cluster No.	Catchment No.	LFP	Cluster No.	Catchment No.	DRD	Cluster No.	Catchment No.	ELV	Cluster No.	Catchment No.	ARE	Cluster No.	Catchment No.	ASP	Cluster No.	Catchment No.	SLP
CL1	14-14	32987.08	CL1	14-29	0.29	CL1	14-14	656.74	CL1	14-15	725.50	CL1	14-20	203.47	CL1	14-11	9.91
	14-20	27063.20		14-32	0.32		14-42	644.37		14-23	504.80		14-78	220.42		14-19	8.32
	14-26	38327.64		14-62	0.34	CL2	14-11	1086.52		14-26	420.40		14-83	194.15		14-23	11.91
	14-80	42804.55	CL2	14-14	0.38		14-20	1172.98		14-42	502.50		14-92	205.80		14-46	11.27
	14-83	37062.90		14-50	0.39		14-26	1094.58		14-80	338.60		14-93	203.09		14-62	9.90
	14-88	28908.96		14-95	0.39		14-32	1112.16		14-88	317.70		14-95	199.07		14-75	11.92
	14-92	31422.96	CL3	14-11	0.43		14-50	1226.78		14-92	477.70		1424	193.61		14-95	11.18
	14-95	26420.12		14-23	0.43		14-75	1235.02		14-102	613.00	CL2	14-11	150.02		1409	9.58
	14-102	39529.39		14-26	0.42		14-78	1181.58		1419	513.20		14-19	134.38		1412	7.71
CL2	14-11	17158.35		14-42	0.43		14-93	1236.26	CL2	14-11	145.10		14-46	136.34		1419	8.75
	14-19	16941.34		14-46	0.41		1426	1143.81		14-14	259.00		14-50	143.40		1424	8.98
	14-29	1976.31		14-75	0.41	CL3	14-19	902.95		14-19	52.60		14-88	143.94	CL2	14-26	4.25
	14-32	16164.60		14-78	0.41		14-23	958.68		14-20	102.40	CL3	14-23	162.43		14-29	5.70
	14-46	14435.01		14-80	0.41		14-88	986.98		14-29	6.80		14-26	154.11		14-50	4.18
	14-50	22325.33		14-83	0.42		14-102	993.09		14-32	94.10		14-32	164.73		14-78	5.16
	14-62	5625.96		14-92	0.44		1412	1076.64		14-46	72.50		14-62	158.85		14-93	6.39
	14-75	16297.05		1401	0.42		1419	941.24		14-50	150.40		14-75	150.81		1426	6.82
	14-78	15970.78		1409	0.42	CL4	14-15	1900.12		14-62	21.50		14-102	157.74	CL3	14-14	15.22
	14-93	20057.65		1418	0.41		14-80	1608.43		14-75	100.40	CL4	14-14	172.08		14-15	13.40
CL3	1401	317980.90		1419	0.42		1401	1643.46		14-78	129.40		14-15	178.71		14-32	14.23
CL4	1409	163498.29		1422	0.41		1418	1599.61		14-83	179.80		14-29	193.14		14-80	14.26
CL5	1412	125472.68		1423	0.42		1422	1836.13		14-93	138.00		14-42	179.23		14-83	13.06
CL6	1418	92403.96		1424	0.44		1423	1723.57		14-95	212.40		14-80	184.00		14-88	16.26
	1426	87308.01	CL4	14-88	0.55	CL5	14-29	1270.15	CL3	1401	10048.80		1401	181.13		14-92	14.09
CL7	1423	212127.10	CL5	14-15	0.45		14-46	1404.52	CL4	1409	5267.60		1409	187.35		1401	14.73
CL8	14-15	52818.79		14-19	0.48		14-62	1370.91	CL5	1412	3668.80		1412	183.10		1422	12.90
	14-23	48443.64		14-20	0.48		14-83	1262.78	CL6	1418	1608.00		1418	181.90		1423	14.49
	14-42	68725.28		14-93	0.46		14-92	1449.46		1422	1714.00		1419	186.36	CL4	14-20	21.44
	1419	56894.20		14-102	0.48		14-95	1440.10		1426	1817.20		1422	180.95		14-42	17.18
	1422	71885.55		1412	0.48		1409	1273.43	CL7	1423	8302.80		1423	181.12		14-102	18.49
	1424	57383.89		1426	0.47		1424	1333.56	CL8	1424	1032.80		1426	182.94		1418	17.80

Cluster No.	Catchment No.	PPT	Cluster No.	Catchment No.	PET	Cluster No.	Catchment No.	ARI
CL1	14-11	488.79	CL1	14-11	1040.51	CL1	14-20	0.44
	14-15	481.03		14-14	1060.55		14-23	0.42
	1401	513.77		14-19	998.06		14-26	0.42
	1419	476.72		14-20	1025.39		14-50	0.41
	1423	496.15		14-32	1019.85		14-88	0.42
CL2	14-14	593.05		14-42	1075.93	CL2	14-11	0.47
CL3	14-32	708.21		1419	1031.15		14-19	0.44
CL4	14-42	766.40	CL2	14-23	935.49		14-29	0.47
CL5	14-23	393.75		14-26	937.13		14-46	0.46
	14-26	390.81		14-50	932.93		14-78	0.45
	14-29	403.82		14-88	951.46		14-93	0.47
	14-46	407.94		14-102	924.53		14-102	0.45
	14-50	386.27		1418	939.34		1409	0.47
	14-78	401.92	CL3	14-46	883.56		1412	0.45
	14-80	401.89		14-62	878.95		1419	0.46
	14-88	395.93		14-75	874.67		1426	0.47
	14-92	410.16		14-78	893.41	CL3	14-62	0.48
	14-93	403.90		14-83	897.76		14-75	0.48
	14-95	401.84		1409	866.74		14-80	0.48
	1409	408.41		1412	894.12		14-83	0.49
	1412	404.77		1424	891.31		14-92	0.48
CL6	1418	546.30		1426	878.17		14-95	0.48
CL7	14-19	442.21	CL4	14-15	797.62		1422	0.50
	14-20	449.47		14-29	852.39		1424	0.48
	14-62	419.62		14-80	834.10	CL4	14-14	0.56
	14-75	423.17		14-92	850.33		14-15	0.60
	14-83	436.63		14-93	852.03		14-32	0.69
	14-102	420.05		14-95	838.78		14-42	0.71
	1422	417.24		1401	842.50		1401	0.61
	1424	423.64		1422	837.74		1418	0.58
	1426	415.87		1423	821.00		1423	0.60